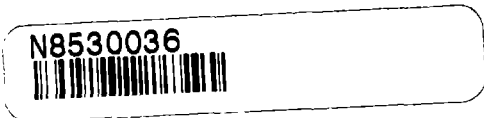
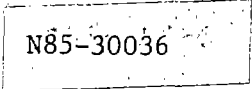


NASA CONTRACTOR REPORT 177357



(NASA-CR-177357) POLYMER MATRIX AND GRAPHITE FIBER INTERFACE STUDY Final Report, Apr. 1984 - Dec. 1984 (Wyoming Univ.) p HC A18/MF A01 CSCI 11D



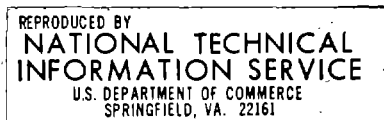
Unclas G3/24 29863

Polymer Matrix and Graphite Fiber Interface Study

D.F.Adams  
R.S.Zimmerman  
E.M.Odom

June 1985

CONTRACT NAS2-11612





1. Report No NASA CR 177357		2. Government Accession No.		3. Recipient's Catalog No.	
4. Title and Subtitle Polymer Matrix and Graphite Fiber Interface Study				5. Report Date June 1985	
				6. Performing Organization Code	
7. Author(s) Donald F. Adams Richard S. Zimmerman Edwin M. Odom				8. Performing Organization Report No UWME-DR-501-102-1	
9. Performing Organization Name and Address Composite Materials Research Group University of Wyoming Laramie, Wyoming 82071				10. Work Unit No	
				11. Contract or Grant No. NAS2-11612	
12. Sponsoring Agency Name and Address NASA-Ames Research Center Moffett Field, California 94035				13. Type of Report and Period Covered Final Report April 1983 - Dec. 1984	
				14. Sponsoring Agency Code 505-33-31	
15. Supplementary Notes NASA-Ames Technical Contact: Demetrius A. Kourtidis, Ames Research Center, MS 234-1 (415) 694-6079, FTS 464-6079					
16. Abstract  <p>Hercules AS4 graphite fiber, unsized, or with EPON 828, PVA, or polysulfone sizing, was combined with three different polymer matrices. These included Hercules 3501-6 epoxy, Hercules 4001 bismaleimide, and Hexcel F155 rubber-toughened epoxy. Unidirectional composites in all twelve combinations were fabricated and tested in transverse tension and axial compression. Quasi-isotropic laminates were tested in axial tension and compression, flexure, interlaminar shear, and tensile impact. All tests were conducted at both room temperature, dry and elevated temperature, wet conditions. Single fiber pull-out testing was also performed.</p> <p>Extensive scanning electron microphotographs of fracture surfaces are included, along with photographs of single fiber pullout failures. Analytical/experimental correlations are presented, based on the results of a finite element micromechanics analysis.</p> <p>Correlations between matrix type, fiber sizing, hygrothermal environment, and loading mode are presented. Results indicate that the various composite properties were only moderately influenced by the fiber sizings utilized.</p>					
17. Key Words (Suggested by Author(s)) Graphite/Polymer Composites Fiber-Matrix Interface Mechanical Properties Micromechanics Analyses			18. Distribution Statement  Unclassified, Unlimited Subject Category 24		
19. Security Classif. (of this report) Unclassified		20. Security Classif. (of this page) Unclassified		21. No. of Pages 396	22. Price*

\* For sale by the National Technical Information Service, Springfield, Virginia 22161



## PREFACE

This technical report presents the results of a thirteen-month study of the graphite fiber-polymer matrix interface, sponsored by NASA-Ames Research Center under Research Contract No. NAS2-11612. Mr. D.A. Kourtides served as the NASA-Ames Project Monitor.

All work was conducted by the Composite Materials Research Group (CMRG) within the Department of Mechanical Engineering at the University of Wyoming, except the fiber surface treatment characterization, which was performed by Midwest Research Institute of Kansas City, Missouri. Co-Principal Investigators were Dr. Donald F. Adams, Professor, and Mr. Richard S. Zimmerman, Staff Engineer. Mr. Edwin M. Odom, Staff Engineer, initially was assigned to this program but was succeeded by Mr. Zimmerman in June 1984. Making significant contributions to this program were Messrs. Mathew Graf, William Pressnall, Gregory Morrison, Merrill Bishop, and Kenneth Bauer, undergraduate students in Mechanical Engineering and members of the Composite Materials Research Group. Special appreciation is extended to Dr. Norman J. Johnston of NASA-Langley Research Center for supplying the thermoplastic-sized graphite fibers for use in this study.

Numerous material acquisition problems were encountered during the first six months of this contract, resulting in some delay in completing the work. All materials were not received until January 1984, a full eight months into the program. Once materials were received, good progress was made in the fabrication of composites and the testing of all samples.

Use of commercial products or names of manufacturers in this

report does not constitute official endorsement of such products or manufacturers, either expressed or implied, by the National Aeronautics and Space Administration.

## TABLE OF CONTENTS

<u>Section</u>		<u>Page</u>
1	SUMMARY . . . . .	1
2	INTRODUCTION . . . . .	19
3	EXPERIMENTAL PROCEDURES . . . . .	21
	3.1 Test Matrix . . . . .	21
	3.2 Fiber Sizings . . . . .	21
	3.3 Preparation of Composite Materials . . . . .	23
	3.4 Composite Test Specimen Preparation . . . . .	28
	3.5 Neat Resin Test Specimen Preparation . . . . .	30
	3.5.1 Tensile Test Specimens . . . . .	30
	3.5.2 Iosipescu Shear Test Specimens . . . . .	30
	3.5.3 Coefficient of Thermal Expansion Tests . . . . .	31
	3.5.4 Coefficient of Moisture Expansion Tests . . . . .	31
	3.6 Testing Equipment . . . . .	34
	3.6.1 Unidirectional Composite Transverse Tension . . . . .	35
	3.6.2 Laminate Axial Tension . . . . .	35
	3.6.3 Unidirectional Composite Axial Compression . . . . .	35
	3.6.4 Laminate Axial Compression . . . . .	37
	3.6.5 Laminate Flexure . . . . .	37
	3.6.6 Laminate Interlaminar Shear . . . . .	37
	3.6.7 Neat Resin Properties . . . . .	39
	3.6.8 Single Fiber Pullout . . . . .	39

TABLE OF CONTENTS  
(Continued)

<u>Section</u>		<u>Page</u>
4	EXPERIMENTAL RESULTS . . . . .	43
4.1	Fiber Surface Treatment Characteristics . . . . .	43
4.2	Neat Resin Properties . . . . .	43
4.3	Composite Fiber Volume Contents . . . . .	48
4.4	Unidirectional Composites . . . . .	51
	4.4.1 Transverse Tension . . . . .	53
	4.4.2 Axial Compression . . . . .	65
4.5	Quasi-Isotropic Laminates . . . . .	76
	4.5.1 Axial Tension . . . . .	77
	4.5.2 Axial Compression . . . . .	87
	4.5.3 Flexure . . . . .	99
	4.5.4 Interlaminar Shear . . . . .	109
	4.5.5 Tensile Impact . . . . .	114
4.6	Single Fiber Pullout . . . . .	127
5	SCANNING ELECTRON MICROSCOPE RESULTS . . . . .	141
5.1	Introduction . . . . .	141
5.2	Specimen Preparation . . . . .	141
5.3	Explanation of SEM Photographs . . . . .	141
6	ANALYTICAL/EXPERIMENTAL CORRELATIONS . . . . .	195
6.1	Micromechanics Analysis . . . . .	195
6.2	Constituent Properties . . . . .	198
6.3	Analysis Procedure . . . . .	205
6.4	AS4/3501-6 Correlations . . . . .	207



TABLE OF CONTENTS  
(Continued)

<u>Section</u>	<u>Page</u>
6.4.1	Thermal Residual Stress . . . . . 207
6.4.2	Moisture-Induced Stresses . . . . . 212
6.4.3	Transverse Tensile Loading . . . . . 216
6.4.3.1	Room Temperature, Dry . . . . . 216
6.4.3.2	Elevated Temper- ature, Wet (93°C, 1%M) . . . . . 221
6.5	AS4/4001 Correlations . . . . . 226
6.5.1	Thermal Residual Stresses . . . . . 226
6.5.2	Moisture-Induced Stresses . . . . . 227
6.5.3	Transverse Tensile Loading . . . . . 228
6.5.3.1	Room Temperature, Dry . . . . . 228
6.5.3.2	Elevated Temper- ature, Wet . . . . . 231
6.6	AS4/F155 Correlations . . . . . 235
6.6.1	Thermal Residual Stresses . . . . . 236
6.6.2	Moisture-Induced Stresses . . . . . 236
6.6.3	Transverse Tensile Loading . . . . . 237
6.6.3.1	Room Temperature, Dry . . . . . 237
6.6.3.2	Elevated Temper- ature, Wet . . . . . 241
6.7	Summary of Results . . . . . 245
7	CONCLUSIONS AND RECOMMENDATIONS . . . . . 247

TABLE OF CONTENTS  
(Continued)

<u>Section</u>	<u>Page</u>
References . . . . .	251
Appendices	
Appendix A - Tables of Individual Specimen Test Results . . . . .	255
Appendix B - Individual Data Plots . . . . .	327
Appendix C - Additional Photographs of Single Fiber Pullout Specimen Fracture Surfaces . . . . .	369
Appendix D - Characterization of Graphite Fiber Surface Coatings . . . . .	379

## SECTION 1

### SUMMARY

Three polymer matrix materials and four fiber sizings, including an unsized fiber, were chosen by NASA-Ames for this Hercules AS4 graphite fiber/polymer matrix interface study. A baseline epoxy, viz, Hercules 3501-6, plus Hercules 4001, a bismaleimide, and Hexcel F155, a rubber-toughened epoxy, were selected as the three polymer matrix materials. Three common graphite fiber sizings, i.e., EPON 828 epoxy, PVA polyvinylalcohol, and Udel P1700 polysulfone thermoplastic, were used, along with an unsized fiber, to create a total of twelve fiber sizing/matrix combinations. These sizings were applied by Hercules, Inc. and NASA-Langley Research Center, to fibers supplied from a common batch. Samples of these sized fibers were then sent to Midwest Research Institute for surface characterization using infrared spectroscopy. These sizing characterization results are included here as Appendix D. Hercules AS4 high strength graphite fiber, in the form of 12,000 filament tow, was used in fabricating all test panels. This provided a common fiber base for this interface study.

All composite material prepregging, test panel fabrication, specimen fabrication, and mechanical testing was performed by the Composite Materials Research Group (CMRG) at the University of Wyoming.

An extensive mechanical characterization study was completed on

the 12 fiber surface treatment/polymer matrix composites, at two different environmental conditions, viz, room temperature, dry (RTD) and elevated temperature, wet (ETW). Unidirectional, i.e.,  $[0]_g$ , composites were tested under transverse tensile and axial compressive loadings, and quasi-isotropic, i.e.,  $[\pm 45/0/90]_g$ , laminates under axial tensile, axial compressive, three-point flexure, short beam (interlaminar) shear, and instrumented tensile impact loadings. Single fiber pullout testing was conducted on all 12 fiber/matrix combinations also, as an aid in the determination of interfacial shear strengths. Neat resin testing was performed on two of the matrix materials, viz, Hercules 4001 and Hexcel F155, to determine their mechanical properties, i.e., tensile and shear strengths, moduli, and ultimate strains, for use as input to the finite element micromechanics computer program. Coefficient of thermal expansion and coefficient of moisture expansion measurements were also made on these two neat resin systems. All of the above data were already available for the Hercules 3501-6 epoxy.

Scanning electron microscopy was performed on all of the unidirectional composite fracture surfaces, for both transverse tensile and axial compressive loadings. An extensive collection of SEM photographs is included in Section 5 of this report.

A summary of the mechanical test results is presented here in Figures 1 through 8, in simple bar chart forms. For brevity, only strength properties are summarized in these figures (except for the laminated composite tensile impact testing, for which a total impact energy absorption plot is included instead, as being of greater relevance). Complete results, including tables of numerical averages

## AVERAGE TRANSVERSE TENSILE STRENGTHS

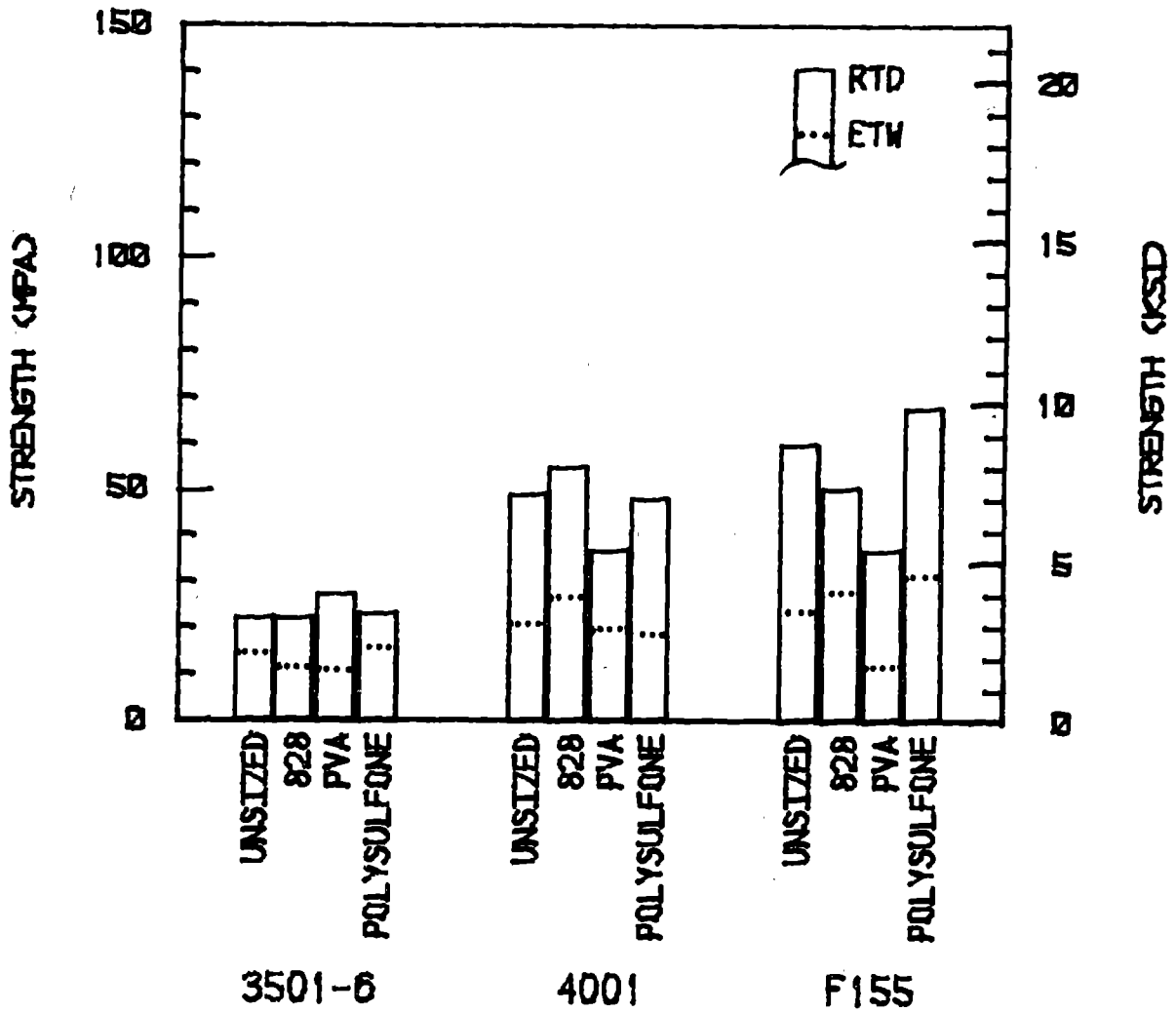


Figure 1. Unidirectional Composite Transverse Tensile Strengths of the Twelve Fiber Sizing/Matrix Combinations.

## AVERAGE AXIAL COMPRESSIVE STRENGTHS

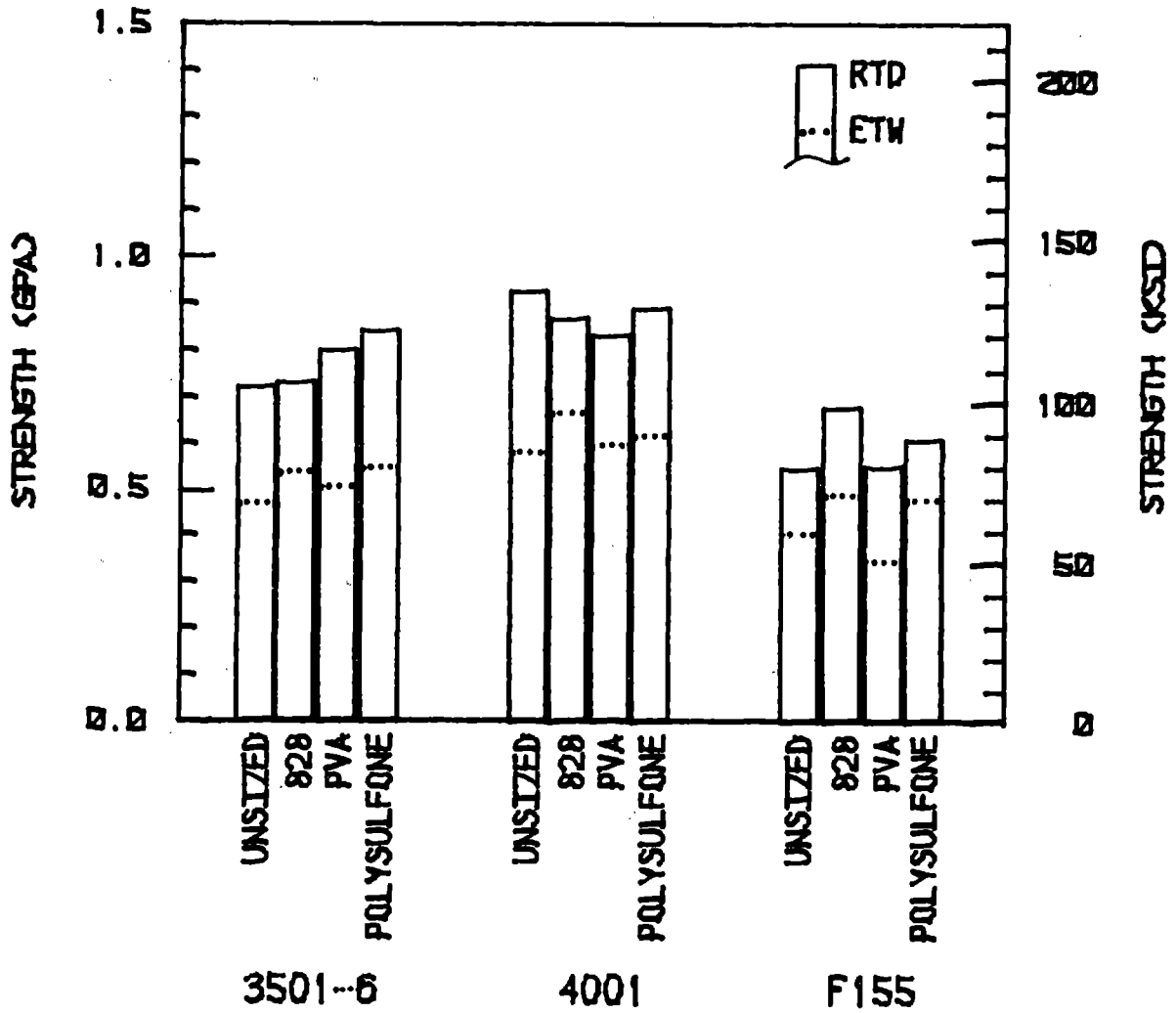


Figure 2. Unidirectional Composite Axial Compressive Strengths of the Twelve Fiber Sizing/Matrix Combinations.

ORIGINAL PAGE IS  
OF POOR QUALITY

### AVERAGE LAMINATE TENSILE STRENGTHS

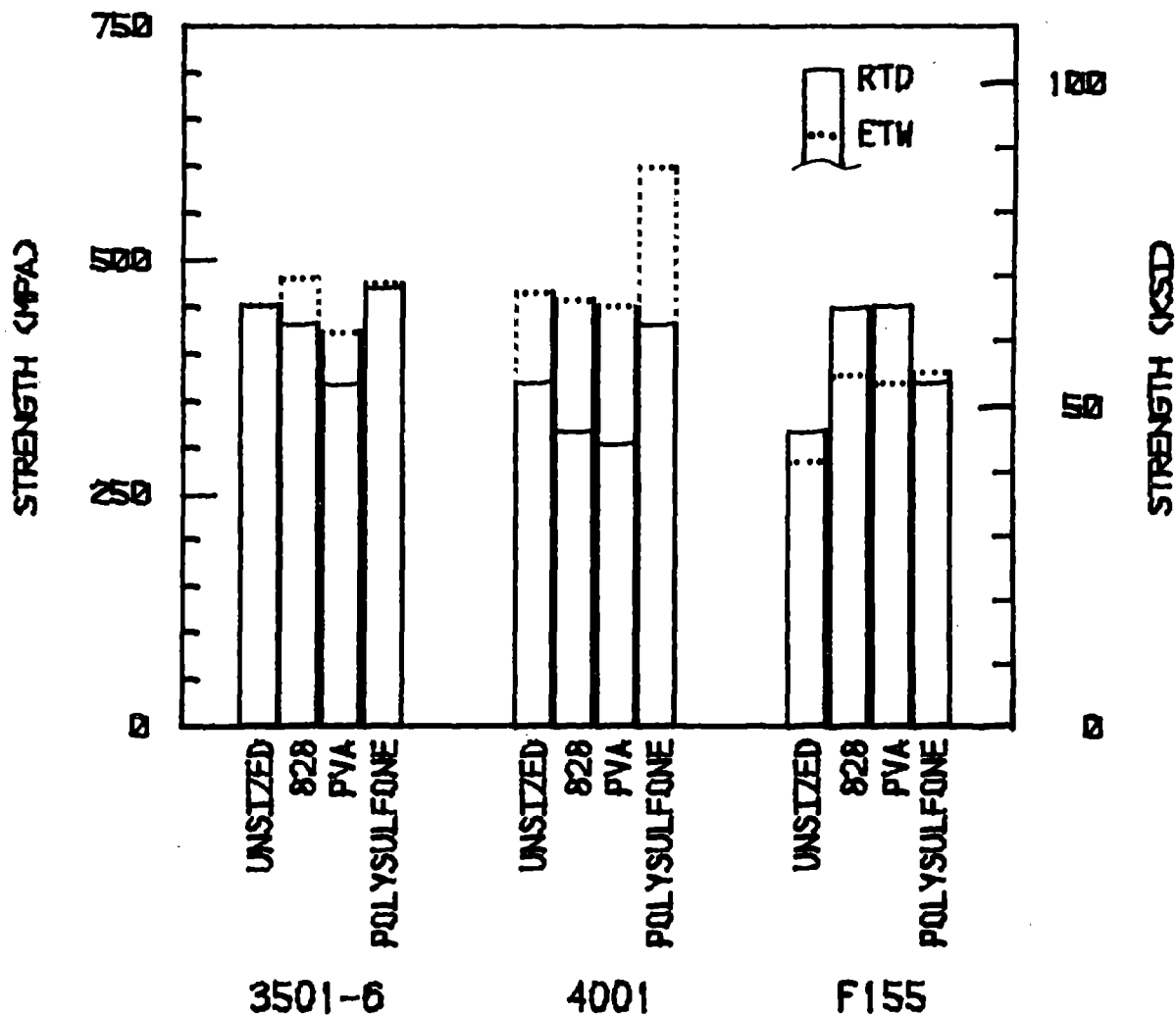


Figure 3. Quasi-Isotropic Laminate Axial Tensile Strengths of the Twelve Fiber Sizing/Matrix Combinations.

## AVERAGE LAMINATE COMPRESSIVE STRENGTHS

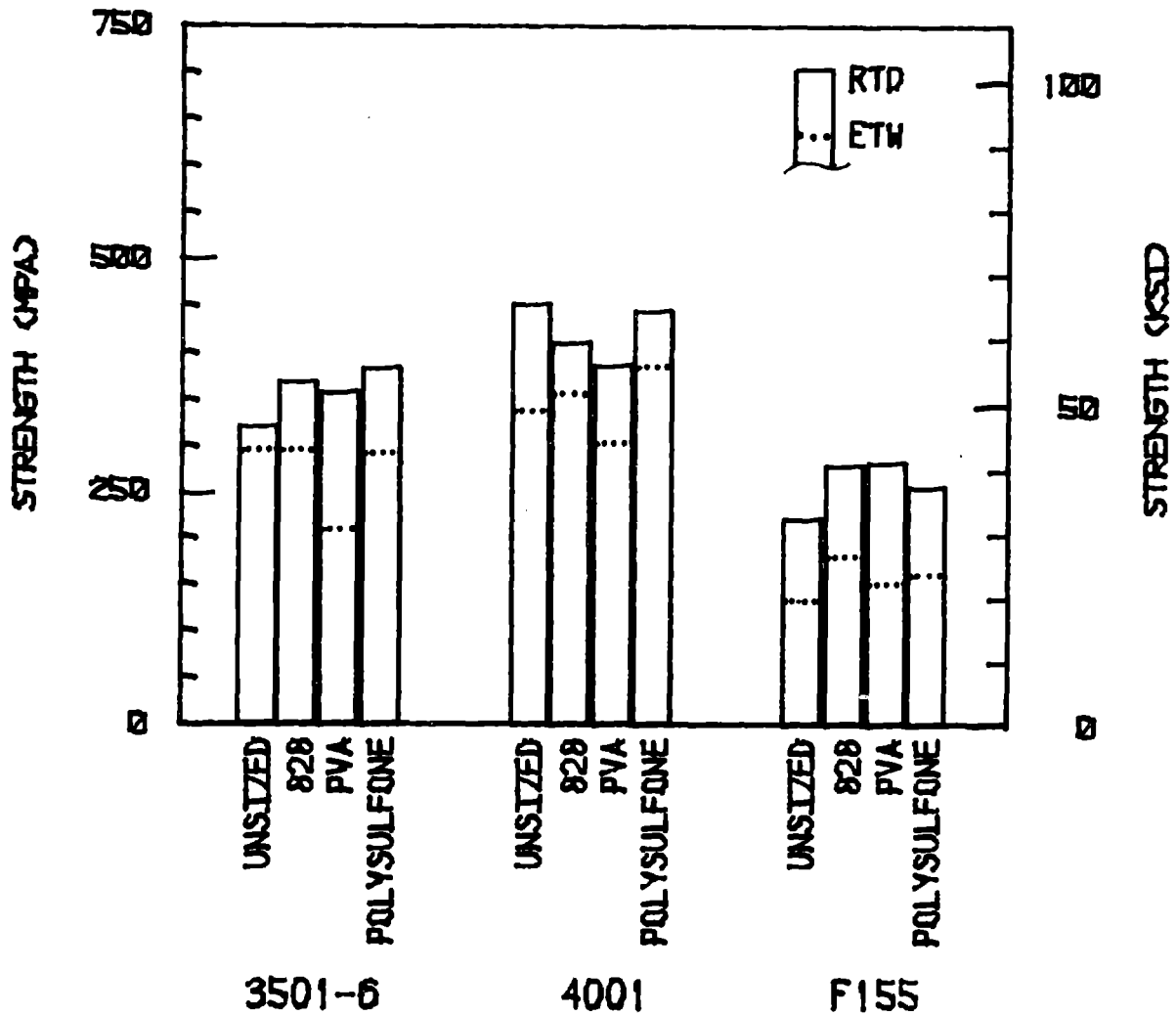


Figure 4. Quasi-Isotropic Laminate Axial Compressive Strengths of the Twelve Fiber Sizing/Matrix Combinations.



ORIGINAL PAGE IS  
OF POOR QUALITY

### AVERAGE LAMINATE FLEXURAL STRENGTHS

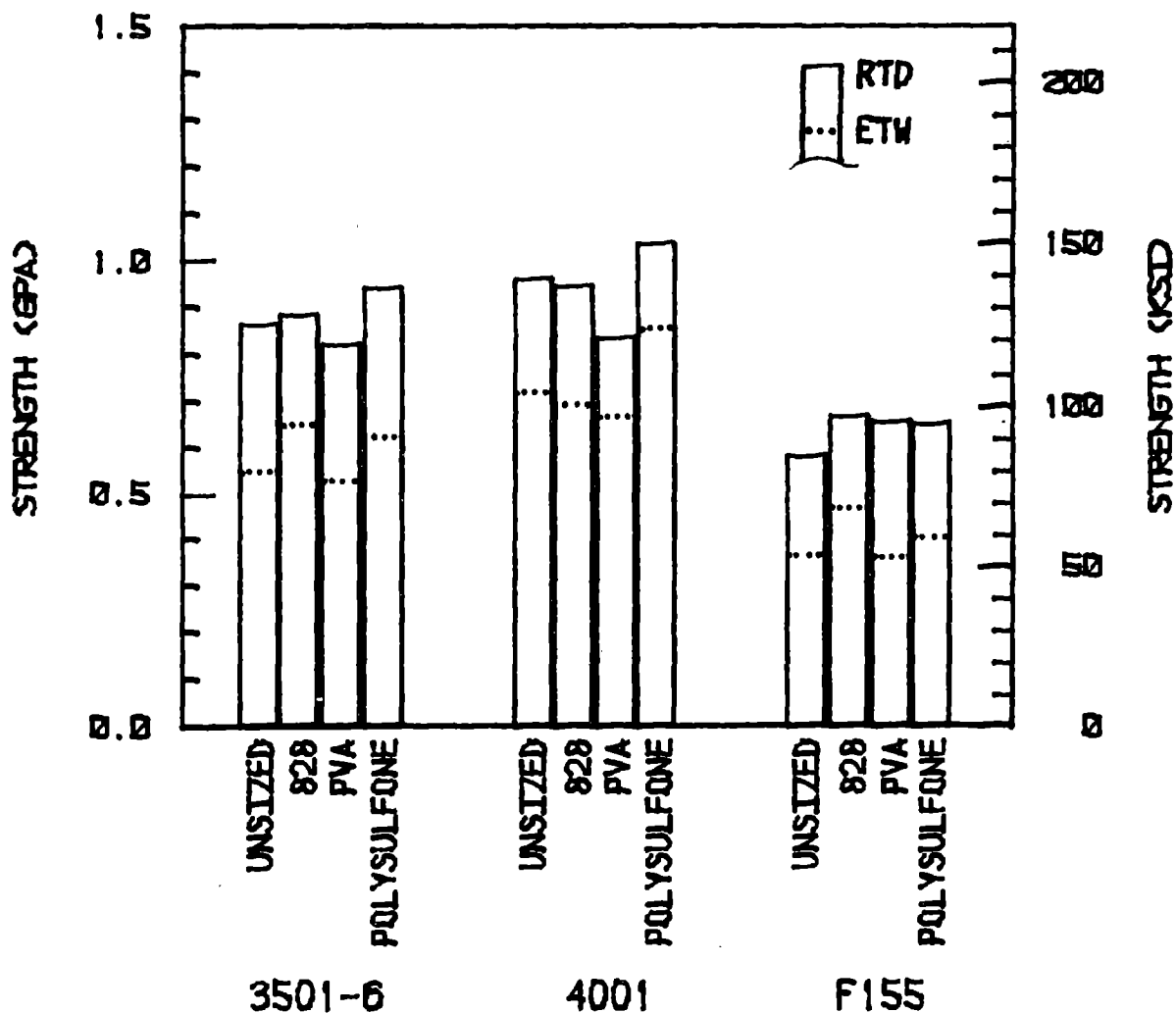


Figure 5. Quasi-Isotropic Laminate Flexural Strengths of the Twelve Fiber Sizing/Matrix Combinations.

## AVERAGE INTERLAMINAR SHEAR STRENGTHS

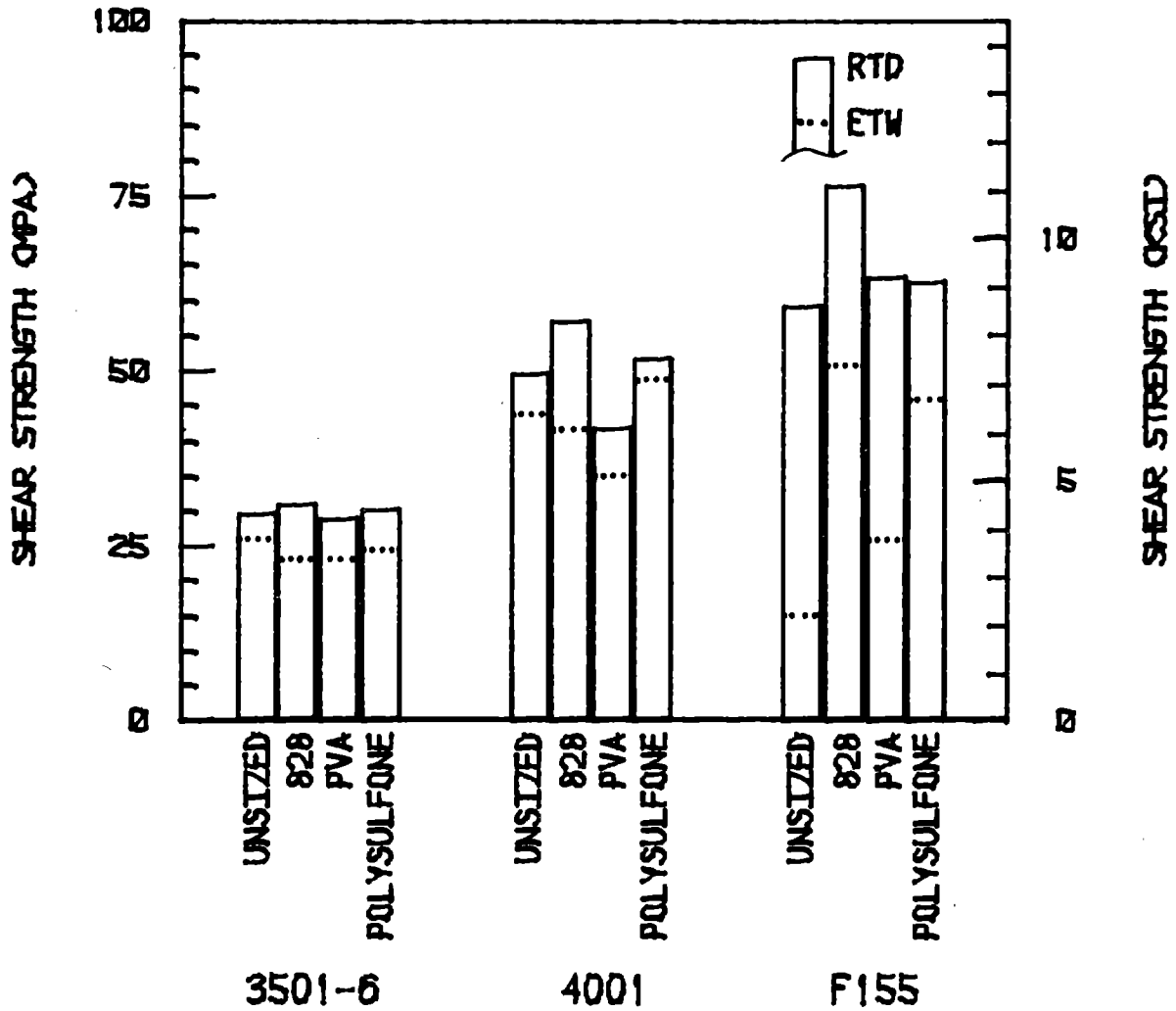


Figure 6. Quasi-Isotropic Laminate Interlaminar Shear Strengths of the Twelve Fiber Sizing/Matrix Combinations.

## AVERAGE TENSILE IMPACT ENERGIES

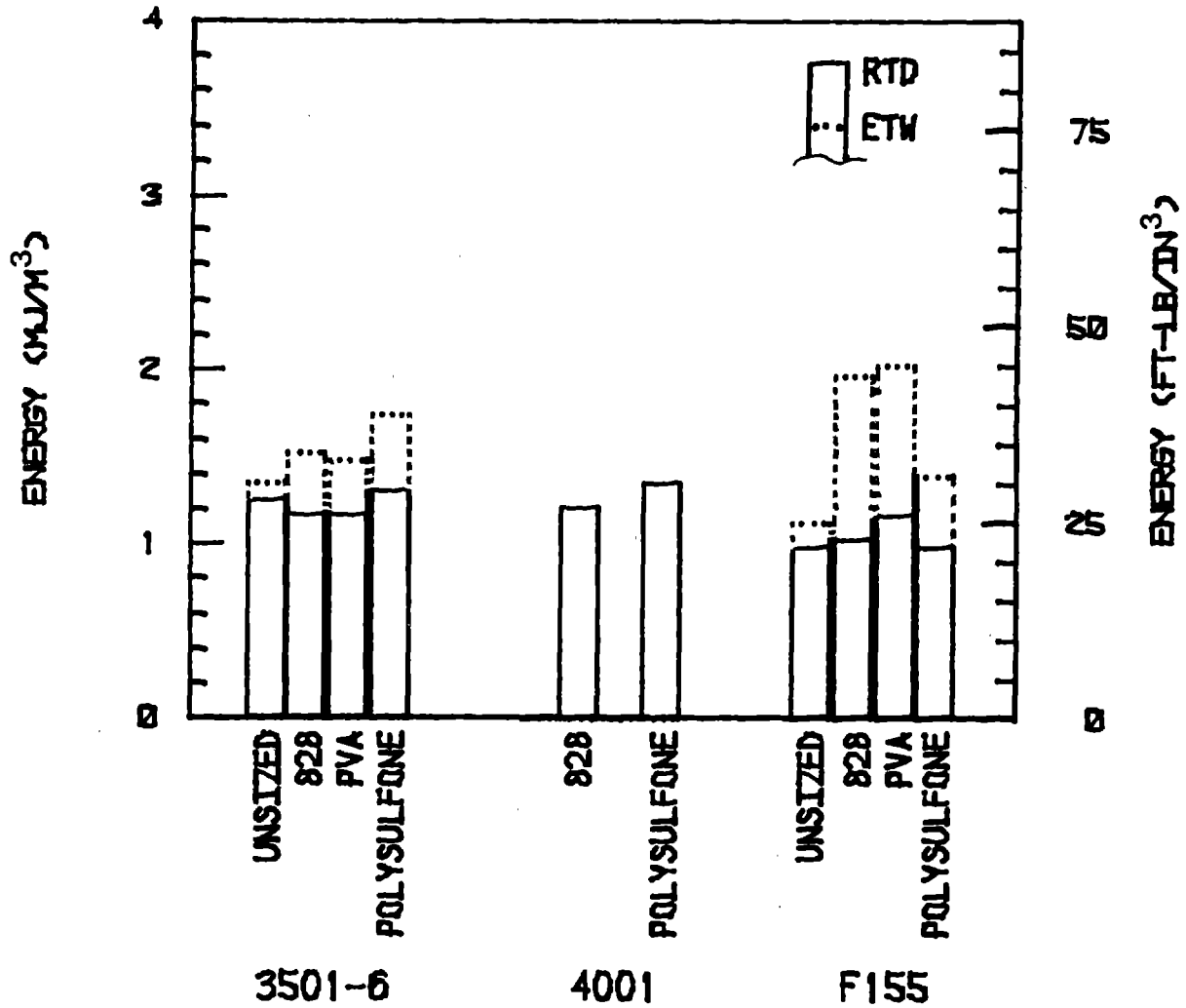


Figure 7. Quasi-Isotropic Laminate Tensile Impact Energies of the Ten Fiber Sizing/Matrix Combinations Successfully Tested.

# AVERAGE SINGLE FIBER PULLOUT STRENGTHS

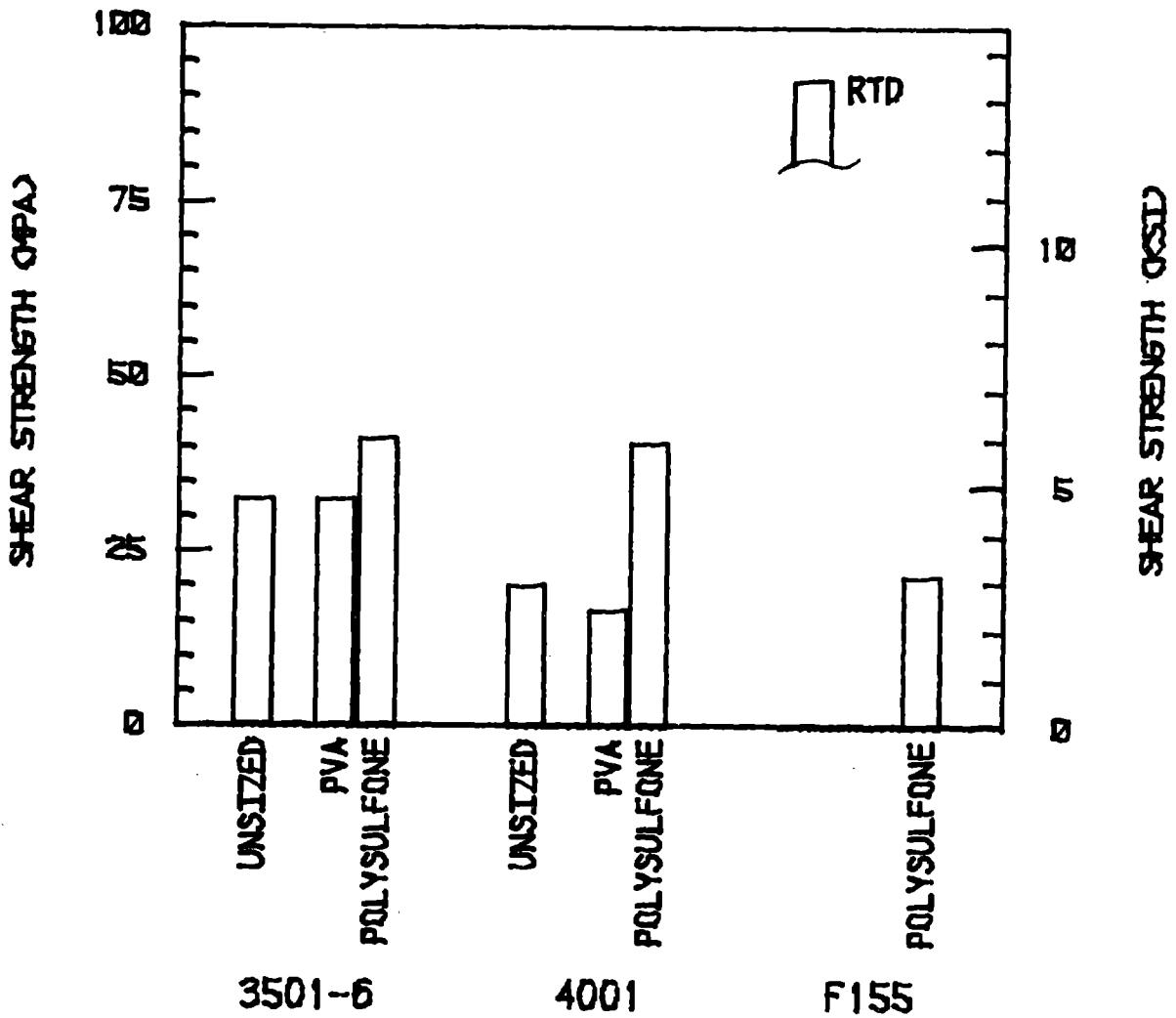


Figure 8. Single Fiber Pullout Shear Strengths of the Seven Fiber Sizing/Matrix Combinations Successfully Tested.

and three-dimensional bar chart plots, are presented in Section 4. Included there also are modulus and strain to failure data as appropriate.

Figure 1 is a plot of the unidirectional composite transverse tensile strengths of the 12 fiber sizing/matrix combinations, at both the room temperature, dry (RTD) and elevated temperature, wet (ETW) test conditions. The wet condition was an approximately one percent moisture weight gain in the composite in all cases. Since the graphite fibers do not absorb this moisture, this one percent weight gain of the composite corresponds to two to three percent moisture weight gain in the matrix itself, the exact value depending on the actual fiber volume of the particular composite. Individual composite fiber volumes and matrix neat (unreinforced) resin moisture saturation levels are tabulated in Section 4. The elevated test temperature was selected as 93°C (200°F) for the AS4/3501-6 and AS4/4001 composites, and 38°C (100°F) for the AS4/F155 composites. The Hercules 3501-6 epoxy is a 177°C (350°F) cure temperature matrix material, and Hercules 4001 bismaleimide is a 204°C (400°F) postcure matrix, while Hexcel F155 rubber-toughened epoxy is a 120°C (250°F) cure temperature matrix. Thus, all composites incorporating the Hexcel F155 matrix were tested at the lower elevated temperature, to permit ETW comparisons on a somewhat equivalent basis between systems.

As indicated in Figure 1, the transverse tensile strengths of the AS4/3501-6 unidirectional composites, for all four fiber sizings, were clearly lower than the strengths of the other two matrix composites, particularly at the RTD test condition. This is not

surprising in that the Hercules 3501-6 is a relatively low strain to failure epoxy, and thus so is the composite. That the fiber sizing expected to provide the poorest interface bond, viz, the PVA sizing, resulted in the highest composite transverse tensile strength is also not totally unexpected. The slightly poorer bond allows local fiber-matrix debonding (microcracking) in local regions of high stress concentrations in this brittle matrix, thus providing some stress relief. These aspects are discussed in detail in Section 6, in relation to the experimental/analytical correlation micromechanics results. The transverse tensile strength results for the other two composite systems also indicate significant differences between the different fiber sizings. In particular, the polysulfone sizing produced high RTD strength values, and the PVA sizing lower values, as expected. At the ETW condition, however, the polysulfone-sized AS4/4001 composite strength was not retained.

Figure 2 is a plot of the unidirectional composite axial compressive strength averages. At room temperature, the axial compressive strengths of the AS4/F155 composites were clearly lower than those of the other two composite systems. As discussed in greater detail in Section 4, this was due to a combination of lower fiber volumes and a lower matrix modulus. Axial compressive strength being a fiber-dominated property, a lower fiber volume would be expected to result in a lower composite strength. Also, since the matrix laterally supports the individual fibers against microbuckling, a lower modulus matrix can be expected to lead to lower composite axial compressive strength. These same trends were maintained at the ETW condition. It will be noted in Figure 2,

however, that there was no clear influence of fiber sizing. That is, axial compression of a unidirectional composite does not appear to be a good discriminator of fiber-matrix interface bond strength.

Axial tensile strengths of the quasi-isotropic laminates are summarized in Figure 3. There was no clear trend in the results, although it will be noted that the AS4/4001 strengths were actually significantly higher at the ETW condition than at room temperature. Likewise, the AS4/3501-6 composites at least maintained their RTD strengths. The strengths of the AS4/F155 composites did tend to be lower, however. These trends are associated with the reduction of the curing residual stresses at the higher temperatures combined with the generally beneficial effects of moisture swelling in offsetting the cooldown-induced thermal contraction stresses, as discussed in Section 6.

The quasi-isotropic laminate axial compressive strengths plotted in Figure 4 tended to follow the same trends as the unidirectional composite axial compressive strengths (Figure 2). That is, while there was no strong influence of fiber sizing, the AS4/4001 composites were clearly stronger than the AS4/3501-6 composites at both test conditions. The fiber volumes of these two types of laminates were similar. On the other hand, the fiber volumes of the AS4/F155 laminates were lower, accounting for the lower strengths of these composite systems. As for unidirectional composite axial compression, laminate axial compression is not a sensitive indicator of interface bond strength.

Quasi-isotropic laminate, three-point flexural strengths are plotted in Figure 5. As expected, the trends follow those of the

axial compression tests (Figure 4). The laminate axial tensile strengths of graphite/epoxy composites tend to be higher than the axial compressive strengths (for example, compare Figures 3 and 4). Thus, in a flexural test, the laminate tends to fail on the compression side, i.e., the compressive strength dictates failure.

No unidirectional composite shear tests were specified by NASA-Ames. This test might have been a relatively sensitive indicator of interface performance. Short beam shear tests of the quasi-isotropic laminates were called for, however. While not expected to be as sensitive an indicator as a unidirectional composite shear test, it was hoped that it would be adequate. The short beam shear strength results are summarized in Figure 6. At room temperature there was not a strong influence of fiber sizing. The EPON 828 and polysulfone sizings performed well, but were not exceptional. As might be expected, the high strain-to-failure Hexcel F155 rubber-toughened epoxy produced the highest interlaminar shear strengths. However, at the ETW condition, the unsized and PVA-sized AS4/F155 laminate shear strengths were severely degraded. This presumably was due to interface bond degradation by the absorbed moisture. On the other hand, the other two, higher cure temperature, matrix materials exhibited shear strength reductions uniformly, somewhat independent of fiber sizing.

As discussed in Section 4, the quasi-isotropic laminate tensile impact tests were only successful for some of the fiber sizing/matrix combinations. Specifically, the AS4/4001 laminates tended to delaminate, resulting in questionable results. Thus, the tensile impact total energy absorption plots of Figure 7 do not include these



data, except for the RTD tests of the EPON 828 and polysulfone-sized AS4/4001 laminates. Like the static tensile tests (Figure 3), the tensile impact tests did not indicate strong influences of the different fiber sizings. The AS4/F155 laminates did perform about as well as the AS4/3501-6 laminates at room temperature, in spite of lower fiber volumes, presumably because of the offsetting favorable influence of high matrix strain to failure as an energy absorption mechanism. The impact energy absorptions of the 120°C (250°F) cure temperature Hexcel F155 matrix laminates tended to increase more at the ETW test conditions than did the higher cure temperature Hercules 3501-6 epoxy matrix laminates. This reflects the greater moisture sensitivity of the Hexcel F155 epoxy matrix. (It will be recalled that the test temperature used was lower, to compensate for the lower cure temperature, but the amounts of absorbed moisture were the same.) Considering the greater complexity of the tensile impact test method relative to the simple static short beam shear test, it is not an attractive screening test.

Single fiber pullout test results are plotted in Figure 8. As discussed in Section 4, the EPON 828-sized fibers were not tested successfully. The matrix films could not be made thin enough to cause the fibers to pull out rather than fail in tension. Thus, no EPON 828 results are presented in Figure 8. The implication is that the interface bond strengths produced by this fiber sizing were higher than those produced by the other three. Of course the unidirectional and quasi-isotropic laminate data presented in the previous seven figures do not seem to support this conclusion. It will also be noted in Figure 8 that only the polysulfone-sized fibers

were successfully pulled out of the Hexcel F155 matrix. For the other two matrix materials, the polysulfone-sized fibers resulted in the highest pullout shear strengths. Thus, it would have been expected that this sizing would have been the most difficult to work with, rather than be the only one successfully utilized.

As will be noted in Figure 8, the calculated interface shear strengths in all cases were relatively low compared to typical unidirectional composite shear strengths. This has been observed by other investigators as well, as discussed in Section 4.6 in detail. That is, while the single fiber pullout test is interesting, it does not adequately simulate an actual multifiber, high fiber volume composite. Stress concentrations induced where the fiber exits the matrix film at each surface undoubtedly reduce the pullout force, and hence, the calculated shear strength. Thus, considering the difficulties involved in performing the single fiber pullout test, it is concluded that it is not a practical interfacial bond screening test.

In addition to the unidirectional and laminated composite mechanical properties tests summarized in Figures 1 through 8 above, uniaxial tensile, Iosipescu shear, thermal expansion and moisture expansion tests were performed on the neat (unreinforced) Hercules 4001 bismaleimide and Hexcel F155 rubber-toughened epoxy matrix materials. Test results were already available from a prior study for the Hercules 3501-6 epoxy, these data being included here in Section 4.2 also, for completeness.

These neat resin matrix properties were needed as input to the finite element micromechanics analysis utilized in Section 6, in

making predictions of the influence of matrix type and fiber sizing on unidirectional composite transverse tensile properties. These analytical predictions were then correlated with the corresponding experimental data generated here.

The correlations presented in Section 6 indicate that the University of Wyoming's WYO2D finite element micromechanics analysis is fully capable of predicting unidirectional composite response, including the influence of a degraded interface. Thus, it is likely to become an extremely valuable tool in future experimental studies, in identifying the proper tests, and testing conditions, to be utilized.

In summary, the present study has provided a large quantity of experimental data, generated under carefully controlled conditions. One group of experienced researchers made all of the required prepreg, fabricated the composites and the neat resin specimens, conducted all of the testing, did the scanning electron microscopy, and performed the finite element analyses. Thus, the data presented in this report are believed to be accurate and reliable. Experimental procedures and interpretations of results are presented in detail in the following sections.



## SECTION 2

### INTRODUCTION

The influence of the fiber-matrix interface bond on the performance of the composite has been a topic of research by the Composite Materials Research Group (CMRG) at the University of Wyoming for some time. Thermal and moisture effects on the mechanical properties of composite material have also been of foremost interest in the numerous prior programs undertaken involving graphite fibers and a variety of polymer matrix systems.

Initially, a program to study four polymer matrices and a graphite fiber with three different surface treatments was proposed to NASA-Ames. Due to the unavailability of PEEK thermoplastic [1], a fourth surface treatment was added to the program, thus maintaining the twelve combinations of polymer matrices and fiber treatments. Hercules AS4 graphite fiber [2] was obtained from Hercules Aerospace and NASA-Langley Research Center with the four required surface treatments. Hercules AS4 high strength graphite fiber was chosen because of its general availability and extensive current usage within the aerospace industry. The Hercules AS4 fiber in 12,000 filament tow form was acquired with three different sizings, viz, EPON 828 epoxy [3], polyvinylalcohol (PVA), Ultem P1700 polysulfone [4], and unsized. Three polymer resins were acquired, viz, Hercules 3501-6, a standard epoxy matrix [5] selected as the baseline material, Hercules 4001, a bismaleimide [6], and Hexcel F155, a

19 16

Preceding Page Blank

BLANK

rubber-toughened epoxy [7].

The twelve combinations were prepregged, and fabricated into unidirectional and quasi-isotropic plates, being cured according to manufacturer's specifications. Specimens were machined from these plates for mechanical property measurements, to provide comparisons of performance between the four fiber surface treatments of the Hercules AS4 graphite fiber when combined with each of the three polymer matrices.

Testing was performed at two conditions, viz, room temperature, dry, (RTD), and elevated temperature, wet, (ETW), wet defining a one percent moisture weight gain condition. Tests performed included transverse tension and axial compression of the unidirectional composites, axial tension, axial compression, flexure, interlaminar shear, and tensile impact of the quasi-isotropic laminates, and single fiber pullout testing. Fracture surfaces were examined using a scanning electron microscope (SEM) to evaluate the fiber-matrix interface.

The Composite Materials Research Group's finite element micromechanics analysis and associated WYO2D computer program was used to predict unidirectional composite properties, and to infer the interface strengths resulting from the different fiber surface treatments combined with the various matrix materials. Conclusions were thus arrived at as to the most efficient method of fiber surface treatment associated with the three different types of resin systems.

## SECTION 3

### EXPERIMENTAL PROCEDURES

#### 3.1 Test Matrix

A comprehensive series of tests was completed for each of the twelve fiber/matrix combinations and three neat resin systems. Table 1 indicates the specific tests performed, and the test conditions utilized.

The dry test specimens were stored in dessicators until tested, to insure that they remained dry after fabrication. Moisture-conditioned (wet) specimens were suspended above distilled water in closed glass containers maintained at 74°C (165°F) in a Tenney Benchmaster environmental chamber until they had absorbed the one weight percent of moisture desired. This elevated temperature allowed the test specimens to reach the desired moisture level more rapidly than if they had been exposed to moisture at room temperature. Witness specimens were weighed periodically to determine the level of moisture absorption. Specimens were conditioned to one percent moisture weight gain prior to testing.

#### 3.2 Fiber Sizings

All of the AS4 graphite fiber was supplied by Hercules, Inc., Magna, Utah, in the form of 12,000 fiber tow [2]. Hercules provided unsized fiber, fiber sized with Shell EPON 828 epoxy [3], and fiber sized with polyvinylalcohol (PVA). The shipping dates were May, August and December 1983, respectively.

Table 1

## Test Matrix for Each Fiber/Matrix Combination

<u>Loading Mode</u>	Number of Specimens	
	<u>Room Temperature, Dry (RTD)</u>	<u>Elevated Temperature, Wet (ETW)</u>
<u>Quasi-Isotropic Laminate Tests</u>		
Tension	5	5
Compression	5	5
Flexure	5	5
Interlaminar Shear	5	5
Instrumented Tensile Impact	5	5
<u>Fiber-Matrix Interface Tests</u>		
Transverse Tension	10	10
Axial Compression	10	10
Single Fiber Pullout	10	10
<u>Neat Resin Tests</u>		
Uniaxial Tension	5	5
Iosipescu Shear	5	5
Thermal Expansion	3	3
Moisture Expansion	<u>3</u>	<u>3</u>
Subtotals	71	68
Total Specimens/Combination		139

Total specimens for 12 fiber/matrix combinations and neat 3 resin systems; less neat resin tests for Hercules 3501-6 (data already available): 1378



One pound of the unsized AS4 graphite fiber was sent to NASA-Langley to receive a General Electric UDEL P-1700 polysulfone sizing [4]. The solvent used was methylene chloride. The amount of residual sizing after solvent removal was approximately 0.37 percent by weight of the weight of the graphite fiber itself. The shipping date from NASA-Langley was December 1983.

All work as part of the present study, and reported here, was performed using these same batches of fibers.

### 3.3 Preparation of Composite Materials

All twelve combinations of Hercules AS4 graphite fiber with one of four different surface treatments and three different matrix resins were prepregged using one of two techniques. A drum winder batch prepregger previously developed at the University of Wyoming was used to prepare sufficient prepreg for the four Hercules AS4 graphite fiber/Hercules 3501-6 epoxy matrix composite combinations. This technique had been used in prior programs at Wyoming to produce good quality prepreg. Figure 9 is a photograph of this prepreg unit, showing the fiber spool in the lower rear of the apparatus and the heated resin bath on the front. The fiber passes around various rollers, up to the heated resin bath. Internal wipers direct the fiber down into the resin, which is typically heated to approximately 120°C (250°F), where the fiber tow becomes saturated with resin. Between the resin bath and the drum, the impregnated fiber passes through a sequence of wipers to spread out the tow and wipe off excess resin. The drum speed and resin bath transverse speed can be individually adjusted to accurately align the fiber tows in a uniform pattern across the release paper taped to the drum. Once a complete

ORIGINAL PAGE IS  
OF POOR QUALITY

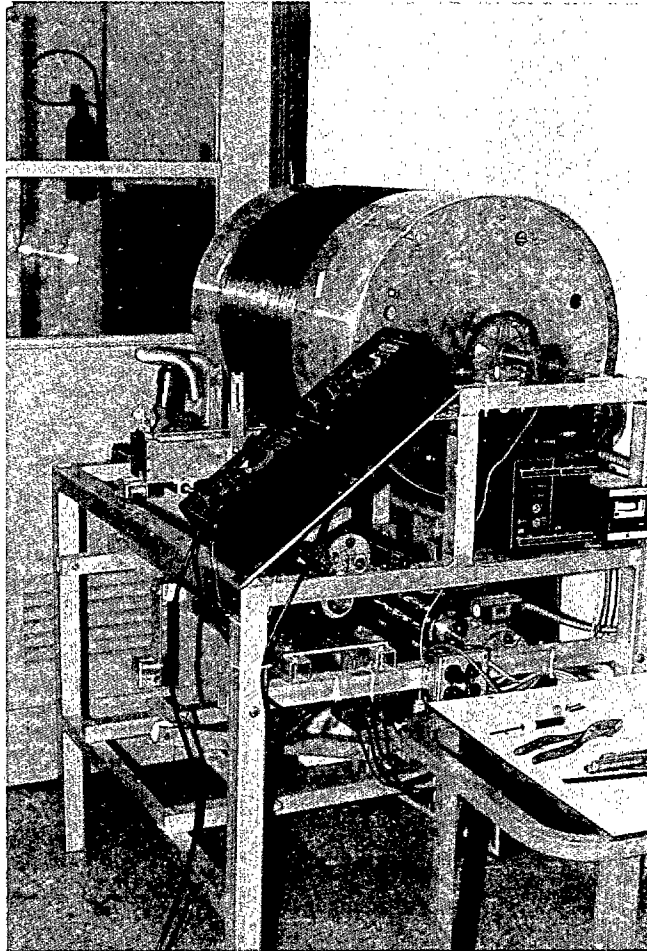


Figure 9. Drum Winder Prepreg Unit Used.

width of prepreg is wound, a second sheet of release paper is placed over the prepreg and the prepreg is removed from the drum, by cutting across it in a groove in the drum. Laid out flat, this produces a piece of prepreg about 180 cm (70 in) long, and of the desired width. For the present study, 36 cm (14 in) wide prepreg was made. This prepreg was then cut into uniform 30.5 cm (12 in) long pieces, stacked up, and placed in moisture-proof plastic bags for storage in a freezer. The bags prevented moisture accumulation while the prepreg was being stored in the freezer.

The Hercules 4001 and Hexcel F155 resins were prepregged using a technique developed as part of the present study for use with highly viscous resins. A thin film of resin was produced using the film prepregger shown in Figure 10. A heated plate melts the hot-melt (solid) resin on top of the release paper, and then the paper is drawn through a flat die arrangement, leaving a uniform layer of resin on the release paper. The Hercules 4001 and Hexcel F155 resins were heated to only 75°C (167°F) in this process, to minimize cure advance and to maintain a consistent viscosity for the film forming. Sufficient resin film was drawn to allow being wrapped completely around the drum of the drum winder prepreg unit previously shown in Figure 9. This resin film backed with release paper was securely taped to the drum, and then the dry AS4 graphite fiber tow was wound onto the film in a manner similar to that used in the normal wet winding process. A second layer of film backed with release paper was then placed over the fiber and resin film already on the drum. This prepreg was removed from the drum, cut into uniform lengths, stacked, placed in plastic bags, and stored in a freezer. As for the

ORIGINAL PAGE IS  
OF POOR QUALITY

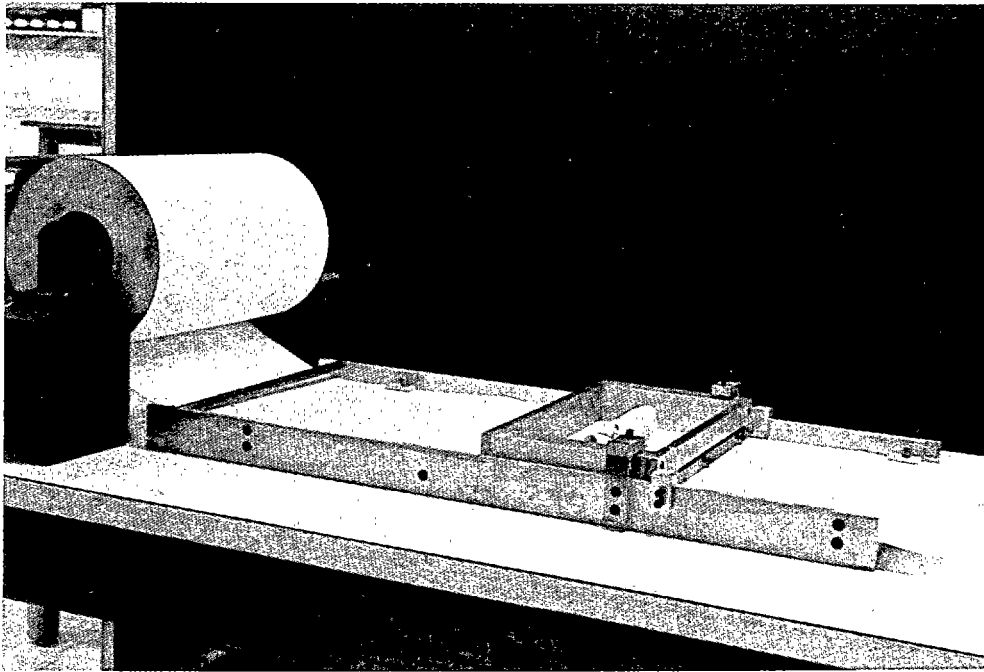


Figure 10. Film Prepregger Unit Used.

Hercules 3501-6 matrix, 36 cm (14 in) wide prepreg was made.

Once enough prepreg was made to lay up a plate, this was done. This minimized storage time for the prepreg. Both eight-ply unidirectional,  $[0]_8$ , and eight-ply quasi-isotropic,  $[\pm 45/0/90]_8$ , plates were laid up for this program. The Hercules 3501-6 and 4001 matrix composite plates were fabricated and cured into 30.5 cm (12 in) long by 30.5 cm (12 in) wide plates. The Hexcel F155 plates were also 30.5 cm (12 in) long, but only 15.2 cm (6 in) wide. The Hexcel F155 matrix composite plates were made smaller to accommodate the platen size of the heated platen cure press used. The Hercules 3501-6 and 4001 matrix composite plates were cured in a blanket press. All three types of composites were cured using the manufacturer's recommended cure schedules as given below:

Hercules 3501-6 Cure Schedule

23°C to 150°C heatup at 3°C/min, at 20 psi pressure

150°C to 177°C heatup at 3°C/min, at 90 psi pressure

Hold for 3 hours at 177°C

Post-cure in an air circulating oven for 4 hours at 177°C

Hercules 4001 Cure Schedule

23°C to 150°C heatup at 3°C/min, at 20 psi pressure

150°C to 177°C heatup at 3°C/min, at 90 psi pressure

Hold for 3 hours at 177°C

Post-cure in an air circulating oven for 4 hours at 177°C,

followed by 8 hours at 204°C

Hexcel F155 Cure Schedule

Heat in full vacuum to 85°C

Hold for 4 hours at 85°C

Heat to 121°C at 20 psi pressure

Hold for 3 hours at 121°C

The 12,000 filament fiber tows used in this program handled fairly well in the prepregging process. The polysulfone-coated fibers had a tendency to stick together and did not spread as evenly in the wet-wind and film-wind processes as the other three types of surface treated fiber tows. The unsized fiber tows produced a large volume of fuzz balls during the wet-wind and film-wind processes, as might be expected. The EPON 828 and PVA treated fibers were easily handled, and produced the best quality prepreg. The wet-wind technique used with the Hercules 3501-6 epoxy, and the film/dry wind technique used with the Hexcel F155 and Hercules 4001 resins, were judged equal in terms of the quality of the prepreg produced, with the film/dry wind process being easier to perform. It was also easier to clean up this apparatus afterward. Both techniques impregnated the fiber tows with sufficient resin, and allowed the uniform distribution of fibers across the release paper, this producing uniform thickness prepregs.

#### 3.4 Composite Test Specimen Preparation

All composite test specimens were machined from cured plates using diamond abrasive tooling. Water cooling was used to prevent overheating of the composites during these operations. A converted machinist's surface grinder was used to machine most of the specimens to final dimensions. Tensile specimens were machined into dogbone shapes using a Tensilkut router.

All finished specimens were clearly marked and stored in plastic bags until used.

The specimens designated for the hot, wet testing were suspended over distilled water in containers kept in a temperature chamber and maintained at 74°C (165°F). Witness specimens were periodically weighed to record the percent weight gain being experienced by the various composite systems. After a moisture weight gain of one percent was measured, these specimens were removed from the temperature chamber, but left in the moisture chambers, until just prior to testing.

The unidirectional composite transverse tensile specimens were nominally 15 cm (6 in) long and 2.5 cm (1 in) wide. Quasi-isotropic laminate tensile specimens were 15 cm (6 in) long by 1.3 cm (0.5 in) wide. Unidirectional and laminated composite axial compression specimens were 10 cm (4 in) long by 1.3 cm (0.5 in) wide. Laminate flexural specimens were 7.6 cm (3 in) long by 2.5 cm (1 in) wide. Short beam (interlaminar) shear specimens were 1.5 cm (0.6 in) long by 1.3 cm (0.5 in) wide. Instrumented tensile impact specimens were 18 cm (7 in) long by 1.3 cm (0.5 in) wide.

Only the tensile impact specimens required tabbing prior to testing. Glass/epoxy tabs, 5.1 cm (2 in) long, were bonded onto these specimens using a Techkits A-12 two-part epoxy adhesive [8]. This tabbing adhesive has been used at the University of Wyoming for a number of years, with excellent results. Single-axis strain gages were bonded onto one surface of the tensile impact specimens (using a standard strain gage adhesive), to allow for dynamic strain measurement.

Strain gage extensometers were used on the static tension and compression specimens to measure strains.

### 3.5 Neat Resin Test Specimen Preparation

Unreinforced (neat) resin testing was performed on the Hexcel F155 rubber-toughened epoxy and the Hercules 4001 bismaleimide, to determine the matrix properties required as input to the finite element micromechanics computer program. Uniaxial tensile and Iosipescu shear properties as a function of temperature and moisture content were measured for these two resin systems. The Hercules 3501-6 matrix material properties did not have to be measured in this program since they had been evaluated in previous programs [9,10].

#### 3.5.1 Tensile Test Specimens

Both the Hexcel F155 and Hercules 4001 resin systems were fabricated into tensile test specimens using the well documented procedures developed during prior programs for NASA-Langley [11,12] and the Naval Air Development Center [13].

Tensile specimens were 15.2 cm (6.0 in) long, 1.27 cm (0.5 in) wide, and 0.25 cm (0.1 in) thick. A Tensilkut router tool was used to machine the rectangular resin pieces into the dogbone shape required for tensile testing. A gage section 7.6 cm (3.0 in) long and 0.51 cm (0.2 in) wide was used for all tension testing in this program. Two extensometers were attached to each specimen, to permit the measurement of both axial and transverse strains during each tensile test.

#### 3.5.2 Iosipescu Shear Test Specimens

Iosipescu shear test specimens were 7.6 cm (3.0 in) long by 1.3 cm (0.5 in) wide by 0.25 cm (0.1 in) thick. The standard 90° notch was machined into both edges of the test specimen using an abrasive grinding wheel. A dual-element +45 degree strain gage rosette was



then bonded to one surface of each specimen to allow for the measurement of shear strain. The Iosipescu shear test had been used previously in a large number of test programs at Wyoming, with excellent results [14-17]. It is presently also being considered by Committee D-30 of ASTM for inclusion as an ASTM Standard Test Method.

### 3.5.3 Coefficient of Thermal Expansion Tests

Coefficient of thermal expansion (CTE) testing was performed on the Hercules 4001 and Hexcel F155 neat resins using a computer-controlled quartz tube dilatometer test apparatus [18,19]. Figure 11 is a photograph of the test set up. Typically, three identical specimens were tested, each specimen being subjected to three temperature excursions from  $-40^{\circ}\text{C}$  ( $-40^{\circ}\text{F}$ ) to  $120^{\circ}\text{C}$  ( $250^{\circ}\text{F}$ ) for the Hercules 3501-6 and 4001, and up to  $66^{\circ}\text{C}$  ( $150^{\circ}\text{F}$ ) for the Hexcel F155 neat resin. The heating rate was  $1.7^{\circ}\text{C}/\text{min}$  ( $3^{\circ}\text{F}/\text{min}$ ). The specimens were 12.7 cm (5.0 in) long, 0.95 cm (0.38 in) wide, and 0.25 cm (0.10 in) thick.

### 3.5.4 Coefficient of Moisture Expansion Tests

Coefficients of moisture expansion (CME) were measured for the Hercules 4001 and Hexcel F155 neat resins using a special quartz tube dilatometer test apparatus previously developed at the University of Wyoming [18,19]. Figure 12 is a photograph of the CME test setup. Two very thin, i.e., 0.90 mm (0.035 in) thick, 70 mm (2.75 in) square plates of the material to be tested were placed in a closed temperature/humidity chamber maintained at  $66^{\circ}\text{C}$  ( $150^{\circ}\text{F}$ ) and 98 percent relative humidity. One specimen was suspended from an electronic analytical balance while the other identical specimen was placed in a quartz tube dilatometer apparatus. The weight gain due

ORIGINAL PAGE IS  
OF POOR QUALITY

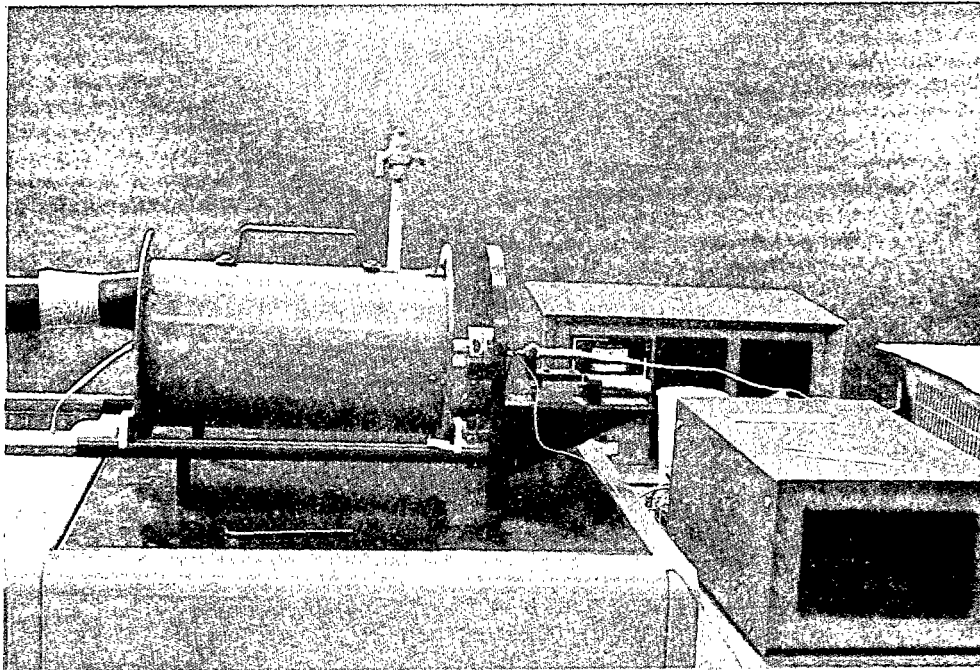


Figure 11. Coefficient of Thermal Expansion Apparatus.

ORIGINAL PAGE IS  
OF POOR QUALITY

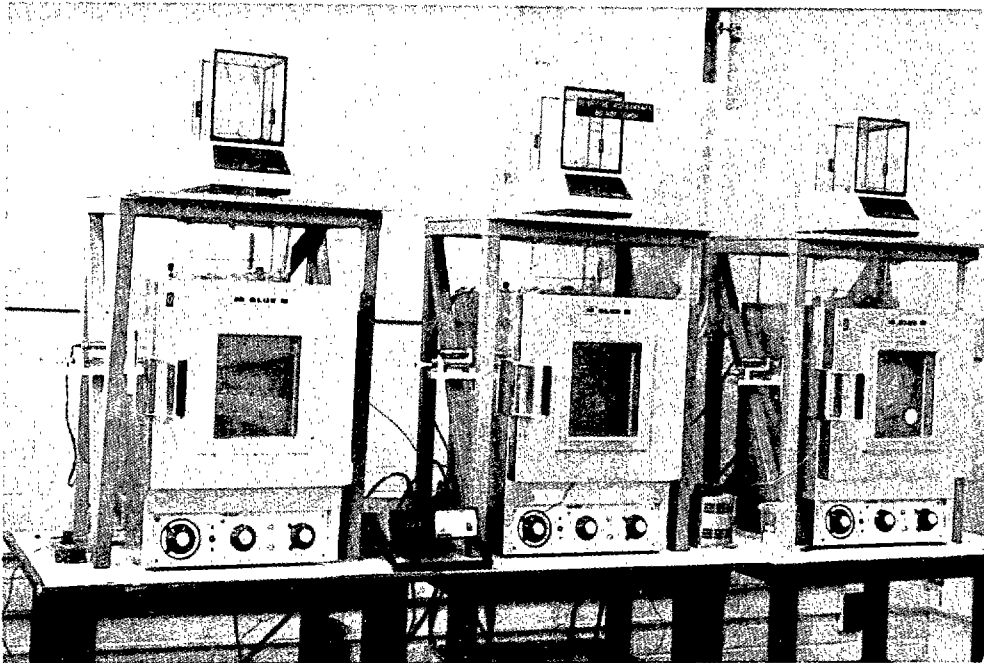


Figure 12. Coefficient of Moisture Expansion Apparatus.

to moisture absorption and the corresponding expansion are recorded concurrently for the two specimens, and input to the equipment's computer program to calculate the coefficient of moisture expansion (CME) directly.

Typically, three pairs of specimens of each material were tested to obtain an average value. Because of the slow rate of moisture diffusion even at 66°C (150°F), a typical test required 7 to 10 days to complete.

### 3.6 Testing Equipment

All static testing was performed using an Instron Model 1125 electromechanical test machine coupled to a Hewlett-Packard Model HP 21MX-E minicomputer for control and data acquisition. Data were reduced on the Hewlett-Packard 21MX-E computer and then read to a data tape for later transfer to the University of Wyoming's CDC CYBER 760 mainframe computer. All plotting and further data reduction was accomplished on the CYBER 760 computer. Additional plotting of average test results was done on the Department of Mechanical Engineering's PRIME 550 computer, coupled to a Hewlett-Packard Model 7550 digital plotter. Data handling involved very large quantities of information, but this was managed relatively efficiently using magnetic tapes for data transfer.

Tensile impact testing was performed using a modified Satec Model SI-1D pendulum-type impact testing machine incorporating special wedge-type tensile grips and a load cell to accommodate the tensile impact specimens [20,21]. A single-element strain gage was bonded to each test specimen to monitor strain, and a piezoelectric load ring was used to measure load. Data were acquired using a

Nicolet Explorer III Model 206-2 digital oscilloscope, and then transferred to the HP 21MX-E minicomputer for subsequent reduction and plotting.

A Bemco FTU 3.8 environmental chamber was used in the Instron Model 1125 testing machine to perform the elevated temperature testing. A hot air gun and thermocouple arrangement was used with the Satec impact testing machine to perform the elevated temperature instrumented impact testing.

### 3.6.1 Unidirectional Composite Transverse Tension

Transverse tension testing was performed using an Instron strain gage extensometer to measure axial strain for each specimen. Complete stress-strain curves were recorded for each test, which allowed for the calculation of Young's modulus,  $E$ , ultimate strength,  $\sigma_u$ , and ultimate strain,  $\epsilon_u$ .

### 3.6.2 Laminate Axial Tension

Quasi-isotropic, i.e.,  $[\pm 45/0/90]_s$ , specimens were tested in axial tension using a strain gage extensometer on each specimen to measure axial strain and thus permit the calculation of composite modulus, and the recording of a complete stress-strain curve for each specimen.

### 3.6.3 Unidirectional Composite Axial Compression

An end-loaded, side-supported test fixture (shown in Figure 13) was used for all axial compression testing. This test method had been used in several previous testing programs [22,23] producing very consistent results. Two sets of steel blocks clamp on each end of a flat rectangular specimen, providing rigid support at each end. Two polished steel guide rods maintain alignment of the two fixture

ORIGINAL PAGE IS  
OF POOR QUALITY

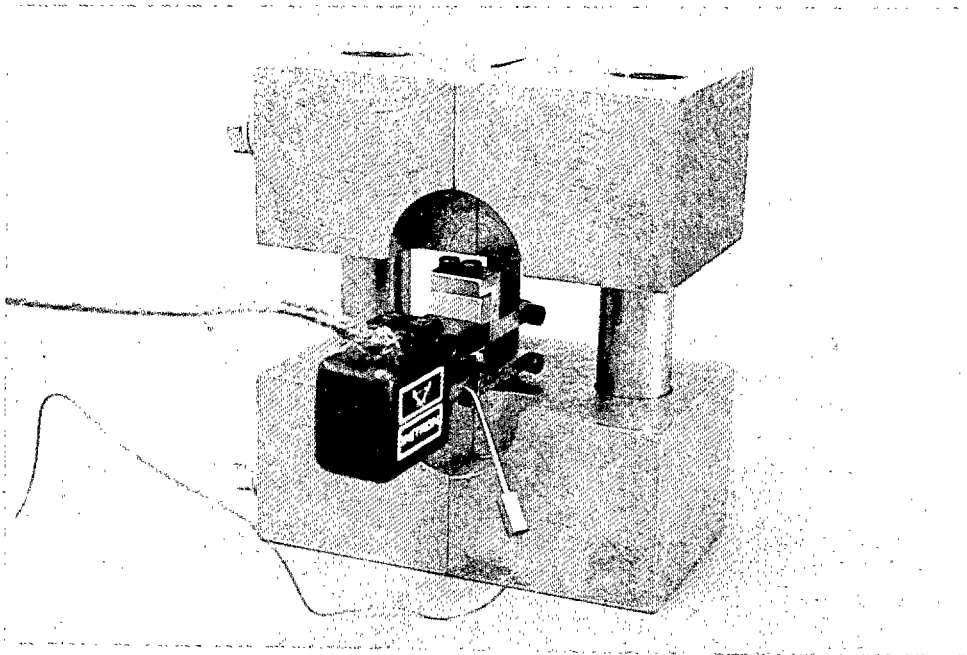


Figure 13. . End Loaded, Side Supported Compression Test Fixture.

halves. An extensometer is attached in the short gage section of the specimen to measure strain. The specimen is loaded in compression between two flat platens, with the steel fixture taking the majority of the direct loading, transferring it into the specimen along its length. Failure almost always occurs in the gage section, with failure at the specimen ends (crushing or brooming), occurring very infrequently.

#### 3.6.4 Laminate Axial Compression

Quasi-isotropic laminates, i.e., [+45/0/90]<sub>s</sub>, were also tested in axial compression, using the same end-loaded, side-supported test configuration used in the axial compressive testing of unidirectional composites, as described in Section 3.6.3.

#### 3.6.5 Laminate Flexure

Quasi-isotropic laminates, i.e., [+45/0/90]<sub>s</sub>, were tested in flexure to determine the flexure strength and modulus. A standard three-point bend flexure setup shown in Figure 14 was used for all of the flexural testing. Test specimens 25 mm (1.0 in) wide, 76 mm (3.0 in) long, and 2.3 mm (0.09 in) thick were used for this testing. Crosshead movement was monitored to allow the calculation of the flexural moduli.

#### 3.6.6 Laminate Interlaminar Shear

Quasi-isotropic laminates, i.e., [+45/0/90]<sub>s</sub>, were tested to determine their interlaminar shear strength, following ASTM Standard STD D2344-76. Test specimens 15 mm (0.6 in) long, 13 mm (0.5 in) wide, and 2.3 mm (0.09 in) thick were used for all short beam shear testing. Load was monitored for each test specimen, allowing the calculation of shear strength.

ORIGINAL PAGE IS  
OF POOR QUALITY

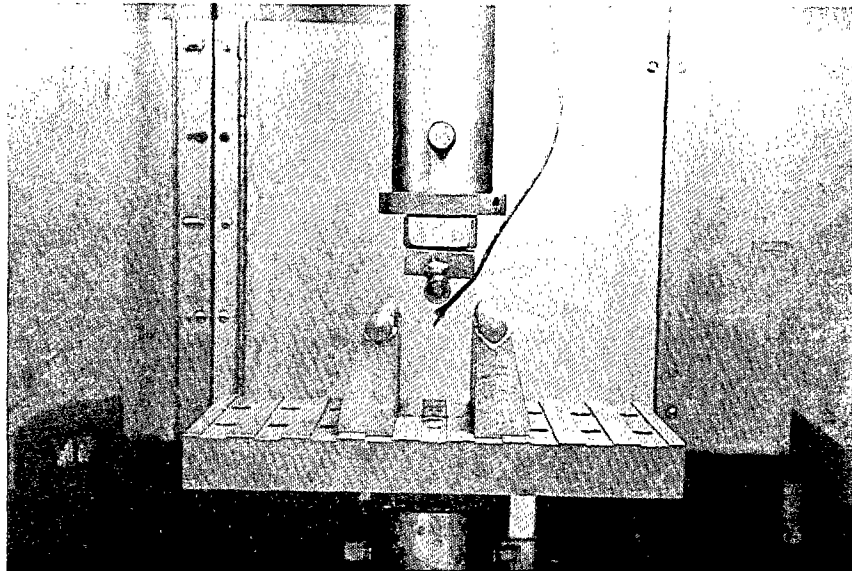


Figure 14. Three-Point Loading Flexure Fixture.



### 3.6.7 Neat Resin Properties

Neat resin specimens of the Hexcel F155 and Hercules 4001 matrix material systems were fabricated using the same types of steel molds used in many previous programs at Wyoming [11-13,18,19]. Both uniaxial tensile and Iosipescu shear specimens were fabricated to characterize these two resins. The Hercules 3501-6 epoxy had already been characterized in previous programs [9,10] and thus was not tested in this program.

### 3.6.8 Single Fiber Pullout

Single fiber pullout tests were conducted to evaluate the interfacial bond between the AS4 graphite fiber, with the four different surface treatments, and the three matrix resins. Unsized fibers, and fibers treated with EPON 828 epoxy, polyvinylalcohol (PVA), or polysulfone (Udell P1700) thermoplastic, were used in combination with the Hercules 3501-6 epoxy, the Hercules 4001 bismaleimide, and the Hexcel F155 rubber-toughened epoxy.

The method used by Penn and Bowler [24] was adopted for this study. A single fiber was separated from the 12,000 filament tow and bonded onto a C-shaped metal tab using Techkits A-12 epoxy [8]. A small piece of masking tape was used to hold the fiber in place until the epoxy hardened. The tabs with the attached fibers were hung on a metal crossbar, as shown in Figure 15. The fibers were then threaded through individual 2.5 mm (0.1 in) holes in 0.025 mm (0.001 in) thick stainless steel shim stock. A small piece of masking tape was then attached the lower edge of each fiber, as a weight to ensure that the fibers hung straight down through each hole. Frozen resin was then pulverized into small granules and enough placed in each hole to

ORIGINAL PAGE IS  
OF POOR QUALITY

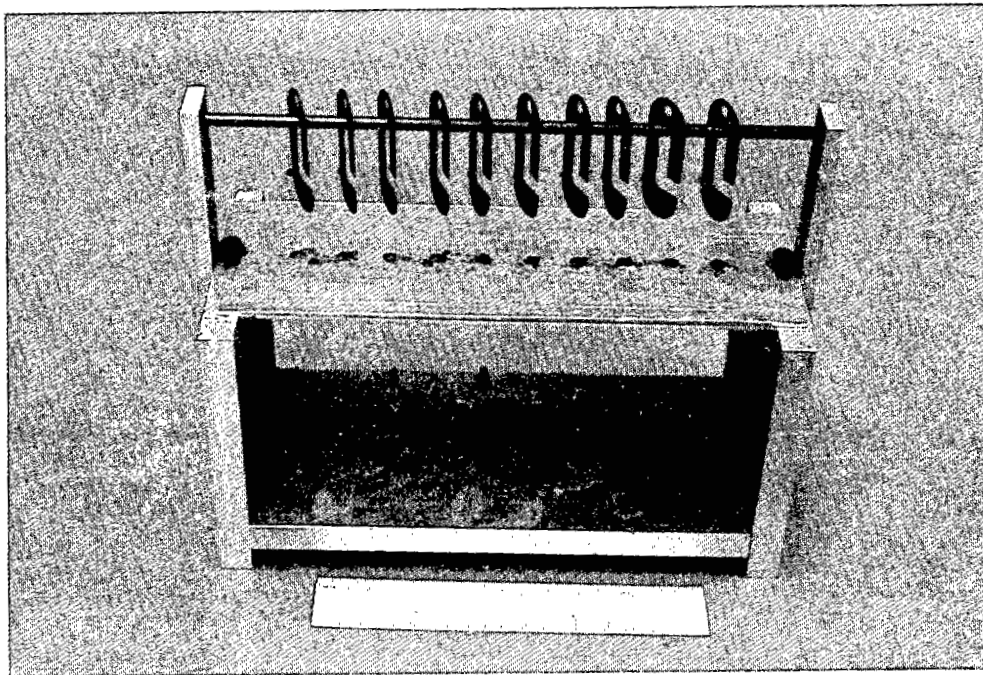


Figure 15. Single Fiber Pullout Test Fixture.

completely cover the hole. The resin was used in frozen form to minimize its tack, thus keeping the resin from sticking to the fiber too soon in the process. The fabrication fixture with ten suspended fibers was then placed into a preheated oven at 140°C (285°F) for the Hercules 3501-6 and 4001 resins, and 100°C (212°F) for the Hexcel F155 resin. The resin films were cured for 3 hours at these temperatures. The Hercules 3501-6 was then post-cured at 177°C (350°F) for 4 hours. The Hercules 4001 was post-cured at 177°C (350°F) for 4 hours, then for 8 hours at 204°C (400°F). The Hexcel F155 was post-cured for 3 hours at 127°C (260°F).

All fiber pullout testing was performed using an Instron Model 1125 electromechanical universal test machine. A metal hook attached to the crosshead of the testing machine engaged the C-shaped tab at the end of the fiber. Pulling on the tab thus pulled the fiber through the resin film.

Initially, many fibers were broken due to the resin films being too thick, thus requiring too much force for pullout. After many trials, a technique was developed for achieving an extremely thin membrane of resin around each fiber, and success was achieved in pulling fibers out of the films. Loads required to pull out the fibers were recorded on a strip chart recorder using a 0.2 N (0.05 lb) full scale load cell. The fibers were then mounted on glass microscope slides to aid in making pullout length measurements. Polaroid photographs of the fiber debond region were taken, to document the determination of the debond length. Fiber diameters were also measured from these photographs, knowing the magnification.

Interfacial shear strengths were then calculated using the

simple formula:

$$\tau = \frac{P}{\pi DL}$$

where:

P = load at debond

D = fiber diameter

L = debonded length

## SECTION 4

### EXPERIMENTAL RESULTS

#### 4.1 Fiber Surface Treatment Characterization

All four fiber surface treatments were chemically characterized, to verify the presence of the proper chemical treatments on the surface of the AS4 fiber used in this study. This fingerprinting of fiber sizings was performed by Midwest Research Institute (MRI), Kansas City, Missouri, on a subcontract basis to the University of Wyoming. Four fiber yarn samples were sent to Midwest Research Institute, these being taken from the same fiber spools used to make prepreg for the program. Internal reflectance infrared spectroscopy was used to characterize the graphite fiber coatings present on the four fiber samples. The fiber coatings were dissolved from the fiber surface using methylene chloride for the unsized, 828-sized, PVA-sized, and polysulfone-sized fibers, with water also being used on the PVA-sized fiber sample. The extracted sizings were dried and then analyzed using IR spectroscopy. Spectra were then compared with handbook spectra for the same polymers. Coating weight percents were calculated also, for reference. The infrared spectra obtained for the fiber sizings corresponded to the handbook spectra in all cases. A copy of the MRI report is reproduced as Appendix D of this report.

#### 4.2 Neat Resin Properties

Both the Hercules 4001 and the Hexcel F155 matrix materials were tested in neat resin (unreinforced) form, as discussed in Section 3.5. Uniaxial tensile and Iosipescu shear tests were performed, as

functions of both temperature and moisture content.

Average uniaxial tensile test results are presented in Table 2. Individual tensile test specimen results are given in Tables A1 and A2 of Appendix A, with individual stress-strain plots given in Appendix B. As will be noted, the two resin systems were tested at each of four environmental conditions, i.e., 23°C (73°F) and 38°C (100°F), dry and wet, for both the Hercules 4001 and the Hexcel F155. The F155 epoxy is a 121°C (250°F) cure epoxy; it was tested at a relatively low temperature to allow properties to be measured consistent with its lower cure temperature and lower glass transition (T<sub>g</sub>) temperature. The Hercules 4001 bismaleimide resin was cured at 204°C (400°F); but it was tested at the same temperatures as the F155.

As previously noted, the Hercules 3501-6 epoxy neat resin had been tested in prior studies [9,10], and thus data were already available. These results are also presented in Table 2. A complete presentation of Hercules 3501-6 properties is given in Reference [12].

Referring to Table 2, it can be seen that the Hercules 3501-6 and 4001 neat resin tensile properties are reasonably comparable at both environmental conditions. The higher Poisson's ratio and the better modulus retention of the Hercules 4001, a bismaleimide resin, will be noted. The Hexcel F155 rubber-toughened epoxy exhibited a lower tensile modulus, as expected, and a relatively high strain to failure.

The saturation moisture contents of the three matrix materials are also given in Table 2. While the Hercules 3501-6 epoxy, at 6

Table 2

## Average Neat Resin Tensile Test Results

Matrix Material	Temperature (°C)	Moisture Content at Saturation (weight %)	Tensile Strength (MPa)	Tensile Strength (ksi)	Tensile Modulus (GPa)	Tensile Modulus (Msi)	Poisson's Ratio	Strain to Failure (percent)
Hercules 3501-6*	23	0	61	8.8	5.1	0.62	0.34	1.4
	38	6.0	36	7.4	3.2	0.47	0.34	1.6
Hercules 4001	23	0	53	7.7	3.6	0.52	0.44	1.6
	38	7.0	32	4.6	2.4	0.35	0.40	1.4
Hexcel 155	23	0	77	11.2	3.1	0.45	0.41	3.6
	38	9.6	41	5.9	2.1	0.30	0.38	3.5

\*Data taken from References [9,10,12,18,19,25]

percent by weight moisture absorption, is near the upper end of the range of most structural polymers, it will be noted that the other two systems tested here were even higher. This has special implications in terms of moisture swelling-induced internal stresses in the composite, as will be discussed in Section 6.

Iosipescu shear testing was also performed on both the Hercules 4001 and Hexcel F155 neat resins, to allow measurement of their shear strengths and shear moduli. Complete shear stress-shear strain curves were recorded for each specimen at the four different environmental conditions indicated in Table 3. The Iosipescu shear test specimens were machined from 0.25 cm (0.10 in) thick plates cast at the same time as the tensile test specimens. The Iosipescu shear test results for the Hercules 4001 and Hexcel F155 neat resins are summarized in Table 3, along with previously measured values for the Hercules 3501-6. Individual test specimen data are included in Tables A3 and A4 of Appendix A, with individual shear stress-shear strain curves given in Appendix B.

These shear stress-shear strain curves were subsequently curve-fit and the resulting equations used as input to the finite element micromechanics computer program. Details of this curve-fit procedure and the micromechanics results are given in Section 6.

Referring again to Table 3, it will be noted that the shear strength of the Hercules 4001 bismaleimide at the room temperature, dry condition was measured to be very low, i.e., only 17 MPa (2.4 ksi). This is due to the relatively brittle nature of this resin at the RTD condition, which makes it particularly sensitive to stress concentration effects. It will be noted that the shear strength more



Table 3  
Average Neat Resin Shear Test Results

Matrix Material	Temperature (°C)	Moisture Content at Saturation (weight %)	Shear Strength (MPa)	Shear Strength (ksi)	Shear Modulus (GPa)	Shear Modulus (Msi)	Shear Strain to Failure (Percent)
Hercules 3501-6*	23	0	101	14.7	1.6	0.23	9.2
	23	6.0	76	11.1	1.5	0.22	9.5
	100	0	55	8.0	1.0	0.15	10.0
	93	6.0	34	5.0	1.0	0.14	10.5
Hercules	23	0	17	2.4	1.2	0.18	1.2
	23	7.0	41	5.9	1.1	0.16	3.2
	100	0	40	5.8	1.1	0.16	4.6
	93	7.0	16	2.3	0.7	0.11	22.0
Hexcel	23	0	48	7.0	1.1	0.15	5.4
	23	9.6	46	6.7	1.0	0.15	5.8
	75	0	43	6.2	1.0	0.14	8.8
	38	9.6	34	4.9	0.9	0.14	5.6

\*Data taken from References [10,12,18,19,25]

than doubled with the increase of either temperature or moisture. However, the combined influence of temperature and moisture lowered the shear strength again. The shear modulus also decreased significantly. This is typical response [11,12], the hygrothermal environment plasticizing the matrix material and hence reducing its strength and stiffness properties. As can be seen in Table 3, the Hercules 3501-6 epoxy was affected similarly. The Hexcel F155 was not subjected to as high a temperature in the ETW condition, and hence did exhibit as severe a loss of properties.

The coefficient of thermal expansion of both the Hercules 4001 and Hexcel F155 matrix materials also were measured, as described in Section 3.5.3. Averages of the six tests for each resin are presented in Table 4. Individual test results and plots of thermal strain versus temperature are included in Appendix B. The values for Hercules 3501-6 epoxy, also included in Table 4, were taken from References [12,18,19].

The coefficients of moisture expansion of the two matrix materials were also measured, using the techniques described in Section 3.5.4. Average values are reported in Table 5. Individual test data and plots are contained in Appendix B. The values for Hercules 3501-6 epoxy also included in Table 5 were taken from References [12,18,19].

#### 4.3 Composite Fiber Volume Contents

Fiber volumes were measured on all sets of composite panels. The fiber volume determinations were made using the acid digestion method described in ASTM Standard STD D3171-76. Three replicates were measured for each panel, with good correlation between the three

Table 4

Average Coefficients of Thermal Expansion  
for the Three Polymer Matrix Materials

Neat Resin System	Moisture Condition	Coefficient of Thermal Expansion ( $10^{-6}/^{\circ}\text{C}$ )	Coefficient of Thermal Expansion ( $10^{-6}/^{\circ}\text{F}$ )
Hercules 3501-6*	Dry	41.2	22.9
	Moisture-Saturated	47.6	26.4
Hercules 4001	Dry	53.1	29.5
	Moisture-Saturated	61.0	33.9
Hexcel F155	Dry	63.4	35.2
	Moisture-Saturated	73.0	40.6

\*From References [18,19]

Table 5

Average Coefficients of Moisture Expansion  
and the Moisture Saturation Levels of the Three Polymer Matrix Materials  
at 66°C, 98% Relative Humidity

Neat Resin System	Coefficient of Moisture Expansion ( $10^{-3}/\%M$ )	Moisture Saturation Level (%M)
Hercules 3501-6	3.20	6.2
Hercules 4001	2.33	7.0
Hexcel F155	3.12	9.4

\*From References [18,19]

samples. Table 6 gives the average fiber volumes for each set of plates tested. Detailed results are presented in Tables A5 through A7 of Appendix A.

For the unidirectional composite panels, there was considerable variation from one fiber surface treatment/matrix combination to another, which must be taken into consideration when comparing the measured composite strength and stiffness properties. This will be done later in this section, and also in Sections 6 and 7 when making analytical/experimental correlations.

The fiber volumes of the quasi-isotropic laminate panels also varied significantly, as indicated in Table 6. The fiber volumes of the AS4/F155 composites in general were lower than those of the Hercules 3501-6 and 4001 matrix composites, because of the different prepregging procedures used. Of particular note is the very low value for the unsized AS4/F155 quasi-isotropic composite laminate. Because of the different handling characteristics of the graphite fibers having different surface finishes, it was difficult to control the resin content accurately during the prepregging and curing processes. In a larger program, as in a commercial prepregging operation, this desired uniformity would be achieved by successive iterations over a period of time. This was not practical to attempt in the present study.

#### 4.4 Unidirectional Composites

The 12 combinations of unidirectional composites were subjected to transverse tensile and axial compressive loadings, at both room temperature, dry, and elevated temperature, wet conditions. Results are presented in the next two subsections.

Table 6  
Average Fiber Volumes  
For the Various Graphite/Polymer Matrix Composite Plates

	Unidirectional Panels	Quasi-Isotropic Panels
<u>AS4/3501-6</u>		
Unsize	47.3	54.5
EPON 828	58.9	58.8
PVA	56.7	64.1
Polysulfone	52.4	52.0
<u>AS4/4001</u>		
Unsize	52.5	54.5
EPON 828	56.7	52.2
PVA	56.2	53.5
Polysulfone	62.8	57.2
<u>AS4/F155</u>		
Unsize	37.7	28.4
EPON 828	40.0	43.8
PVA	39.7	47.4
Polysulfone	44.0	42.2

#### 4.4.1 Transverse Tension

Both unidirectional composite transverse tensile and quasi-isotropic laminate axial tensile testing was performed for all 12 fiber/matrix combinations. Results for the quasi-isotropic laminates are presented in Section 4.6. Measurements of tensile modulus, ultimate tensile strength, and ultimate tensile strain were made, at two environmental conditions, viz, room temperature, dry (RTD) and elevated temperature, wet (ETW), i.e., 93°C (200°F) for the Hercules 3501-6 and 4001 matrix composite specimens and 38°C (100°F) for the Hexcel F155 matrix composite specimens. The Hexcel F155 composites were tested at a lower temperature because the F155 matrix is a 121°C (250°F) cure temperature system while the Hercules 3501-6 is cured at 177°C (350°F) and the Hercules 4001 at 204°C (400°F). Testing the Hexcel F155 matrix composites at 93°C (200°F) would have resulted in very low mechanical properties, which would have made it difficult to evaluate the fiber/matrix interface for that resin system. Therefore, the Hexcel F155 was tested at what was considered an equivalent temperature, considering its cure temperature relative to the Hercules 3501-6 and 4001 cure temperatures.

Transverse tensile testing of unidirectional composites was performed to help evaluate the effectiveness of the interface bond between the Hercules AS4 graphite fiber (with four different surface treatments) and the three polymer matrices. Average values of the test results for all 12 fiber/matrix combinations are presented in Tables 7 and 8, for the RTD and ETW test conditions, respectively. These same data are also plotted in bar chart form in Figures 16 through 21, for ease of visualization of possible trends. Individual

test specimen results are included in Tables A8 through A13 of Appendix A, with individual stress-strain curves being included in Appendix B.

Reference will be made first to the transverse tensile strength results (Figures 16 and 17 for the RTD and ETW conditions, respectively). At the room temperature, dry condition, the AS4/3501-6 unidirectional composites clearly exhibited the lowest strengths, for all fiber surface treatments. The AS4/4001 composites exhibited strengths about twice as high, the PVA sizing being the poorest performer. There were variations in fiber volume from one fiber/matrix combination to another (as previously presented in Table 6). However, there does not appear to be a correlation between high transverse tensile strength and low fiber volume content, as might be expected based upon the well established fact that more closely spaced fibers result in higher stress concentrations in the matrix material [26-28].

The room temperature, dry (RTD) transverse tensile strengths of the AS4/F155 unidirectional composites were as high, or higher, than those of the AS4/4001 composites.

At the ETW condition (see Figure 17), the transverse tensile strengths were all significantly lower. (It should be noted that Figure 17 is plotted to the same scale as Figure 16. This will be true also for all other comparison plots to be presented subsequently, to make comparisons easier.) The AS4/F155 composites appear to have the better strength retention in general, but it must be noted (see Table 8) that these tests were conducted at only 38°C (100°F).



Table 7

Average Unidirectional Composite Transverse Tensile Test Results  
At the Room Temperature, Dry Condition

Composite Material System	Ultimate Strength		Tensile Modulus		Ultimate Strain (percent)
	(MPa)	(ksi)	(GPa)	(Msi)	
<u>AS4/3501-6</u>					
Unsize	22	3.2	7.9	1.2	0.29
EPON 828	22	3.2	7.7	1.1	0.28
PVA	27	4.0	7.9	1.2	0.34
Polysulfone	23	3.4	7.6	1.1	0.30
<u>AS4/4001</u>					
Unsize	49	7.1	9.5	1.4	0.56
EPON 828	55	8.0	8.8	1.3	0.61
PVA	37	5.4	8.1	1.2	0.46
Polysulfone	48	7.0	9.1	1.3	0.55
<u>AS4/F155</u>					
Unsize	60	8.7	6.9	1.0	0.84
EPON 828	50	7.3	7.9	1.2	0.63
PVA	37	5.4	7.5	1.1	0.51
Polysulfone	67	9.8	7.7	1.1	0.92

Table 8

Average Unidirectional Composite Transverse Tensile Test Results  
At the Elevated Temperature, Wet Condition

Composite Material System	Test Temperature (°C)	Ultimate Strength (MPa) (ksi)		Tensile Modulus (GPa) (Msi)		Ultimate Strain (percent)
<u>AS4/3501-6</u>	93°C					
Unsized		15	2.2	5.2	0.8	0.34
EPON 828		12	1.7	6.0	0.9	0.21
PVA		11	1.6	3.4	0.5	0.25
Polysulfone		16	2.3	5.4	0.8	0.28
<u>AS4/4001</u>	93°C					
Unsized		21	3.1	6.6	1.0	0.39
EPON 828		27	3.9	6.6	1.0	0.44
PVA		20	2.9	6.9	1.0	0.29
Polysulfone		19	2.8	8.0	1.2	0.28
<u>AS4/F155</u>	38°C					
Unsized		24	3.5	3.8	0.6	0.78
EPON 828		28	4.1	5.4	0.8	0.77
PVA		12	1.8	3.5	0.5	0.38
Polysulfone		33	4.7	5.1	0.7	0.69

# Unidirectional Composite Transverse Tension Room Temperature, Dry (RTD)

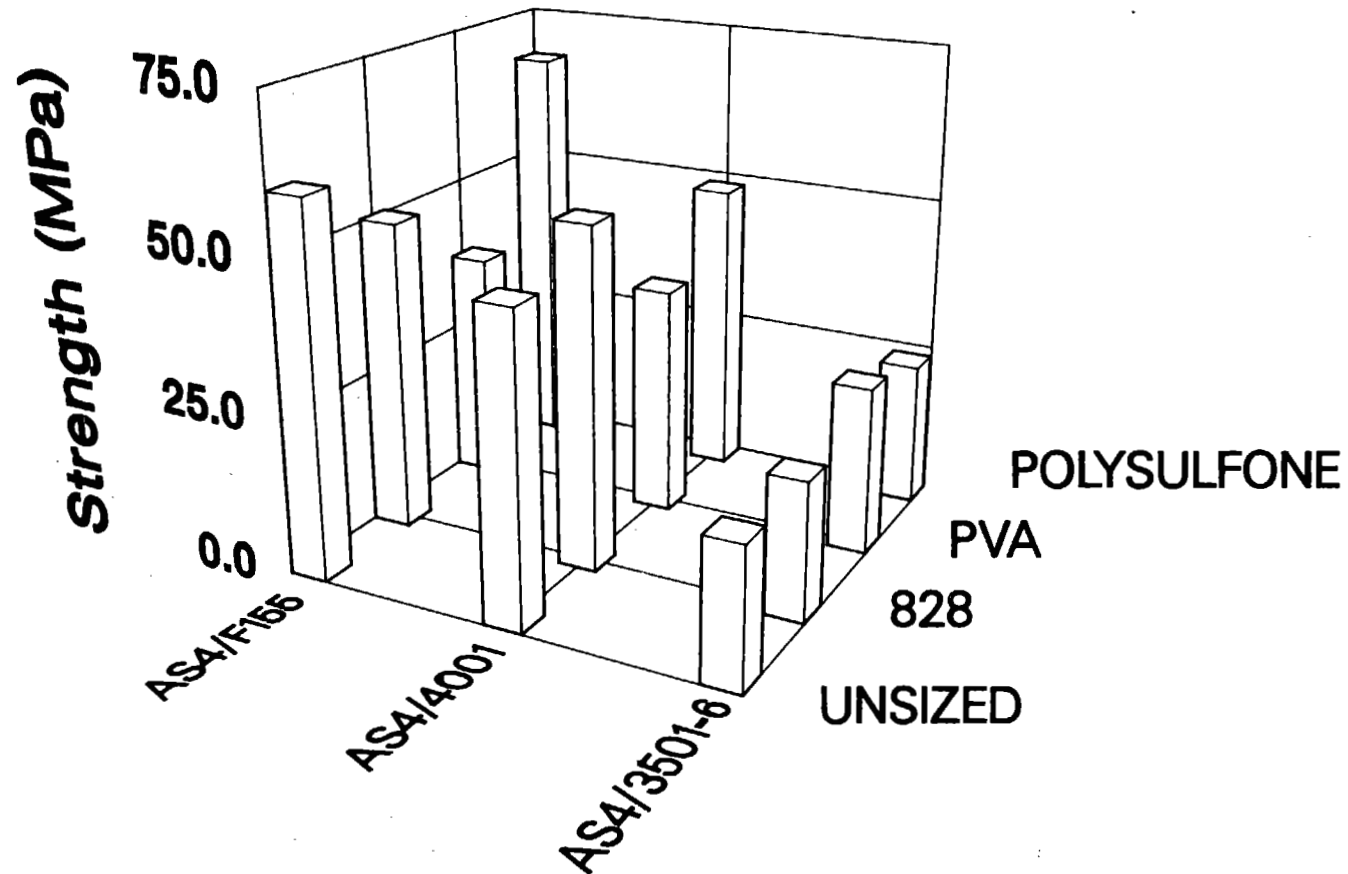


Figure 16. Unidirectional Composite Transverse Tensile Strengths of the Twelve Fiber Sizing/Matrix Combinations at the Room Temperature, Dry Condition.

## Unidirectional Composite Transverse Tension Elevated Temperature, Wet (ETW)

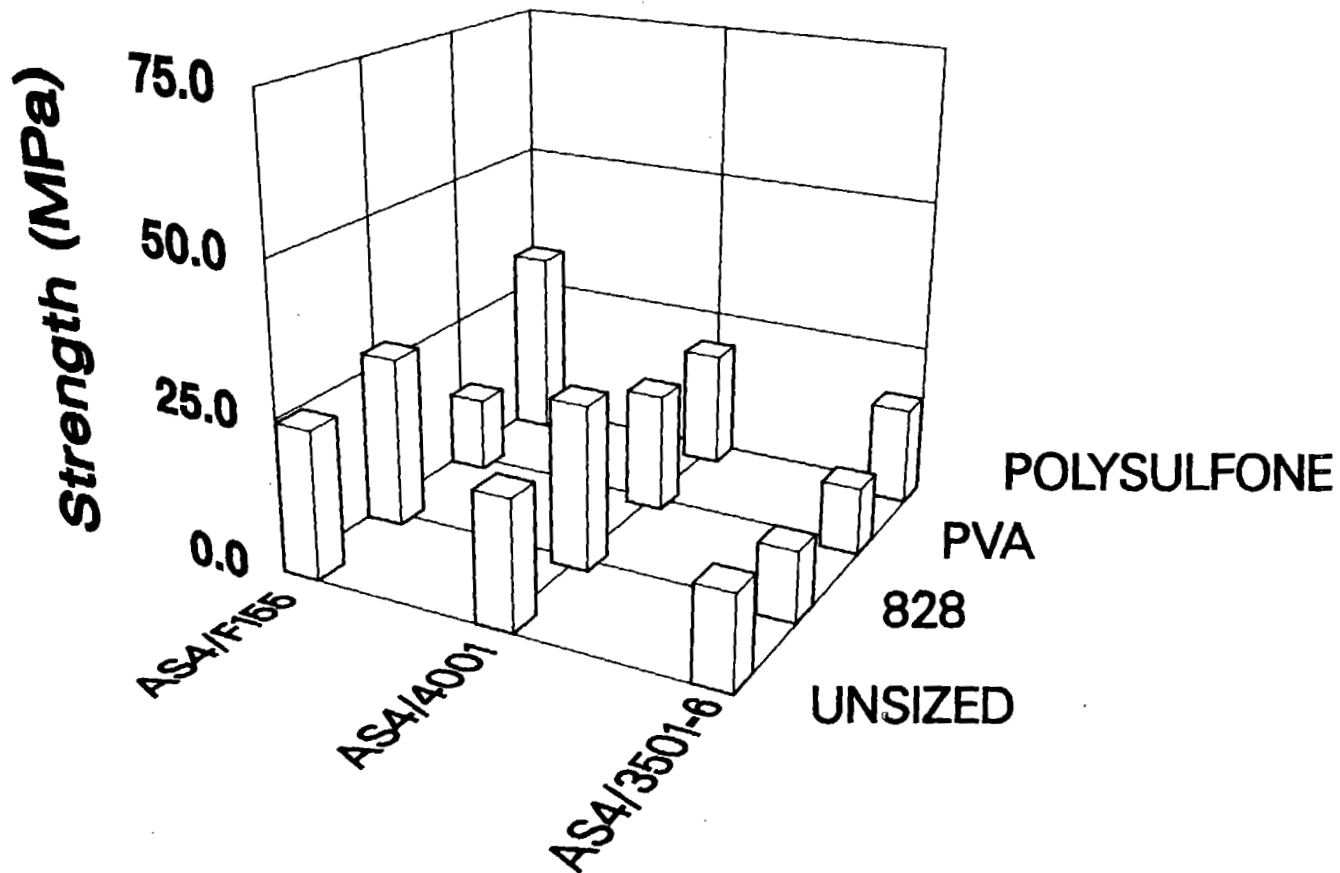


Figure 17. Unidirectional Composite Transverse Tensile Strengths of the Twelve Fiber Sizing/Matrix Combinations at the Elevated Temperature, Wet Condition.

# Unidirectional Composite Transverse Tension Room Temperature, Dry (RTD)

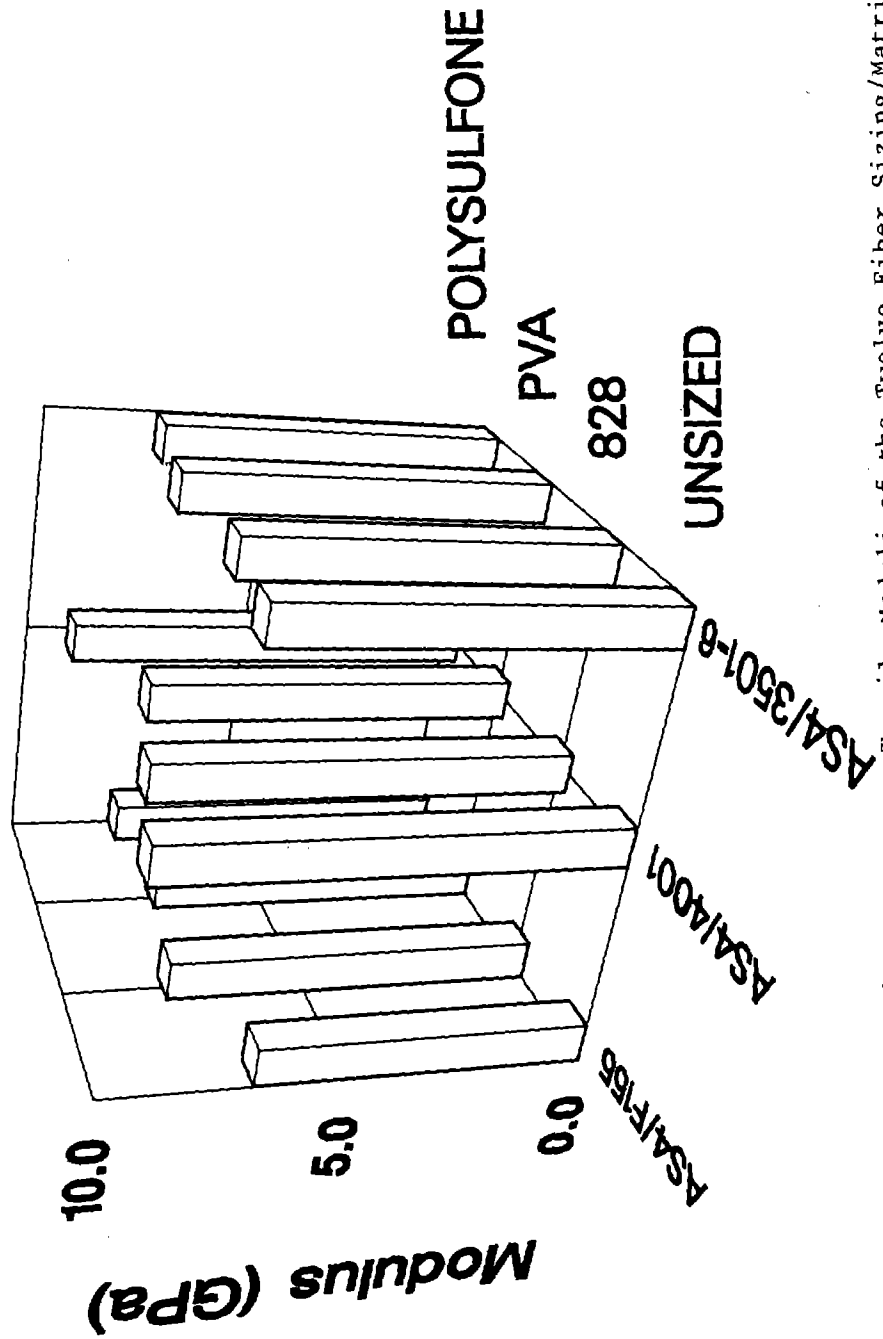


Figure 18. Unidirectional Composite Transverse Tension Moduli of the Twelve Fiber Sizing/Matrix Combinations at the Room Temperature, Dry Condition.

# Unidirectional Composite Transverse Tension Elevated Temperature, Wet (ETW)

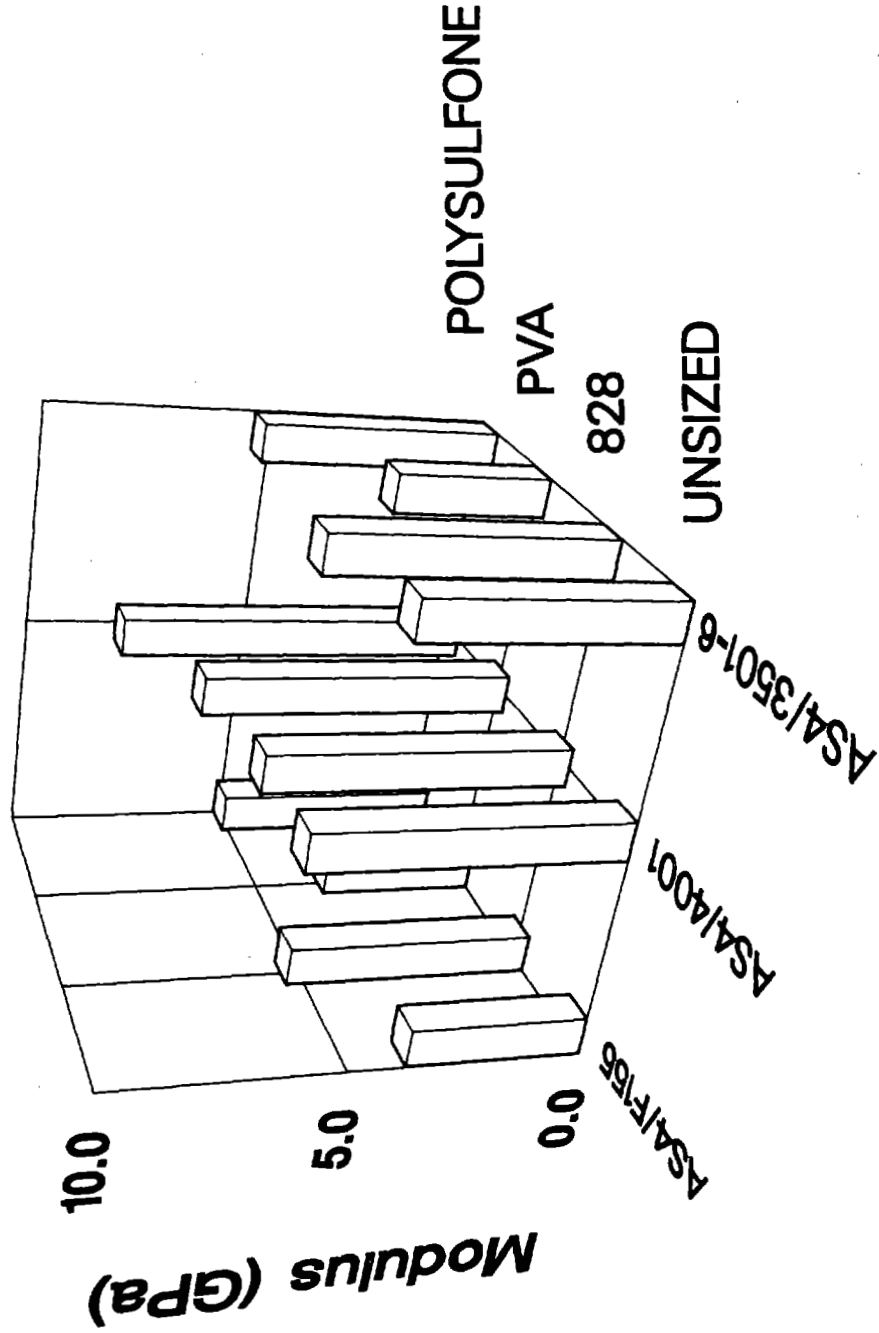


Figure 19. Unidirectional Composite Transverse Tensile Moduli of the Twelve Fiber Sizing/ Matrix Combinations at the Elevated Temperature, Wet Condition.

# Unidirectional Composite Transverse Tension Room Temperature, Dry (RTD)

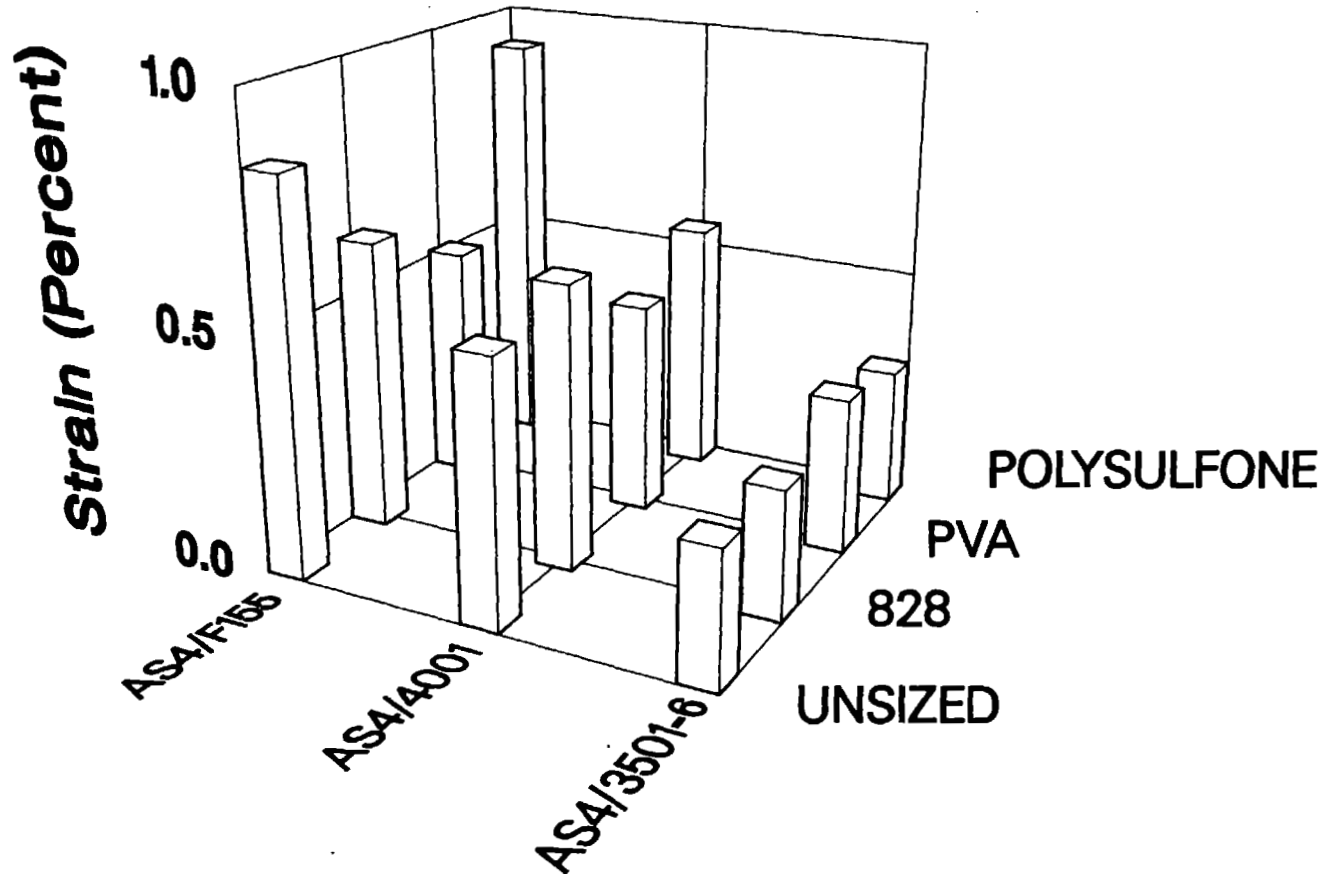


Figure 20. Unidirectional Composite Transverse Tensile Strains to Failure of the Twelve Fiber Sizing/Matrix Combinations at the Room Temperature, Dry Condition.

# Unidirectional Composite Transverse Tension Elevated Temperature, Wet (ETW)

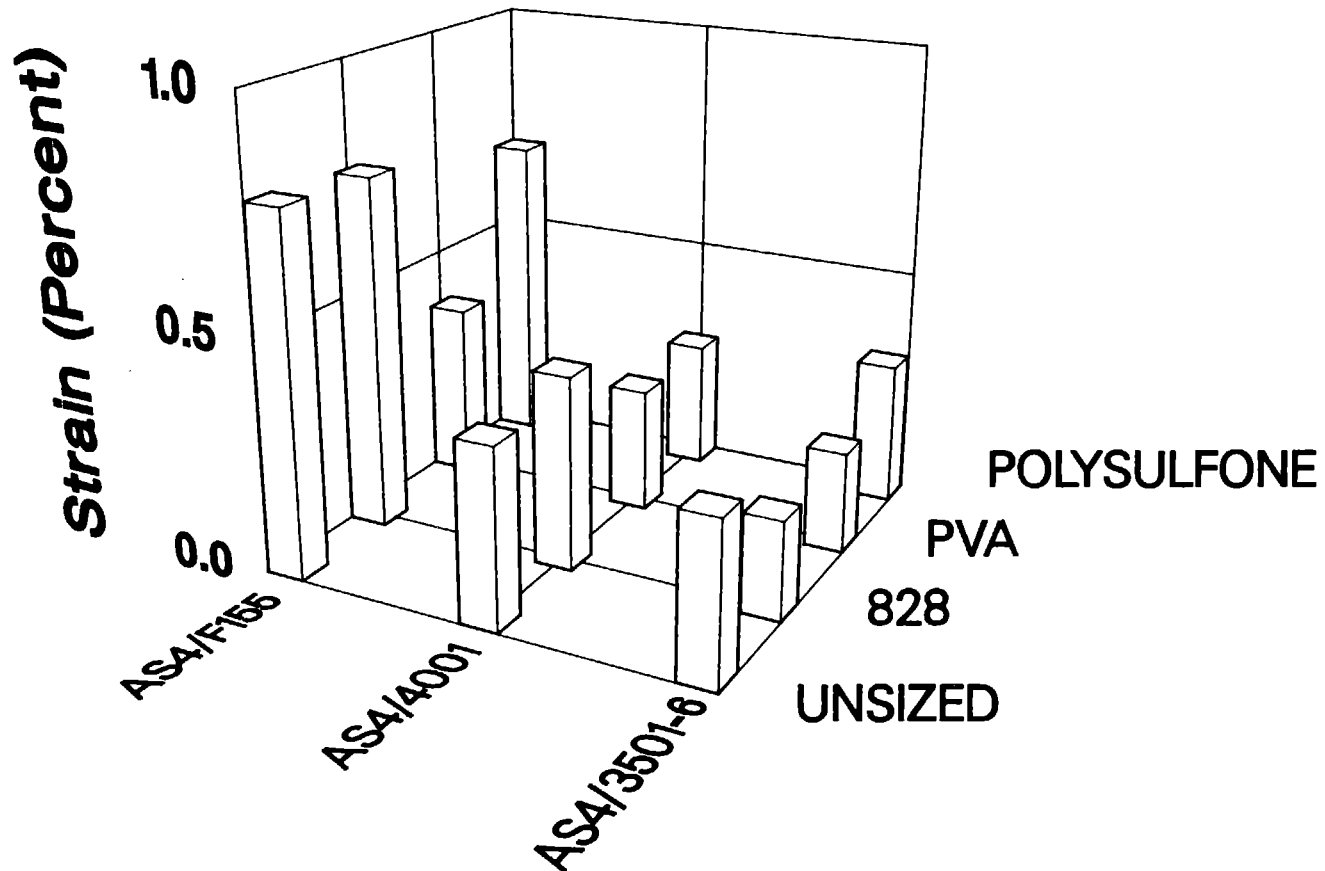


Figure 21. Unidirectional Composite Transverse Tensile Strains to Failure of the Twelve Fiber Sizing/Matrix Combinations at the Elevated Temperature, Wet Condition.



The transverse tensile moduli, tabulated in Tables 7 and 8 for the RTD and ETW conditions, respectively, are also shown as three-dimensional plots in Figures 18 and 19. At room temperature, there was relatively little variation in modulus. The AS4/4001 composites did exhibit the highest moduli, which can perhaps be best seen in Table 7. It would have been expected that the Hercules 3501-6 matrix composites have the highest moduli, since the fiber volumes were comparable to those of the Hercules 4001 matrix composites (see Table 6) and the matrix tensile modulus is higher (Table 2). In fact, the composite transverse moduli of the Hexcel F155 matrix composites were about as high, even though the modulus of this matrix material is lower (Table 2) and the composite fiber volumes were also lower (Table 6). These trends will be discussed further in Section 6 in relation to the finite element micromechanics predictions of composite response.

At the ETW condition, the transverse tensile moduli of the various composites decreased by 20 to 40 percent relative to the corresponding RTD values, as can be seen by comparing Tables 7 and 8. The AS4/F155 composites were degraded the most, even though these ETW tests were conducted at only 38°C (100°F), as opposed to 93°C (200°F) for the other two matrix systems. The suggestion is that a fiber-matrix interface debond may have occurred during the hygrothermal conditioning prior to testing, or during the very early stages of the transverse tensile loading. The former is more likely, as will be discussed further in relation to the analytical/experimental correlations of Section 6. This may have occurred for the PVA-sized AS4/3501-6 composite also, as suggested by

the significant drop in composite modulus.

Transverse tensile strains to failure for all 12 fiber surface treatment/matrix conditions, for the RTD conditions, are plotted in Figure 20. As indicated also in Table 7, the transverse tensile strains of the Hercules 3501-6 matrix composites were the lowest, for all fiber surface treatments. This is consistent with the low transverse tensile strengths also observed (Figure 16). The higher strain to failure values for the Hexcel F155 matrix composites reflect the higher strains to failure of this rubber-toughened matrix material (Table 2). It will also be noted, however, that this higher matrix strain to failure is not translated fully to composite strain. The Hercules 4001 matrix exhibited a RTD strain to failure only about 45 percent as high as the Hexcel F155 (see Table 2), yet the AS4/4001 composite transverse strains averaged at least 75 percent as high. This is even more significant when the differences in fiber volumes are taken into account. As indicated in Table 6, the fiber volume of the AS4/4001 composites averaged 57 percent, while the AS4/F155 composites averaged only about 40 percent. That is, there was much more of the high strain to failure Hexcel F155 matrix in the AS4/F155 composites than there was lower strain to failure Hercules 4001 matrix in the AS4/4001 composites. Thus, even though the transverse tensile strengths were comparable, the higher strain to failure of the matrix did not translate directly to the composite. This is typical [12], and indicates one practical limitation of developing "tough" matrix materials for use in composites. As indicated in Figure 21, the ETW strains to failure for all composite systems followed essentially the same trends as the RTD data.

#### 4.4.2 Axial Compression

Axial compression testing was also performed on both the unidirectional composites and the quasi-isotropic laminates, at both room temperature, dry (RTD) and elevated temperature, wet (ETW) conditions. The temperatures and moisture contents were the same as previously defined in Section 4.4.1 for the tensile tests. Again, it should be emphasized that the cure temperatures were different for all three matrix materials, viz, 121°C (250°F) for the Hexcel F155, 177°C (350°F) for the Hercules 3501-6, and 204°C (400°F) for the Hercules 4001. The axial compressive test results for the quasi-isotropic laminates will be presented in Section 4.

Axial compression testing was performed on the unidirectional composites to assist in the evaluation of the fiber-matrix interfacial strength, by observing microbuckling of the graphite fibers. In theory, as the interfacial strength is decreased, the fiber-matrix bond will fail earlier under compressive loading, causing the fibers to become laterally unsupported. They then will buckle to cause total failure of the composite.

The unidirectional composite axial compressive properties are summarized in Tables 9 and 10 for the RTD and ETW test conditions, respectively. These data are also plotted in bar chart form in Figures 22 through 27, as an alternative form of observing trends. Individual test specimen data are presented in Tables A14 through A19 of Appendix A, and stress-strain curves are included in Appendix B.

At the room temperature, dry (RTD) test condition, the axial compressive strengths of the Hexcel F155 matrix composites were consistently lower than those of the other two composite systems,

Table 9

Average Unidirectional Composite Axial Compression Test Results  
At the Room Temperature, Dry Condition

Composite Material System	Ultimate Strength		Compressive Modulus		Ultimate Strain
	(MPa)	(ksi)	(GPa)	(Msi)	(percent)
<u>AS4/3501-6</u>					
Unsize	719	104	100	14.5	1.33
EPON 828	728	106	114	16.6	0.62
PVA	797	116	122	17.7	0.62
Polysulfone	839	122	116	16.9	0.97
<u>AS4/4001</u>					
Unsize	923	134	105	15.2	1.05
EPON 828	870	126	124	17.9	0.87
PVA	828	120	108	15.6	0.84
Polysulfone	887	129	128	18.6	0.60
<u>AS4/F155</u>					
Unsize	547	79	68	9.9	0.97
EPON 828	674	98	86	12.4	0.91
PVA	549	80	79	11.5	0.75
Polysulfone	608	88	91	13.2	0.69

Table 10

Average Unidirectional Composite Axial Compression Test Results  
At the Elevated Temperature, Wet Condition

Composite Material System	Test Temperature (°C)	Ultimate Strength (MPa)	Ultimate Strength (ksi)	Compressive Modulus (GPa)	Compressive Modulus (Msi)	Ultimate Strain (percent)
<u>AS4/3501-6</u> 93°C						
Unsize		469	68	79	11.5	0.55
EPON 828		536	78	87	12.7	0.54
PVA		512	74	93	13.5	0.56
Polysulfone		555	80	95	13.7	0.65
<u>AS4/4001</u> 93°C						
Unsize		581	84	91	13.2	0.80
EPON 828		670	97	122	17.7	0.73
PVA		596	87	107	15.5	0.55
Polysulfone		619	90	123	17.9	0.49
<u>AS4/F155</u> 38°C						
Unsize		406	59	53	7.7	0.70
EPON 828		486	71	69	10.0	0.69
PVA		354	51	74	10.8	0.59
Polysulfone		482	70	86	12.5	0.59

# Unidirectional Composite Axial Compression Room Temperature, Dry (RTD)

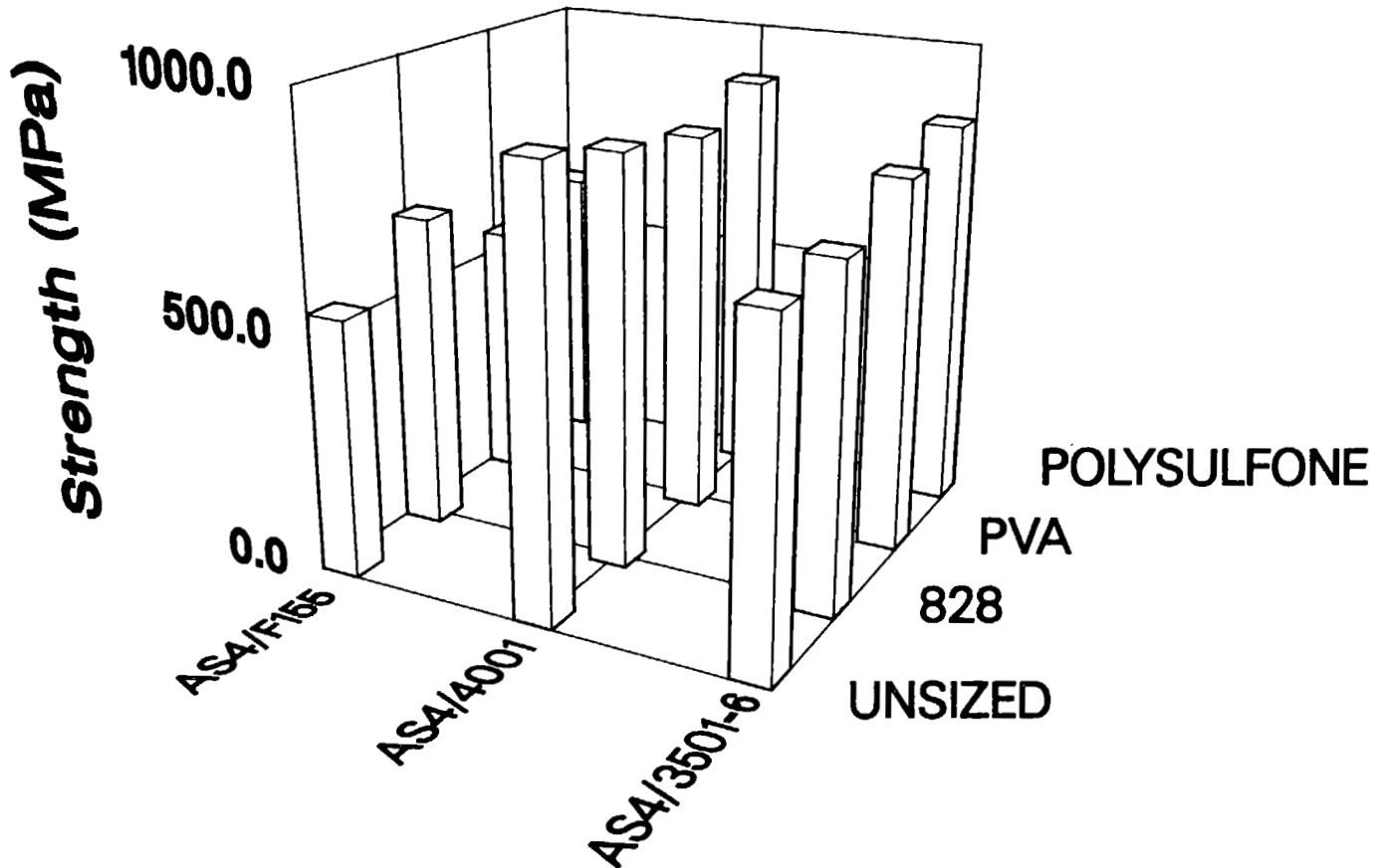


Figure 22. Unidirectional Composite Axial Compressive Strengths of the Twelve Fiber Sizing/ Matrix Combinations at the Room Temperature, Dry Condition.

# Unidirectional Composite Axial Compression Elevated Temperature, Wet (ETW)

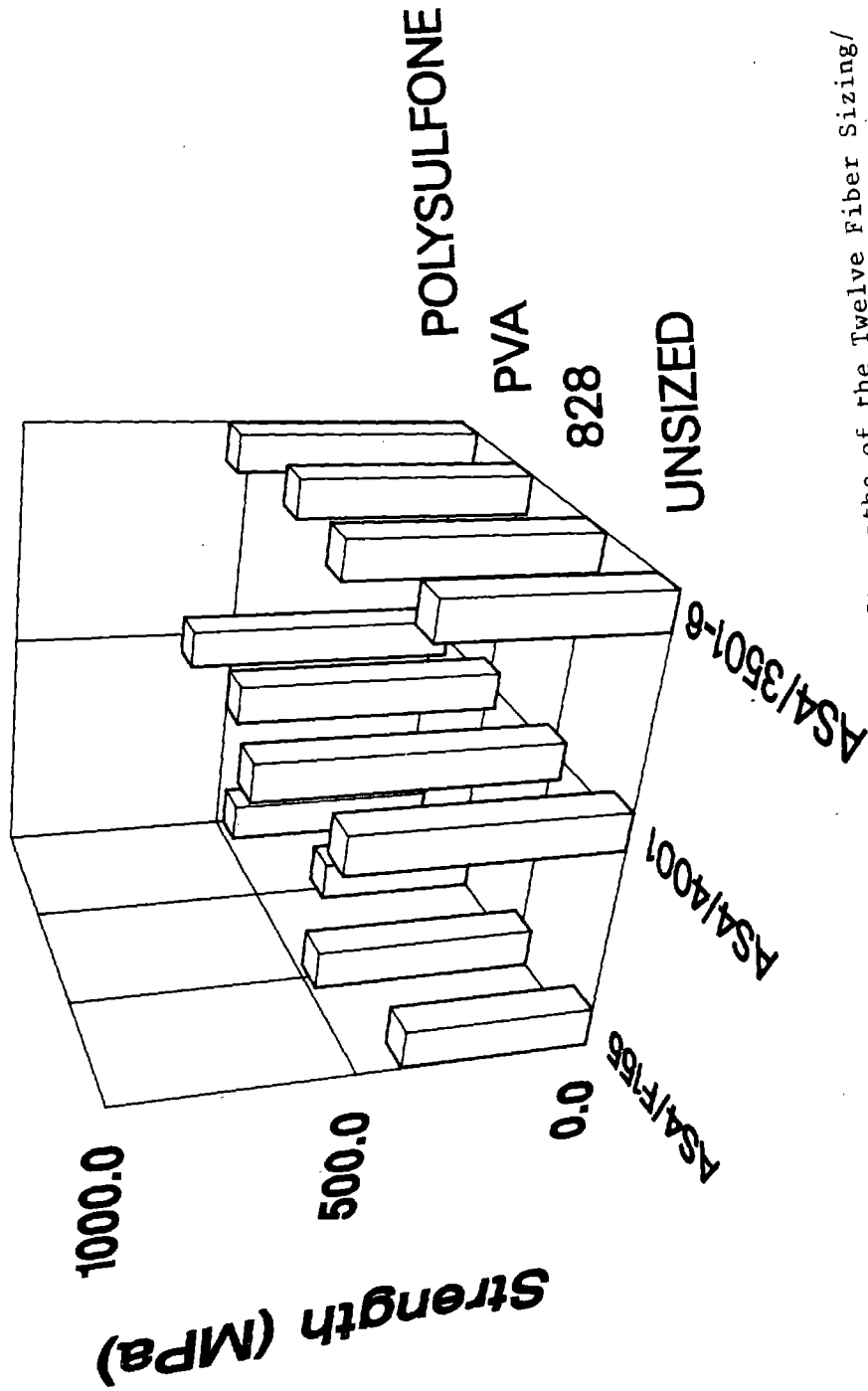


Figure 23. Unidirectional Composite Axial Compressive Strengths of the Twelve Fiber Sizing/Matrix Combinations at the Elevated Temperature, Wet Condition.

# Unidirectional Composite Axial Compression Room Temperature, Dry (RTD)

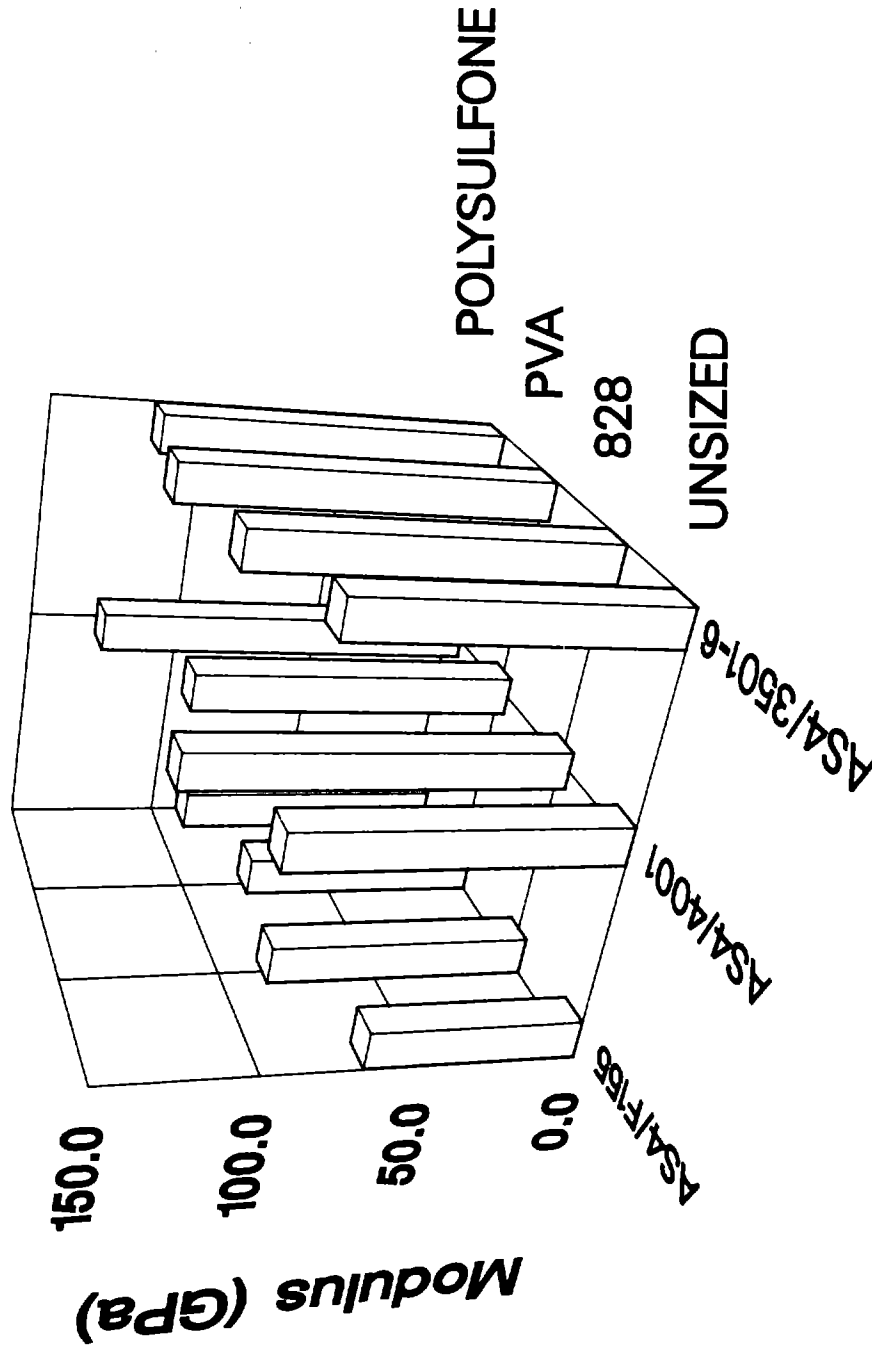


Figure 24. Unidirectional Composite Axial Compressive Moduli of the Twelve Fiber Sizing/Matrix Combinations at the Room Temperature, Dry Condition.



# Unidirectional Composite Axial Compression Elevated Temperature, Wet (ETW)

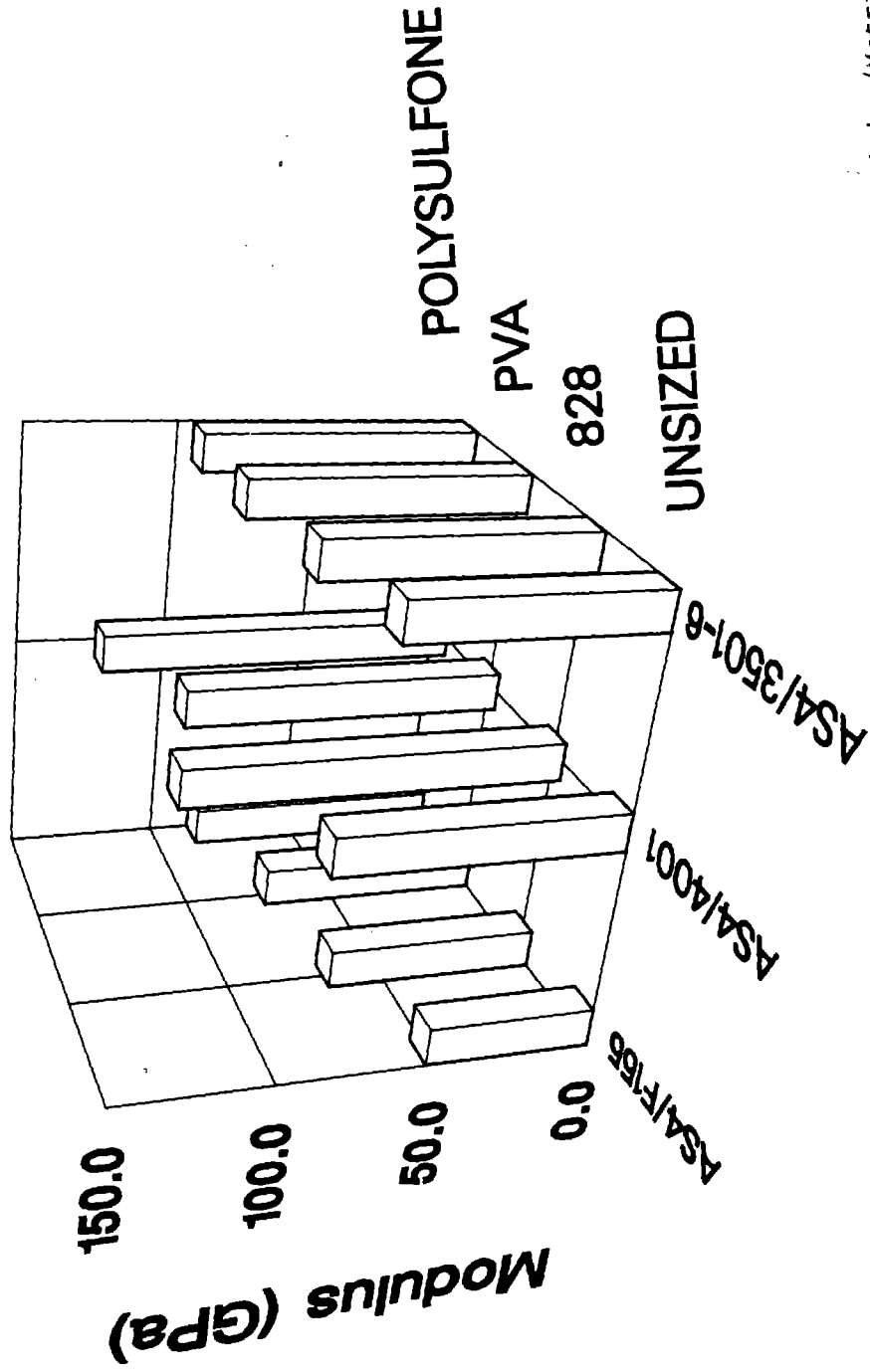


Figure 25. Unidirectional Composite Axial Compressive Moduli of the Twelve Fiber Sizing/Matrix Combinations at the Elevated Temperature, Wet Condition.

# Unidirectional Composite Axial Compression Room Temperature, Dry (RTD)

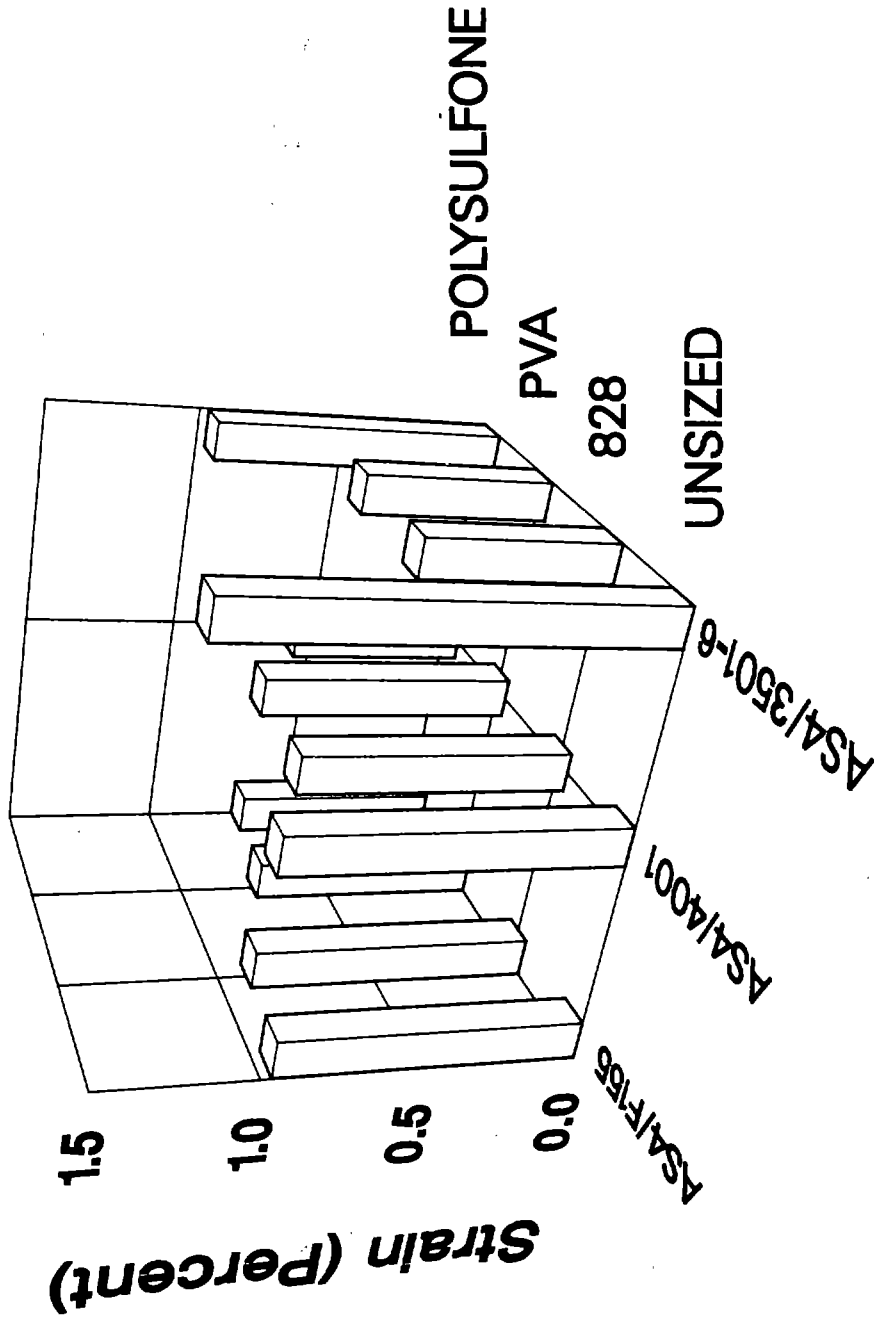


Figure 26. Unidirectional Composite Axial Compressive Strains to Failure of the Twelve Fiber Sizing/Matrix Combinations at the Room Temperature, Dry Condition.

# Unidirectional Composite Axial Compression Elevated Temperature, Wet (ETW)

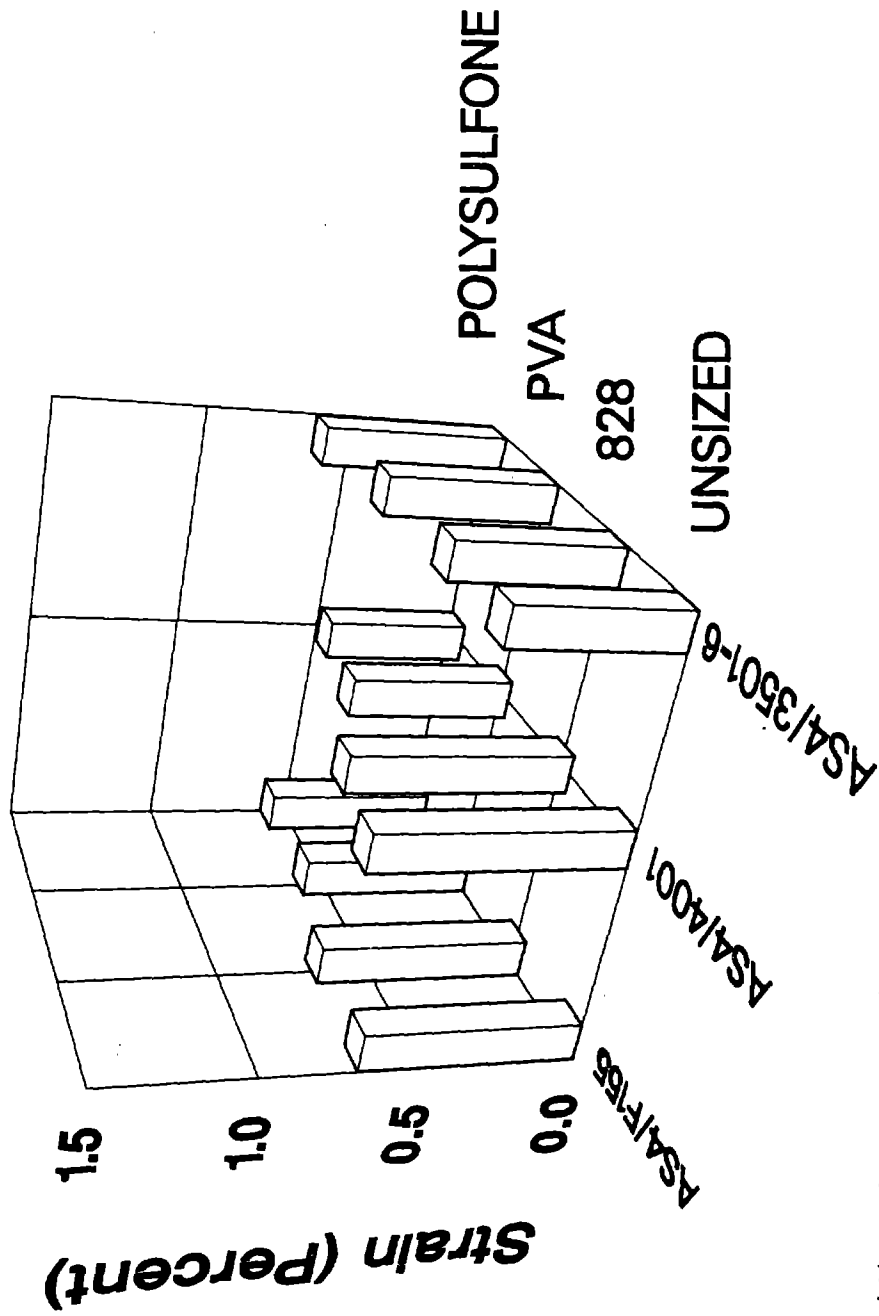


Figure 27. Unidirectional Composite Axial Compressive Strains to Failure of the Twelve Fiber Sizing/Matrix Combinations at the Elevated Temperature, Wet Condition.

independent of fiber surface treatment, the EPON 828 sizing producing the highest compressive strength. The poorer performance of the AS4/F155 unidirectional composites was probably associated with the fact that the Hexcel F155 has the lowest modulus of the three matrix materials (see Table 2). The lower matrix stiffness implies less lateral support for the fibers, and hence, an earlier occurrence of fiber microbuckling under axial compressive loading. This also accounts for the intermediate compressive strengths of the AS4/3501-6 composites. Within each composite system, the axial compressive strength was not strongly influenced by type of fiber sizing. This suggests that axial compression testing of unidirectional composites is not a very sensitive indicator of the efficiency of the interface bond strength. The present data do suggest the importance of matrix stiffness on axial compressive strength, however.

By observing Table 10 and Figure 23, similar comments can be made concerning the interpretation of the ETW data. It will be further noted, however, that the axial compressive strengths of all of the 12 fiber sizing/matrix combinations were significantly reduced in the presence of a hygrothermal environment. The strength reduction was relatively uniform at about 30 percent for all three matrix materials, keeping in mind that the AS4/F155 was tested at a lower temperature. Presumably these reductions in composite axial compressive strengths were due to the reduced stiffnesses of the matrix materials at the hot, wet conditions of these tests.

The axial compressive moduli of the 12 unidirectional composite combinations at the RTD condition are plotted in Figure 24. The compressive moduli of the Hercules 3501-6 and 4001 matrix composites

were similar in magnitude. The measured values are slightly below what would be predicted for the Hercules AS4 graphite fiber, a 235 GPa (34 Msi) modulus fiber [2], using the fiber volumes of Table 6 and a simple rule-of-mixtures calculation [29] for this fiber-dominated property. However, the variations from one type of surface-treated fiber composite to another appear to be accounted for by the corresponding variations in fiber volume.

The much lower fiber volumes of the AS4/F155 composites also explain why their composite moduli were lower. Also, corrected for fiber volume, the composite moduli for all four surface treatments would be similar. The rule-of-mixtures relation would suggest an AS4 graphite fiber modulus of only about 207 GPa (30 Msi). This was also true for the other two groups of composites. This could suggest that the Hercules AS4 graphite fibers used did not have as high a modulus as advertised by the manufacturer [2]. However, it is more likely that the composite modulus values were lower than predicted by a simple rule-of-mixtures relation because of the occurrence of slight fiber misalignments within the composites [29].

As can be seen by comparing Figures 24 and 25, the general trends in composite compressive modulus at the ETW condition were similar to those observed at room temperature. That is, unidirectional composite axial compressive modulus at a hot, wet condition is also not a satisfactory discriminator of relative interface bond strength. As an aside, however, it will be noted that the AS4/4001 composites suffered very little modulus loss with increasing temperature and moisture content, while the AS4/3501-6 composites decreased in axial compressive modulus by 20 percent or

more. The AS4/F155 composites were not as consistently lower, but also tended to decrease in modulus at the ETW condition. That the AS4/4001 did not decrease in modulus is somewhat surprising since the Hercules 4001 matrix itself did decrease in modulus at the hot, wet condition (see Table 2).

The unidirectional composite axial compressive strains to failure, tabulated in Tables 9 and 10, are also plotted in bar chart form in Figures 26 and 27, for the RTD and ETW conditions, respectively. At room temperature, the AS4/3501-6 composites incorporating unsized and polysulfone-sized AS4 graphite fibers exhibited unusually high strains, with the unsized fiber composites in general exhibiting the highest strains. At the ETW condition (see Figure 27), the differences tended to disappear.

Axial compressive failure of a unidirectional composite is a very complex fracture process, involving fiber-matrix debonding due to transverse tensile stresses developed by the Poisson effect, gross longitudinal splitting also caused by the Poisson-induced transverse tensile stresses, fiber microbuckling, local longitudinal shear failures, and gross 45° angle shear failures. Which mode predominates within a specific specimen during failure can have a strong influence on the composite strain to failure actually measured.

#### 4.5 Quasi-Isotropic Laminates

As indicated in the test matrix of Table 1 in Section 3.1, considerable attention was given to the performance of the fiber surface treated composites in laminate form. Five different test methods were selected, to characterize  $[\pm 45/0/90]_S$  quasi-isotropic

laminates. Since it is in laminate form that most high performance graphite/epoxy composites are used in aerospace applications, NASA-Ames was particularly interested in this composite form. A quasi-isotropic layup was selected as being of general interest.

#### 4.5.1 Axial Tension

Quasi-isotropic laminate axial tensile testing was conducted on all 12 fiber sizing/matrix combinations. The room temperature, dry (RTD) test results are summarized in Table 11. Elevated temperature, wet (ETW) results are included in Table 12. Individual specimen data are given in Tables A20 through A25 of Appendix A, and individual stress-strain curves in Appendix B. For use in making comparisons, these data are also plotted in three-dimensional bar chart form in Figures 28 through 33.

Considering first the RTD axial tensile strength results, these data are plotted in Figure 28. In general, the AS4/3501-6 and AS4/F155 composite laminates tended to exhibit higher axial tensile strengths than the AS4/4001 laminates. However, there do not appear to be any clear trends in the data of Figure 28. Likewise, there is not a strong correlation between fiber volume content and laminate strength, suggesting that the 0° plies did not dominate the strength response.

At the ETW condition, the laminate strengths (Figure 29) tended to be higher than at room temperature for the Hercules 3501-6 and 4001 matrix composites, but generally lower for the Hexcel F155 matrix composites. It should again be noted that the ETW test temperatures for this 177°C (250°F) cure rubber-toughened epoxy was only 38°C (100°F), whereas it was 93°C (200°F) for the other two

Table 11

Average Quasi-Isotropic Laminate Tensile Test Results  
At the Room Temperature, Dry Condition

Composite Material System	Ultimate Strength		Tensile Modulus		Ultimate Strain
	(MPa)	(ksi)	(GPa)	(Msi)	(percent)
<u>AS4/3501-6</u>					
Unsize	452	65.5	40.9	5.93	1.13
EPON 828	430	62.4	41.5	6.02	1.21
PVA	368	53.3	30.8	4.47	1.18
Polysulfone	470	68.2	39.6	5.75	1.20
<u>AS4/4001</u>					
Unsize	371	53.8	35.7	5.18	1.06
EPON 828	317	46.0	29.4	4.27	1.09
PVA	303	44.0	26.9	3.91	1.11
Polysulfone	432	62.6	36.4	5.27	1.21
<u>AS4/F155</u>					
Unsize	317	46.0	22.9	3.32	1.39
EPON 828	449	65.2	32.0	4.65	1.44
PVA	452	65.5	32.5	4.72	1.41
Polysulfone	369	53.5	31.1	4.51	1.20



Table 12

Average Quasi-Isotropic Laminate Tensile Test Results  
At the Elevated Temperature, Wet Condition

Composite Material System	Test Temperature (°C)	Ultimate Strength		Tensile Modulus		Ultimate Strain
		(MPa)	(ksi)	(GPa)	(Msi)	(percent)
<u>AS4/3501-6</u>	93°C					
Unsize		451	65.4	42.0	6.09	1.16
EPON 828		481	69.7	42.3	6.13	1.19
PVA		424	61.5	37.4	5.42	1.37
Polysulfone		474	68.8	42.4	6.15	1.21
<u>AS4/4001</u>	93°C					
Unsize		465	67.4	43.1	6.24	1.12
EPON 828		456	66.2	40.2	5.83	1.15
PVA		452	65.5	37.3	5.41	1.27
Polysulfone		598	86.8	47.0	6.81	1.36
<u>AS4/F155</u>	38°C					
Unsize		286	41.5	21.0	3.05	1.30
EPON		379	55.0	29.8	4.33	1.23
PVA		369	53.5	29.4	4.26	1.29
Polysulfone		380	55.2	28.8	4.17	1.25

# Quasi-Isotropic Laminate Axial Tension Room Temperature, Dry (RTD)

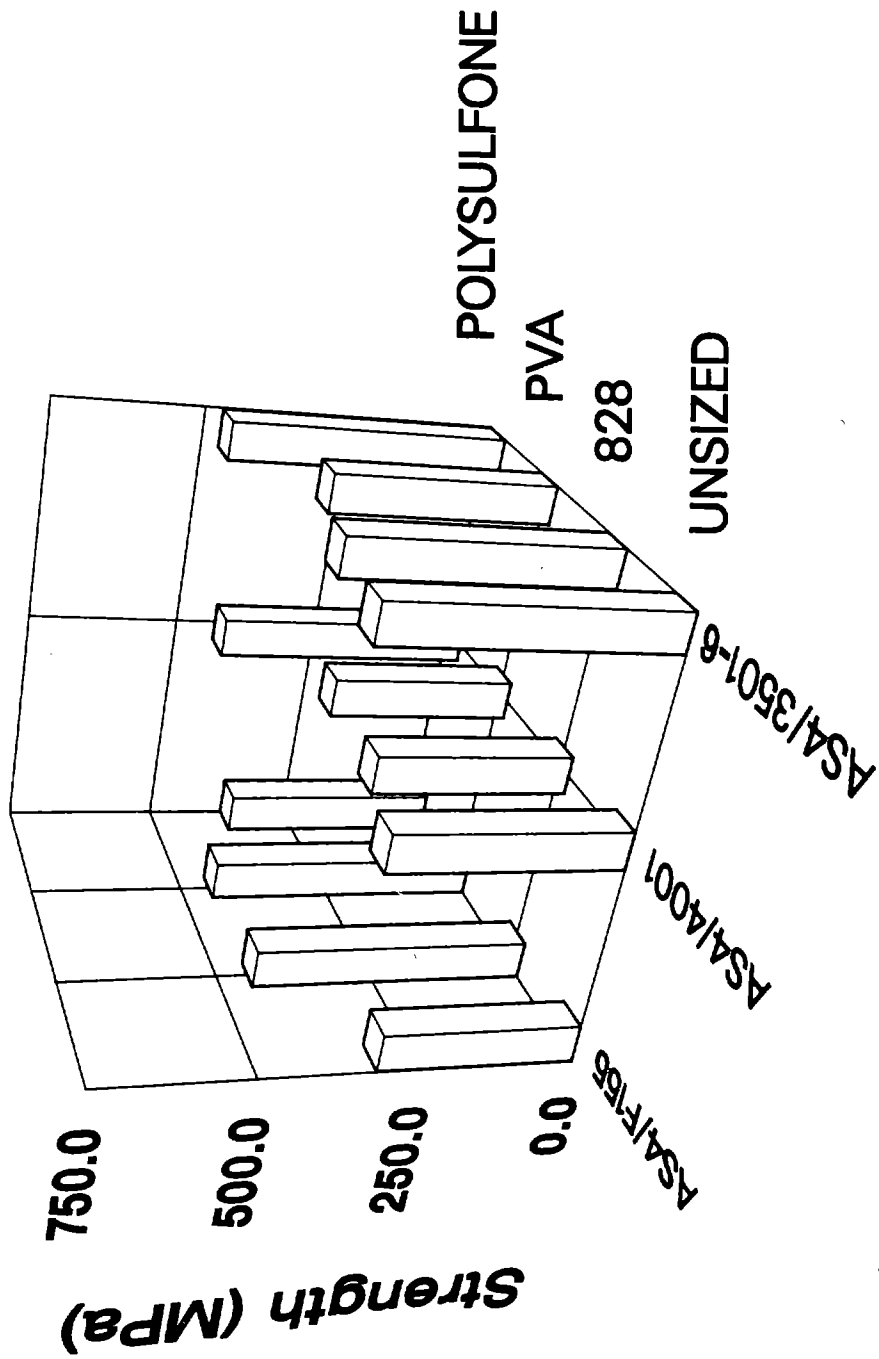


Figure 28. Quasi-Isotropic Laminate Axial Tensile Ultimate Strengths of the Twelve Fiber Sizing/Matrix Combinations at the Room Temperature, Dry Condition.

# Quasi-Isotropic Laminate Axial Tension Elevated Temperature, Wet (ETW)

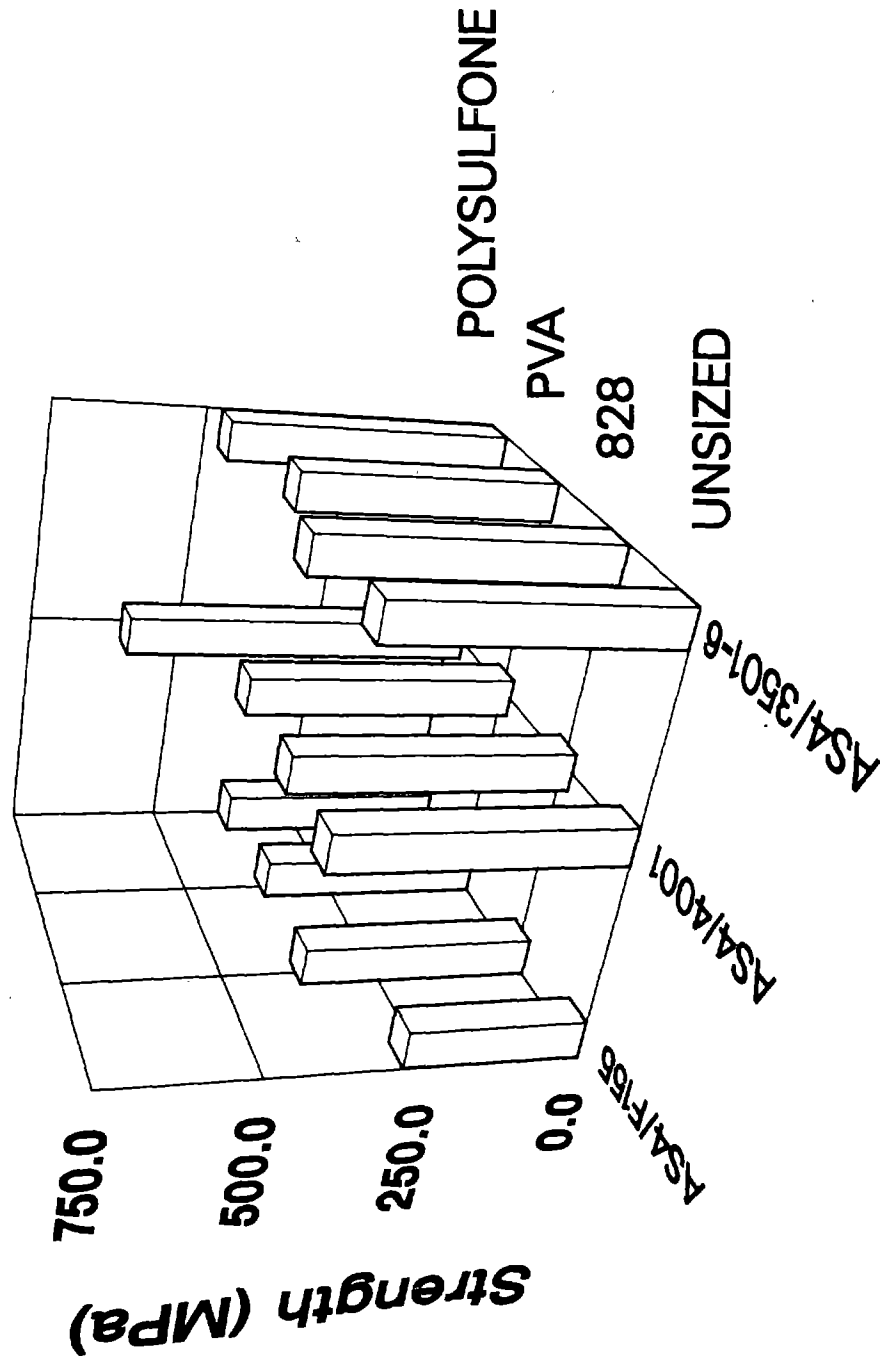


Figure 29. Quasi-Isotropic Laminate Axial Tensile Ultimate Strengths of the Twelve Fiber Sizing/Matrix Combinations at the Elevated Temperature, Wet Condition.

# Quasi-Isotropic Laminate Axial Tension Room Temperature, Dry (RTD)

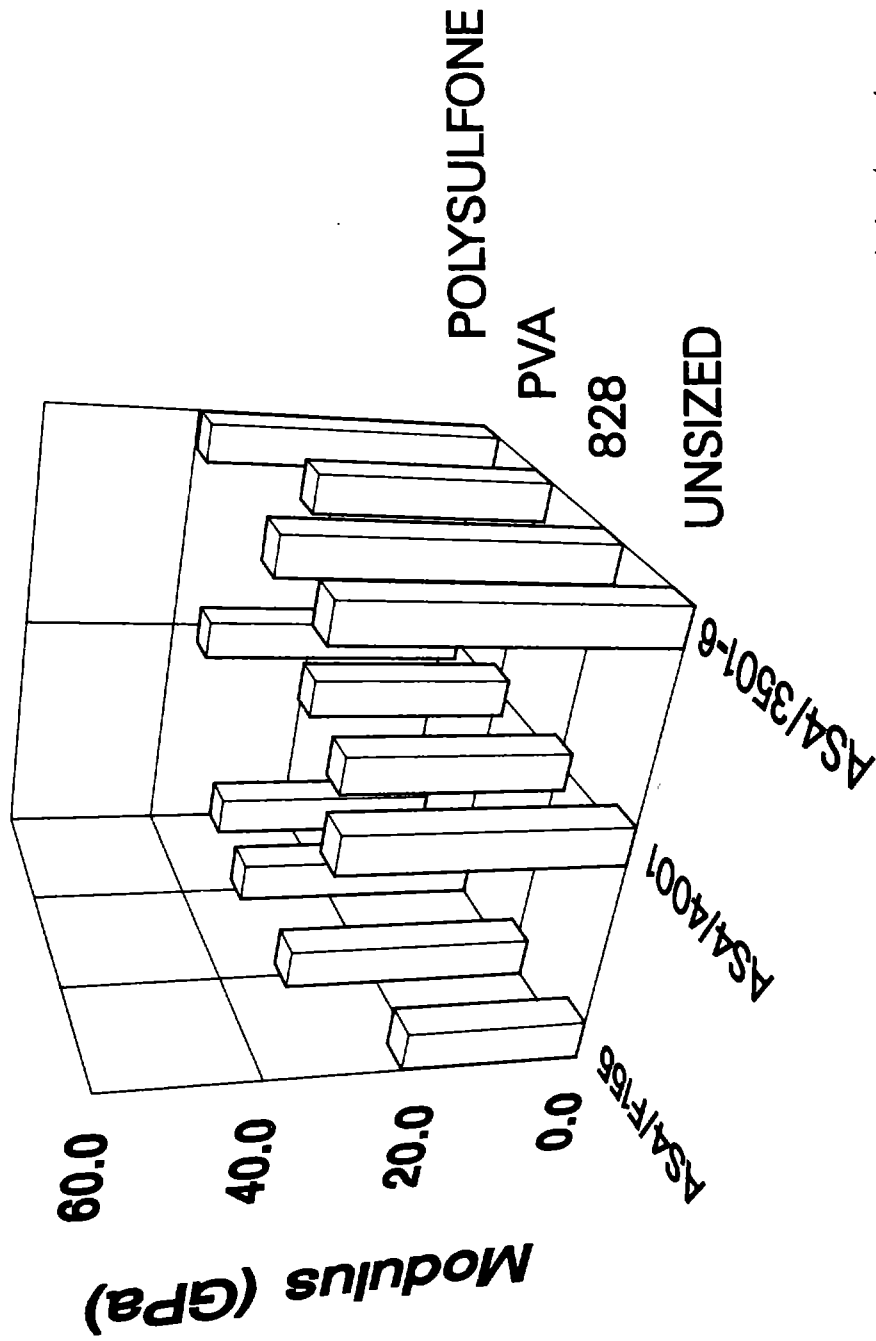


Figure 30. Quasi-Isotropic Laminate Axial Tension Moduli of the Twelve Fiber Sizing/Matrix Combinations at the Room Temperature, Dry Condition.

# Quasi-Isotropic Laminate Axial Tension Elevated Temperature, Wet (ETW)

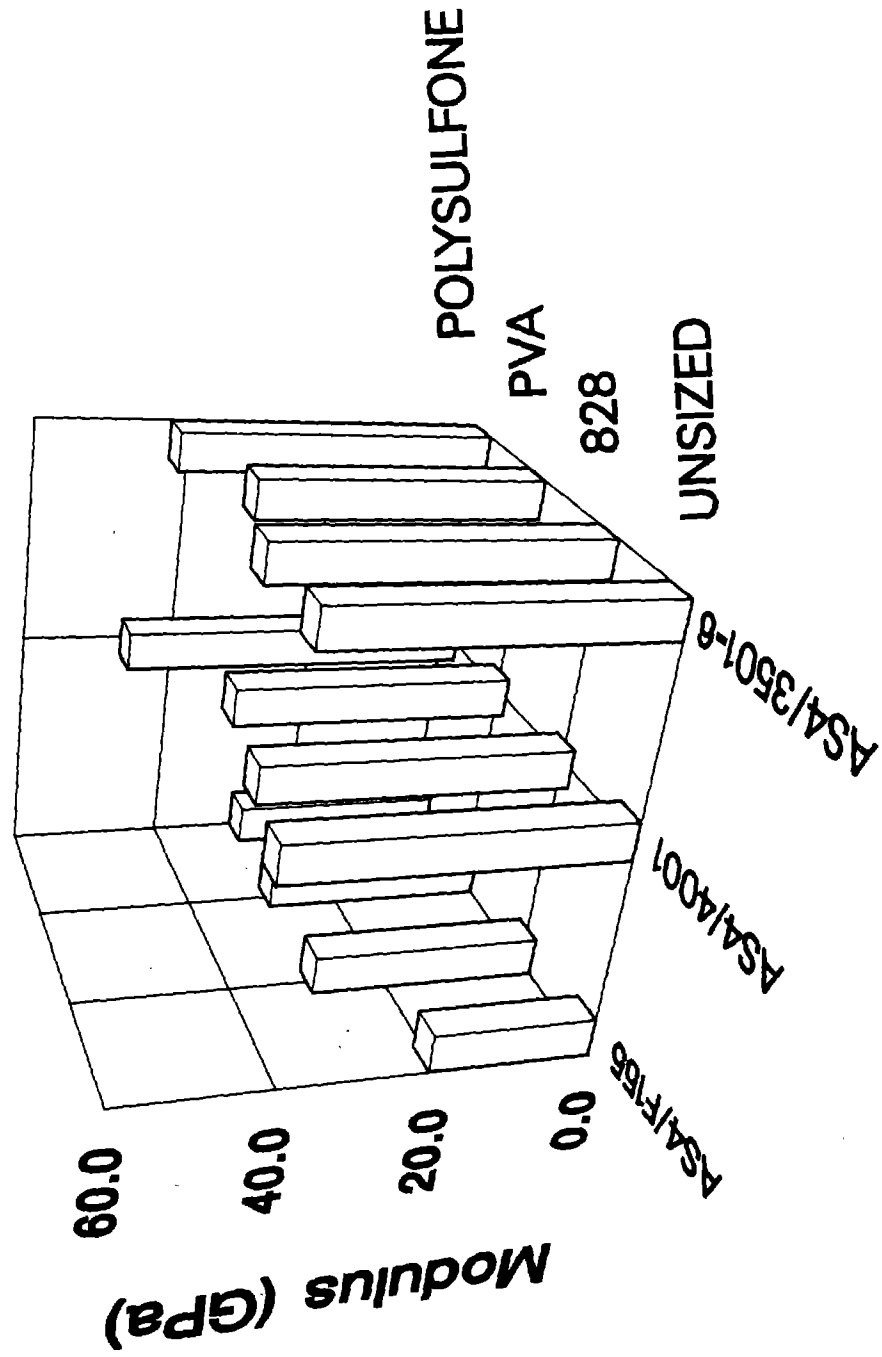


Figure 31. Quasi-Isotropic Laminate Axial Tension Moduli of the Twelve Fiber Sizing/Matrix Combinations at the Elevated Temperature, Wet Condition.

# Quasi-Isotropic Laminate Axial Tension Room Temperature, Dry (RTD)

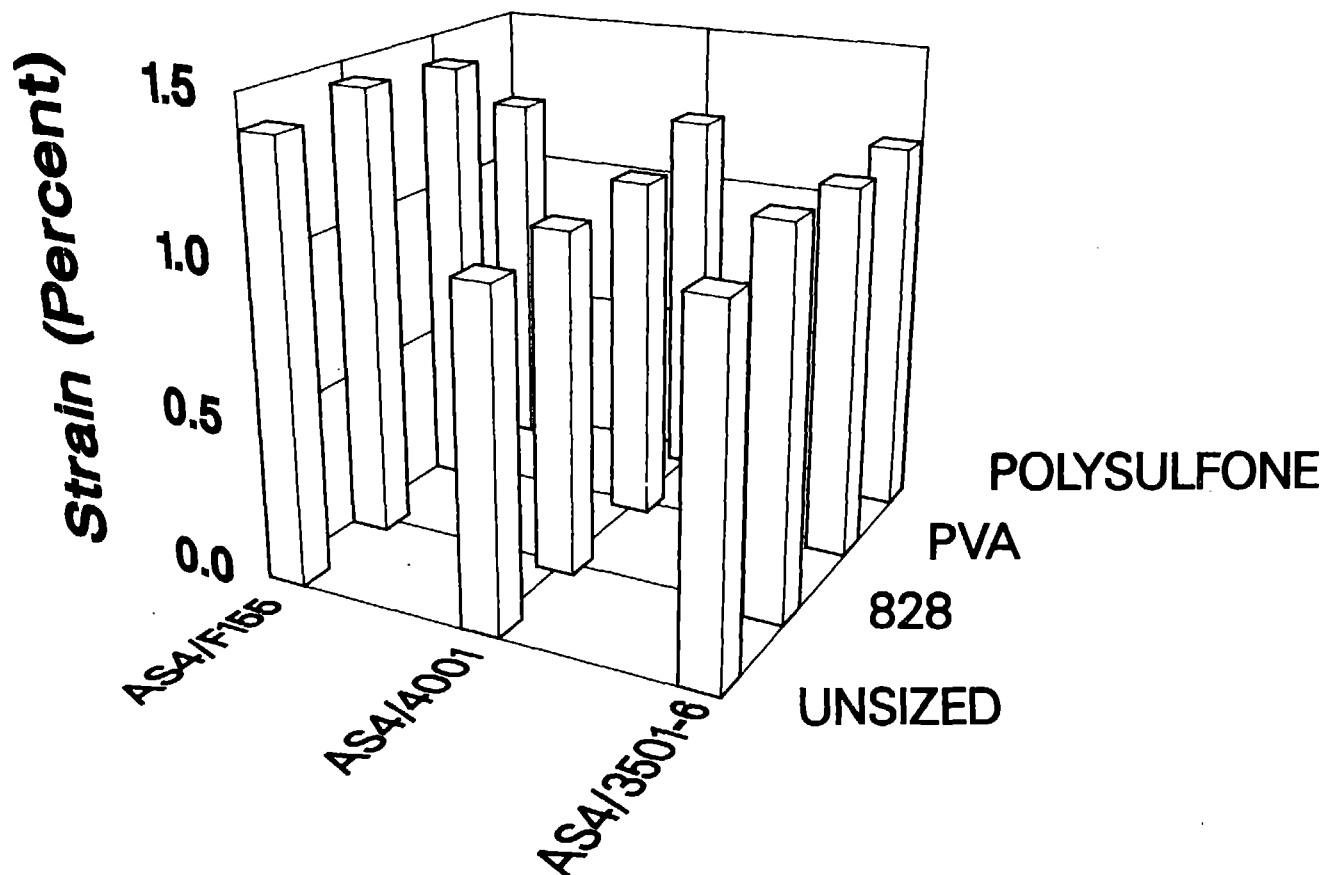


Figure 32. Quasi-Isotropic Laminate Axial Tensile Strains to Failure of the Twelve Fiber Sizing/Matrix Combinations at the Room Temperature, Dry Condition.

# Quasi-Isotropic Laminate Axial Tension Elevated Temperature, Wet (ETW)

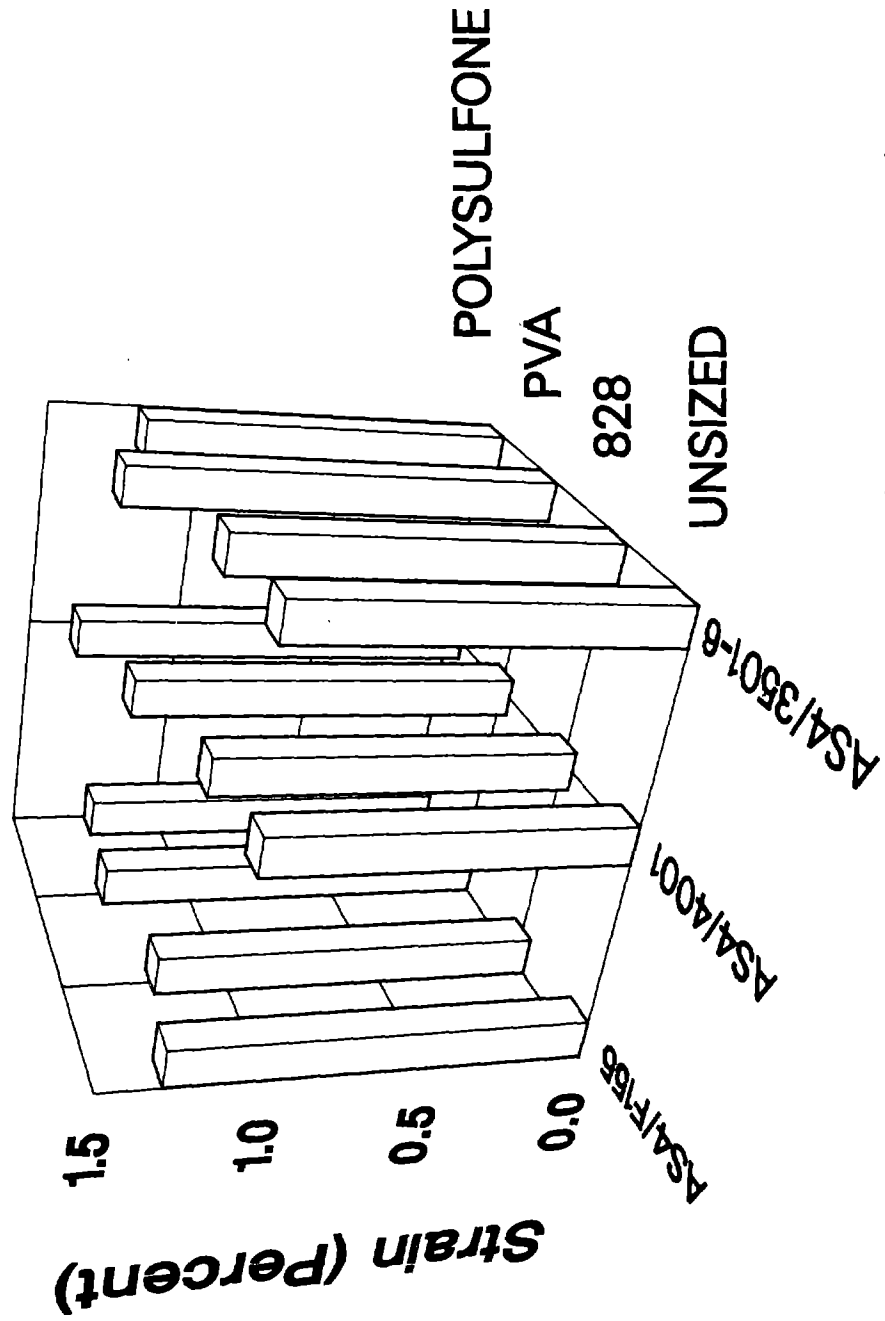


Figure 33. Quasi-Isotropic Laminate Axial Tension Strains to Failure of the Twelve Fiber Sizing/Matrix Combinations at the Elevated Temperature, Wet Condition.

composite systems, as indicated in Table 12. It will also be recalled that the transverse tensile strengths of the unidirectional AS4/F155 composites (see Table 8) stayed relatively high at the ETW condition, and the Hexcel F155 matrix itself exhibited reasonable strength retention, in both tension (Table 2) and shear (Table 3). It is possible that high laminate hygrothermal residual stresses contributed to the axial tensile strength loss of the AS4/F155 composite laminates.

In general, laminate tensile strength does not appear to be a sensitive indicator of fiber-matrix interfacial bond strength.

Axial tensile moduli of the various composite laminates are plotted in Figures 30 and 31 for the two test conditions. At both RTD and ETW conditions, the trends in modulus appeared to be similar to those for strength. That is, at the ETW condition, the axial tensile moduli of the AS4/3501-6 composites increased slightly, the moduli of the AS4/4001 composites increased significantly, and the moduli of the AS4/F155 composites decreased slightly. It is often possible to explain composite strength increases in terms of more favorable residual stresses at the hot, wet condition (lower thermal residual stresses due to being closer to the original cure temperature, and favorable offsetting stresses due to matrix moisture swelling). However, why composite moduli increased is not as obvious. The graphite fibers are unaffected by the temperature and moisture changes, and all three matrix materials become less stiff (as shown in Tables 2 and 3). The unidirectional composite moduli did decrease at the ETW condition, both in transverse tension (Tables 7 and 8) and in axial compression (Tables 9 and 10). Although not



measured here, the in-plane (longitudinal) shear moduli would also be expected to decrease. The occurrence of microcracking or local delamination would also tend to reduce the measured modulus. Obviously, more investigation will be required to explain the results observed here. Needless to say, laminate tensile modulus did not prove to be a suitable indicator of fiber-matrix interface performance.

Laminate axial tensile strains to failure are plotted in Figures 32 and 33. At both room temperature and elevated temperature, there was very little variation from one matrix material to another, or from one fiber sizing to another. At the RTD condition (Figure 32), the Hexcel F155 matrix composites exhibited composite strains to failure which were only about 15 percent higher than those of the Hercules 3501-6 matrix composites, even though the strain to failure of the rubber-toughened Hexcel F155 epoxy itself was over 250 percent higher than that of the Hercules 3501-6 epoxy. Similar comparisons can be made between the Hexcel F155 matrix and the Hercules 4001 bismaleimide matrix, and their composites. That is, neither fiber-matrix interface strength nor matrix strain to failure appeared to influence the measured laminate axial tensile strain to failure.

#### 4.5.2 Axial Compression

The axial compression testing was conducted using the end loaded, side supported test fixture described in Section 3.6.3. Results are summarized in Tables 13 and 14 for the RTD and ETW test conditions, respectively. Individual test specimen data are presented in Tables A26 through A31 of Appendix A. Stress-strain curves are included in Appendix B. As for the test results of the

Table 13

Average Quasi-Isotropic Laminate Compression Test Results  
At the Room Temperature, Dry Condition

Composite Material System	Ultimate Strength		Compressive Modulus		Ultimate Strain
	(MPa)	(ksi)	(GPa)	(Msi)	(percent)
<u>AS4/3501-6</u>					
Unsize	319	46.3	37.6	5.45	1.35
EPON 828	368	53.3	56.0	8.12	1.07
PVA	356	51.7	47.8	6.94	1.09
Polysulfone	383	55.5	49.0	7.10	1.30
<u>AS4/4001</u>					
Unsize	452	65.5	37.7	5.45	2.59
EPON 828	468	59.3	39.7	5.75	1.98
PVA	386	55.9	47.3	6.87	2.46
Polysulfone	445	64.5	44.9	6.52	2.65
<u>AS4/F155</u>					
Unsize	224	32.4	25.7	3.72	1.19
EPON 828	281	40.7	34.0	4.94	0.88
PVA	283	41.1	33.8	4.90	1.02
Polysulfone	256	37.1	26.8	3.88	1.03

Table 14

Average Quasi-Isotropic Laminate Compression Test Results  
At the Elevated Temperature, Wet Condition

Composite Material System	Test Temperature (°C)	Ultimate Strength		Compressive Modulus		Ultimate Strain (percent)
		(MPa)	(ksi)	(GPa)	(Msi)	
<u>AS4/3501-6</u>		93°C				
Unsize		296	42.9	40.4	5.86	0.87
EPON 828		296	43.0	39.6	5.74	0.96
PVA		213	30.9	29.8	4.32	0.80
Polysulfone		294	42.6	35.4	5.14	0.93
<u>AS4/4001</u>		93°C				
Unsize		337	48.9	32.1	4.66	1.41
EPON 828		356	51.6	38.4	5.57	1.10
PVA		305	44.2	34.4	5.00	1.09
Polysulfone		385	55.8	46.8	6.79	1.04
<u>AS4/F155</u>		38°C				
Unsize		135	19.6	16.3	2.36	1.65
EPON 828		182	26.5	23.2	3.37	1.22
PVA		154	22.3	28.8	4.18	0.69
Polysulfone		163	23.7	23.8	3.46	1.26

previous sections, the average strengths, moduli, and strains to failure are also presented in bar chart form, in Figures 34 through 39.

The room temperature, dry (RTD) laminate axial compressive strengths are plotted in Figure 34 for all 12 fiber sizing/matrix combinations. The trends were very similar to those for the unidirectional composites (see Figure 22). That is, while there was no clear trend between fiber surface treatments, there was a distinct trend from one matrix material to another. The AS4/4001 composites were somewhat stronger than the AS4/3501-6 composites, which in turn were considerably stronger than the AS4/F155 composites. For the unidirectional composites in axial compression (Section 4.4.2), this was postulated to be due to the differences in moduli of the different matrix materials (as presented previously in Tables 2 and 3). It is interesting that the same trend is observed here, where only one-fourth of the plies are oriented in the axial direction.

As can be seen by comparing Figure 35 to Figure 34, the reductions in axial compressive strengths at the ETW conditions were significant. The Hercules 3501-6 and 4001 matrix composite laminates decreased an average of about 20 percent in strength; the Hexcel F155 matrix composites lost an average of almost 40 percent. For the unidirectional composites, the strength losses were fairly uniform at 30 percent for all three systems, as discussed in Section 4.4.2. Again, it should be remembered that the AS4/F155 composites were tested at only 38°C (100°F), while the two 177°C (350°F) cure systems were tested at 93°C (200°F). That the AS4/F155 unidirectional composites suffered no more percentage strength loss at the ETW

# Quasi-Isotropic Laminate Axial Compression Room Temperature, Dry (RTD)

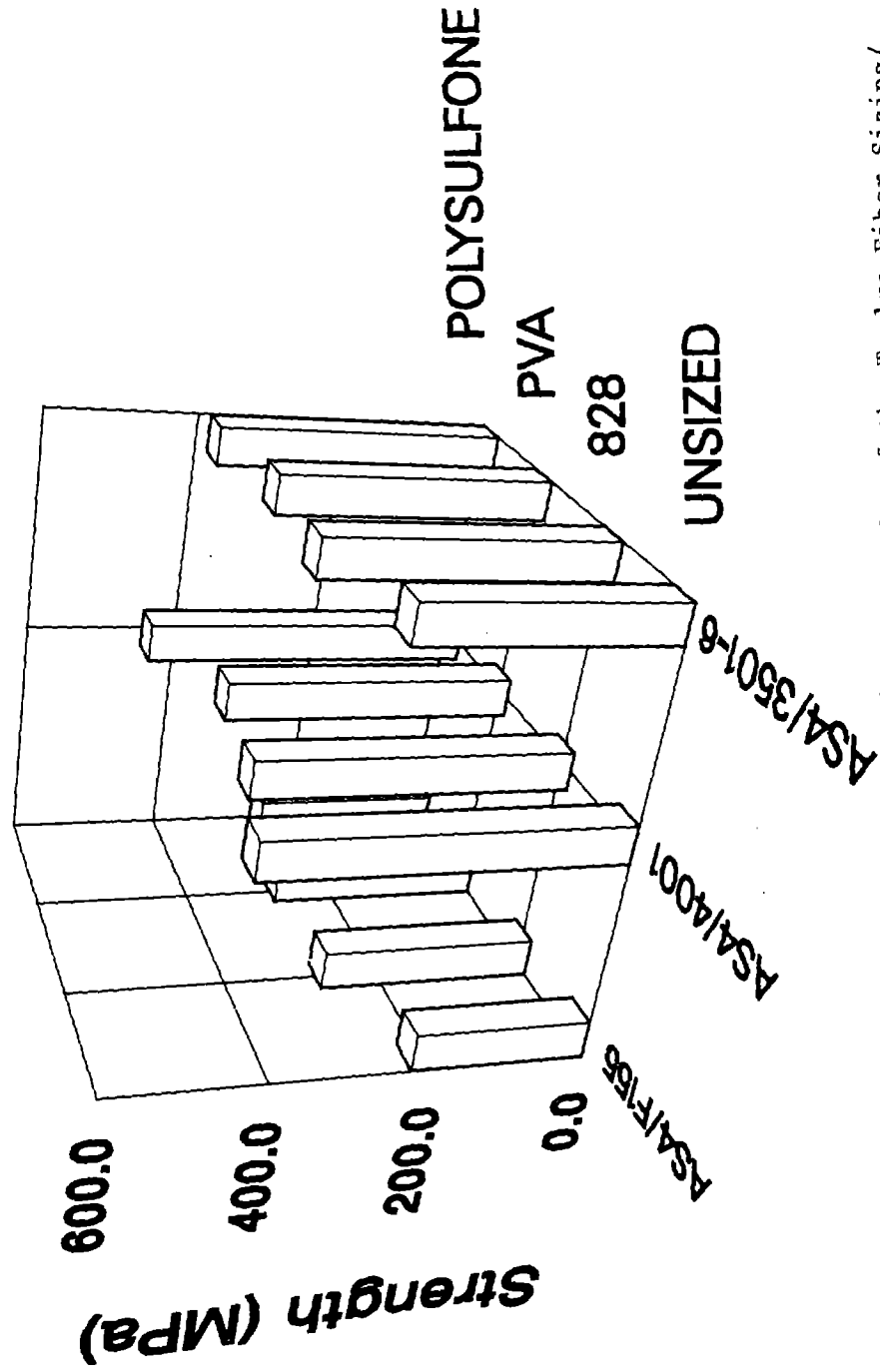


Figure 34. Quasi-Isotropic Laminate Axial Compressive Strengths of the Twelve Fiber Sizing/Matrix Combinations at the Room Temperature, Dry Condition.

# Quasi-Isotropic Laminate Axial Compression Elevated Temperature, Wet (ETW)

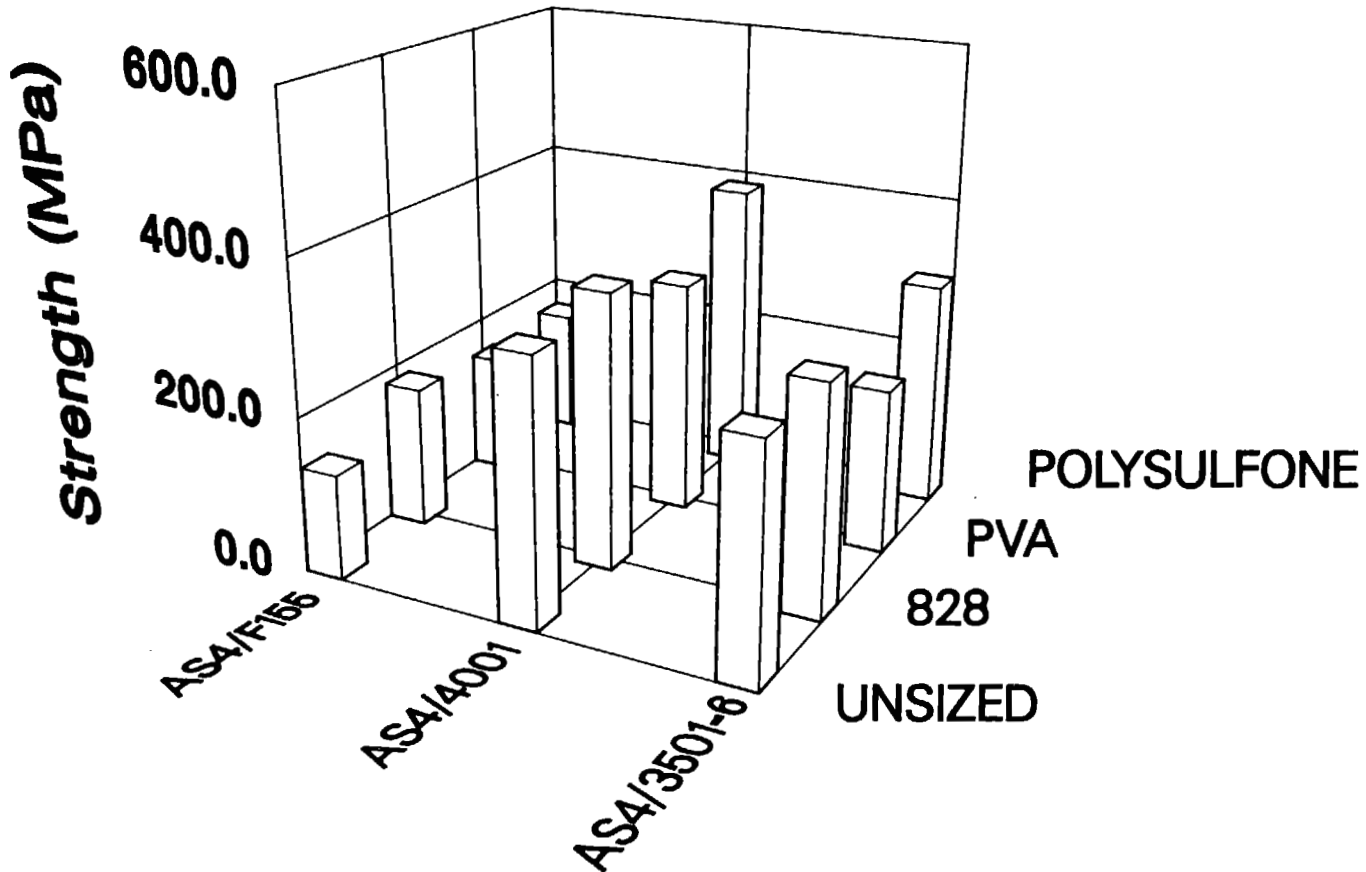


Figure 35. Quasi-Isotropic Laminate Axial Compressive Strengths of the Twelve Fiber Sizing/Matrix Combinations at the Elevated Temperature, Wet Condition.

# Quasi-Isotropic Laminate Axial Compression Room Temperature, Dry (RTD)

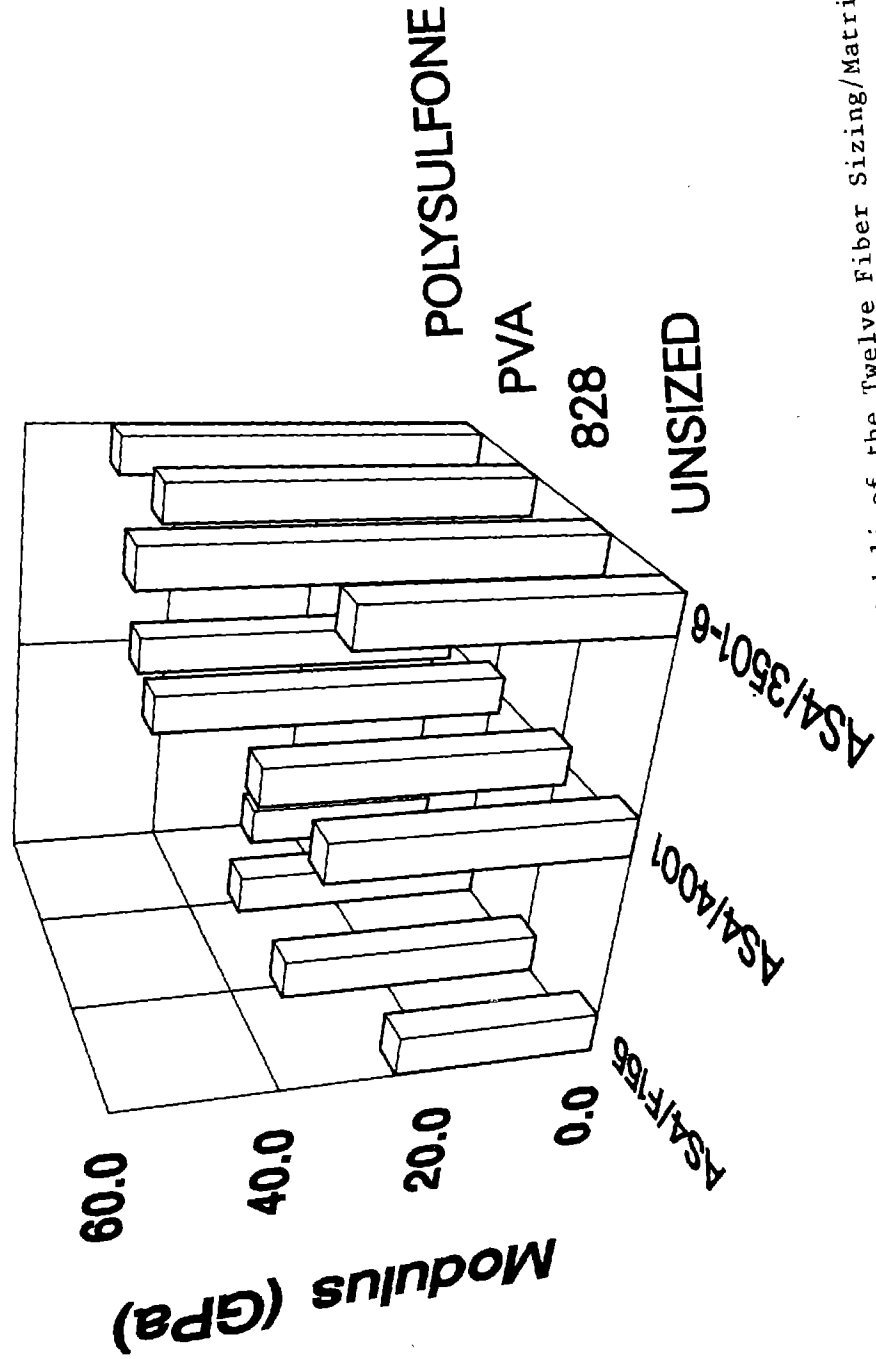


Figure 36. Quasi-Isotropic Laminate Axial Compressive Moduli of the Twelve Fiber Sizing/Matrix Combinations at the Room Temperature, Dry Condition.

# Quasi-Isotropic Laminate Axial Compression Elevated Temperature, Wet (ETW)

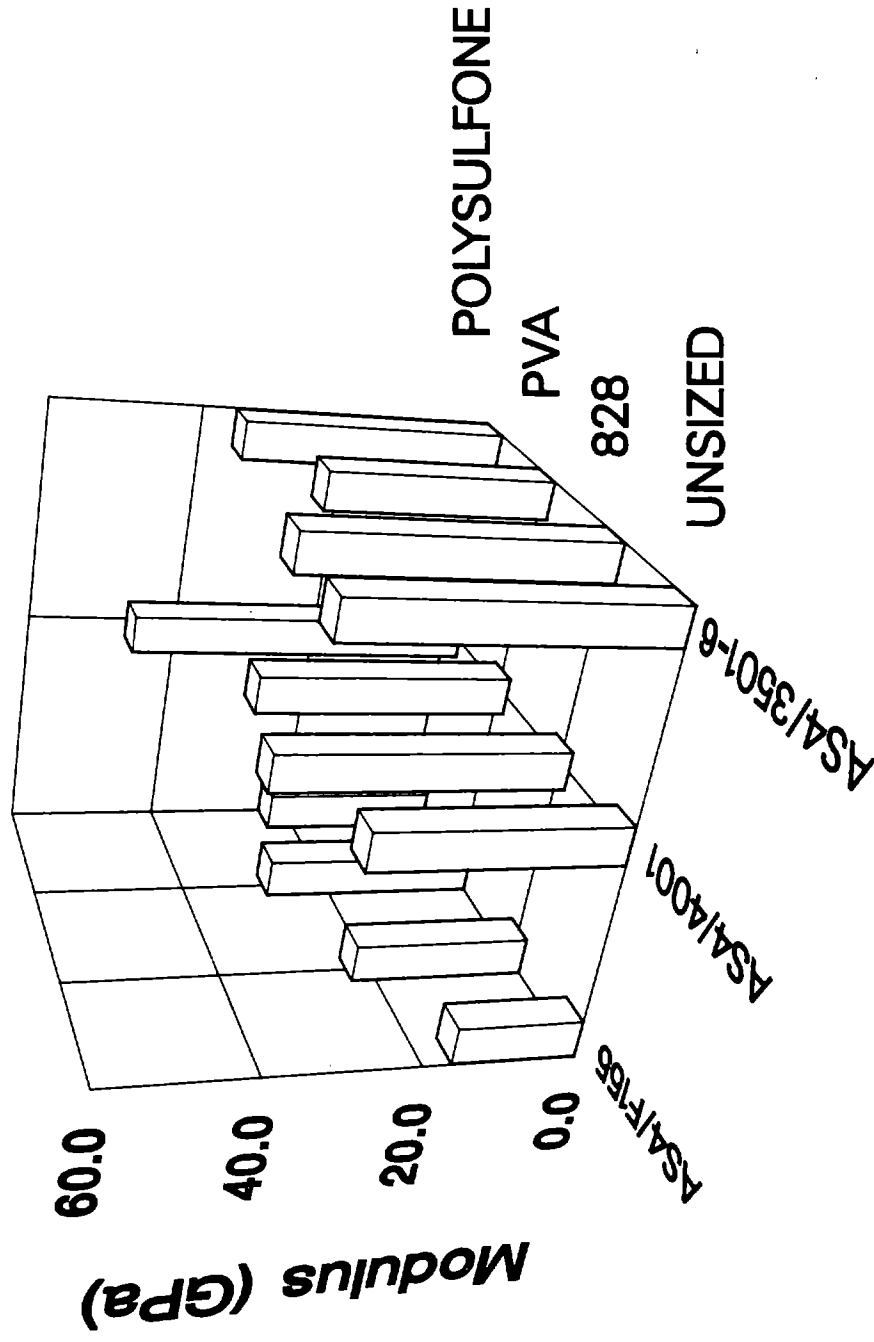


Figure 37. Quasi-Isotropic Laminate Axial Compressive Moduli of the Twelve Fiber Sizing/Matrix Combinations at the Elevated Temperature, Wet Condition.



## Quasi-Isotropic Laminate Axial Compression Room Temperature, Dry (RTD)

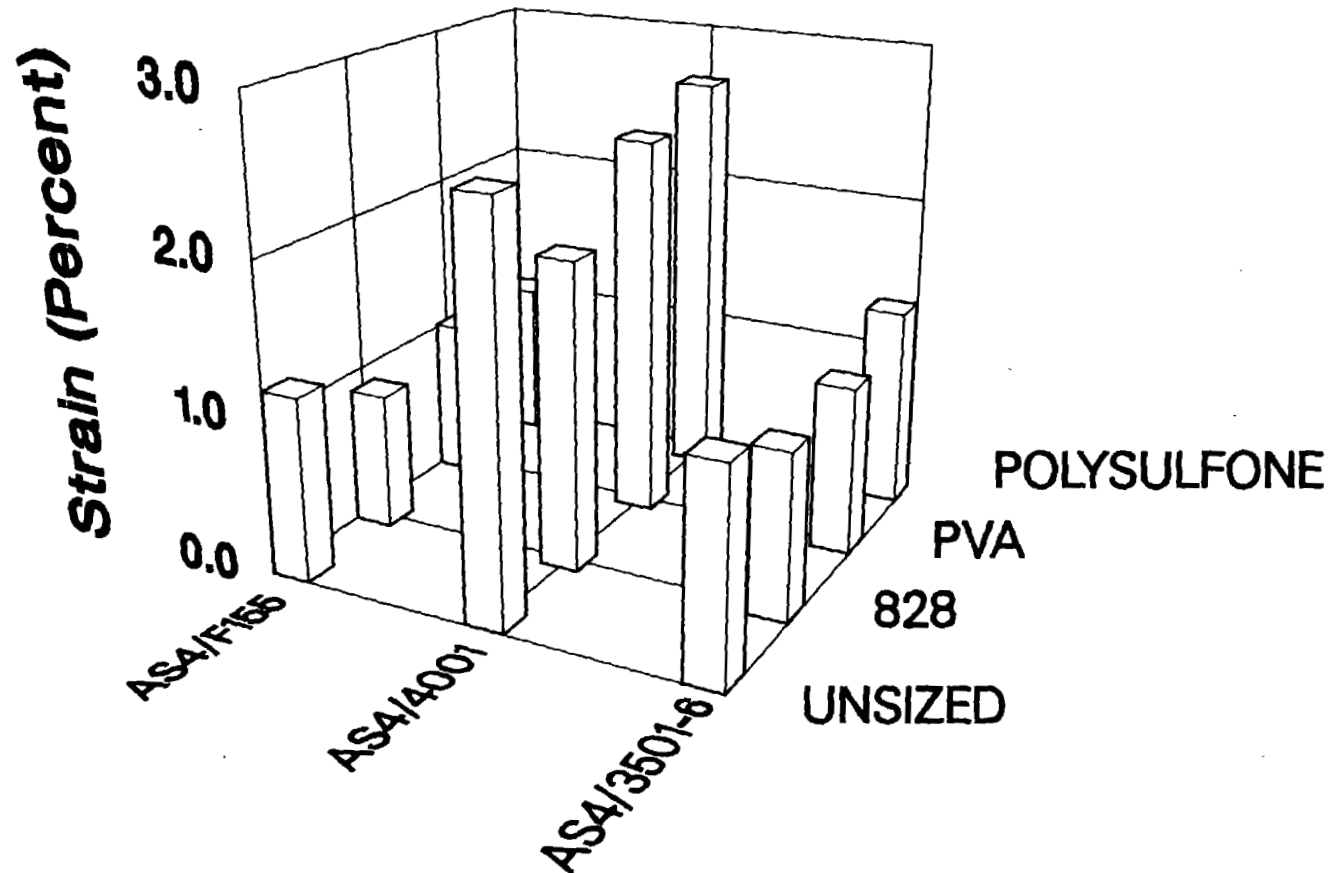


Figure 38. Quasi-Isotropic Laminate Axial Compressive Strains to Failure of the Twelve Fiber Sizing/Matrix Combinations at the Room Temperature, Dry Condition.

# Quasi-Isotropic Laminate Axial Compression Elevated Temperature, Wet (ETW)

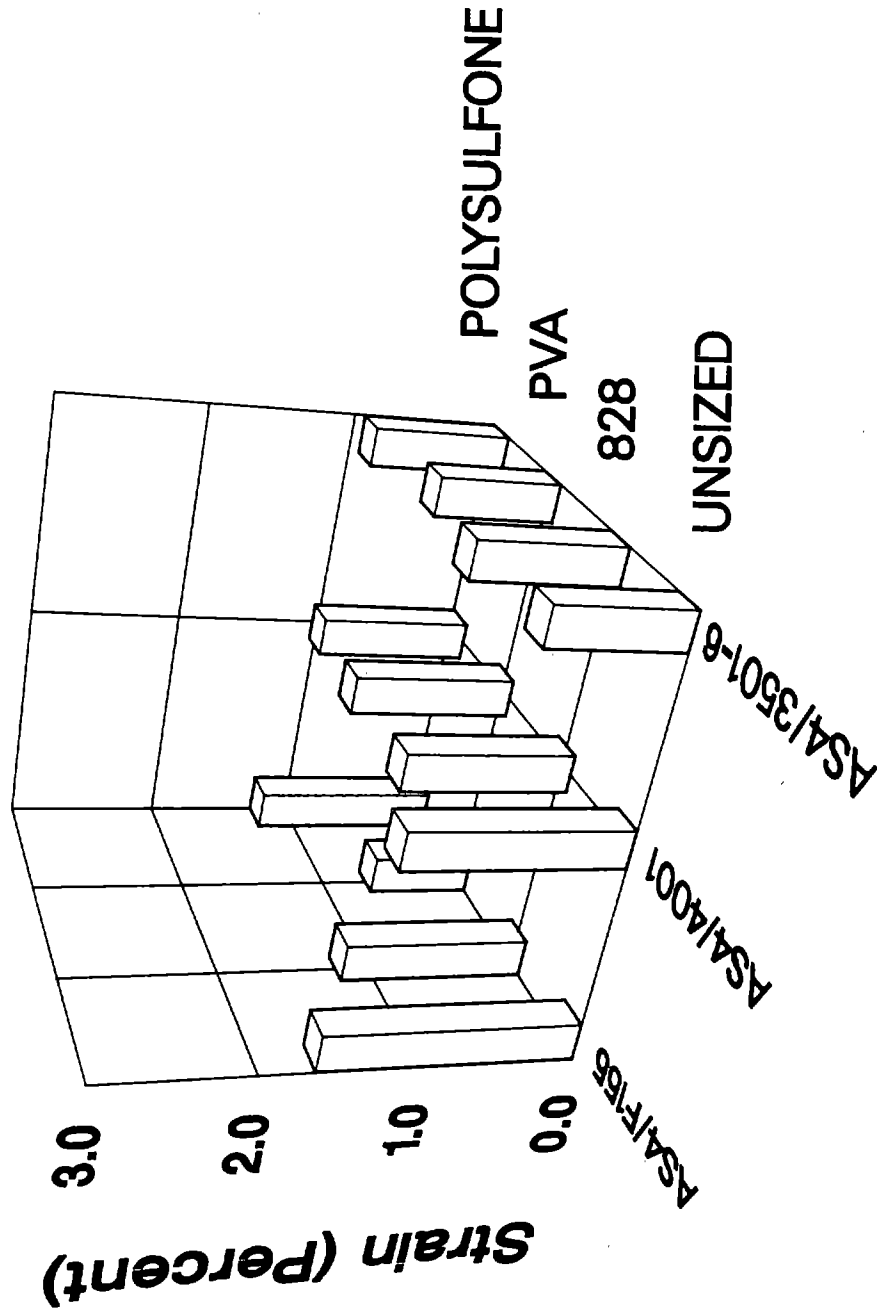


Figure 39. Quasi-Isotropic Laminate Axial Compressive Strains to Failure of the Twelve Fiber Sizing/Matrix Combinations at the Elevated Temperature, Wet Condition.

condition than the other two composites, while the AS4/F155 laminates suffered twice the loss of the other two laminates, is particularly interesting.

At the ETW condition, the PVA-sized fiber composite laminates generally exhibited somewhat lower strengths. This was not as evident in the unidirectional composites (Figure 23).

Room temperature modulus values are plotted in Figure 36. The lower laminate axial compressive stiffnesses of the AS4/F155 composites are presumably strongly associated with the lower fiber volumes of these composites (see Table 6 of Section 4.3). However, there does not seem to be a strong correlation. For example, for the AS4/3501-6 composites, the polysulfone-treated fiber composite had a much lower fiber volume than the PVA-sized fiber composite, viz, 52 versus 64 percent, yet its axial compressive modulus was slightly higher. Likewise, the unsized fiber AS4/F155 laminate had a very low fiber volume (28 percent). Yet its axial compressive modulus was not significantly lower than that of the polysulfone-sized fiber composite, which had a fiber volume of 42 percent.

The laminate axial compressive moduli at the ETW condition are plotted in Figure 37. The general response was similar to that observed for the unidirectional composites (Figure 25). The low modulus of the unsized AS4/F155 composite might be attributed to the low fiber volume previously quoted. But, in contrast, the high modulus of the polysulfone-sized AS4/4001 would not be explained by an abnormally high fiber volume.

Thus, while there are clearly as of yet unexplained anomalies in the data, no obvious trends seem to emerge. Laminate axial

compressive modulus does not appear to be a meaningful indicator of fiber-matrix interfacial bond strength.

The laminated composite axial compressive strain to failure values for all 12 combinations, at the room temperature, dry condition, are plotted in Figure 38. The relatively high strains to failure of the AS4/4001 composites are somewhat surprising. This did not occur for the unidirectional composites (Figure 26). As will be discussed in the next section, the RTD flexural strains to failure of the AS4/4001 laminates were not unusually high; this might have been expected based upon the axial compressive strain data shown in Figure 38. That is, one possible concern would be the occurrence of delaminations in these AS4/4001 laminates, as discussed in relation to the tensile impact data to be presented in Section 4.5.6. But this would be expected to strongly influence the flexure data also, and there was no indication of any anomalous behavior there.

At the elevated temperature, wet condition, unusually high strains to failure in the AS4/4001 did not occur. The test results are plotted in Figure 39. As for the unidirectional composite axial compressive strains, the laminate axial compressive strains tended to become more uniform among the 12 combinations at the ETW condition. For the unidirectional composites, the strains for all three matrix systems were lower at the ETW condition than at the RTD condition, as can be seen by comparing Tables 9 and 10, or Figures 26 and 27. This was associated with the uniformly reduced strengths, as discussed in Section 4.4.2. For the laminates, the axial compressive strains at the ETW conditions were also lower than at room temperature for the Hercules 3501-6 and 4001 matrix systems. The AS4/3501-6 laminates

averaged about a 50 percent reduction, with considerable scatter in both cases. On the other hand, the AS4/F155 laminate strains to failure increased by about 30 percent, except for the PVA-sized laminate, which did decrease by about 30 percent.

The cause of the increasing strains at failure of the AS4/F155 laminates at the ETW condition was the exceptionally low values at room temperature. These, in turn, are associated with the low strengths and moduli recorded. The corresponding strengths and moduli of the unidirectional composites were also low, of course, as previously discussed in Section 4.4.2. Thus, the AS4/F155 composites generally did not perform as well as the other two composite systems.

#### 4.5.3 Flexure

A standard three-point flexure fixture, as described in Section 3.6.5, was used in conducting all of the tests of the quasi-isotropic laminates. The average values of the results obtained are presented in Tables 15 and 16, for the room temperature, dry (RTD) and elevated temperature, wet (ETW) test conditions, respectively. Individual test specimen results are listed in Tables A32 through A37 of Appendix A. Stress-displacement plots are included in Appendix B. Bar chart plots are presented in Figures 40 through 45, for use in comparing data trends.

The RTD flexural strength averages are plotted in Figure 40. By comparing this plot with that for the laminate axial compressive strengths (Figure 34), it can be seen that the trends are very similar. This is as expected, since the axial compressive strengths were generally higher than the axial tensile strengths. That is, the flexural failures typically occurred on the compressive surface of

Table 15

Average Quasi-Isotropic Laminate Flexural Test Results  
At the Room Temperature, Dry Condition

Composite Material System	Ultimate Strength		Flexural Modulus		Ultimate Strain
	(MPa)	(ksi)	(GPa)	(Msi)	(percent)
<u>AS4/3501-6</u>					
Unsize	860	125	54.7	7.94	1.57
EPON 828	881	128	60.1	8.72	1.47
PVA	818	119	49.8	7.23	1.64
Polysulfone	943	137	59.2	8.59	1.59
<u>AS4/4001</u>					
Unsize	963	140	67.2	9.75	1.44
EPON 828	947	137	67.5	9.78	1.50
PVA	835	121	53.1	7.70	1.57
Polysulfone	1034	150	66.0	9.57	1.57
<u>AS4/F155</u>					
Unsize	583	85	32.4	4.70	1.83
EPON 828	669	97	40.0	5.80	1.58
PVA	658	95	42.3	6.13	1.65
Polysulfone	651	94	39.4	5.71	1.75

Table 16

Average Quasi-Isotropic Laminate Flexural Test Results  
At the Elevated Temperature, Wet Condition

Composite Material System	Test Temperature (°C)	Ultimate Strength (MPa)	Ultimate Strength (ksi)	Flexural Modulus (GPa)	Flexural Modulus (Msi)	Ultimate Strain (percent)
<u>AS4/3501-6</u>	93°C					
Unsized		548	80	54.3	7.87	0.97
EPON 828		651	94	59.0	8.55	1.09
PVA		530	77	47.1	6.83	1.13
Polysulfone		625	91	52.9	7.67	1.14
<u>AS4/4001</u>	93°C					
Unsized		718	104	66.2	9.60	1.11
EPON 828		691	100	52.8	7.65	1.31
PVA		668	97	57.3	8.31	1.17
Polsulfone		854	124	74.9	10.86	1.14
<u>AS4/F155</u>	38°C					
Unsized		371	54	25.4	3.69	1.47
EPON 828		472	69	41.1	5.96	1.15
PVA		364	53	33.3	4.83	1.09
Polysulfone		407	59	37.2	5.40	1.10

# Quasi-Isotropic Laminate Flexure Room Temperature, Dry (RTD)

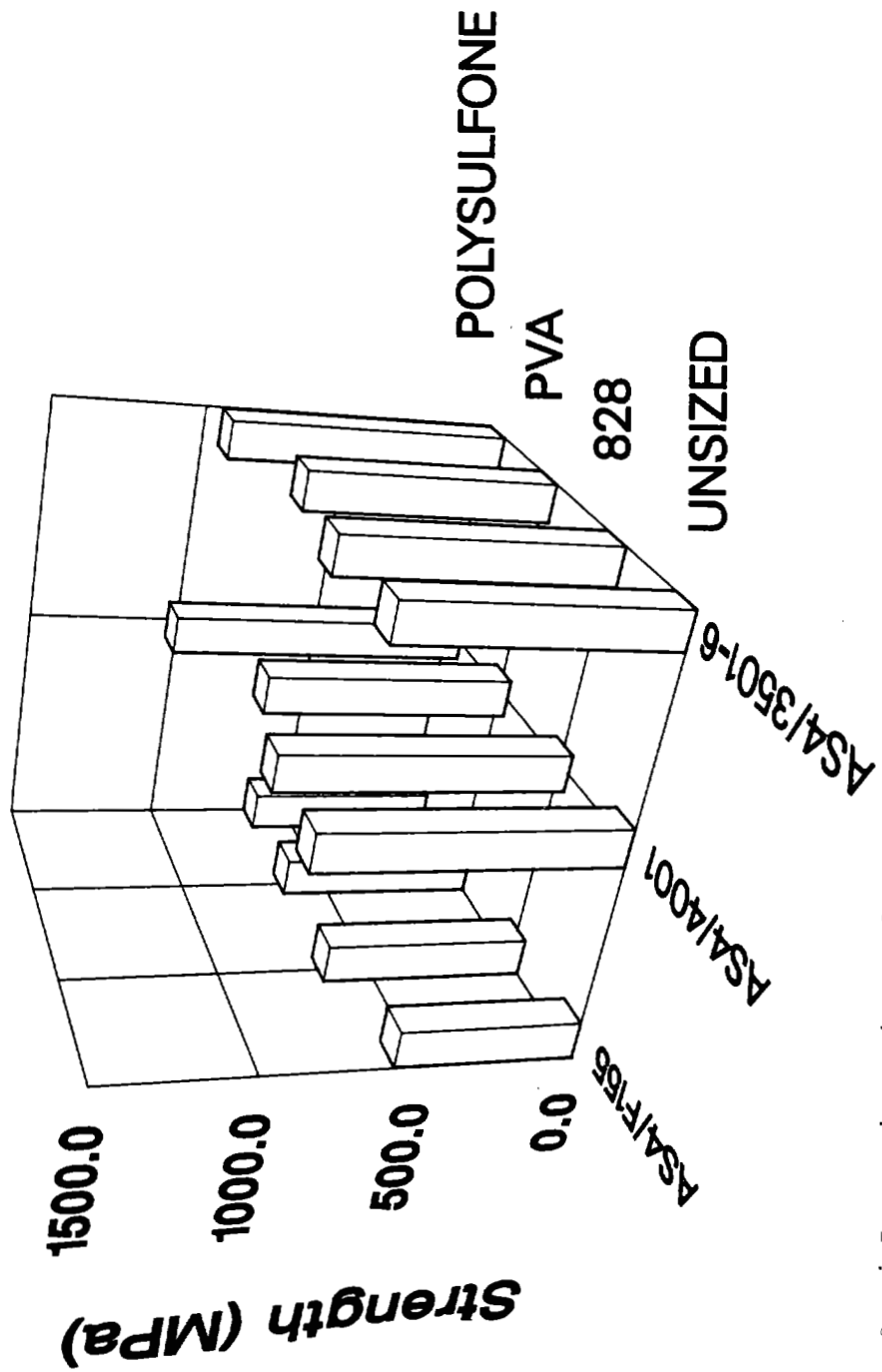


Figure 40. Quasi-Isotropic Laminate Flexural Strengths of the Twelve Fiber Sizing/Matrix Combinations at the Room Temperature, Dry Condition.



## Quasi-Isotropic Laminate Flexure Elevated Temperature, Wet (ETW)

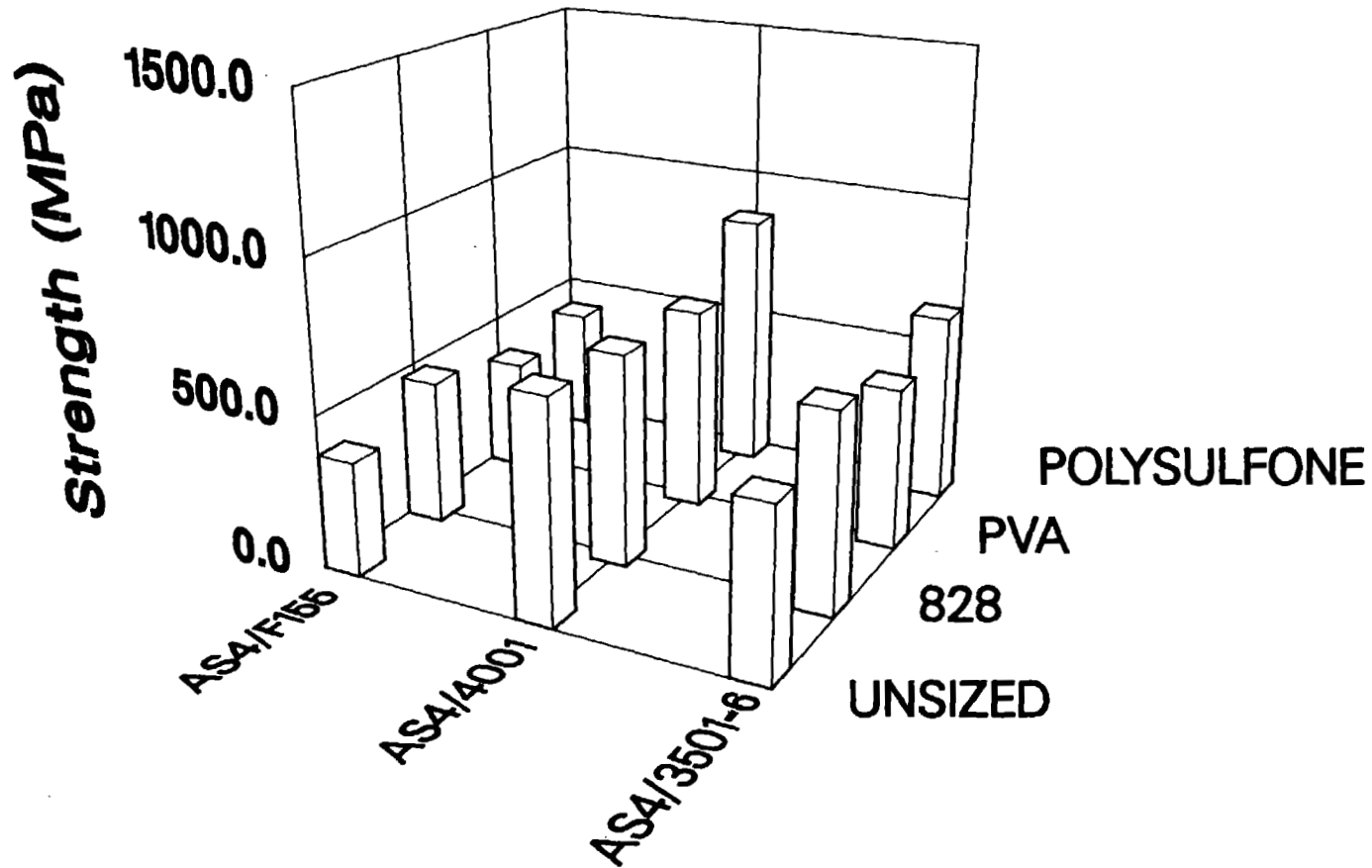


Figure 41. Quasi-Isotropic Laminate Flexural Strengths of the Twelve Fiber Sizing/Matrix Combinations at the Elevated Temperature, Wet Condition.

# Quasi-Isotropic Laminate Flexure Room Temperature, Dry (RTD)

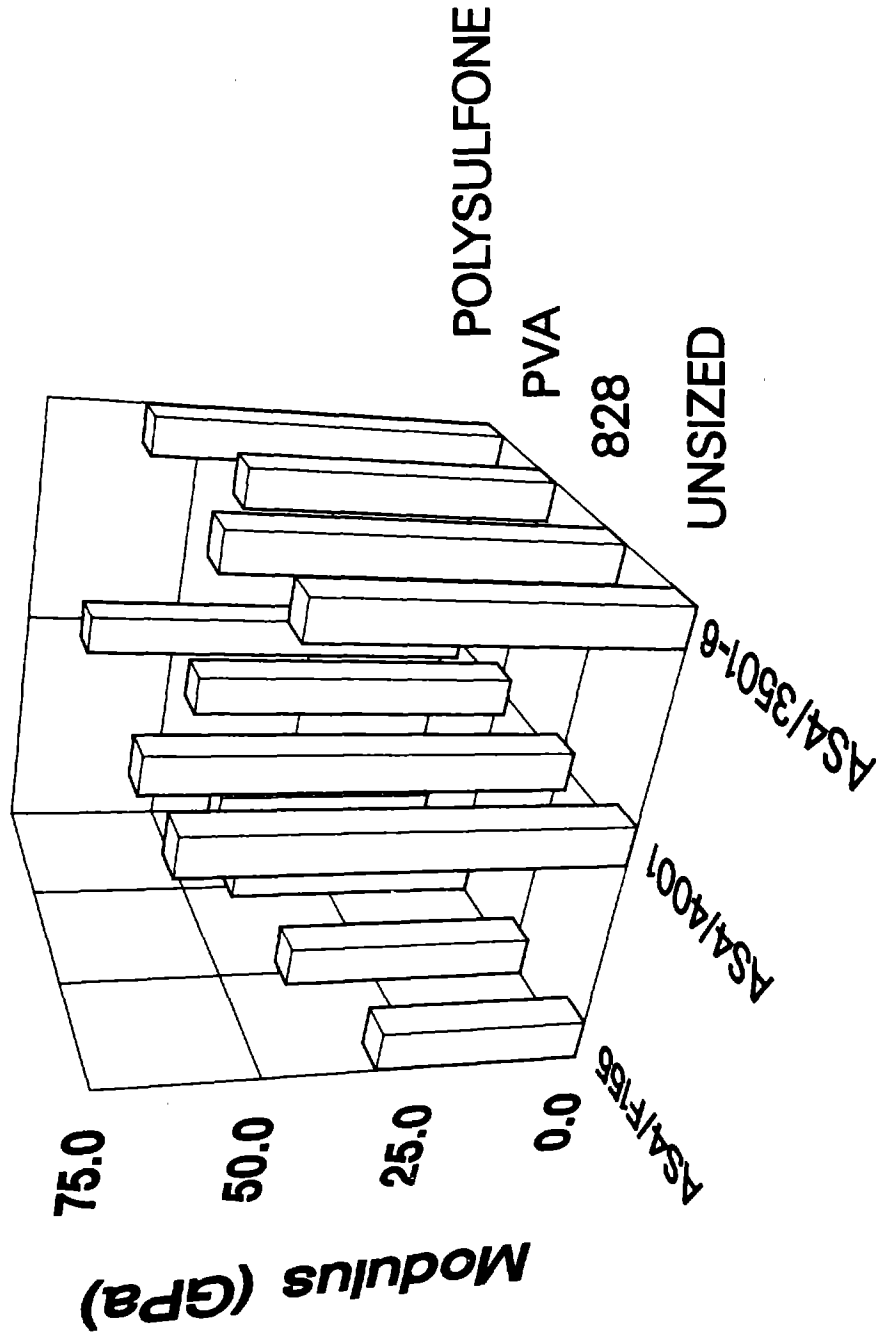
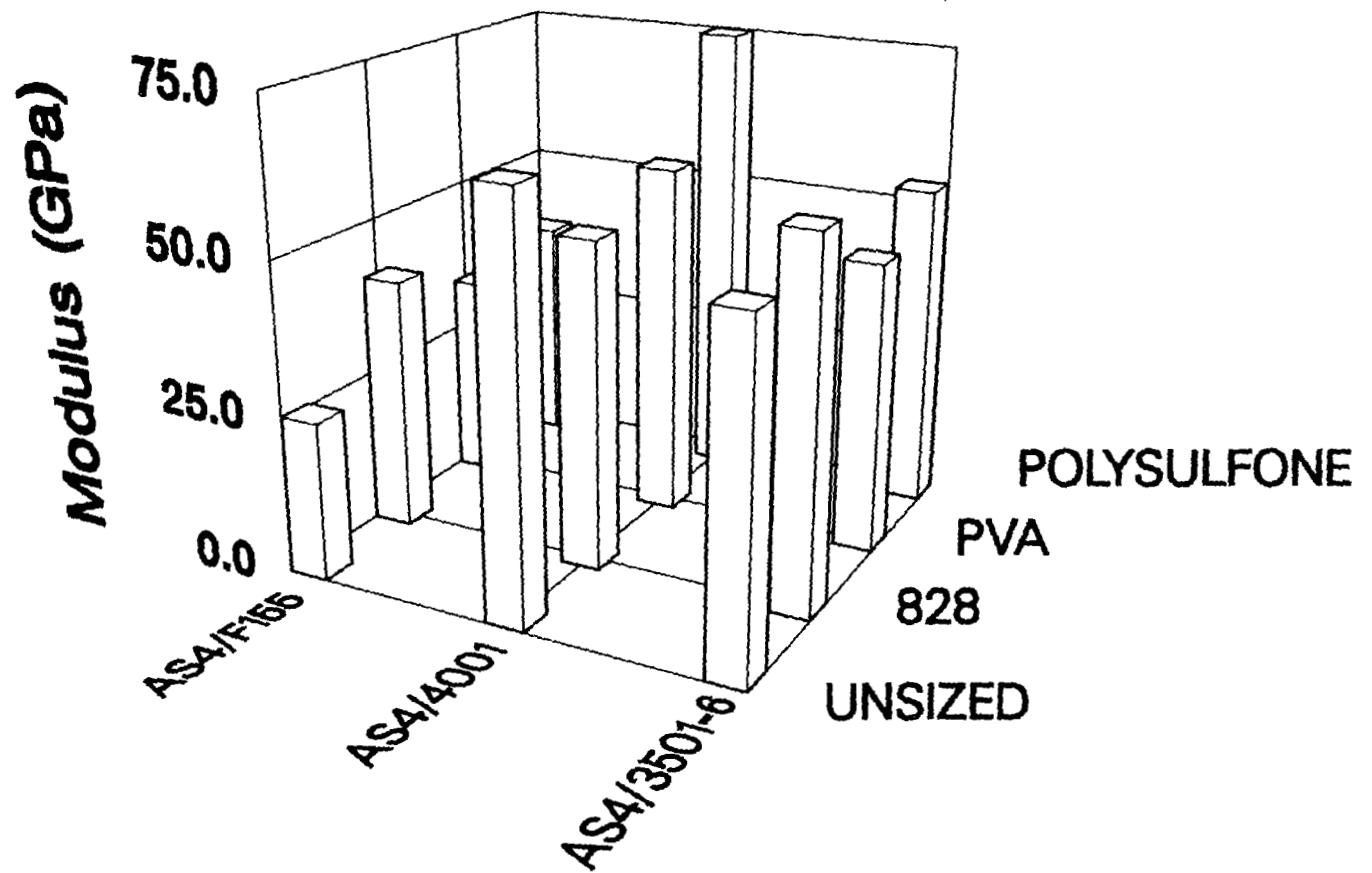


Figure 42. Quasi-Isotropic Laminate Flexural Moduli of the Twelve Fiber Sizing/Matrix Combinations at the Room Temperature, Dry Condition.

# Quasi-Isotropic Laminate Flexure Elevated Temperature, Wet (ETW)



# Quasi-Isotropic Laminate Flexure Room Temperature, Dry (RTD)

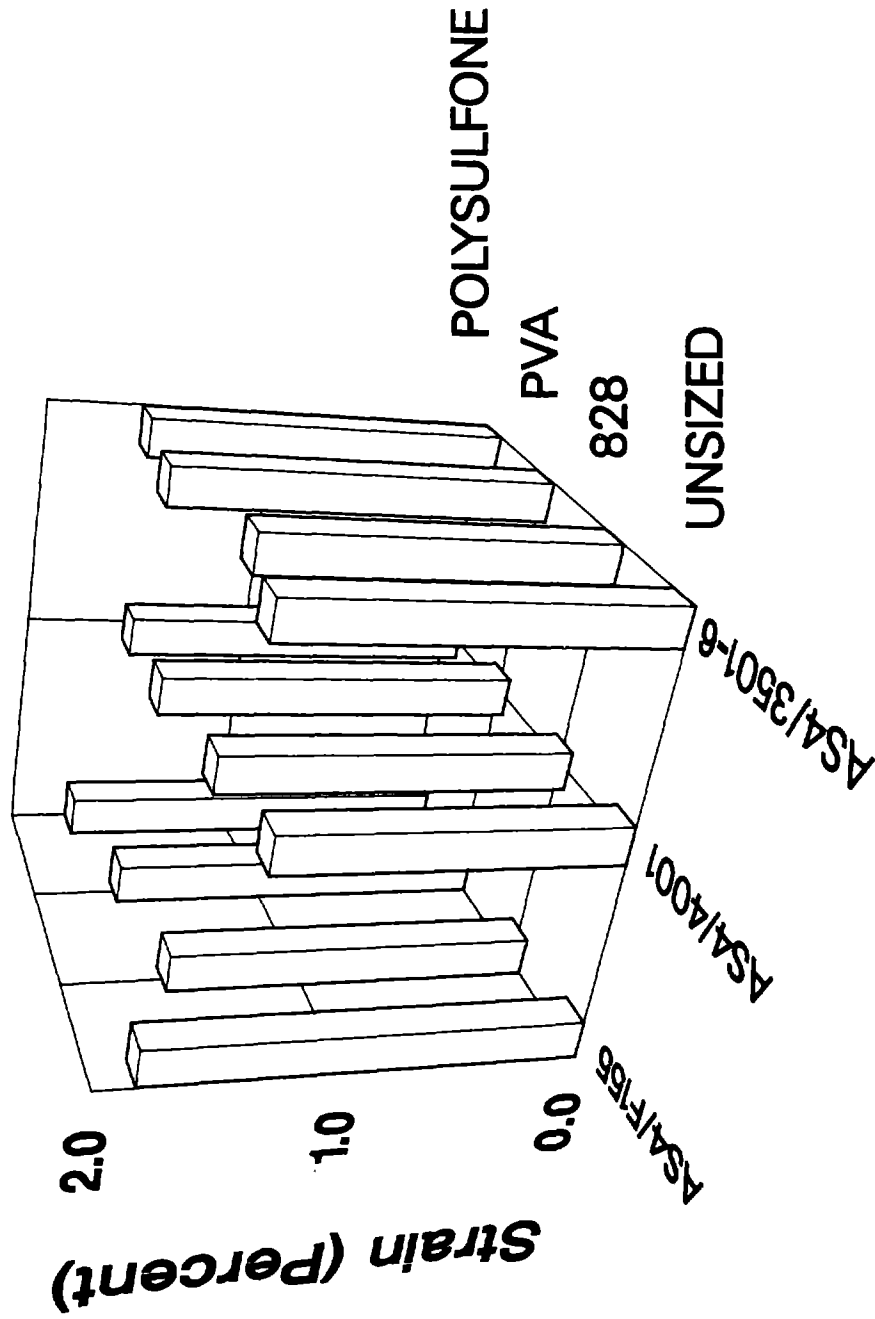


Figure 44. Quasi-Isotropic Laminate Flexural Strains to Failure of the Twelve Fiber Sizing/Matrix Combinations at the Room Temperature, Dry Condition.

# Quasi-Isotropic Laminate Flexure Elevated Temperature, Wet (ETW)

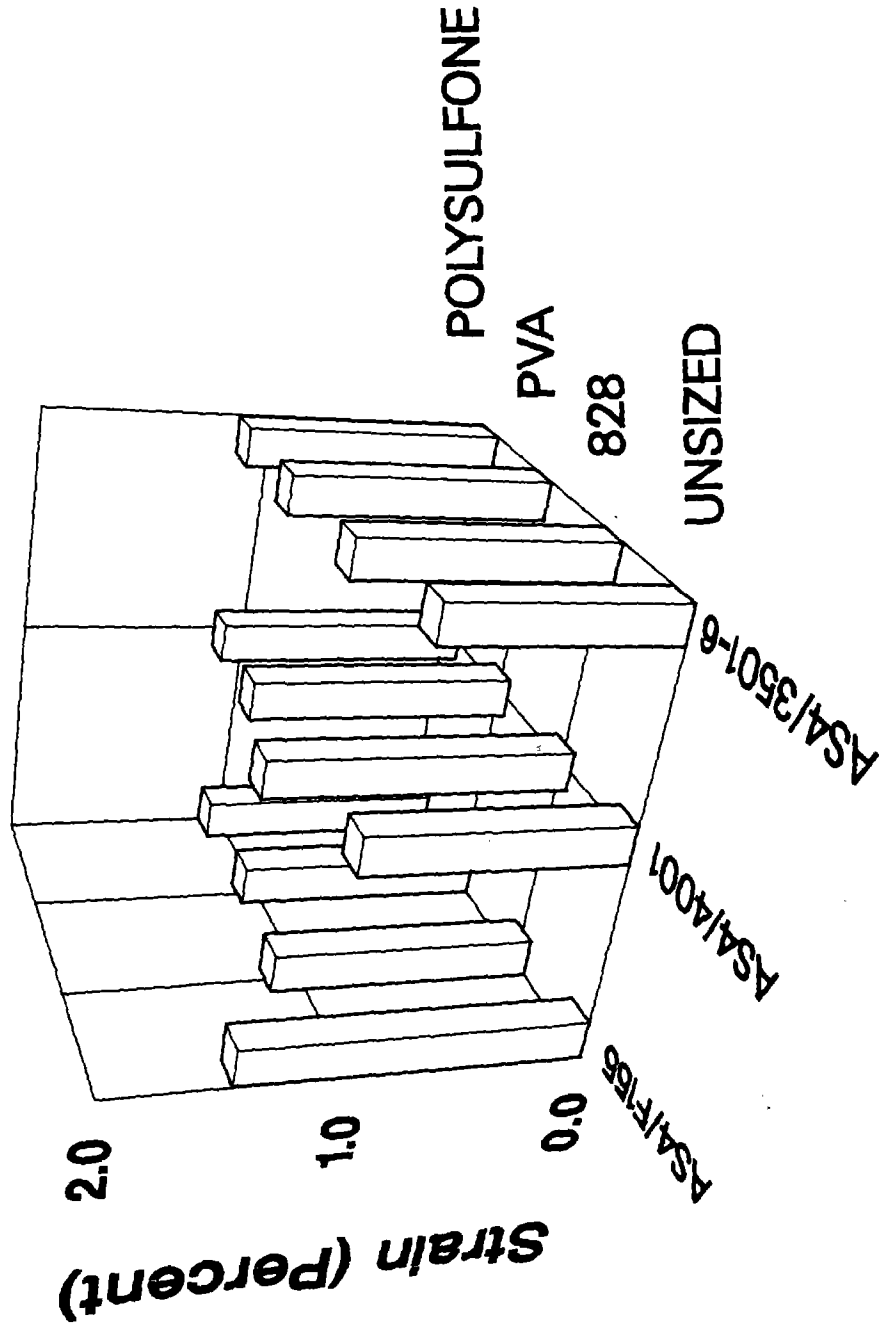


Figure 45. Quasi-Isotropic Laminate Flexural Strains to Failure of the Twelve Fiber Sizing/ Matrix Combinations at the Elevated Temperature, Wet Condition.

the specimen. The RTD axial tensile strengths of the AS4/4001 laminates were an exception, however, being lower than expected, as shown previously in Figure 28. This did not carry over into the flexural strength trends, however. The RTD flexural strengths of the AS4/4001 laminates were the highest of all three composite systems tested.

As shown in Figure 41, the ETW flexural strengths followed the same trends as the RTD strengths. Also, these elevated temperature, wet strengths were consistently lower than the corresponding room temperature, dry strengths, just as the axial compressive strengths were. At the ETW condition, the axial tensile strengths of these laminates were considerably higher than the axial compressive strengths, as can be seen by comparing Tables 12 and 14, or Figures 29 and 35. Thus, it is not surprising that the flexural strength data followed the same trends as the axial compressive strength data.

As for the axial compressive strengths, flexural strengths are not a suitable indicator of interfacial bond efficiency.

The flexural modulus data are plotted in Figures 42 and 43, for the RTD and ETW test conditions, respectively. The general response was similar to that of both the axial tensile and axial compressive moduli, and a similar conclusion can be drawn. That is, there does not appear to be a correlation between flexural modulus and fiber-matrix interface bond strength at either environmental condition.

Laminate flexural strains to failure are presented in Figures 44 and 45 for the RTD and ETW test conditions, respectively. It will be recalled (see Figure 38 of Section 4.5.2) that the laminate axial compressive strains to failure of the AS4/4001 composites were

exceptionally, and unexplainably, high. It will be noted in Figure 44 that this was not carried over to the RTD laminate flexural strains to failure. In fact, these strains were very similar in trend to the laminate axial tensile strains (as plotted in Figure 32), with the AS4/F155 laminates exhibiting the highest values.

Since the AS4/4001 laminates did not indicate this anomalously high axial compressive strain response when tested at the ETW condition, it would be expected that the ETW flexural strains would follow the axial strain values, both tensile and compressive. This was true, as can be seen by comparing Figure 45 with Figures 33 and 39.

In summary, nothing in the flexural test results was unexpected. Unfortunately, this test method does not appear to be a good indicator of fiber-matrix interfacial bond strength.

#### 4.5.4 Interlaminar Shear

Interlaminar shear tests, using the short beam shear test method, were performed on all 12 fiber sizing/matrix combinations as a further aid in evaluating the effectiveness of the various fiber surface treatments. Average laminate interlaminar shear strengths are listed in Tables 17 and 18 for the room temperature, dry and elevated temperature, wet test conditions, respectively. Individual test specimen results are included in Tables A38 through A43 of Appendix A. Bar chart plots are included here, as in Figures 46 and 47.

Room temperature, dry (RTD) interlaminar shear strengths are plotted in Figure 46. Little difference will be noted in the four Hercules 3501-6 epoxy matrix composite laminate combinations. The

Table 17

Average Quasi-Isotropic Laminate Interlaminar Shear Strengths  
At the Room Temperature, Dry Condition

Composite Material System	Shear Strength	
	(MPa)	(ksi)
<u>AS4/3501-6</u>		
Unsize	30	4.3
EPON 828	31	4.5
PVA	29	4.2
Polysulfone	30	4.4
<u>AS4/4001</u>		
Unsize	50	7.2
EPON 828	57	8.3
PVA	42	6.1
Polysulfone	52	7.5
<u>AS4/F155</u>		
Unsize	59	8.6
EPON 828	77	11.1
PVA	63	9.2
Polysulfone	63	9.1



Table 18

Average Quasi-Isotropic Laminate Interlaminar Shear Strengths  
At the Elevated Temperature, Wet Condition

Composite Material System	Test Temperature (°C)	Shear Strength (MPa) (ksi)	
<u>AS4/3501-6</u>	93°C		
Unsize		26	3.8
EPON 828		23	3.4
PVA		24	3.4
Polysulfone		25	3.6
<u>AS4/4001</u>	93°C		
Unsize		44	6.4
EPON 828		42	6.1
PVA		35	5.1
Polysulfone		49	7.1
<u>AS4/F155</u>	38°C		
Unsize		15	2.2
EPON 828		51	7.4
PVA		26	3.8
Polysulfone		46	6.7

# Quasi-Isotropic Laminate Interlaminar Shear Room Temperature, Dry (RTD)

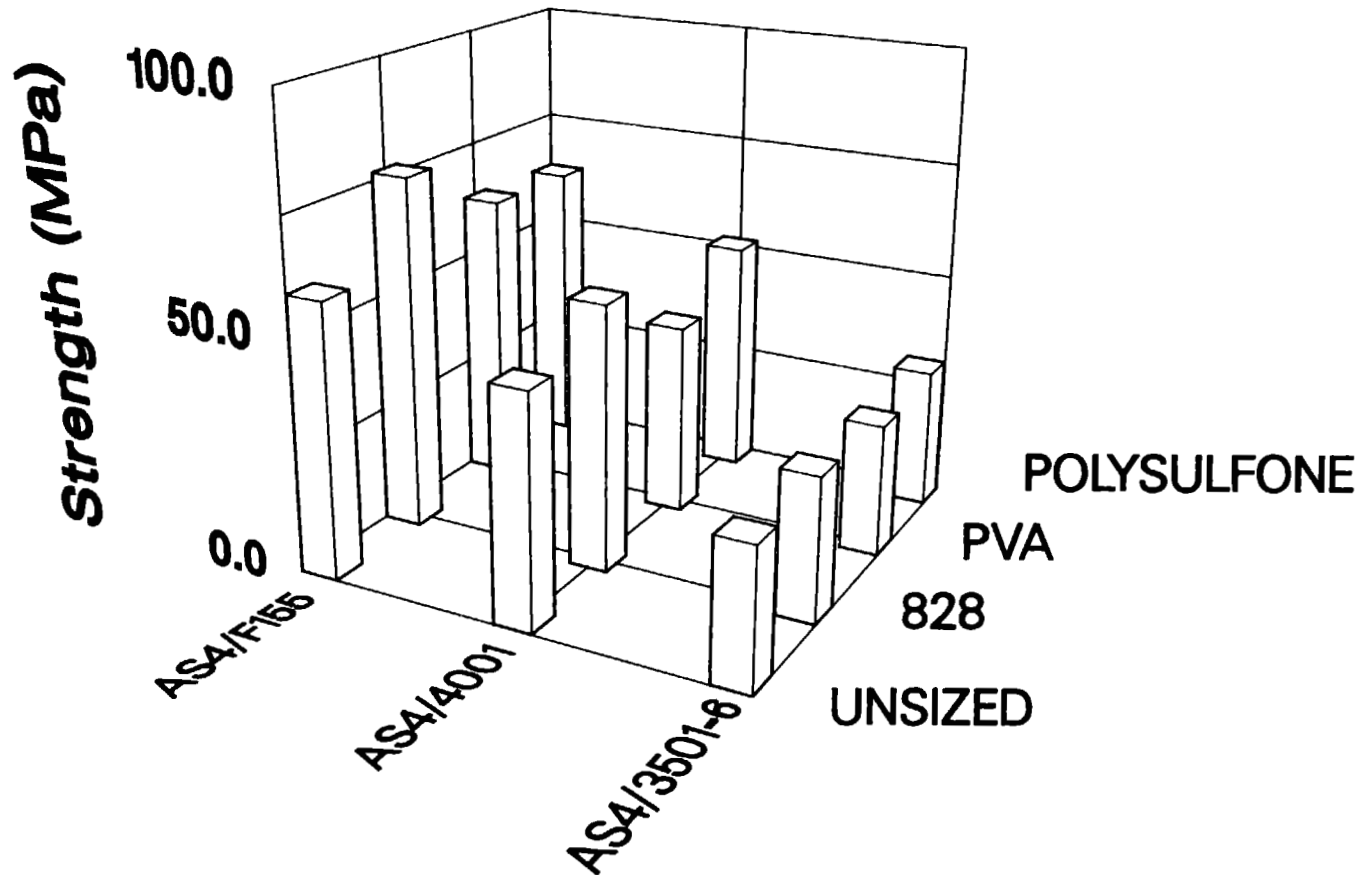


Figure 46. Quasi-Isotropic Laminate Interlaminar Shear Strengths of the Twelve Fiber Sizing/Matrix Combinations at the Room Temperature, Dry Condition.

# Quasi-Isotropic Laminate Interlaminar Shear Elevated Temperature, Wet (ETW)

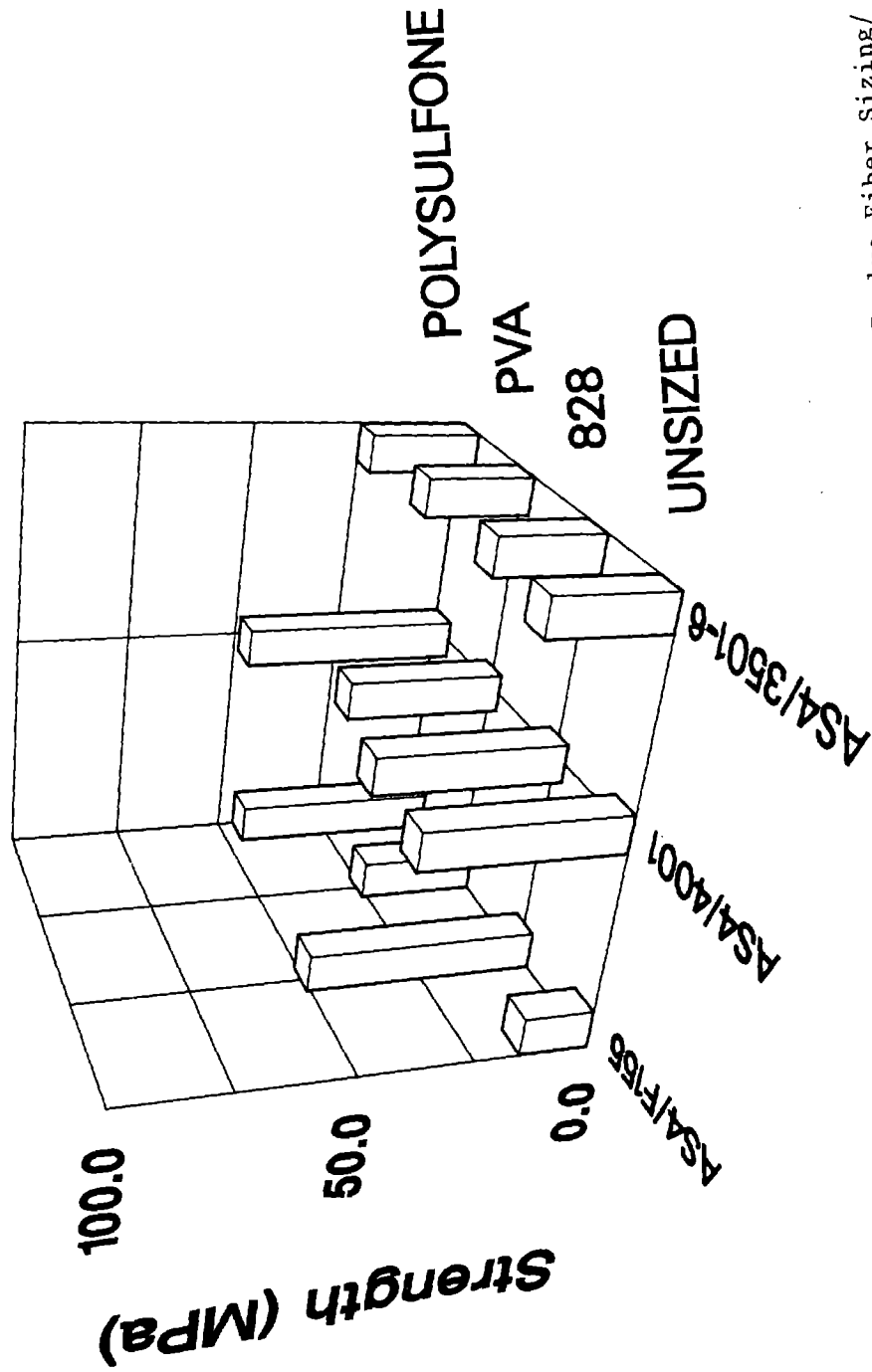


Figure 47. Quasi-Isotropic Laminate Interlaminar Shear Strengths of the Twelve Fiber Sizing/  
Matrix Combinations at the Elevated Temperature, Wet Condition.

EPON 828 and polysulfone fiber sizings yielded the highest shear strengths of the Hercules 4001 bismaleimide matrix composites, with the unsized and PVA-sized fiber combinations still having higher shear strengths than any of the Hercules 3501-6 matrix composites. The Hexcel F155 matrix composites produced the highest shear strengths of any of the three matrix materials at the room temperature, dry (RTD) condition, with the EPON 828 surface treatment being the best.

Elevated temperature, wet (ETW) interlaminar shear strengths are plotted in Figure 47. The baseline AS4/3501-6 graphite/epoxy composites were reduced in shear strength only slightly by the elevated temperature, wet condition, remaining relatively uniform in strength independent of fiber surface treatment. The Hercules 4001 matrix composites were also influenced only slightly, with the EPON 828 sizing resulting in the greatest composite shear strength loss. On the other hand, the Hexcel F155 matrix composites were more strongly, and nonuniformly, influenced by the ETW condition. The composites incorporating the unsized and PVA-sized graphite fibers were degraded in shear strength the most. For example, the unsized fiber/F155 matrix composite had exhibited one of the highest shear strengths in the RTD condition (Figure 46). But in the ETW condition (Figure 47), it displayed the lowest shear strength of all 12 combinations tested.

#### 4.5.5 Tensile Impact

Instrumented tensile impact testing was performed at both environmental conditions on most of the 12 fiber/matrix combinations. Only 10 of the 12 combinations were tested at the room temperature,

dry (RTD) condition, due to an unexplained problem of delamination of the unsized and PVA-treated graphite fiber composite laminates of the Hercules 4001 bismaleimide matrix. A possible cause of these delaminations was the excessive thermal stresses induced during cooldown from the cure temperature, as will be discussed later.

Elevated temperature, wet (ETW) tensile impact testing was conducted only on the Hercules 3501-6 and Hexcel F155 epoxy matrix composites, for all four fiber surface treatments. No Hercules 4001 tensile impact specimens were successfully tested at the elevated temperature, wet (ETW) condition due to the previously mentioned problem of delamination in the Hercules 4001 matrix laminates. Lack of a sufficient amount of extra Hercules 4001 resin prevented preparing additional composite laminates to repeat these tensile impact tests. Since none of the four fiber surface treatment combinations of the Hercules 4001 bismaleimide matrix composites could be successfully tested, this suggests that the ETW condition is even more detrimental than the RTD condition.

The averages of all of the quasi-isotropic laminate tensile impact tests which were successfully performed are included in Tables 19 and 20. Individual test specimen data are presented in Tables A44 through A48 of Appendix A. Individual force versus time and energy versus time plots are shown in Appendix B. For ease in making comparisons, the averages are also plotted in bar chart form in Figures 48 through 53.

Average tensile impact strength values at the RTD condition are plotted in Figure 48. The AS4/3501-6 laminates and the two AS4/4001 laminates which were successfully impact tested all exhibited about

Table 19

Average Quasi-Isotropic Laminate Instrumented Tensile Impact  
Test Results at the Room Temperature, Dry Condition

Composite Material System	Ultimate Strength		Dynamic Modulus		Total Energy	
	(MPa)	(ksi)	(GPa)	(Msi)	(kJ/m <sup>3</sup> )	(ft-lb/in <sup>3</sup> )
<u>AS4/3501-6</u>						
Unsize	414	60.0	36.5	5.3	1259	28
EPON	412	59.8	40.0	5.8	1169	26
PVA	390	56.6	35.2	5.1	1178	26
Polysulfone	407	59.0	35.2	5.1	1322	29
<u>AS4/4001</u>						
Unsize*						
EPON 828	385	55.8	33.8	4.9	1214	27
PVA*						
Polysulfone	427	62.0	40.0	5.8	1349	30
<u>AS4/F155</u>						
Unsize	276	40.0	20.7	3.0	989	22
EPON 828	334	48.5	30.3	4.4	1034	23
PVA	361	52.4	33.1	4.8	1169	26
Polysulfone	370	53.6	35.2	5.1	989	22

\*No data taken - see text.

Table 20

Average Quasi-Isotropic Laminate Instrumented Tensile Impact  
Test Results at the Elevated Temperature, Wet Condition

Composite Material System	Test Temperature (°C)	Ultimate Strength		Dynamic Modulus		Total Energy	
		(MPa)	(ksi)	(GPa)	(Msi)	(kJ/m <sup>3</sup> )	(ft-lb/in <sup>3</sup> )
<u>AS4/3501-6</u>	93°C						
Unsize		381	55.3	40.0	5.8	1349	30
EPON 828		507	73.5	40.0	5.8	1529	34
PVA		374	54.3	27.6	4.0	1484	33
Polysulfone		492	71.3	37.9	5.5	1754	39
<u>AS4/4001</u>	93°C						
Unsize							
EPON 828							
PVA							
Polysulfone							
		No data taken - see text					
<u>AS4/F155</u>	38°C						
Unsize		234	34.0	17.2	2.5	1102	25

Table 20

- Continued -

Composite Material System	Test Temperature (°C)	Ultimate Strength (MPa)	Ultimate Strength (ksi)	Dynamic Modulus (GPa)	Dynamic Modulus (Msi)	Total Energy (kJ/m <sup>3</sup> )	Total Energy (ft-lb/in <sup>3</sup> )
<u>AS4/F155</u>							
EPON 828		384	55.7	29.6	4.3	1979	44
PVA		363	52.7	26.9	3.9	2001	45
Polysulfone		348	50.5	31.7	4.6	1408	31



# Quasi-Isotropic Laminate Tensile Impact Room Temperature, Dry (RTD)

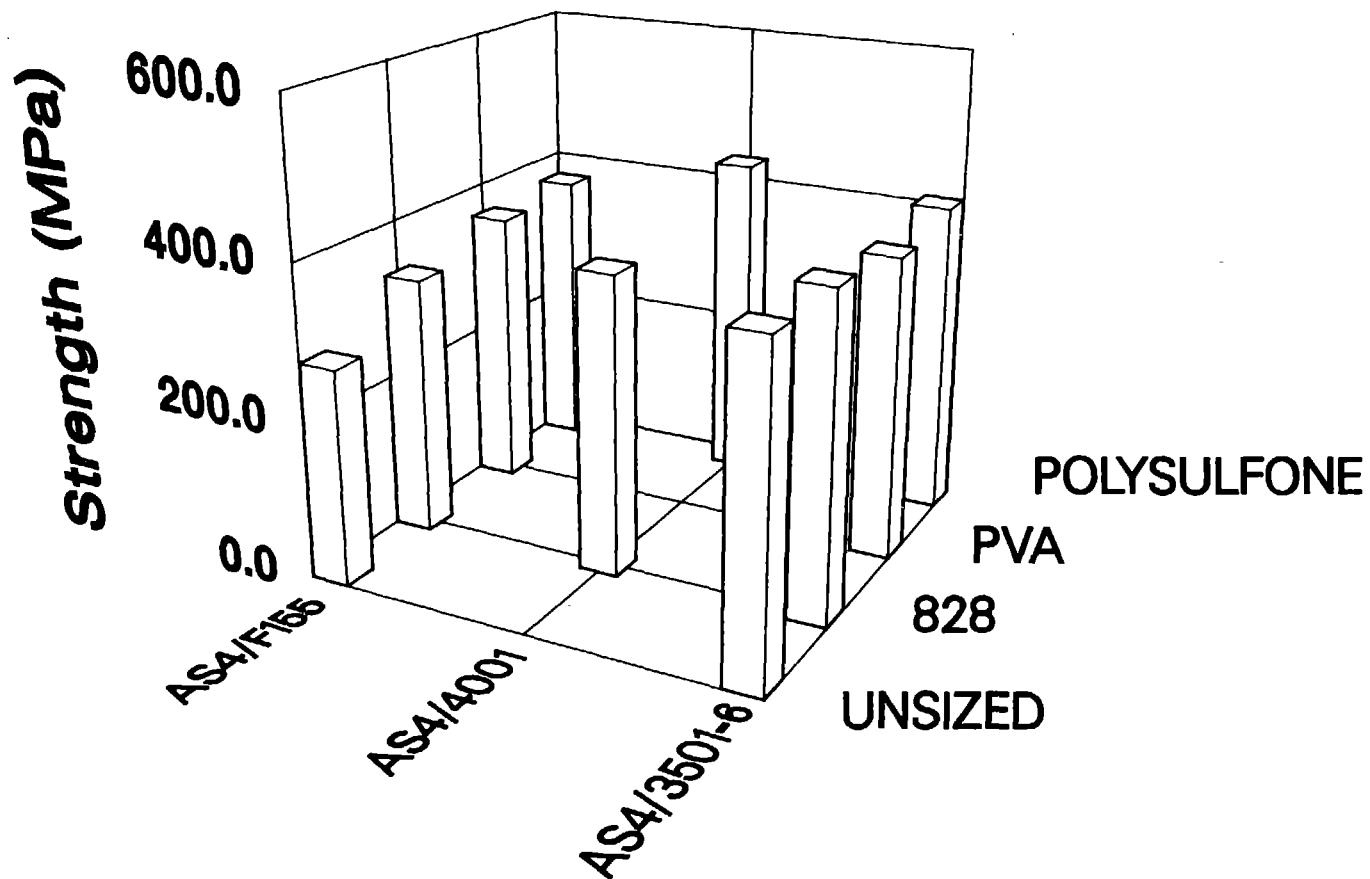


Figure 48. Quasi-Isotropic Laminate Tensile Impact Strengths of the Ten Fiber Sizing/Matrix Combinations Successfully Tested at the Room Temperature, Dry Condition.

# Quasi-Isotropic Laminate Tensile Impact Strength at the Elevated Temperature, Wet (ETW)

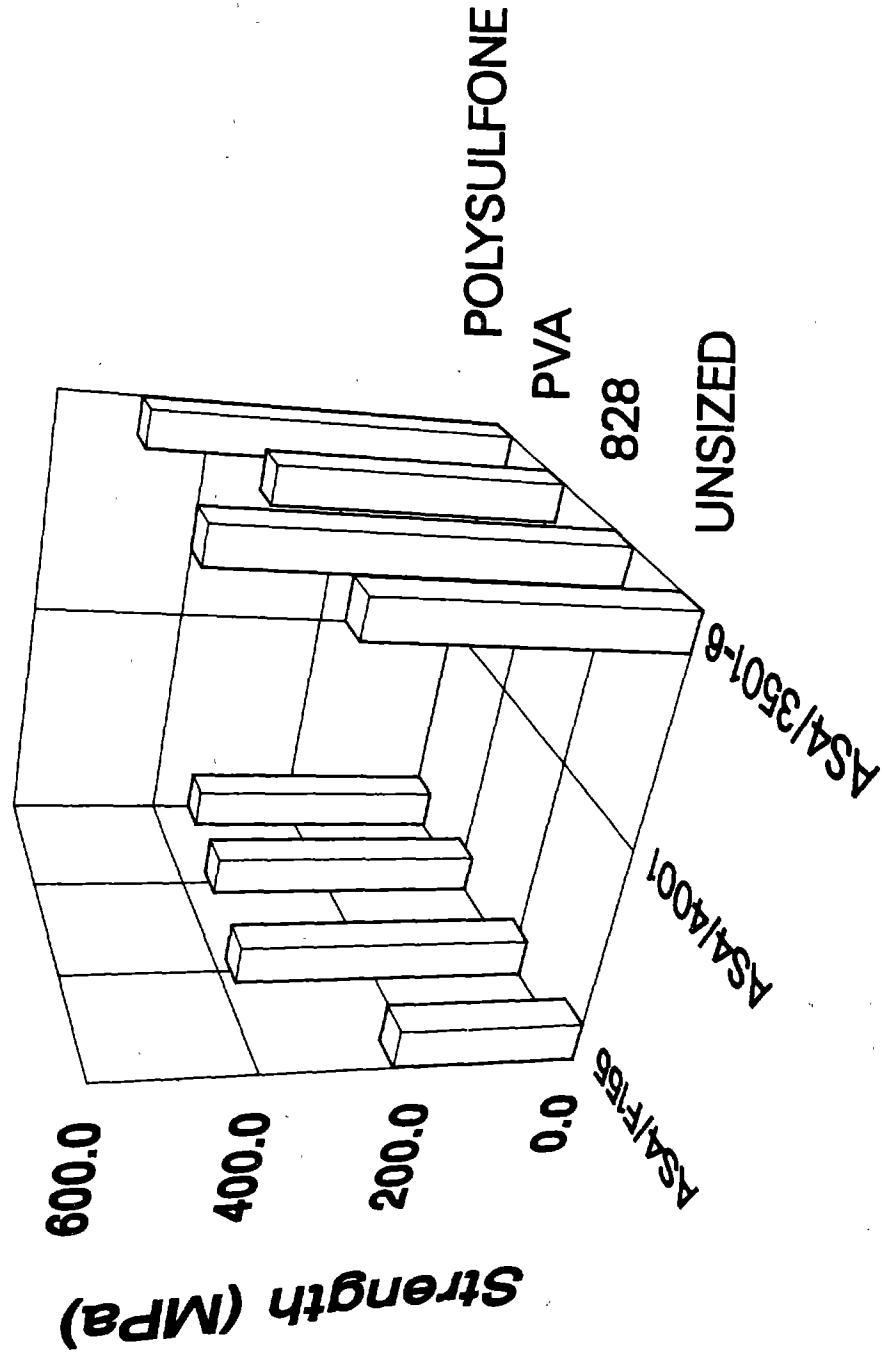


Figure 49. Quasi-Isotropic Laminate Tensile Impact Strengths of the Eight Fiber Sizing/Matrix Combinations Successfully Tested at the Elevated Temperature, Wet Condition.

# Quasi-Isotropic Laminate Tensile Impact Room Temperature, Dry (RTD)

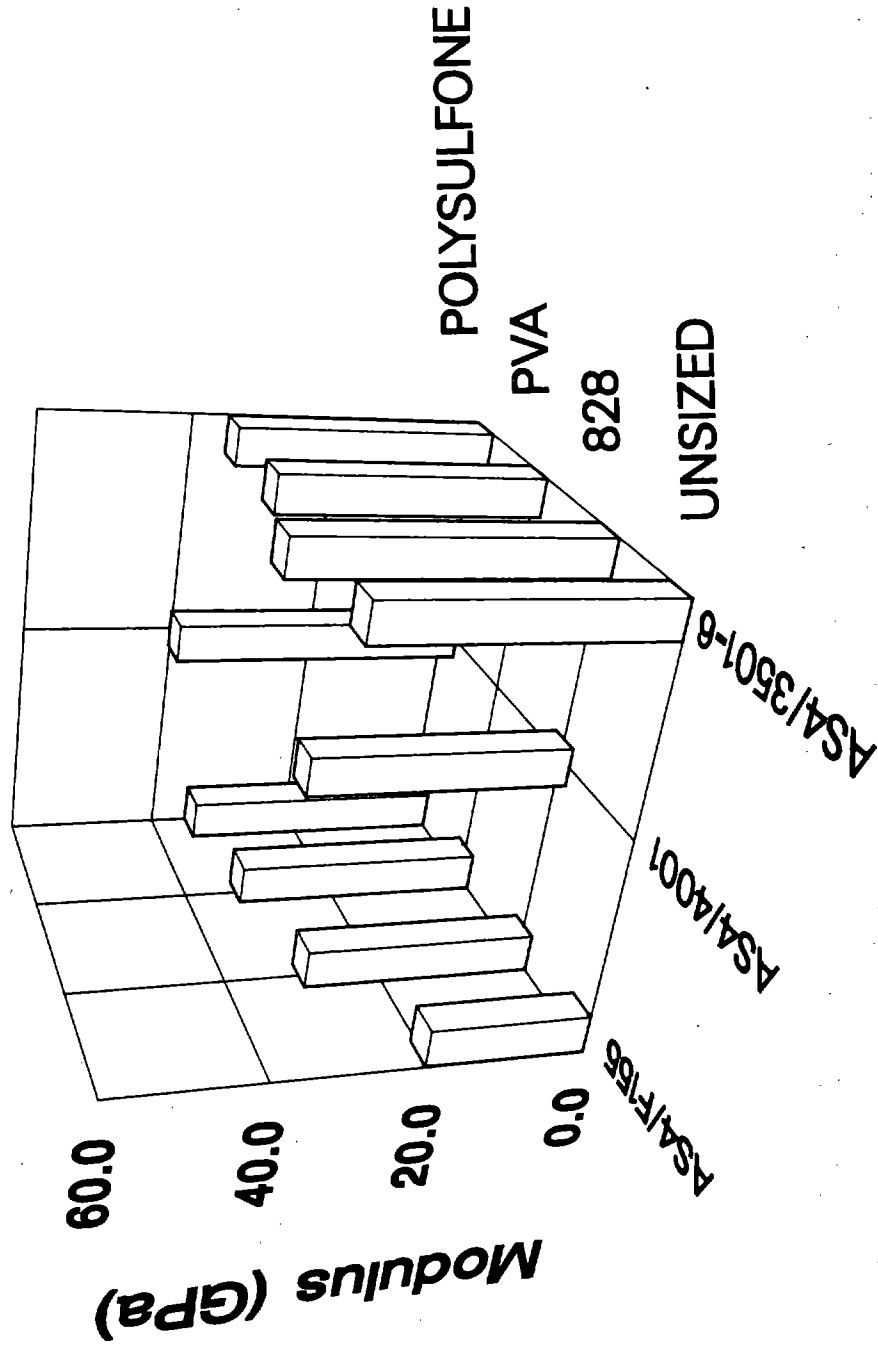


Figure 50. Quasi-Isotropic Laminate Tensile Impact Moduli of the Ten Fiber Sizing/Matrix Combinations Successfully Tested at the Room Temperature, Dry Condition.

# Quasi-Isotropic Laminate Tensile Impact Moduli at Elevated Temperature, Wet (ETW)

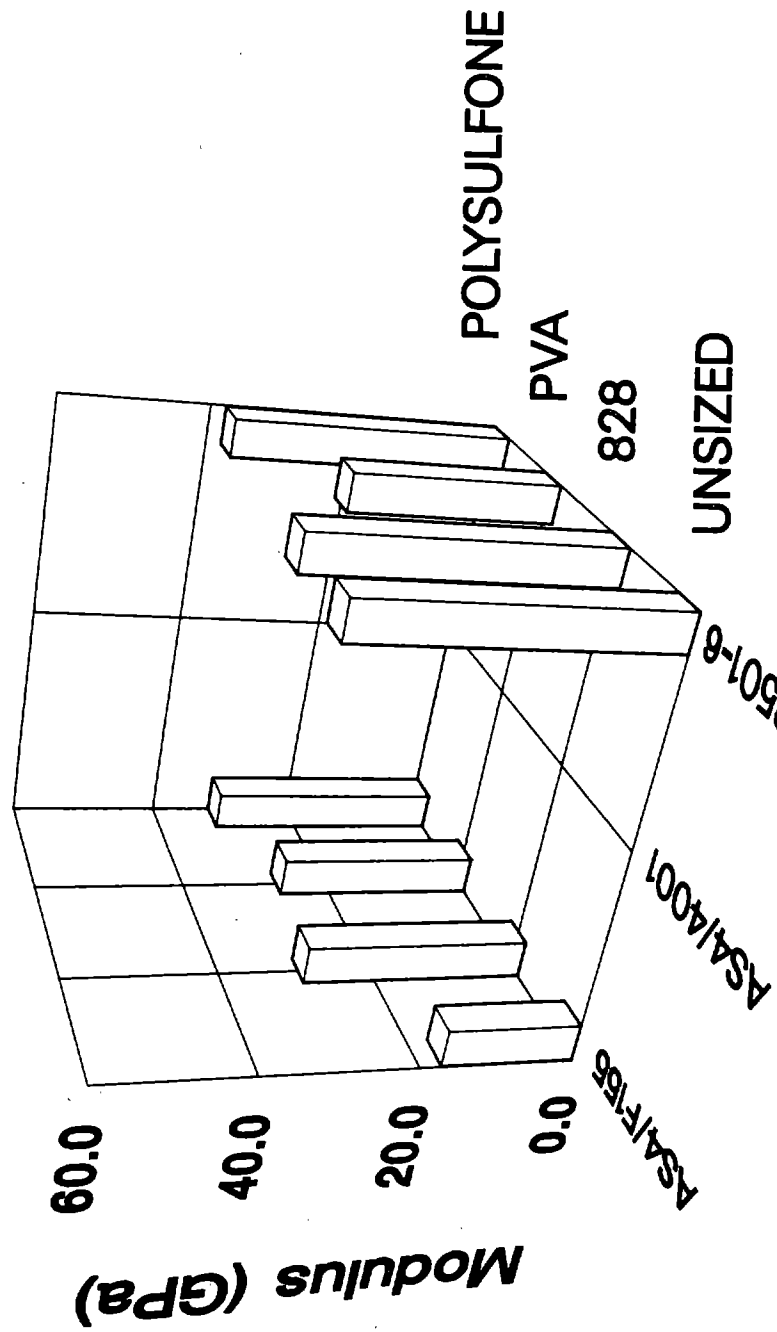


Figure 51. Quasi-Isotropic Laminate Tensile Impact Moduli of the Eight Fiber Sizing/Matrix Combinations Successfully Tested at the Elevated Temperature, Wet Condition.

## Quasi-Isotropic Laminate Tensile Impact Room Temperature, Dry (RTD)

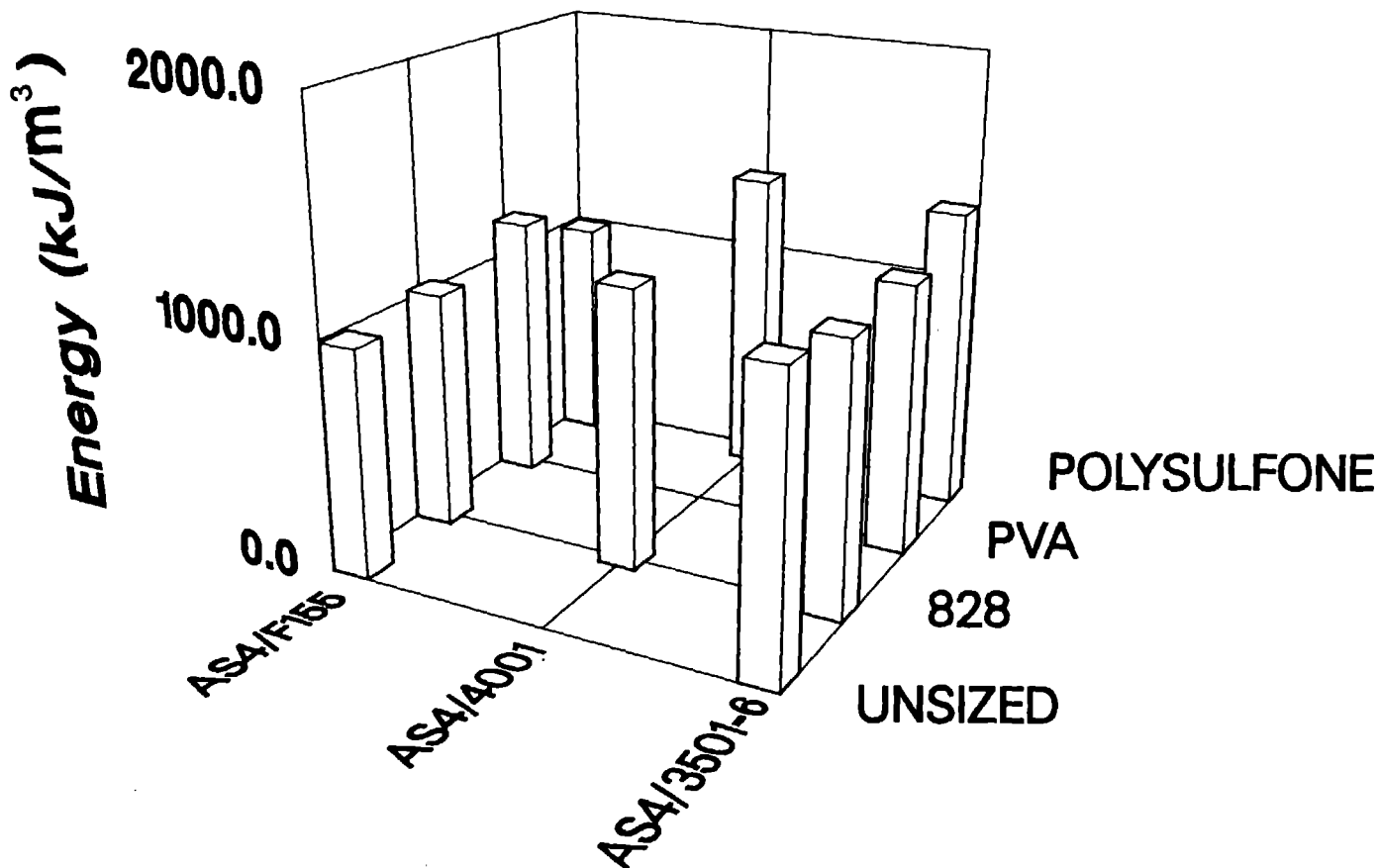


Figure 52. Quasi-Isotropic Laminate Tensile Impact Energies of the Ten Fiber Sizing/Matrix Combinations Successfully Tested at the Room Temperature, Dry Condition.

# Quasi-Isotropic Laminate Tensile Impact Elevated Temperature, Wet (ETW)

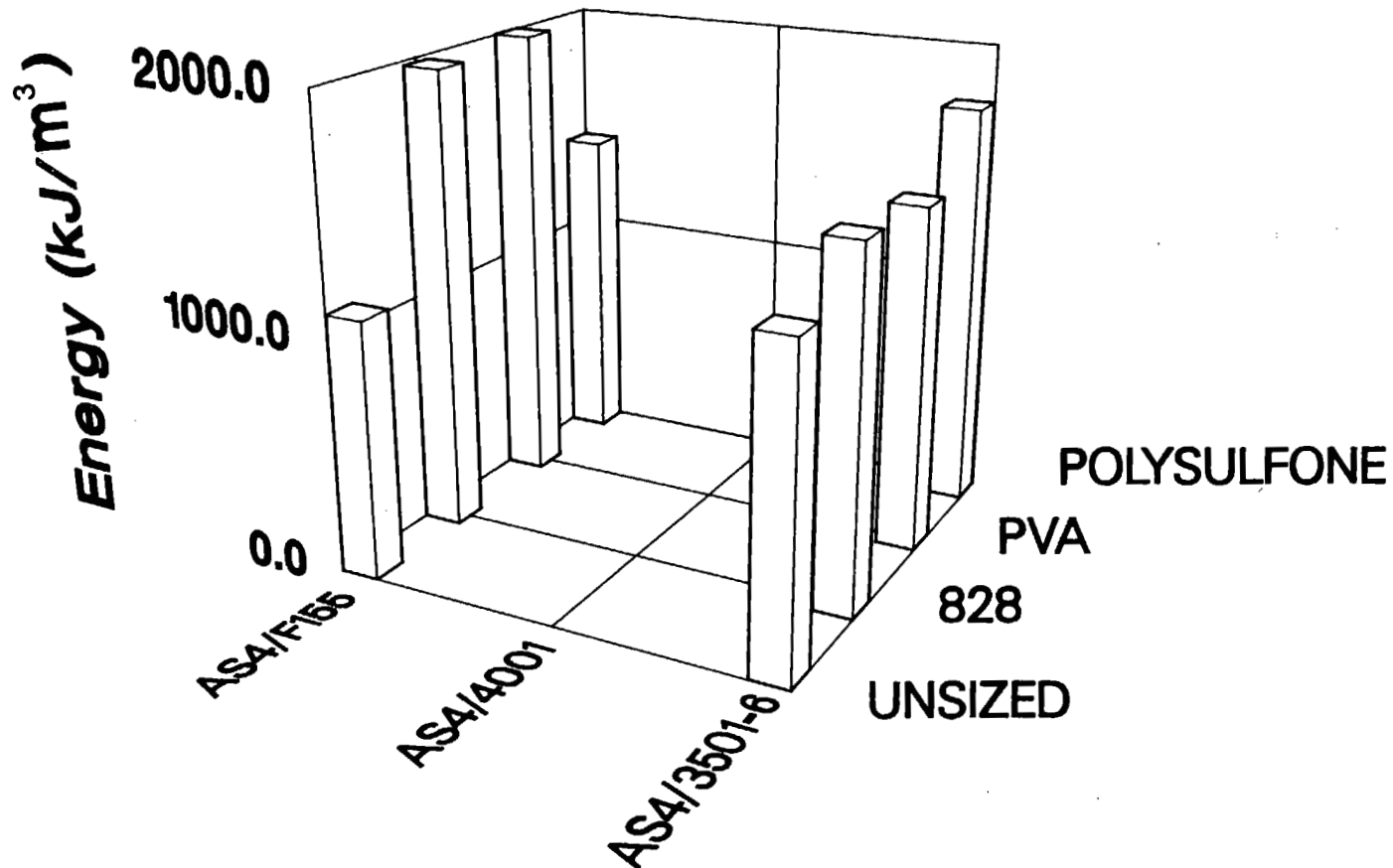


Figure 53. Quasi-Isotropic Laminate Tensile Impact Energies of the Eight Fiber Sizing/Matrix Combinations Successfully Tested at the Elevated Temperature, Wet Condition.

the same tensile strength, viz, approximately 415 MPa (60 Ksi). For the AS4/3501-6 laminates, this was about the same as for the static tensile tests (see Table 11 of Section 4.5.1). For the two AS4/4001 laminates successfully impact tested, this was also true. The RTD tensile impact strengths of the AS4/F155 laminates averaged about 20 percent lower than the corresponding static tensile strength values, except for the polysulfone-sized fiber laminate strengths, which were the same in both tests.

The tensile impact strengths of the Hercules 3501-6 and Hexcel F155 matrix laminates tested at the ETW condition were, on average, about the same as the RTD impact strengths. However, there was more scatter in the data, as can be seen in Figure 49. The low impact strength of the unsized AS4/F155 laminate can be explained by the low fiber volume content for this particular fiber surface treatment/matrix combination (see Table 6 of Section 4.3). On the other hand, the exceptionally high tensile impact strengths of the EPON 828-sized and polysulfone-sized AS4/3501-6 laminates cannot be explained in terms of fiber volume differences. As indicated in Table 6, the fiber volume of the polysulfone-sized laminate was the lowest of all four, while that of the EPON 828-sized laminate was relatively high.

Tensile impact (dynamic) moduli at the room temperature, dry condition are plotted in Figure 50 for the ten fiber surface treatment/matrix combinations which were successfully tested. As for the RTD tensile impact strengths (Figure 48), the tensile impact moduli did not vary significantly from one combination to another, the one exception being the unsized fiber/F155 matrix combination, which was somewhat lower than all the others. As for tensile impact

strength, this can probably be explained by the low fiber volume of this composite. The dynamic modulus values were about the same as the static tensile moduli, in some cases being a bit higher, and in other cases, a bit lower.

The ETW laminate tensile impact moduli (Figure 51) followed the same trends as the RTD values, and exhibited no clear trend of increasing or decreasing modulus with testing environment. These dynamic moduli thus tended to be lower than the corresponding static moduli, as can be seen by comparing the results of Table 20 with those of Table 12 of Section 4.5.1. That the AS4/3501-6 impact moduli were higher than the AS4/F155 impact moduli was probably due to the significantly higher fiber volumes of the AS4/3501-6 laminates.

The RTD tensile impact total energy absorptions are plotted in Figure 52. The total energy absorbed by each of the Hercules 3501-6 and 4001 matrix laminates was about the same, viz, about  $1260 \text{ kJ/m}^3$  ( $28 \text{ ft-lb/in}^3$ ). The total impact energy absorbed by the Hexcel F155 matrix composites averaged only about  $1035 \text{ kJ/m}^3$  ( $23 \text{ ft-lb/in}^3$ ), with the PVA-sized fiber laminate being slightly higher at  $1170 \text{ kJ/m}^3$  ( $26 \text{ ft-lb/in}^3$ ). This higher value might be explained by the slightly higher fiber volume of the PVA-sized fiber/F155 laminate. However, this was not supported by a correspondingly low impact energy value for the unsized fiber/F155 laminate, which had a very low fiber volume.

At the elevated temperature, wet test condition, the total impact energy values increased, as can be seen by comparing Figure 53 with Figure 52. Proportionally, the increase was much greater for



two of the AS4/F155 laminates, viz, the EPON 828 and PVA-sized fiber composites. Why these two laminates should be so much higher than the others is not obvious.

#### 4.6 Single Fiber Pullout

The detailed procedures for performing the single fiber pullout tests were presented in Section 3.6.8. All 12 fiber surface treatment/matrix combinations were tested, with varying degrees of success, this being extremely delicate work.

Although all 12 combinations were tested, it proved to be impossible in the present effort to achieve a proper pullout of the fibers in all cases. The EPON 828 sizing combined with any of the three resins proved to be the most difficult to work with. This EPON 828 fiber surface treatment always resulted in fiber breakage rather than fiber pullout, indicating a high interfacial bond strength for the EPON 828 sizing. Likewise, the Hexcel F155 resin combined with all four fiber surface treatments was difficult to work with. Only the polysulfone-sized fibers were successfully tested with the Hexcel F155 resin. Many iterations were tried, varying the size of the hole in the shim stock and the cure temperature. But the result was always a broken fiber rather than fiber pullout. The resin films could not be made thin enough to pull fibers through the Hexcel F155 film.

The averaged results for the single fiber pullout tests which were successful are presented in Table 21. Individual test specimen results are included in Tables A49 through A51 of Appendix A, for the three matrix materials. Photographs of typical single fibers after pullout are presented in Figures 54 through 60, representing all

Table 21

Average Single Fiber Pullout Test Results  
for AS4 Graphite Fibers in the Three Different Matrix Materials

Matrix Material	Fiber Sizing	Fiber Diameter		Embedded Length		Interfacial Shear Strength	
		( $\mu\text{m}$ )	( $10^{-4}$ in)	(mm)	( $10^{-3}$ in)	(MPa)	(ksi)
Hercules 3501-6 Epoxy	Unsize	8.4	3.3	94	3.7	32.6	4.7
	PVA	7.4	2.9	134	5.2	32.4	4.7
	Polysulfone	8.3	3.3	84	3.3	41.5	6.0
Hercules 4001 Bismaleimide	Unsize	8.4	3.3	201	7.9	20.2	2.9
	PVA	9.3	3.7	169	6.7	16.3	2.4
	Polysulfone	8.9	3.5	102	4.0	40.3	5.9
Hexcel F155 Rubber-Toughened Epoxy	Polysulfone	8.6	3.4	130	5.1	21.1	3.1

ORIGINAL PAGE IS  
OF POOR QUALITY

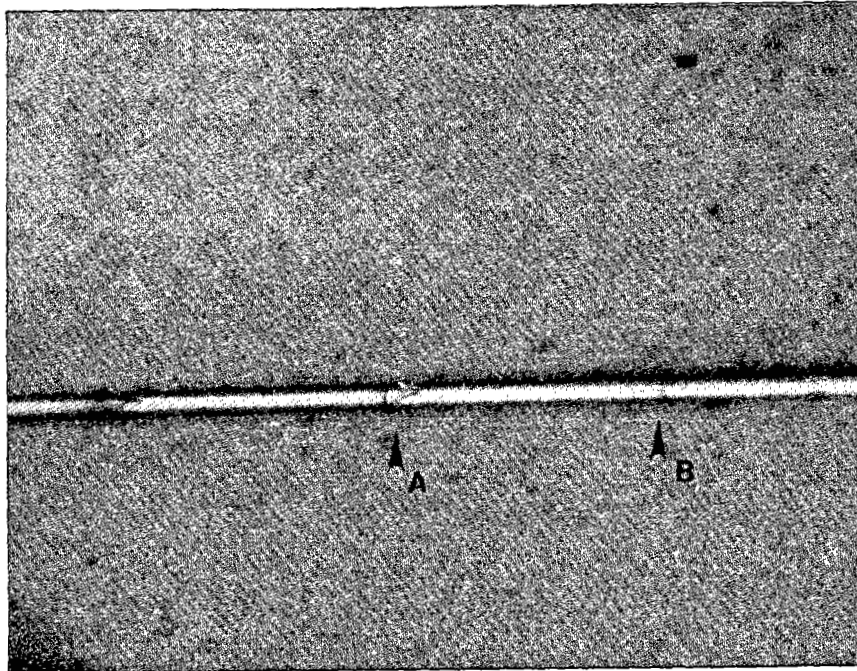


Figure 54. Optical Photomicrograph (80X) of Single Fiber Pullout Specimen AERY04; Unsized AS4 Graphite Fiber and Hercules 3501-6 Epoxy Matrix, Showing the Top Meniscus at A and the Bottom of the Resin Film at B.

ORIGINAL PAGE IS  
OF POOR QUALITY

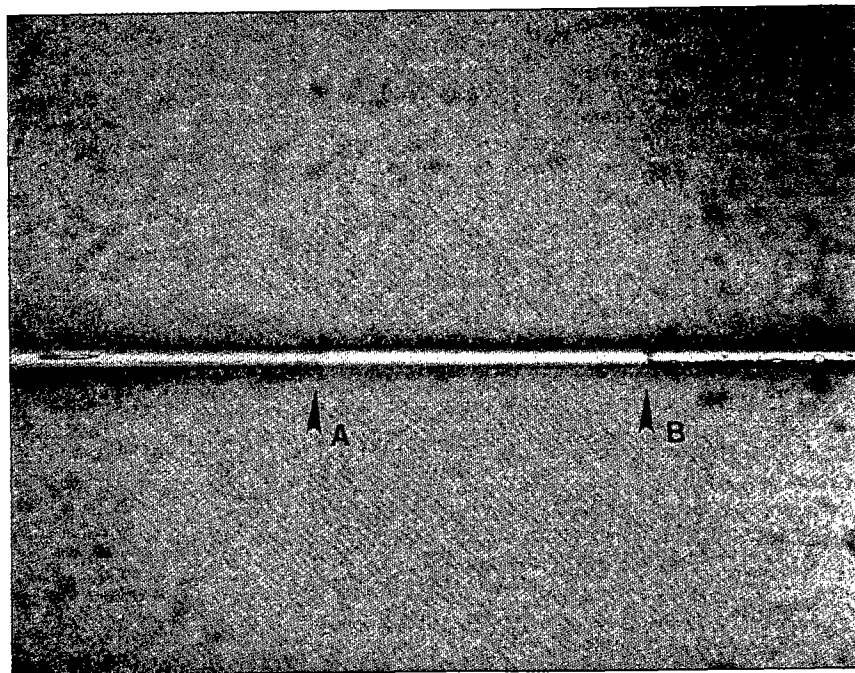


Figure 55. Optical Photomicrograph (50X) of Single Fiber Pullout Specimen AERY21, PVA-Sized AS4 Graphite Fiber and Hercules 3501-6 Epoxy Matrix, Showing the Top Meniscus at A and the Bottom of the Resin Film at B.

ORIGINAL PAGE IS  
OF POOR QUALITY

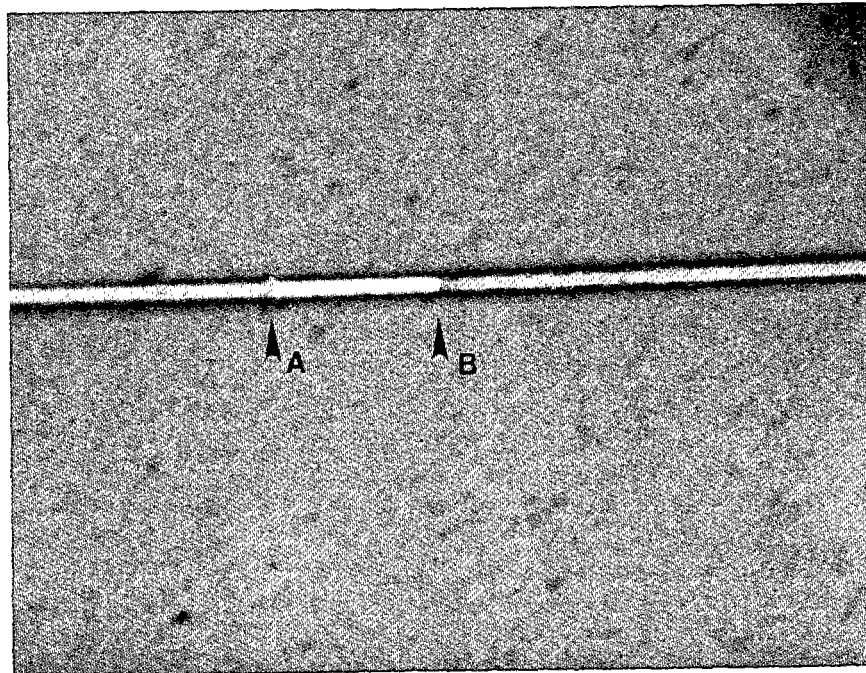


Figure 56. Optical Photomicrograph (64X) of Single Fiber Pullout Specimen AERY32, Polysulfone-Sized AS4 Graphite Fiber and Hercules 3501-6 Epoxy, Showing the Top Meniscus at A and the Bottom of the Resin Film at B.

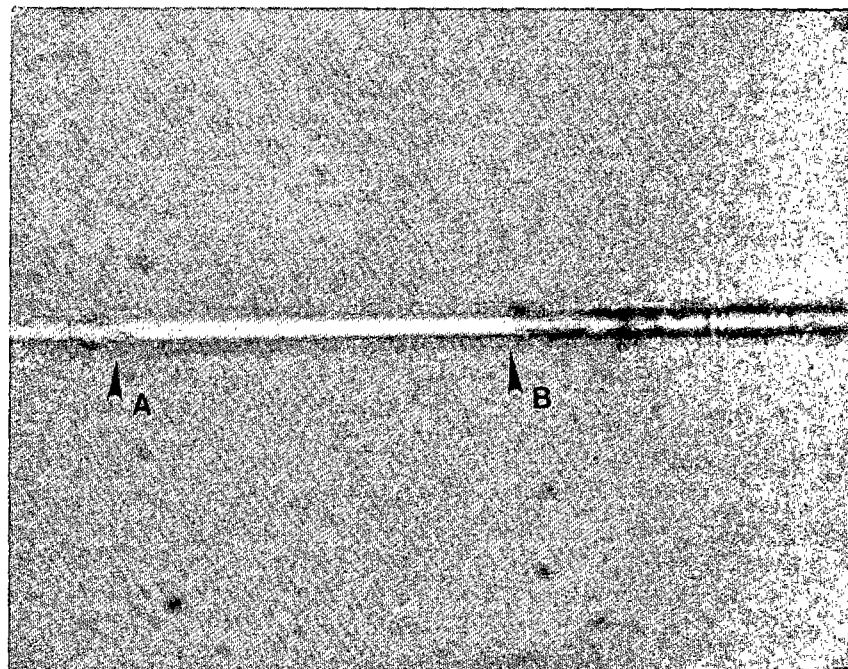


Figure 57. Optical Photomicrograph (320X) of Single Fiber Pullout Specimen AERZ00, Unsized AS4 Graphite Fiber and Hercules 4001 Bismaleimide, Showing the Top Mensicus at A and the Bottom of the Resin Film at B.

ORIGINAL PAGE IS  
OF POOR QUALITY

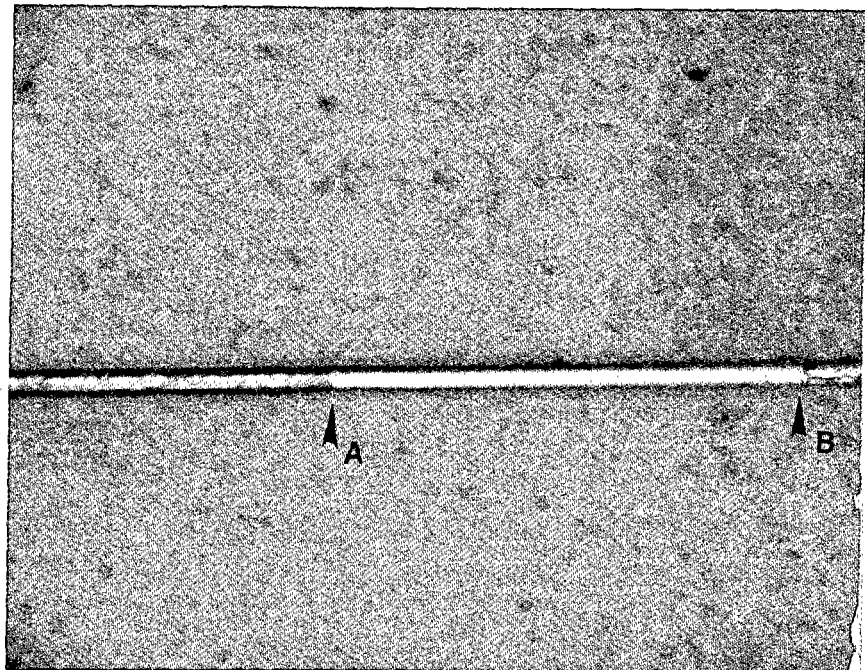


Figure 58. Optical Photomicrograph (320X) of Single Fiber Pullout Specimen AERZ20, PVA-Sized AS4 Graphite Fiber and Hercules 4001 Bismaleimide, Showing the Top Meniscus at A and the Bottom of the Resin Film at B.

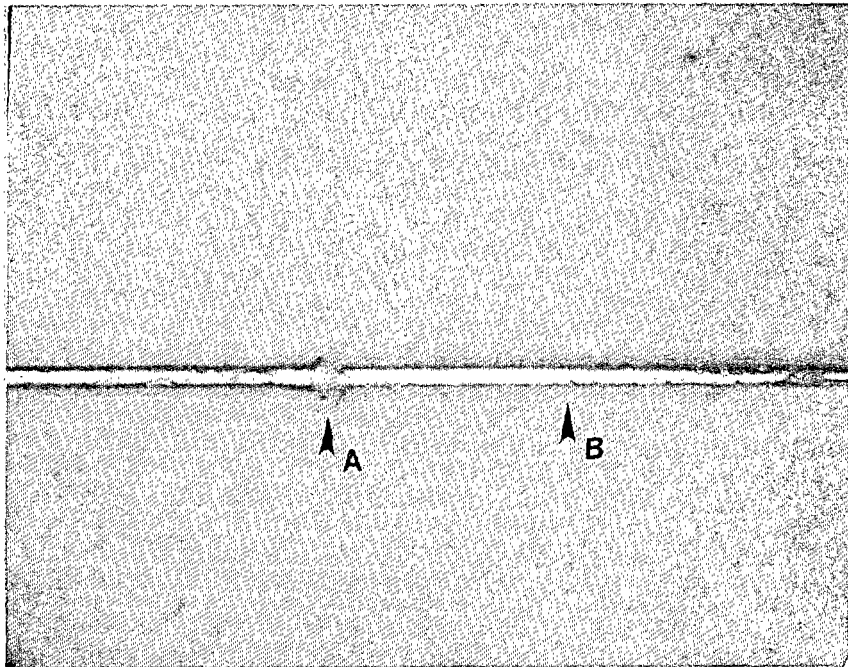


Figure 59. Optical Photomicrograph (50X) of Single Fiber Pullout Specimen AERZ30, Polysulfone-Sized AS4 Graphite Fiber and Hercules 4001 Bismaleimide, Showing the Top Meniscus of A and the Bottom of Resin Film at B.

Residual material to the right of A will be noted, indicating that the debonding was not entirely clean.



ORIGINAL PAGE IS  
OF POOR QUALITY

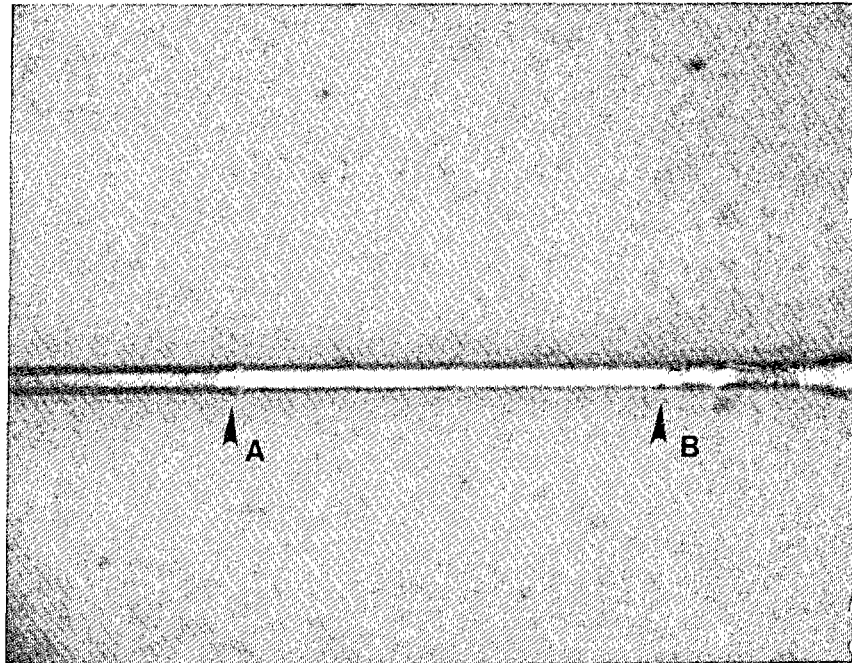


Figure 60. Optical Photomicrograph (320X) of Single Fiber Pullout Specimen AERX31, Polysulfone-Sized AS4 Graphite Fiber and Hexcel F155 Epoxy, Showing the Meniscus at A and the Bottom of the Resin Film at B.

three matrix materials. Additional photographs are included in Appendix C for reference. These photographs show the meniscus at what was the top surface of the resin film, and where the bottom of the film had been. These locations are marked A and B, respectively, on the photographs. Photographs such as these were used to determine fiber diameters and film thicknesses. They also provided some insight as to the nature of the pullouts.

As can be seen in Table 21, the polysulfone-sized fibers resulted in the highest interfacial shear strengths for the Hercules 3501-6 and 4001 resins. The EPON 828 combinations could be inferred to be even higher, since no fiber pullouts were achieved. The PVA-sized fibers performed as well as the unsized fibers in the Hercules 3501-6 epoxy, but not quite as well in the Hercules 4001 bismaleimide.

It will be noted that there was some variation in AS4 graphite fiber diameter, as is typical of the PAN precursor graphite fibers in general (see, for example, Reference [24]). Likewise, the average film thickness (i.e., the embedded length of the fiber) also varied from one resin system to another. The thinnest films were used for the Hercules 3501-6 matrix, being approximately  $80\mu$  to  $130\mu$  thick. Penn, et al. [24] found, using a similar epoxy matrix, that film thicknesses less than  $300\mu$  thick had to be used when testing Kevlar fibers, but for graphite fibers, the thickness had to be less than  $50\mu$ . However, Penn also measured considerably higher shear strengths than indicated here in Table 21, higher by a factor of two to three. Thus, the relative successes in terms of being able to pull graphite fibers out without breaking them appear to be similar. Penn's work

[24] also correlates with the inability to obtain successful fiber pullouts using the EPON 828 sizing in the present study. The thinnest fibers which could be obtained were still too thick.

Unfortunately, no unidirectional composite longitudinal shear tests were called for or performed on the quasi-isotropic laminates, results having been presented previously in Table 17. While not a completely valid comparison, the EPON 828 sized fiber composite laminates did produce the highest shear strengths in all cases. This further supports the assumption that it was the higher interface shear strength of the EPON 828 sized fibers that prevented their being tested successfully in pullout.

For the Hercules 3501-6 matrix, the shear strengths as measured from the single fiber pullout tests (Table 21) agreed reasonably well with the laminate interlaminar shear strengths (Table 17). Penn, et al. [24], using both short beam shear and Iosipescu shear tests of unidirectional graphite/epoxy composites, obtained similar correlations. Penn's single fiber pullout tests tended to be lowest, with the short beam shear results higher, and the Iosipescu shear results the highest of all. The Iosipescu shear results were about 35 percent higher than the single fiber pullout shear strengths. It should be noted that for the Kevlar/epoxy system, Penn's Iosipescu shear results were 270 percent higher (i.e., higher by a factor of 2.7).

As will be noted by comparing the results for the Hercules 4001 matrix in Tables 17 and 21, the laminate shear strengths were about 2.5 times higher than the single fiber pullout shear strengths for the unsized and PVA-sized fibers, but only 1.3 times higher for the

polysulfone-sized fibers.

For the Hexcel F155 matrix, only the polysulfone-sized fibers were successfully pulled out. The shear strength of the quasi-isotropic laminate was 2.9 times higher. As pointed out by Penn [24], the coefficient of thermal expansion mismatch between the graphite fiber and the matrix can be an important parameter. During cooldown from the cure temperature, the matrix contracts more than the fiber diameter, inducing a compressive residual stress at the fiber-matrix interface. This is favorable in terms of enhancing shear properties. The Hexcel F155 matrix is cured at a lower temperature than the other two matrix systems, which results in lower residual stresses.

Since the single fiber pullout specimen has effectively a very low fiber volume content compared to normal composites, the internal stress states are also different. Thus, direct comparisons of test results must be carefully qualified.

As previously noted, the single fiber pullout test used here was developed by Penn, et al. [24]. Drzal [30] has worked extensively with a different single fiber specimen configuration. He casts a single fiber in a dogbone-shaped miniature tensile coupon of matrix material. The single fiber runs from end to end of the resin specimen. A special mechanical loading device was designed, to observe the fiber-matrix interface bonding, fiber fracture, and matrix cracking under a microscope. Drzal's specimen configuration and loading device were duplicated at the University of Wyoming, with Drzal's cooperation and guidance. A photograph of the loading fixture and a typical specimen is shown in Figure 61.

ORIGINAL PAGE IS  
OF POOR QUALITY

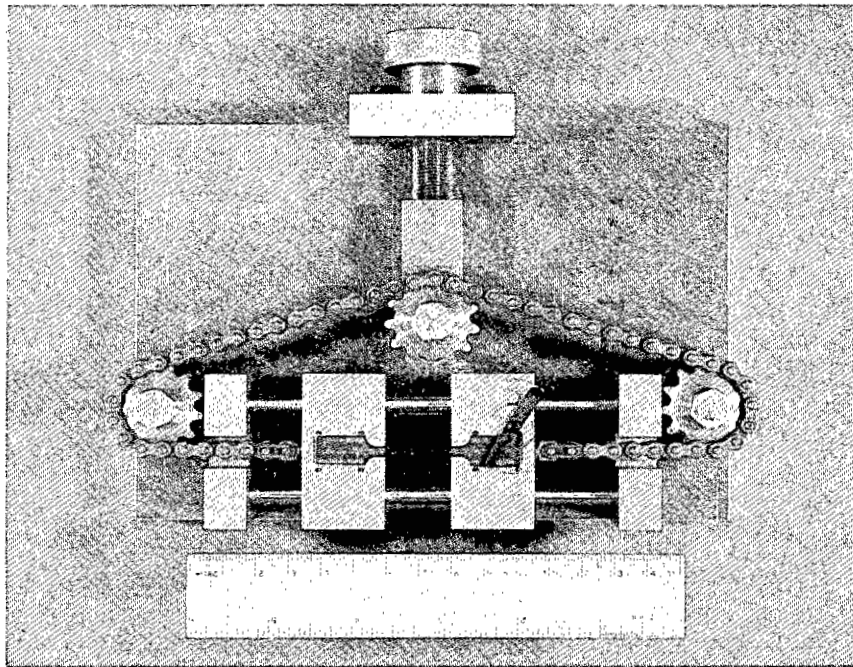


Figure 61. Single Fiber Composite Tensile Specimen and Loading Fixture (after Drzal [30]).

Drzal used low cure temperature, high strain to failure model resins as the matrix material, and achieved well controlled failures. In the present investigation it was, of course, desired to use the three matrix materials already identified, viz, Hercules 3501-6 epoxy, Hercules 4001 bismaleimide, and Hexcel F155 rubber-toughened epoxy. As previously presented in Table 2 of Section 4.2, even the rubber-toughened epoxy exhibited a tensile strain to failure of only about 3.5 percent. The strains to failure of the other two matrix materials were only about half this value. Thus, the test method did not prove to be suitable, producing unstable fractures, and was set aside for the present study. Single fiber specimens of good quality were made, however. Thus, the technique is available for future use, if needed.

In summary, the single fiber pullout tests conducted as part of the present study were only partly successful. Considering the extreme difficulty in performing these very time consuming tests, it is questionable as to whether the data obtained are worth the effort required. It would appear, based both on the extensive effort expended here and the prior efforts by Penn, et al. [24], that it may be much more meaningful to perform shear tests on actual unidirectional composites instead.

## SECTION 5

### SCANNING ELECTRON MICROSCOPE RESULTS

#### 5.1 Introduction

A JEOL JSM-35C scanning electron microscope was used for all of the work of the present study. This instrument has a magnification range from 10X to 180,000X, a depth of field of 30 $\mu$  at 1000X, and a resolution of 60 $\text{\AA}$ .

#### 5.2 Specimen Preparation

A total of 48 specimens were mounted for examination, representing all of the environmental conditions for the transverse tensile and axial compression testing of the 12 graphite fiber/polymer matrix composites. The SEM specimen mounts were 25 mm (1.0 in) in diameter.

A Buehler No. 4150 silicon carbide cutoff blade was used to cut the SEM specimens from the failed test articles. A silver conducting paint was used to bond the SEM specimens to the brass mounts, after which the specimens were ultrasonically cleaned to remove loose surface debris. All specimens were subsequently vapor-coated with gold to make them electrically conductive.

#### 5.3 Explanation of SEM Photographs

Specimens representing both test temperature and moisture conditions, and both unidirectional composite test types, i.e., transverse tension and axial compression, were studied. On the following pages, selected SEM photographs are shown along with, to

the extent possible, a description/interpretation of the fracture surface features. The 48 photographs represent both the RTD and ETW test conditions for all 12 fiber sizing/matrix combinations, for both loading conditions.

The first 24 figures, i.e. Figures 62 through 85, are photographs of fracture surfaces for transverse tensile tests of the unidirectional composites. The first eight of the photographs, i.e., Figures 62 through 69, are for the AS4/3501-6 unidirectional composite: four representing the four different fiber sizings at the RTD test condition, followed by four representing the ETW test condition. The photographs are always presented in the same order, via, unsized, EPON 828, PVA, and polysulfone. The next eight photographs, i.e., Figures 70 through 77, depict the AS4/4001 unidirectional composite transverse tensile failures. The final eight photographs of the group, Figures 78 through 85, represent the AS4/F155 composites.

The next 24 figures, i.e., Figures 86 through 109, are photographs of fracture surfaces of unidirectional composites tested in axial compression. The order of presentation is the same as for the transverse tensile tests. Figures 86 through 93 represent the AS4/3501-6 composites for the four RTD tests followed by the four ETW tests. Figures 94 through 101 are for the AS4/4001 composites, and Figures 102 through 109 represent the AS4/F155 composites.

Each of these 48 SEM photographs was selected as being typical of the failures observed. The inclusion of so many photographs, and presented in the body of this report rather than in an appendix, was deliberate. These photographs are very valuable indicators of



the degree of fiber-matrix interface bonding, and document subtle differences from one system to another. They should also prove to be very useful in future studies, as an archive of fracture modes.

The photographic system of the SEM displays information directly across the bottom of each SEM photograph. Referring, for example, to Figure 62, the caption reads:

25 KV X1000 1131 10.0U UW85

The interpretation is as follows:

25 KV    electron beam accelerating voltage, in kilovolts  
X1000    magnification  
1131    photograph number  
10.0U    length of scale bar, in microns  
UW85    the SEM unit identification number, i.e.,  
          University of Wyoming and the current year, 1985

The specimen numbering system is summarized here for convenience. A typical specimen identification is divided into three sets of characters. For example, the specimen number in Figure 62 is AFRY06. This is interpreted as follows:

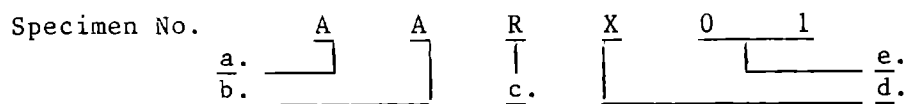
A        identifies the program, for NASA-Ames, related  
          to the graphite fiber/polymer matrix interface  
          study  
FRY      identifies the type of specimen, environmental  
          condition, and polymer matrix, as defined below  
06       identifies the fiber surface treatment and  
          specimen number

The complete set of codes, for all specimens tested, is presented in Table 22.

It should be noted that, by identifying the particular test specimen from which the SEM photograph was taken, it is possible to associate the specific mechanical properties of that specimen, as tabulated in Appendix A, with the specific fracture surface characteristics observed.

Table 22

Test Specimen Identification Code



<u>a.</u>	A	- Ames
<u>b.</u>	A	- Neat Resin Tension
	B	- Neat Resin Iosipescu Shear
	C	- Neat Resin Thermal Expansion
	D	- Neat Resin Moisture Expansion
	E	- Fiber Pullout
	F	- Transverse Tension
	G	- Axial Compression
	H	- Laminate Compression
	I	- Laminate Tension
	J	- Laminate Flexure
	K	- Interlaminar Shear
	L	- Instrumented Tensile Impact
<u>c.</u>	R	- Room Temperature, Dry
	E	- Elevated Temperature, Wet
<u>d.</u>	X	- Hexcel F155 Epoxy
	Y	- Hercules 3501-6 Epoxy
	Z	- Hercules 4001 Bismaleimide
<u>e.</u>	00-09	- Unsized
	10-19	- EPON 828 sizing
	20-29	- PVA sizing
	30-39	- Polysulfone sizing

ORIGINAL PAGE IS  
OF POOR QUALITY

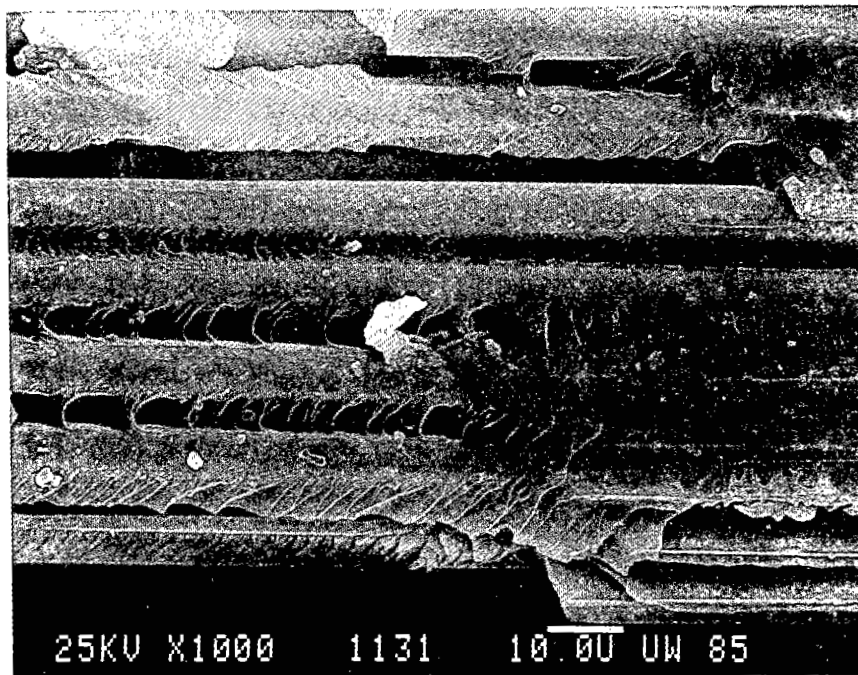


Figure 62. Unsized AS4/Hercules 3501-6 Unidirectional Composite, Transverse Tensile Specimen ARFY06, 23°C, Dry Condition.

Good adhesion of the matrix to the graphite fibers, along with a normal hackle pattern in the matrix caused by the tensile failure, is indicated.

ORIGINAL PAGE IS  
OF POOR QUALITY

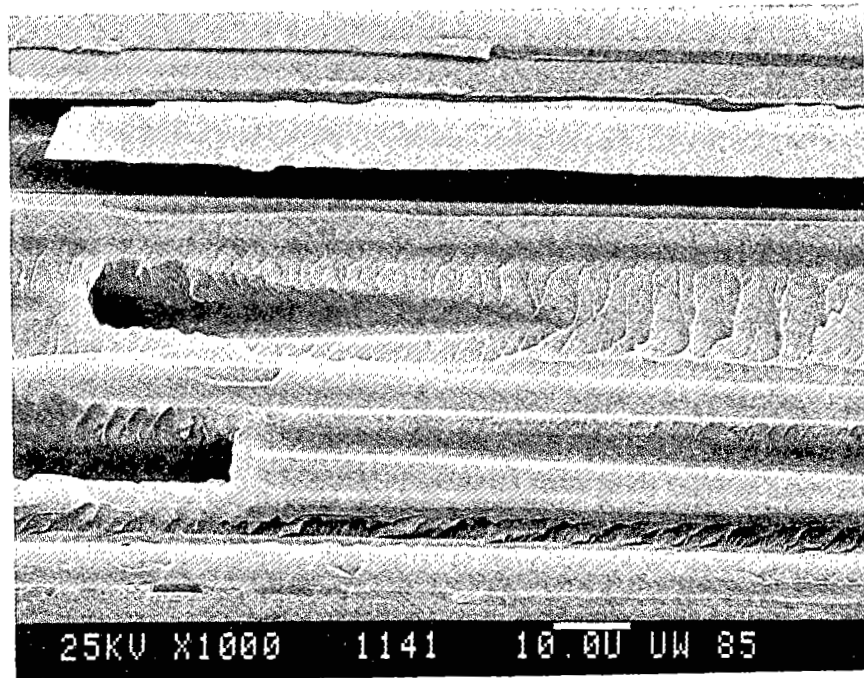


Figure 63. EPON 828-Sized AS4/Hercules 3501-6 Unidirectional Composite, Transverse Tensile Specimen AFRY10, 23°C, Dry Condition.

Good matrix adhesion to the graphite fibers, and a normal matrix hackle pattern caused by the tensile failure is indicated.

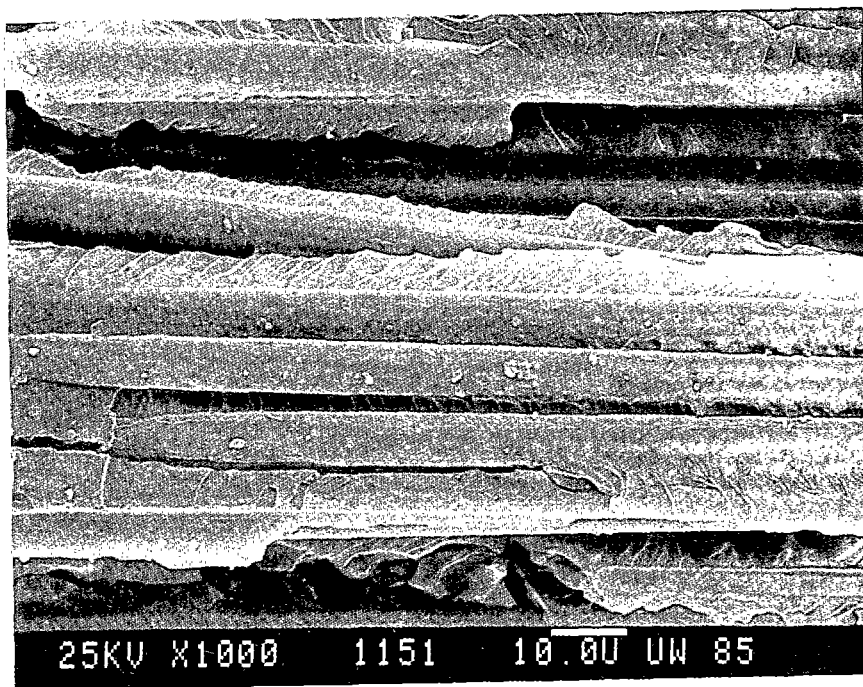


Figure 64. PVA-Sized AS4/Hercules 3501-6 Unidirectional Composite, Transverse Tensile Specimen AFRY26, 23°C, Dry Condition.

Limited fiber/matrix adhesion and somewhat more disruption of the composite from the tensile failure than seen in Figures 62 and 63 will be noted.

ORIGINAL PAGE IS  
OF POOR QUALITY

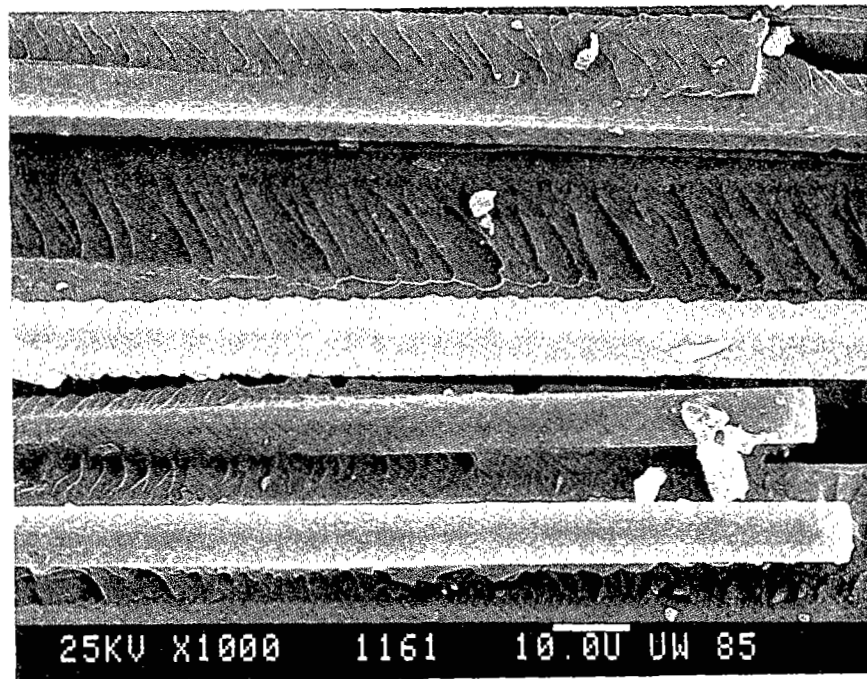


Figure 65. Polysulfone-Sized AS4/Hercules 3501-6 Unidirectional Composite, Transverse Tensile Specimen AFRY33, 23°C, Dry Condition.

Moderate fiber-matrix adhesion and some bulk composite disruption is indicated.

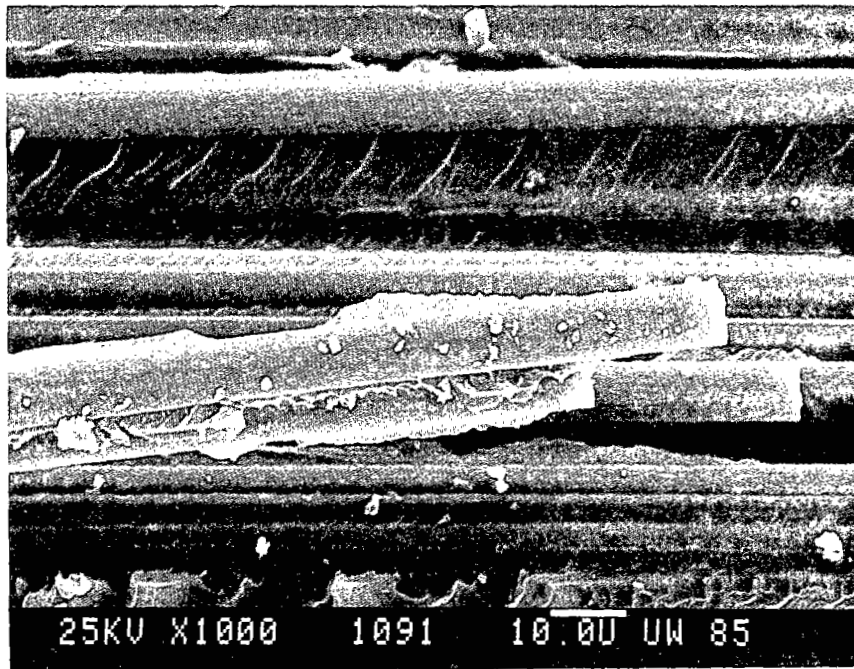


Figure 66. Unsized AS4/Hercules 3501-6 Unidirectional Composite, Transverse Tensile Specimen AFEY04, 100°C, Moisture-Conditioned.

Some minor debris from the failure can be seen, along with bare fibers, empty fiber troughs, and a hackled resin surface caused by the tensile failure.



ORIGINAL PAGE IS  
OF POOR QUALITY

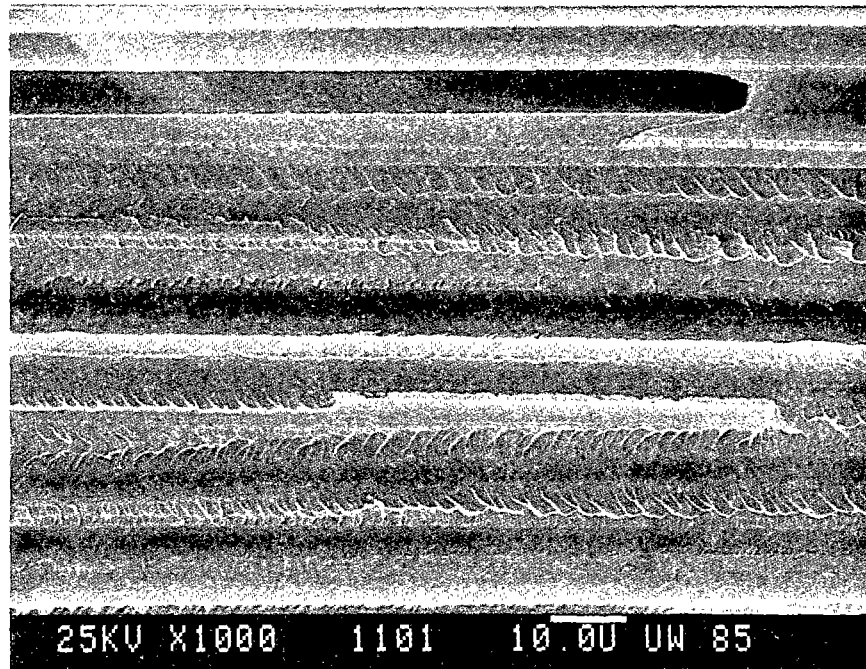


Figure 67. Epon 828-Sized AS4/Hercules 3501-6 Unidirectional Composite, Transverse Tensile Specimen AFEY12, 100°C, Moisture-Conditioned.

Many empty fiber troughs, bare fibers, and the hackled matrix surface caused by the tensile failure will be noted.

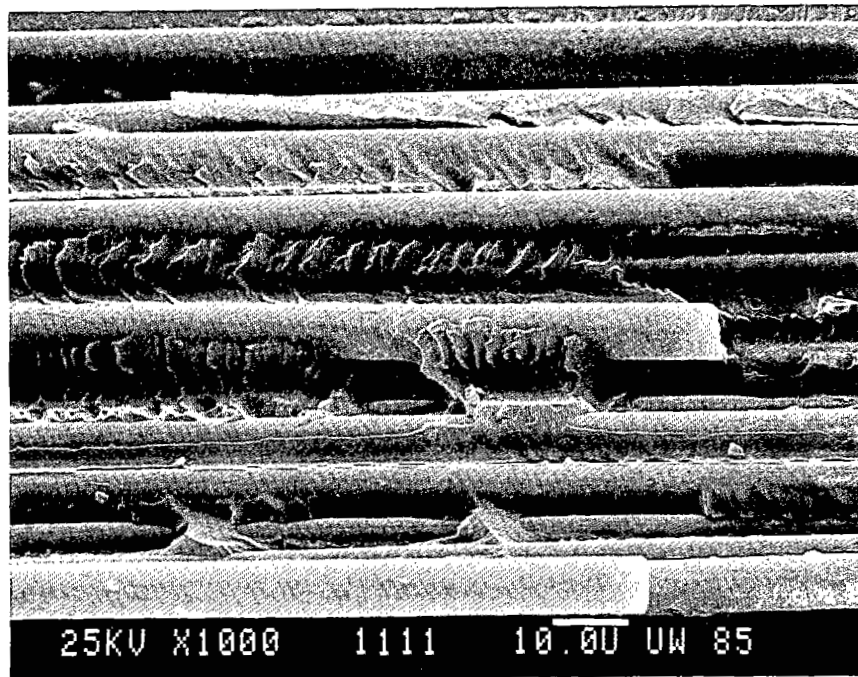


Figure 68. PVA-Sized AS4/Hercules 3501-6 Unidirectional Composite, Transverse Tensile Specimen AFEY28, 100°C, Moisture-Conditioned.

Bare fibers and a somewhat coarser hackle pattern in the matrix than seen in Figure 67 are evident.

ORIGINAL PAGE IS  
OF POOR QUALITY

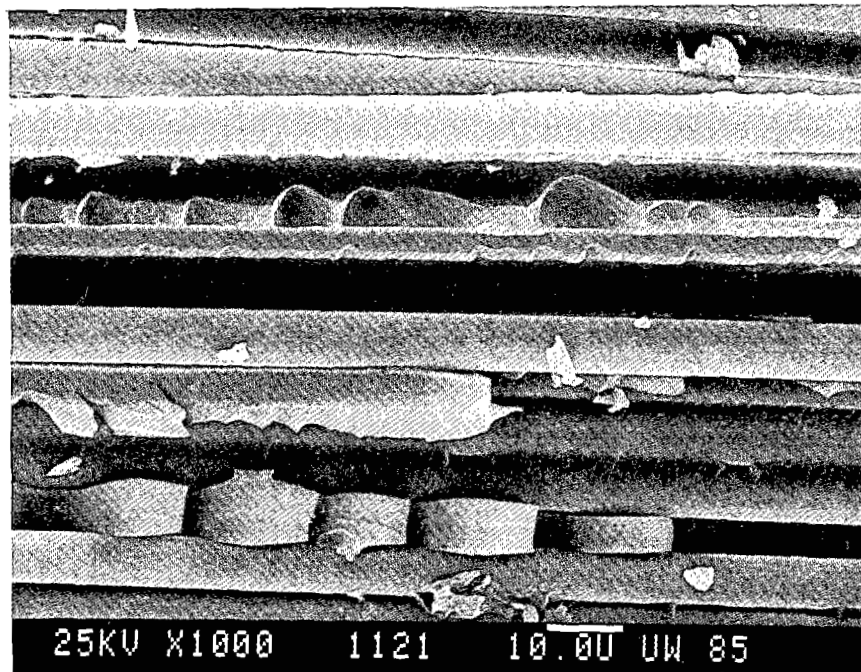


Figure 69. Polysulfone-Sized AS4/Hercules 3501-6 Unidirectional Composite, Transverse Tensile Specimen AFEY35, 100°C, Moisture-Conditioned.

Bare fibers and a very coarse hackle pattern in the matrix are obvious.

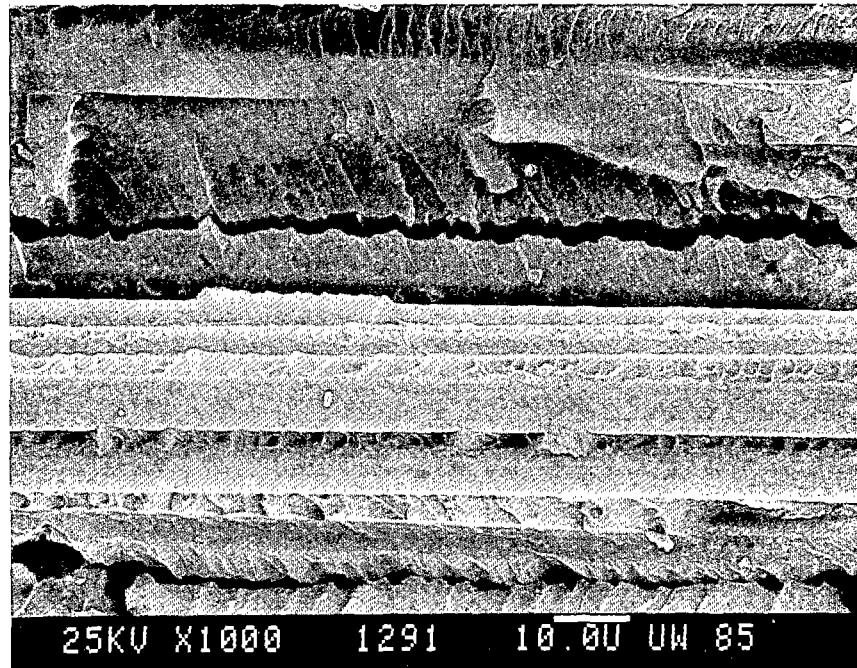


Figure 70. Unsized AS4/Hercules 4001 Unidirectional Composite, Transverse Tensile Specimen AFRZ04, 23°C, Dry Condition.

Limited fiber-matrix interface bonding is indicated.

ORIGINAL PAGE IS  
OF POOR QUALITY

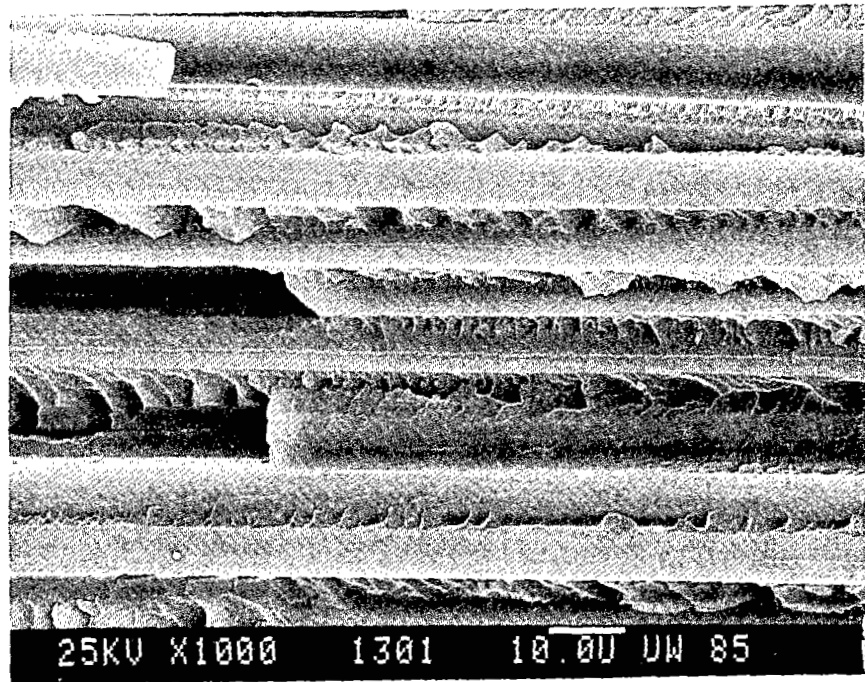


Figure 71. EPON 828-Sized AS4/Hercules 4001 Unidirectional Composite, Transverse Tensile Specimen AFRZ17, 23°C, Dry Condition.

Bare fibers, but some signs of fiber-matrix interface adhesion, are evident.

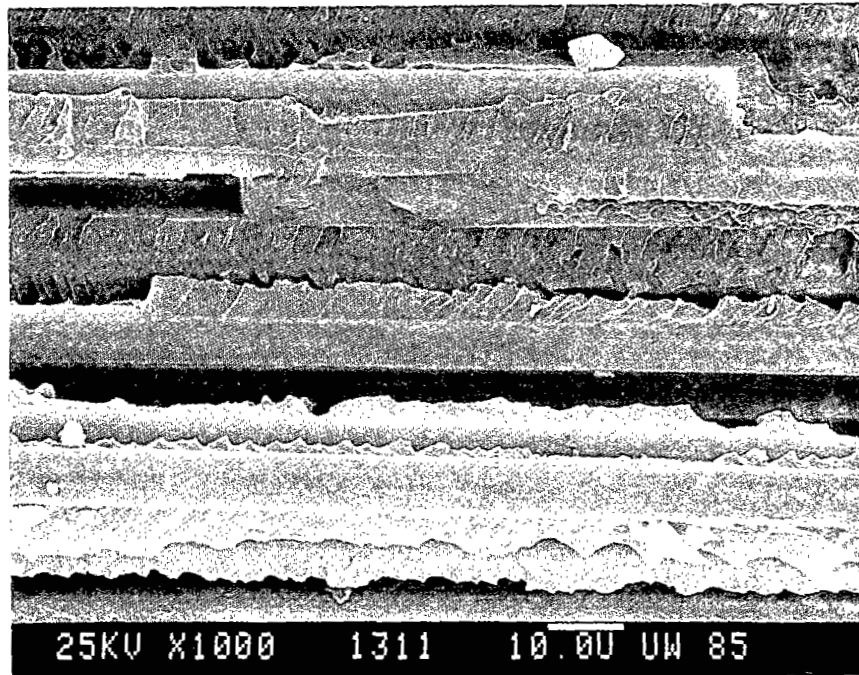


Figure 72. PVA-Sized AS4/Hercules 4001 Unidirectional Composite, Transverse Tensile Specimen AFR223, 23°C, Dry Condition.

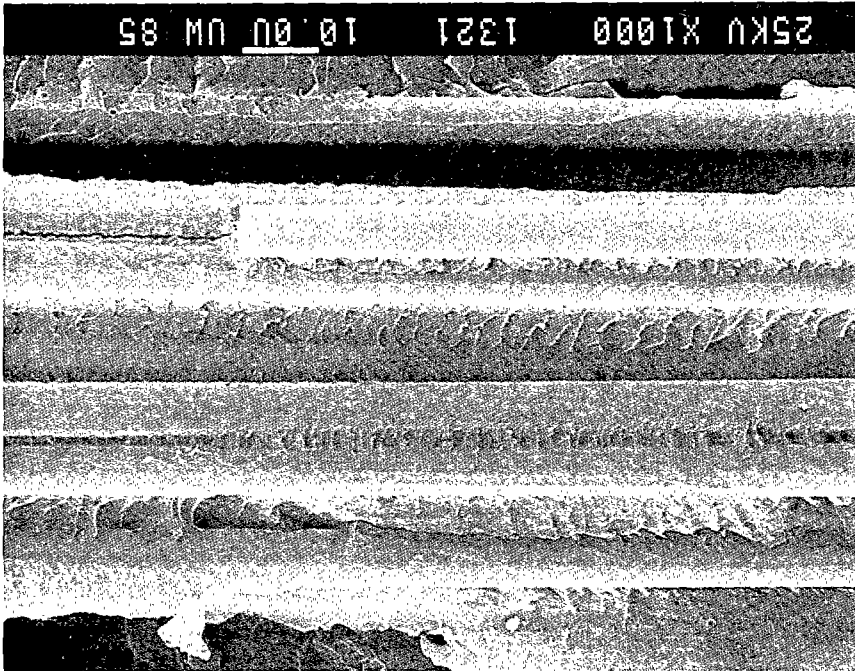
Bare fibers and locations of fiber pullouts can be seen.

suggested.

the other surface treatment cases shown in Figures 70, 71, and 72 is That the fiber-matrix interface adhesion may be higher than for

Dry Condition.  
Composite, Transverse Tensile Specimen AFRZ36, 23°C,  
Polysulfone-Sized AS4/Hercules 4001 Unidirectional

Figure 73.



ORIGINAL PAGE IS  
OF POOR QUALITY

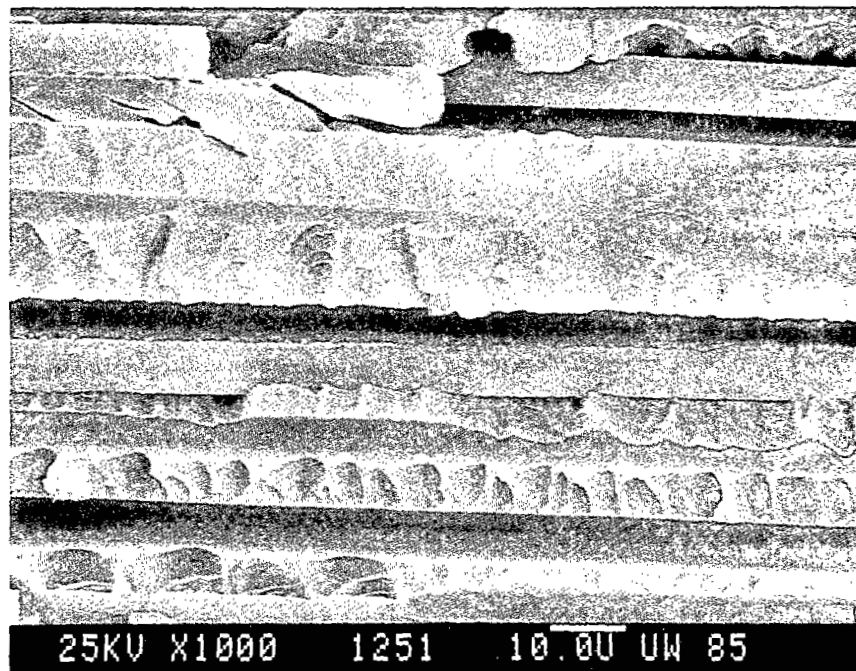


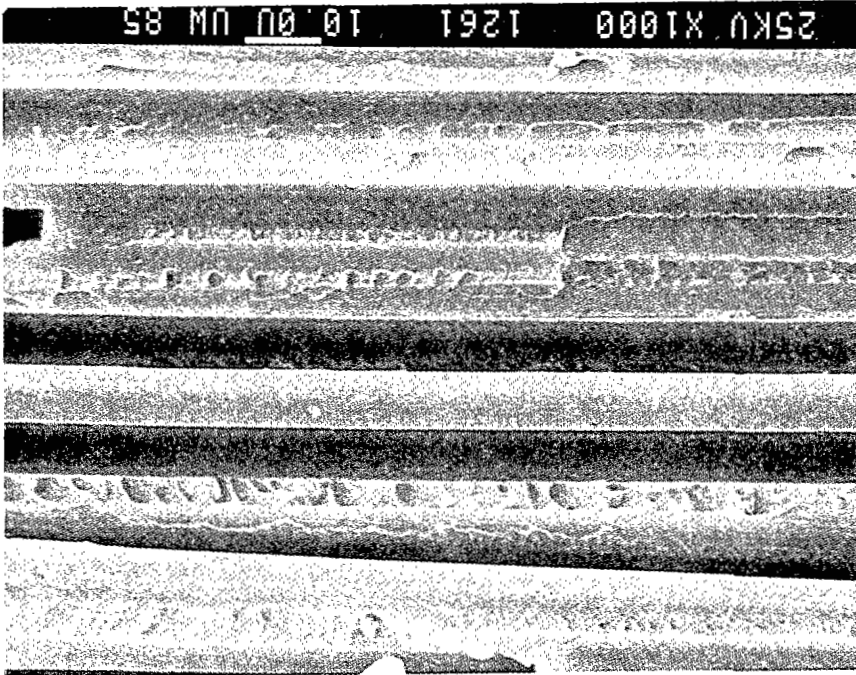
Figure 74. Unsized AS4/Hercules 4001 Unidirectional Composite, Transverse Tensile Specimen AFEZ02, 100°C, Moisture-Conditioned.

Bare fibers and fiber troughs, and a rough hackled appearance of the matrix, are dominant features of this fracture surface.



74, are evident.  
of hackles than indicated for the unsized fiber composite in Figure  
Bare fibers and many empty fiber troughs, with a finer pattern

Figure 75. EPON 828-Sized AS4/Hercules 4001 Unidirectional  
Composite, Transverse Tensile Specimen AFZ15,  
100°C, Moisture-Conditioned.



ORIGINAL PAGE IS  
OF POOR QUALITY

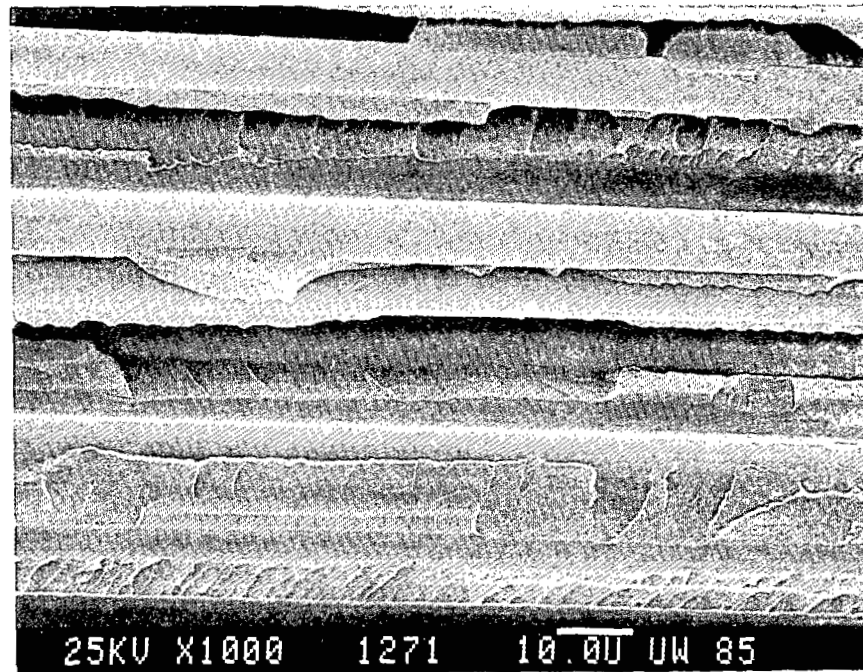


Figure 76. PVA-Sized AS4/Hercules 4001 Unidirectional Composite, Transverse Tensile Specimen AFEZ21, 100°C, Moisture-Conditioned.

A fiber with some resin still adhering to it, indicating better adhesion, and also some porosity in the matrix, can be seen in this photograph.

ORIGINAL PAGE IS  
OF POOR QUALITY

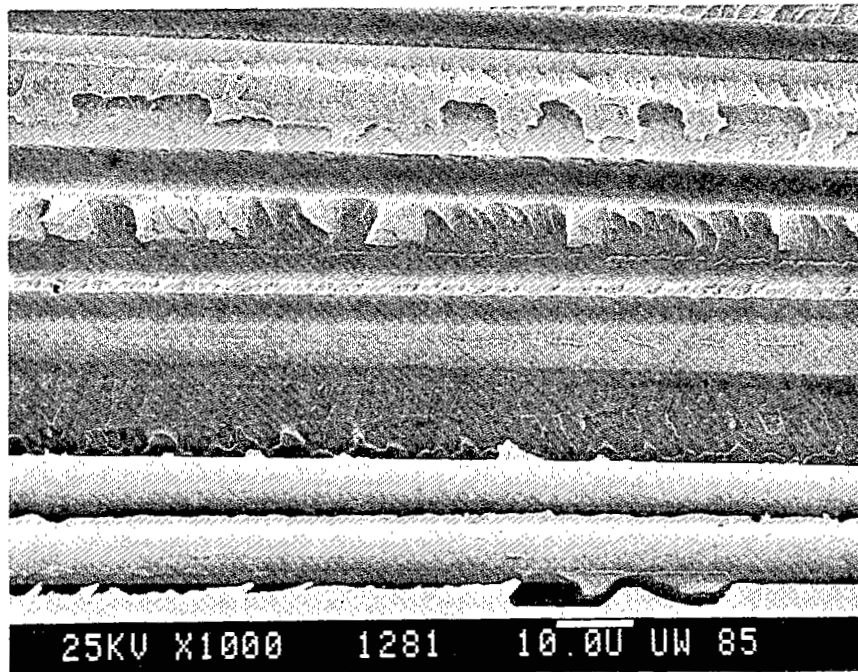


Figure 77. Polysulfone-Sized AS4/Hercules 4001 Unidirectional Composite, Transverse Tensile Specimen AFEZ34, 100°C, Moisture-Conditioned.

Fibers with some matrix material still adhering to them, indicating moderate interface bonding between the fibers and the surrounding matrix, are shown. Porosity in the matrix is also evident.

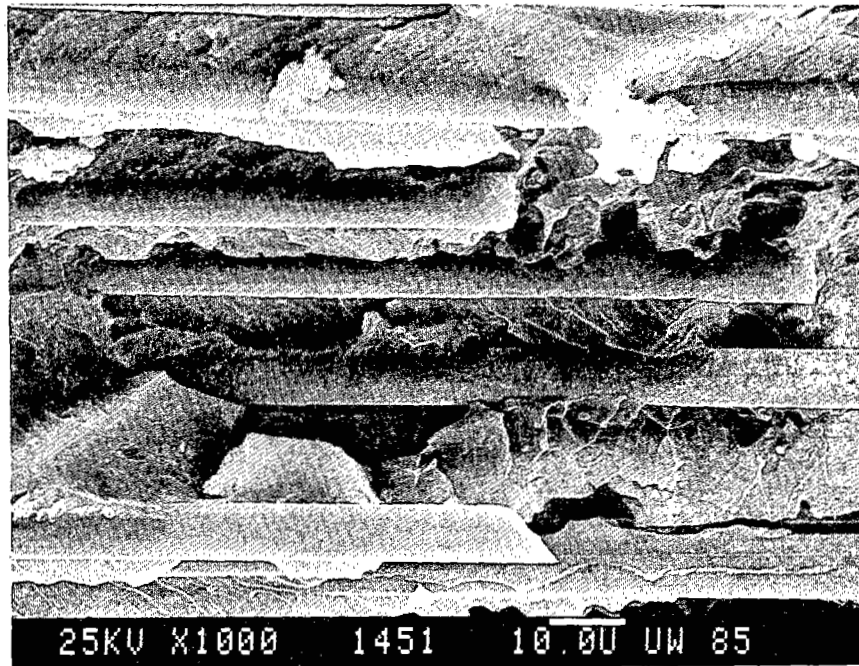


Figure 78. Unsized AS4/Hexcel F155 Unidirectional Composite, Transverse Tensile Specimen AFRX01, 23°C, Dry Condition.

Some broken fibers and a very coarse region of failed matrix are shown. The relatively clean fiber surfaces indicate imperfect fiber-matrix interface bonding.

ORIGINAL PAGE IS  
OF POOR QUALITY

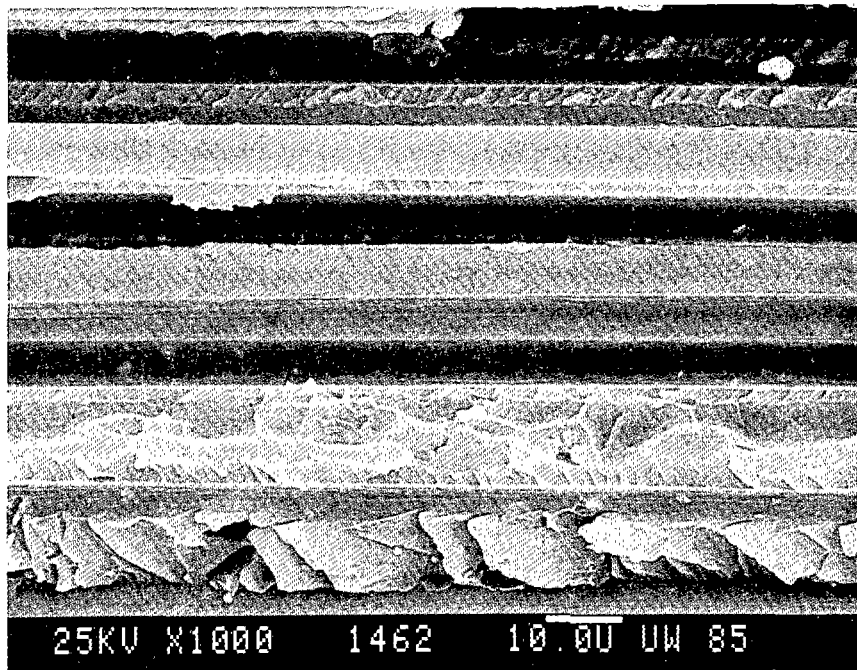


Figure 79. EPON 828-Sized AS4/Hexcel F155 Unidirectional Composite, Transverse Tensile Specimen AFRX10, 23°C, Dry Condition.

Some bare fibers and a somewhat less coarse matrix failure surface than seen in Figure 78 are evident.

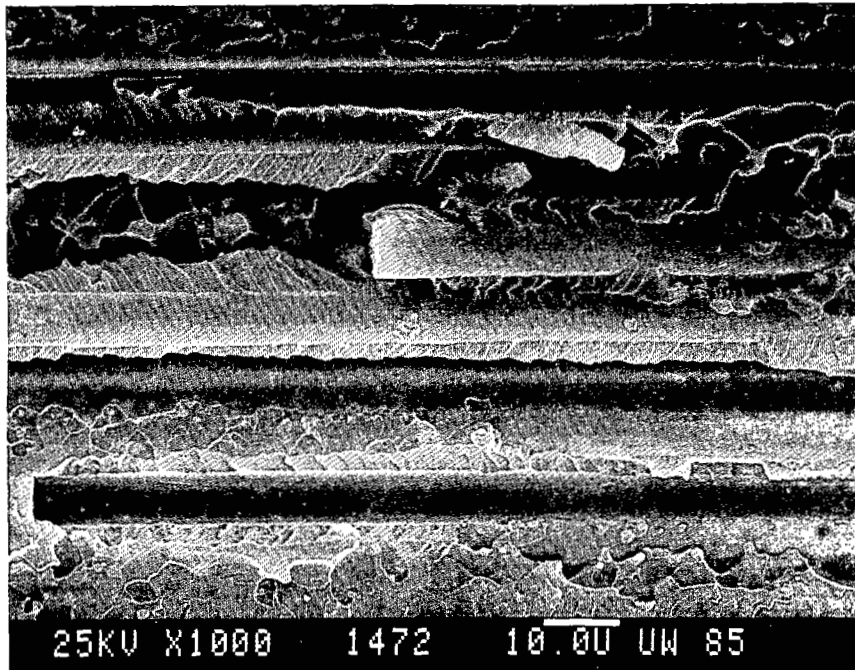


Figure 80. PVA-Sized AS4/Hexcel F155 Unidirectional Composite, Transverse Tensile Specimen AFRX26, 23°C, Dry Condition.

Some broken fibers and moderate fiber/matrix adhesion will be noted.

ORIGINAL PAGE IS  
OF POOR QUALITY

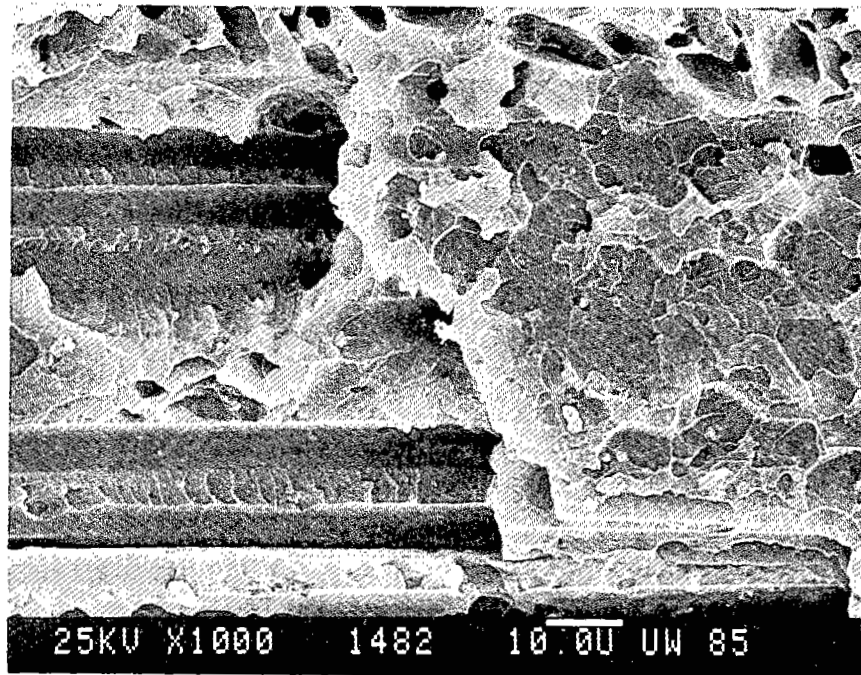


Figure 81. Polysulfone-Sized AS4/Hexcel F155 Unidirectional Composite, Transverse Tensile Specimen AFRX33, 23°C, Dry Condition.

Better fiber/matrix adhesion in the center of the photograph, where a fiber has pulled some matrix away, is indicated.

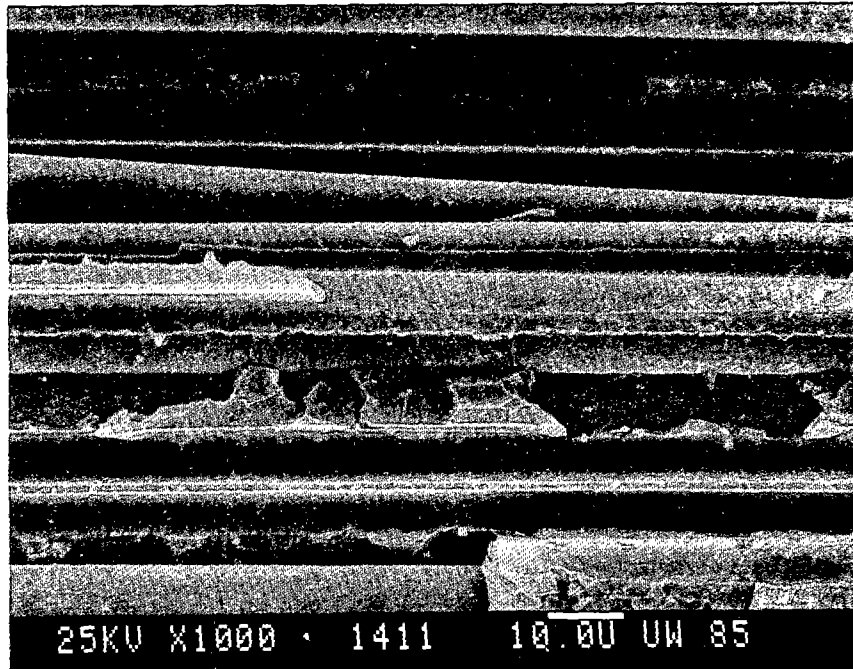


Figure 82. Unsized AS4/Hexcel F155 Unidirectional Composite, Transverse Tensile Specimen AFEX00, 38°C, Moisture-Conditioned.

Some indications of interface breakdown and exposed fibers can be seen.



ORIGINAL PAGE IS  
OF POOR QUALITY

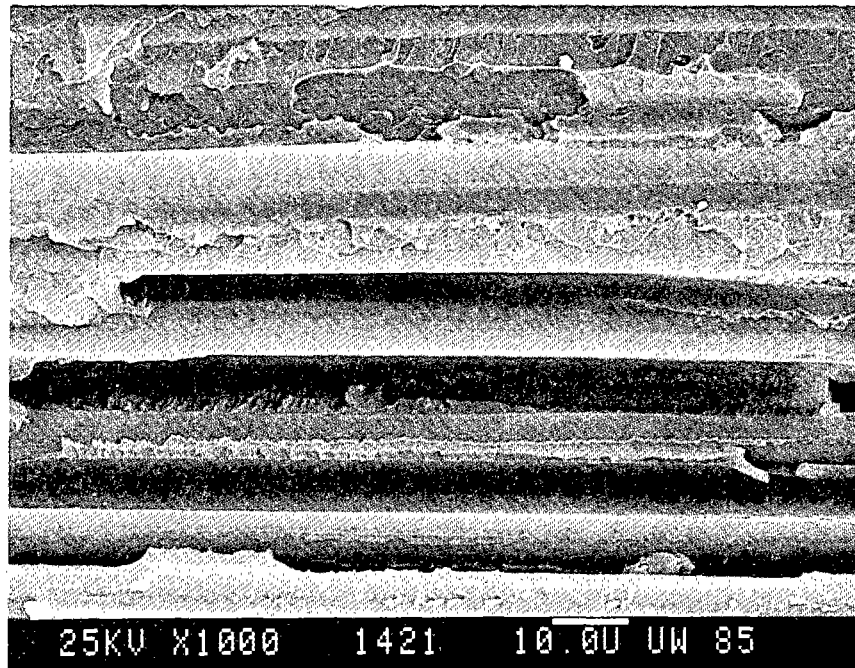


Figure 83. EPON 828-Sized AS4/Hexcel F155 Unidirectional Composite, Transverse Tensile Specimen AFEX13, 38°C, Moisture-Conditioned.

Some indication of reasonable fiber/matrix adhesion is evidenced by the matrix still adhering to the otherwise bare fibers.

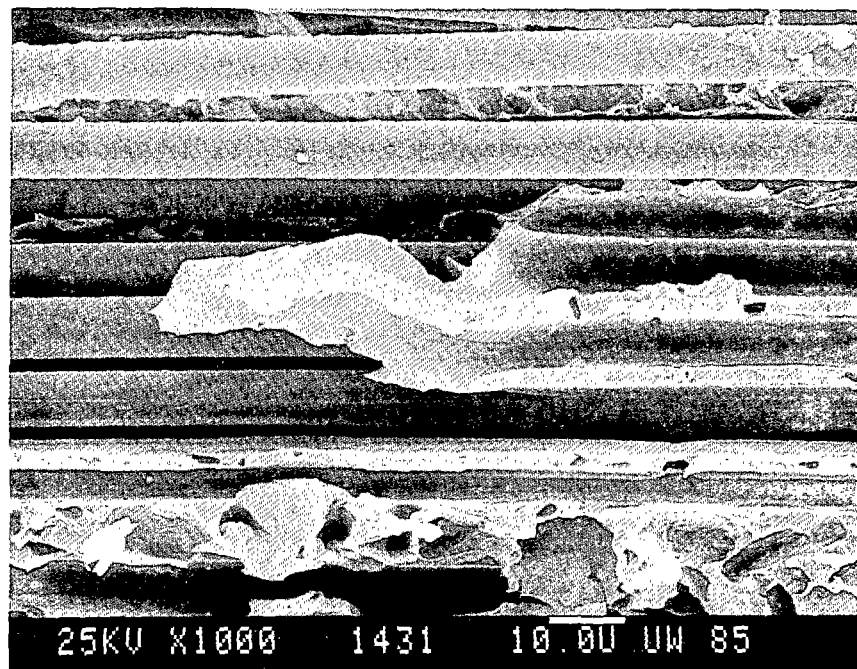


Figure 84. PVA-Sized AS4/Hexcel F155 Unidirectional Composite, Transverse Tensile Specimen AFEX21, 38°C, Moisture-Conditioned.

Matrix ductility is quite evident in the center of the photograph, with some bare fibers also seen.

ORIGINAL PAGE IS  
OF POOR QUALITY

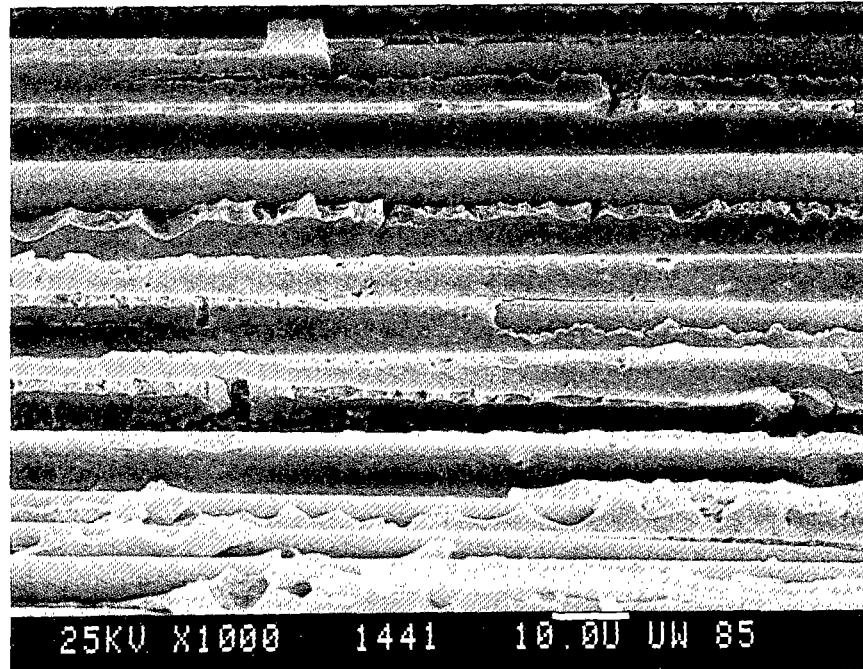


Figure 85. Polysulfone-Sized AS4/Hexcel F155 Unidirectional Composite, transverse Tensile Specimen AFEX33, 38°C, Moisture-Conditioned.

Bare fibers and other indications of inadequate interface bonding can be seen.

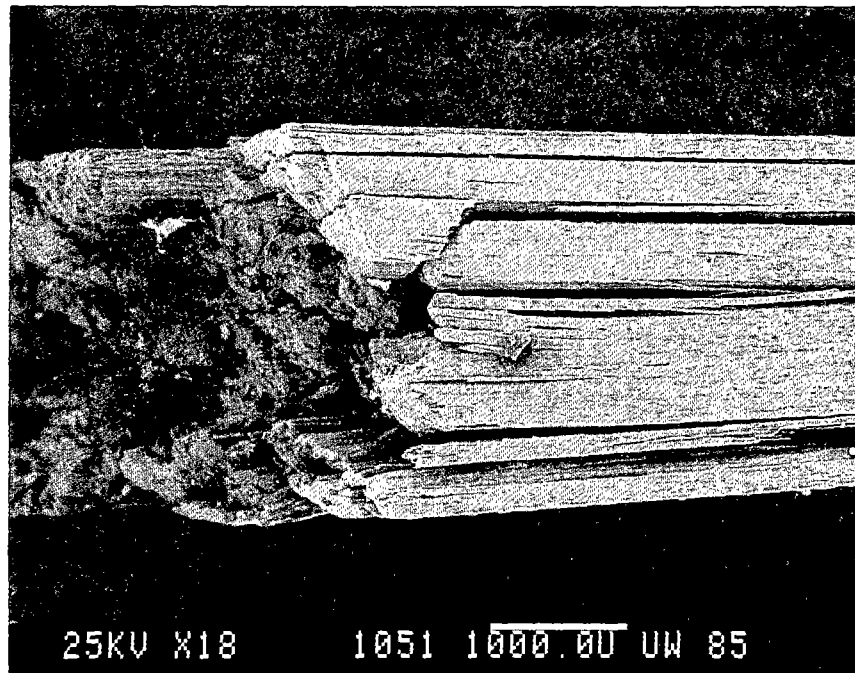


Figure 86. Unsized AS4/Hercules 3501-6 Unidirectional Composite, Axial Compression Specimen AGRY05, 23°C, Dry Condition.

Little indication of fiber buckling, but major longitudinal splitting and gross shear failure, is shown.

ORIGINAL PAGE IS  
OF POOR QUALITY

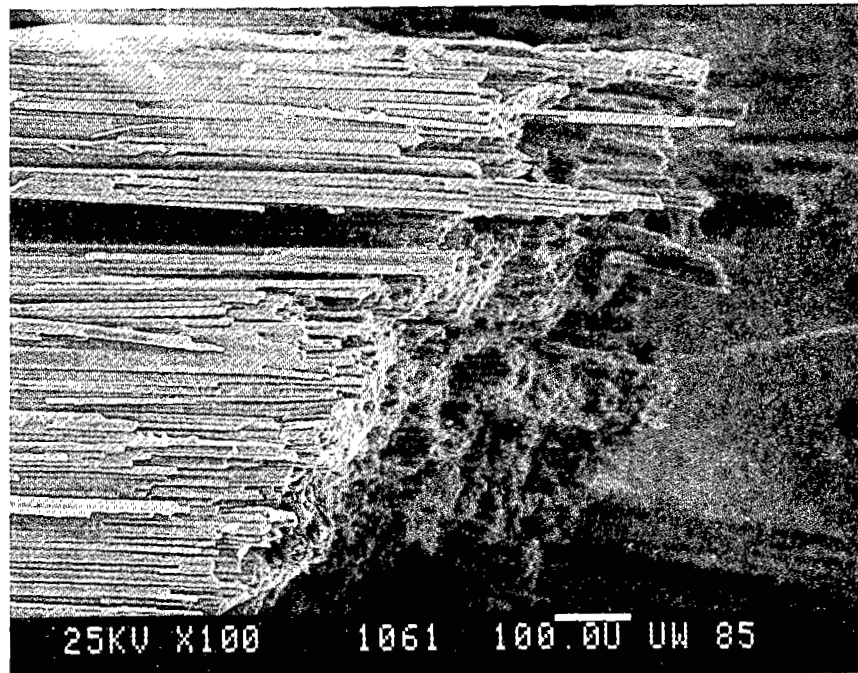


Figure 87. EPON 828-Sized AS4/Hercules 3501-6 Unidirectional Composite, Axial Compression Specimen AGRY17, 23°C, Dry Condition.

No evidence of fiber microbuckling, but some longitudinal splitting and gross shear failure, is indicated.

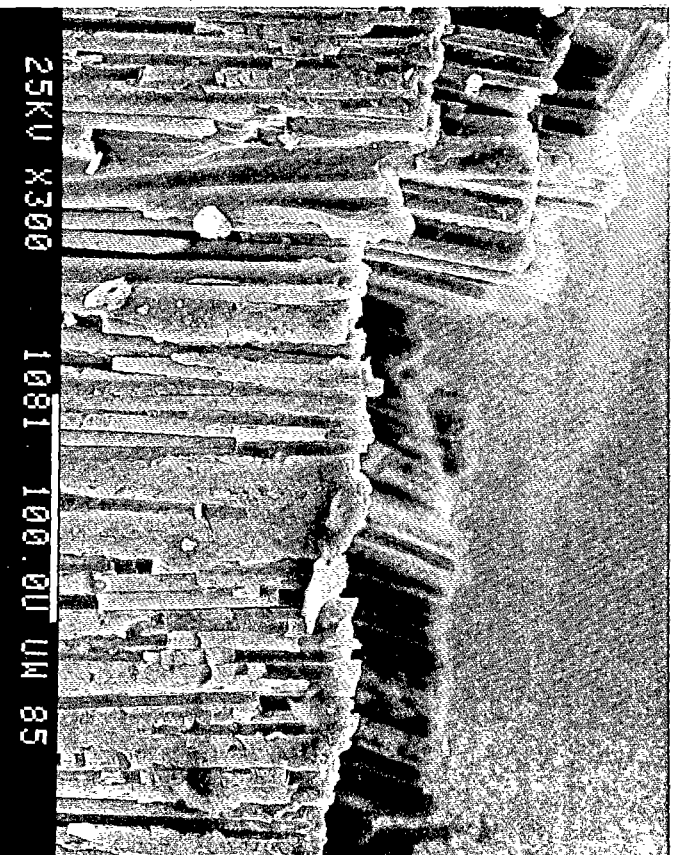


Figure 88. PVA-Sized AS4/Hercules 3501-6 Unidirectional Composite, Axial Compression Specimen AGRY22, 23°C, Dry Condition.

This higher magnification photograph shows individual broken fibers that have sheared off. The gross failure looked similar to that of specimen AGRY30 in Figure 89.

ORIGINAL PAGE IS  
OF POOR QUALITY



Figure 89. Polysulfone-Sized AS4/Hercules 3501-6 Unidirectional Composite, Axial Compression Specimen AGRY30, 23°C, Dry Condition.

Gross longitudinal splitting and extensive shear failures are shown.

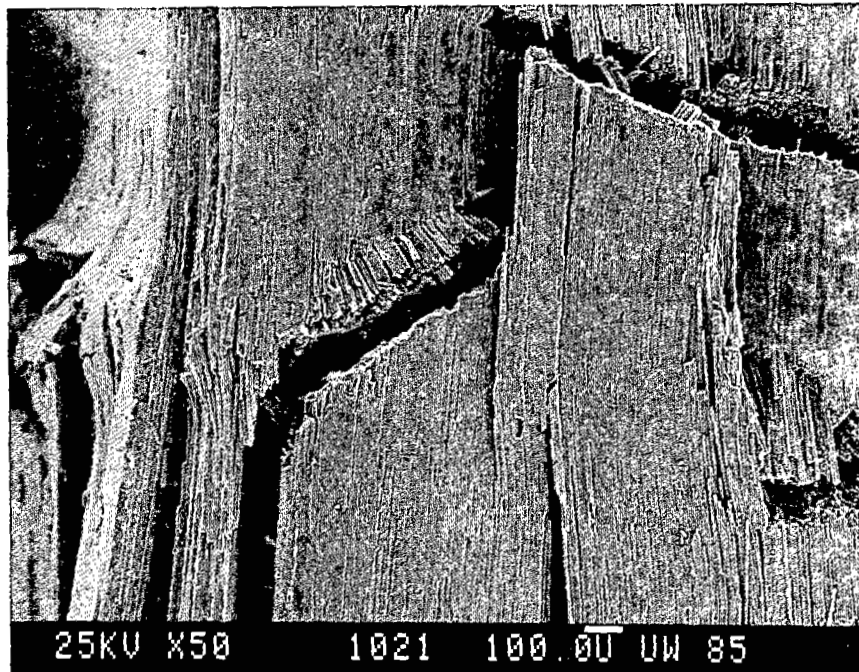


Figure 90. Unsized AS4/Hercules 3501-6 Unidirectional Composite, Axial Compression Specimen AGFY03, 100°C, Moisture-Conditioned.

An edge view of the failure zone is shown. Some buckled fibers can be seen near the center of the photograph, with some longitudinal splitting also evident at the bottom and left side of the photograph.



ORIGINAL PAGE IS  
OF POOR QUALITY

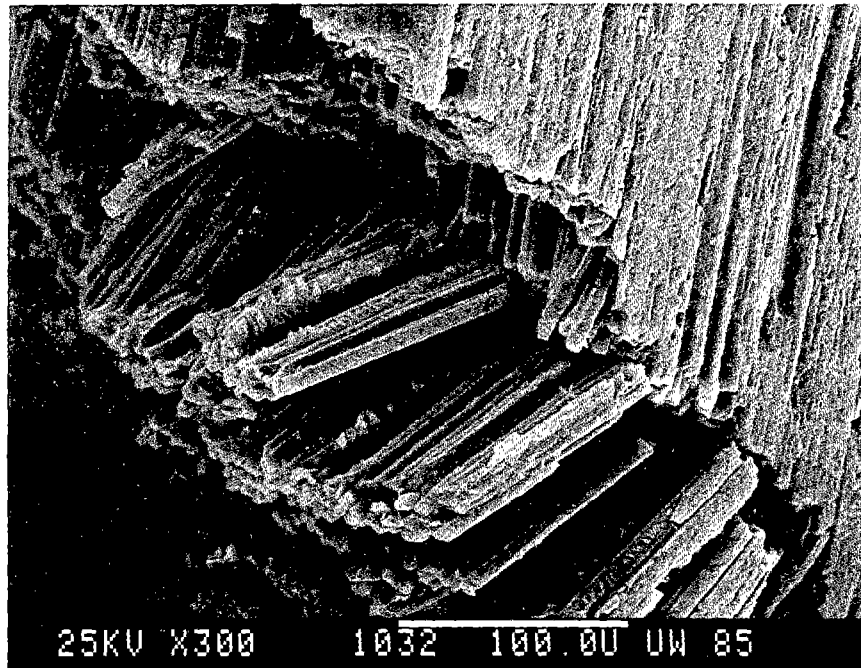


Figure 91. EPON 828-Sized AS4/Hercules 3501-6 Unidirectional Composite, Axial Compression Specimen AGEY13, 100°C, Moisture-Conditioned.

A closeup of the failure zone is shown. Many buckled fibers are evident.

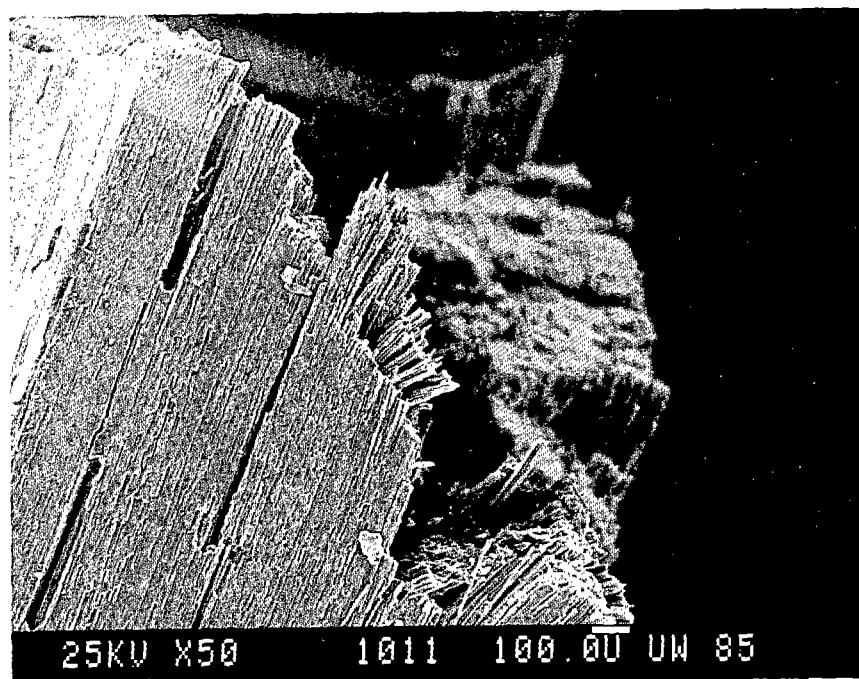


Figure 92. PVA-Sized AS4/Hercules 3501-6 Unidirectional Composite, Axial Compression Specimen AGEY26, 100°C, Moisture-Conditioned.

The edge of the specimen is shown, with some evidence of fiber microbuckling and also some longitudinal splitting.

ORIGINAL PAGE IS  
OF POOR QUALITY

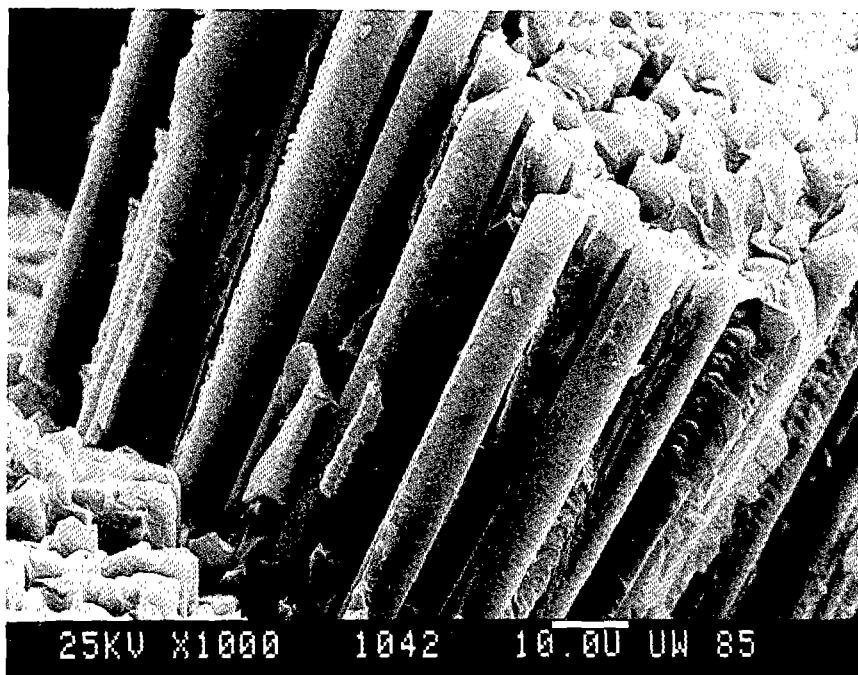


Figure 93. Polysulfone-Sized AS4/Hercules 3501-6 Unidirectional Composite, Axial Compression Specimen AGEY30, 100°C, Moisture-Conditioned.

A closeup of a bundle of buckled fibers is shown. The fibers debonded from the matrix, and some matrix adhering to the surface of the loose fibers will be noted.

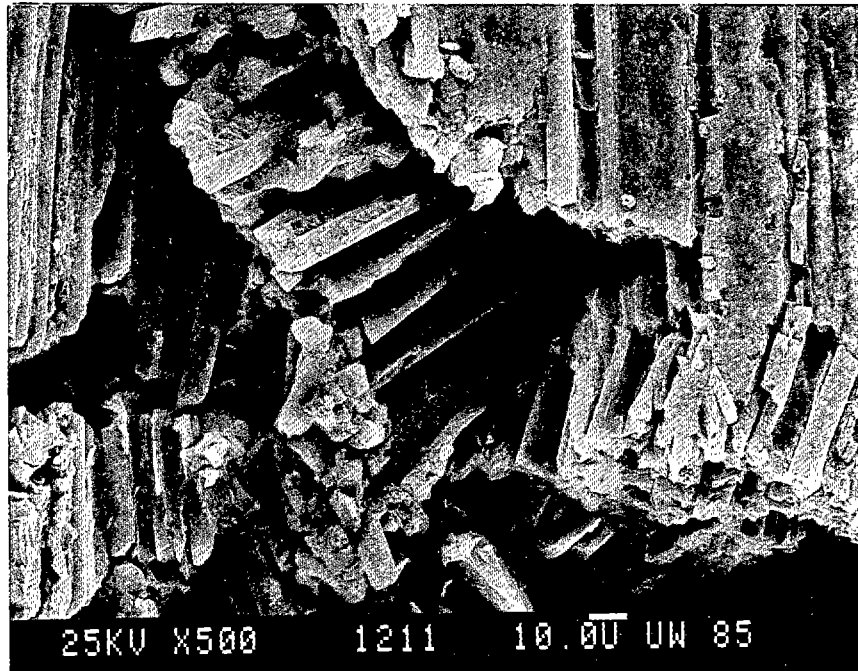


Figure 94. Unsized AS4/Hercules 4001 Unidirectional Composite, Axial Compression Specimen AGRZ00, 23°C, Dry Condition.

A typical section of buckled fibers can be seen in this fractured region.

ORIGINAL PAGE IS  
OF POOR QUALITY

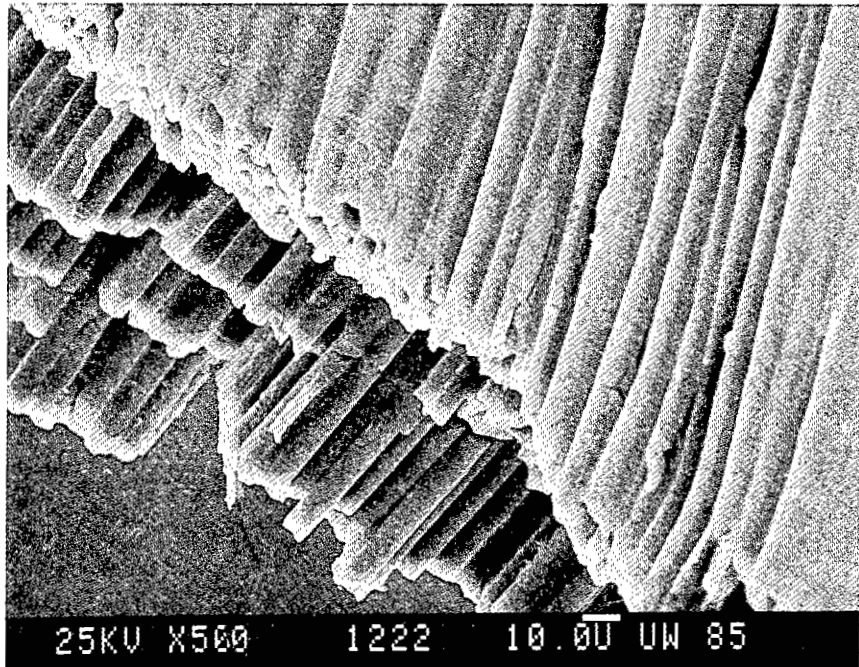


Figure 95. EPON 828-Sized AS4/Hercules 4001 Unidirectional Composite, Axial Compression Specimen AGRZ13, 23°C, Dry Condition.

A section of buckled fibers at the failure zone of the specimen is shown.

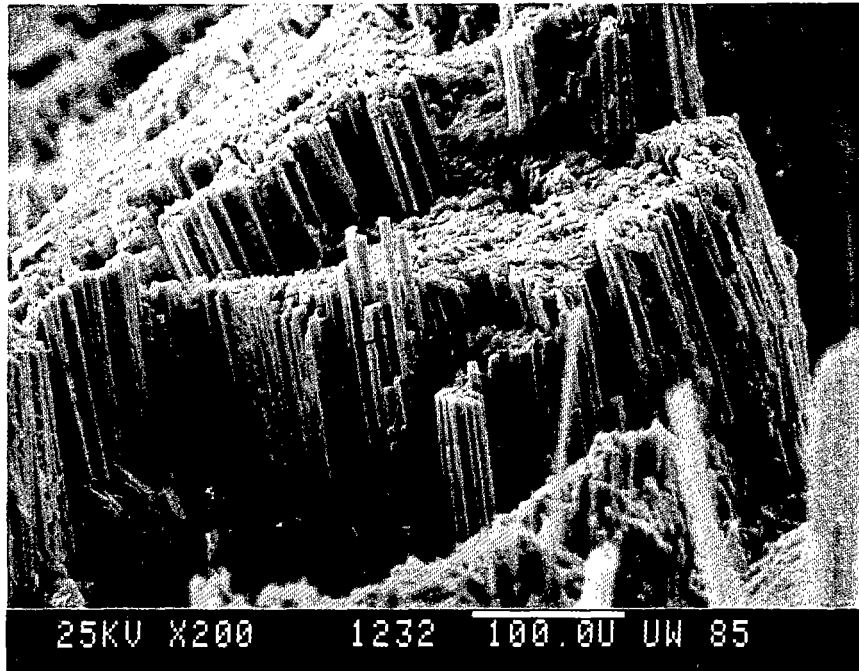


Figure 96. PVA-Sized AS4/Hercules 4001 Unidirectional Composite, Axial Compression Specimen AGRZ27, 23°C, Dry Condition.

A large amount of longitudinal splitting and some buckled fibers near the failure zone can be seen.

ORIGINAL PAGE IS  
OF POOR QUALITY

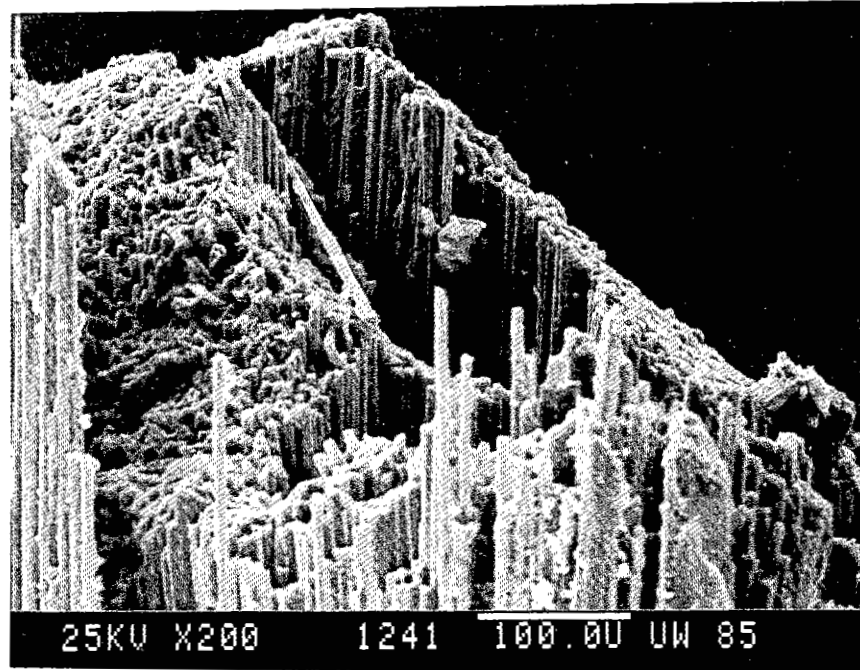


Figure 97. Polysulfone-Sized AS4/Hercules 4001 Unidirectional Composite, Axial Compression Specimen AGRZ39, 23°C, Dry Condition.

Only gross shear failures, with no apparent evidence of fiber buckling, is shown.

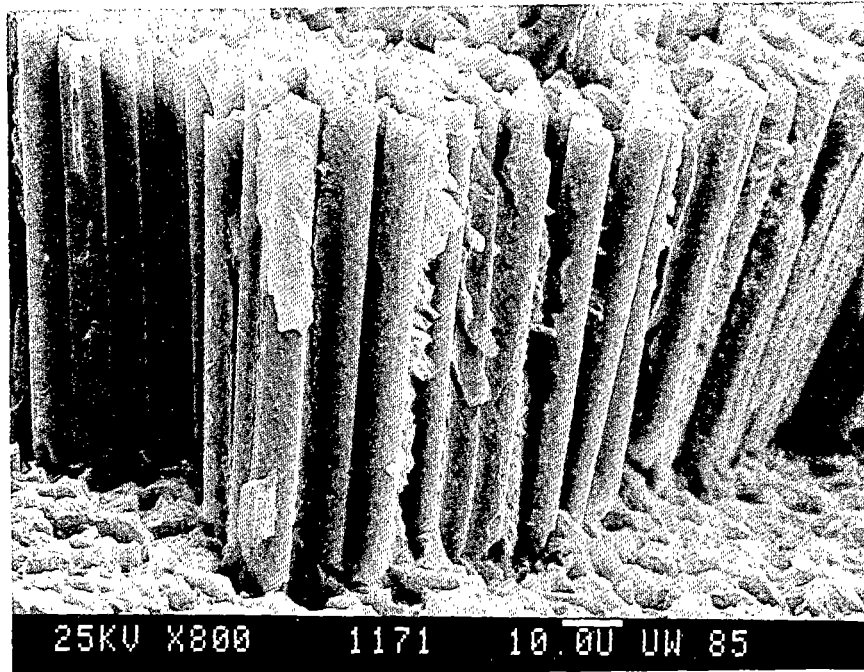


Figure 98. Unsized AS4/Hercules 4001 Unidirectional Composite, Axial Compression Specimen AGEZ08, 100°C, Moisture-Conditioned.

Broken fibers caused by microbuckling of the graphite fibers can be seen. Many longitudinal cracks and fiber/matrix debonds will also be noted.



ORIGINAL PAGE IS  
OF POOR QUALITY

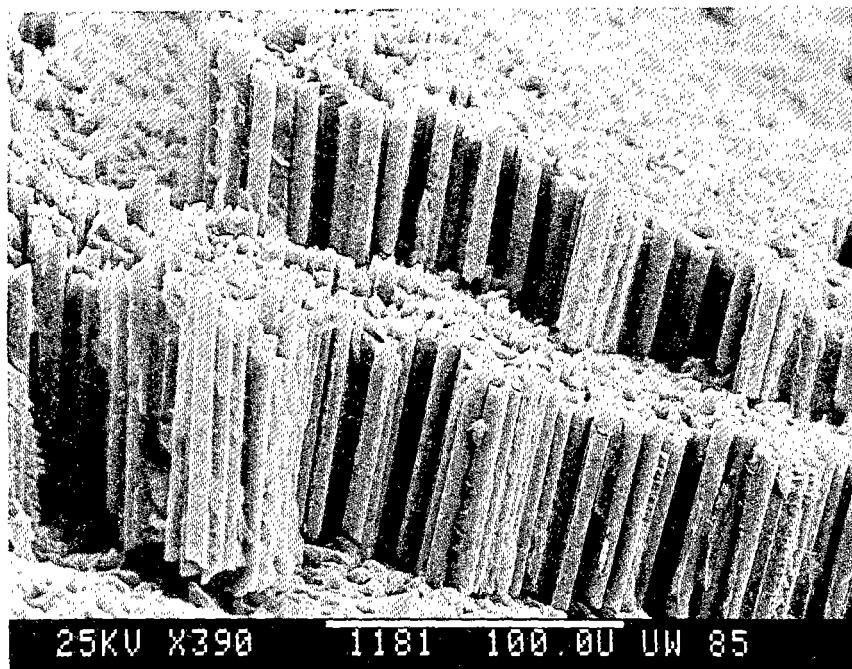


Figure 99. EPON 828-Sized AS4/Hercules 4001 Unidirectional Composite, Axial Compression Specimen AGEZ13, 100°C, Moisture-Conditioned.

A regular pattern of fiber microbuckling will be noted.

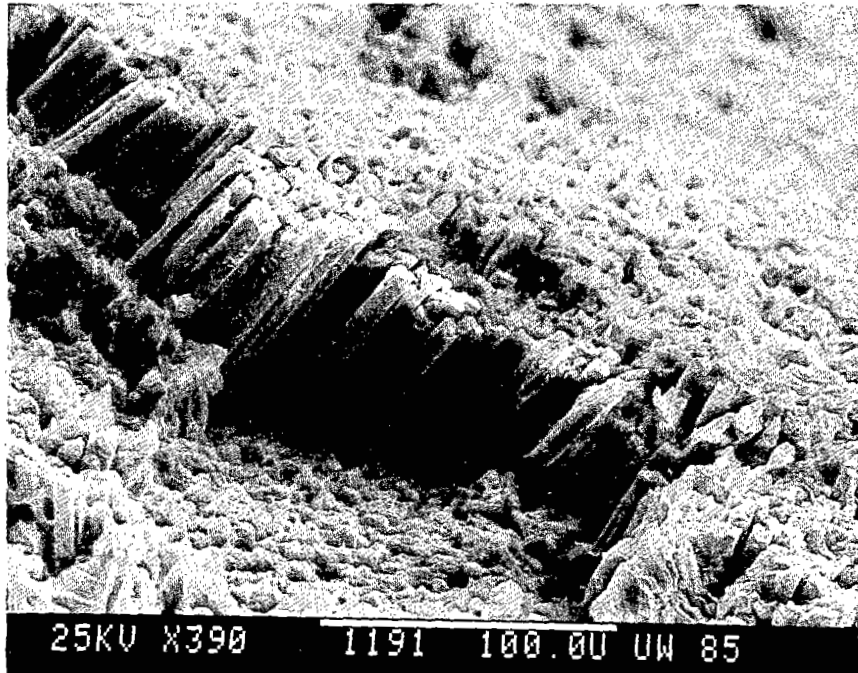


Figure 100. PVA-Sized AS4/Hercules 4001 Unidirectional Composite, Axial Compression Specimen AGEZ28, 100°C, Moisture-Conditioned.

A somewhat shorter broken fiber length in the buckling zone will be noted. This suggests a lower fiber/matrix interface adhesion and therefore, a lower compression strength, due to less lateral fiber support by the matrix.

ORIGINAL PAGE IS  
OF POOR QUALITY

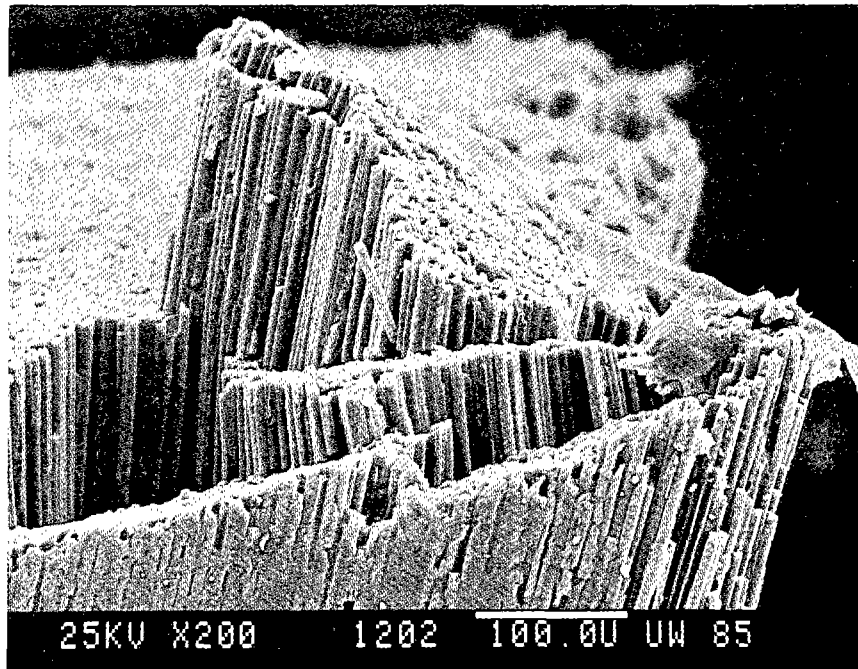


Figure 101. Polysulfone-Sized AS4/Hercules 4001 Unidirectional Composite, Axial Compression Specimen AGEZ34, 100°C, Moisture-Conditioned.

A somewhat longer fiber length in the buckling zone, indicating a higher fiber-matrix interface adhesion than in the PVA-coated fiber composite of Figure 95, and an equal or better fiber-matrix adhesion than in the unsized or EPON 828-sized fiber composites of Figures 98 and 99, will be noted.

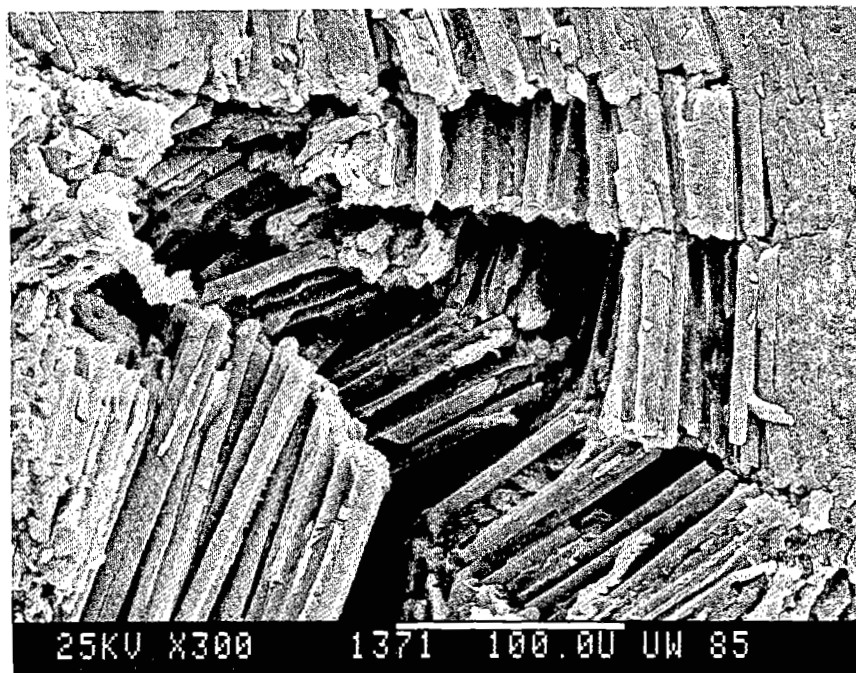


Figure 102. Unsized AS4/Hexcel F155 Unidirectional Composite, Axial Compression Specimen AGRX00, 23°C, Dry Condition.

A good example of fiber microbuckling is shown. Critical fiber lengths are somewhat longer than were observed in the elevated temperature, wet (ETW) specimen failures.

ORIGINAL PAGE IS  
OF POOR QUALITY.

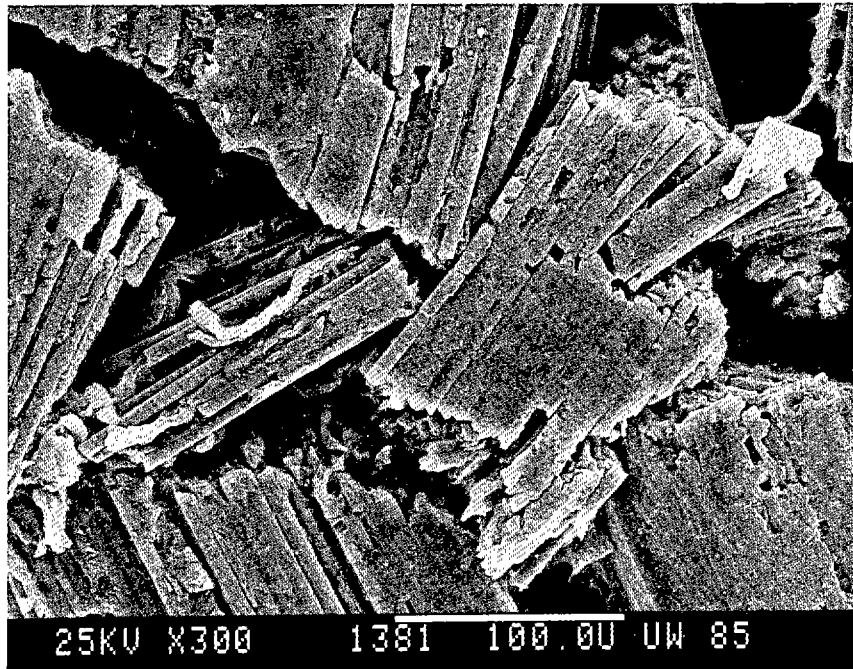


Figure 103. EPON 828-Sized AS4/Hexcel F155 Unidirectional Composite, Axial Compression Specimen AGRX17, 23°C, Dry Condition.

A section of buckled fibers very similar in length to the ETW specimen in Figure 107, but slightly longer than those of the RTD unsized specimen of Figure 102, can be seen.

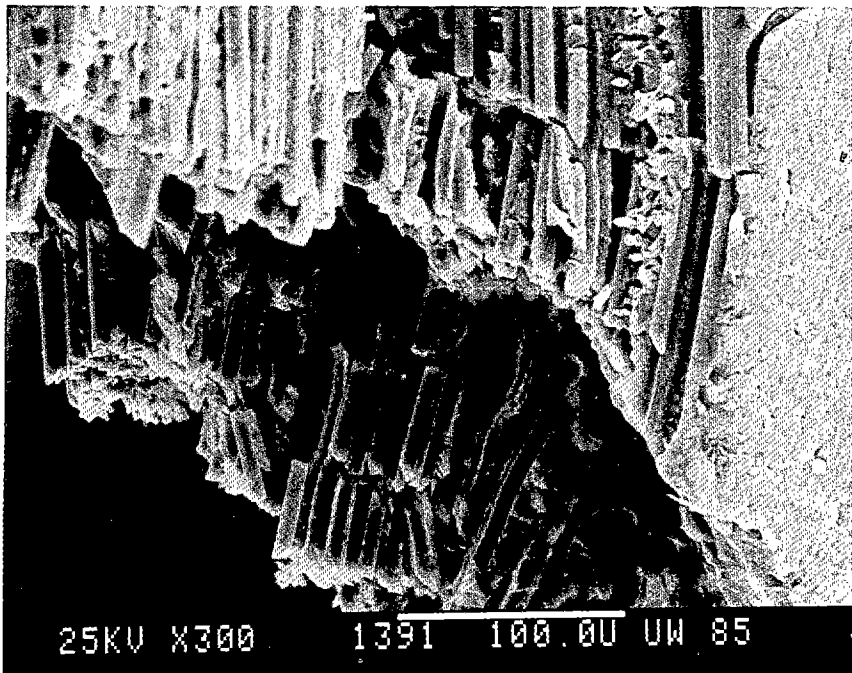


Figure 104. PVA-Sized AS4/Hexcel F155 Unidirectional Composite, Axial Compression Specimen AGRX26, 23°C, Dry Condition.

A region of fibers which appear to have been broken up into smaller segments by post-failure crushing rather than by primary fiber microbuckling is shown.

ORIGINAL PAGE IS  
OF POOR QUALITY

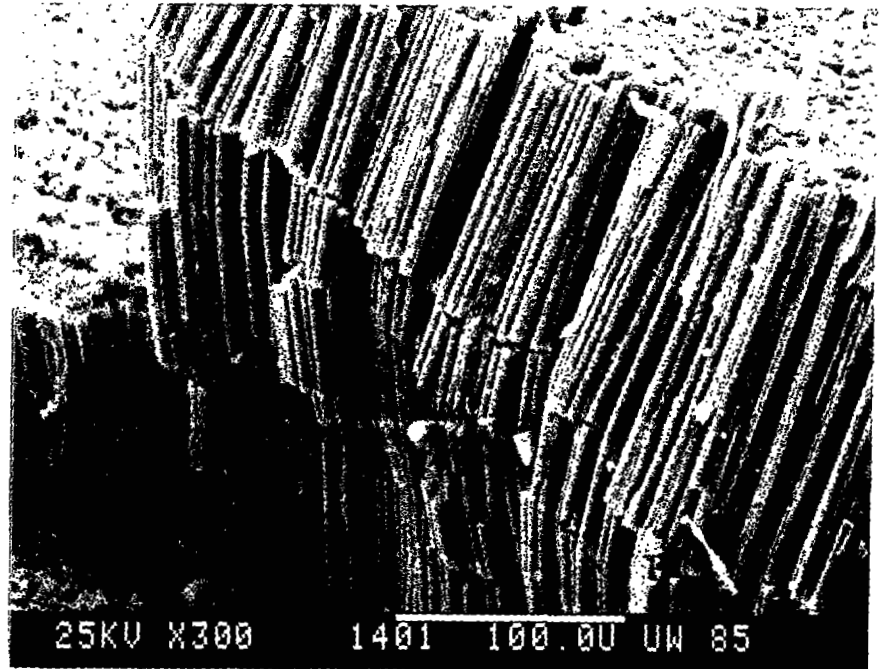


Figure 105. Polysulfone-Sized AS4/Hexcel F155 Unidirectional Composite, Axial Compression Specimen AGRX33, 23°C, Dry Condition.

A section of buckled fibers on the surface, which are of similar critical length to those of the ETW specimen shown in Figure 109, can be seen.

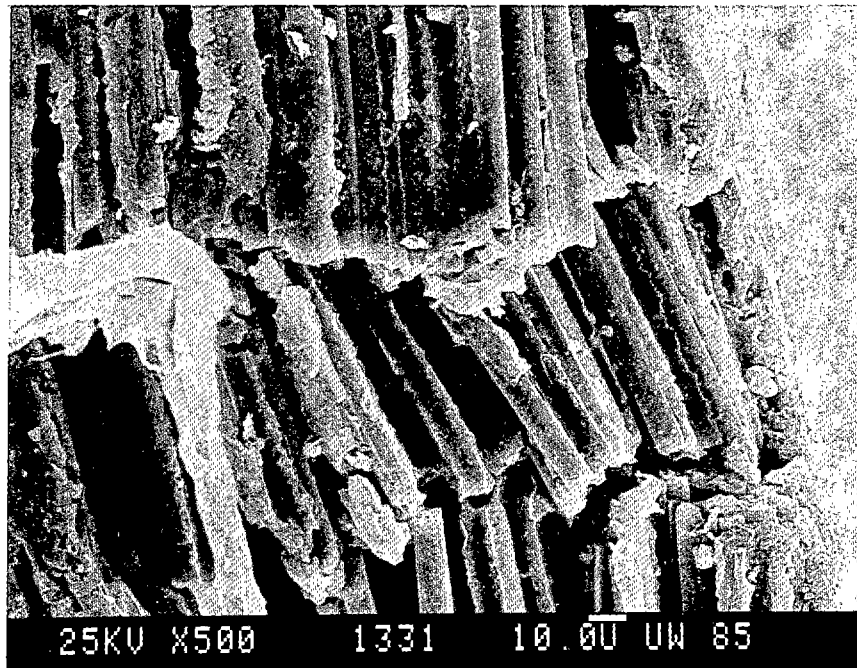


Figure 106. Unsized AS4/Hexcel F155 Unidirectional Composite, Axial Compression Specimen AGEX07, 38°C, Moisture-Conditioned.

The relatively short buckling lengths for these unsized graphite fibers are evident.



ORIGINAL PAGE IS  
OF POOR QUALITY

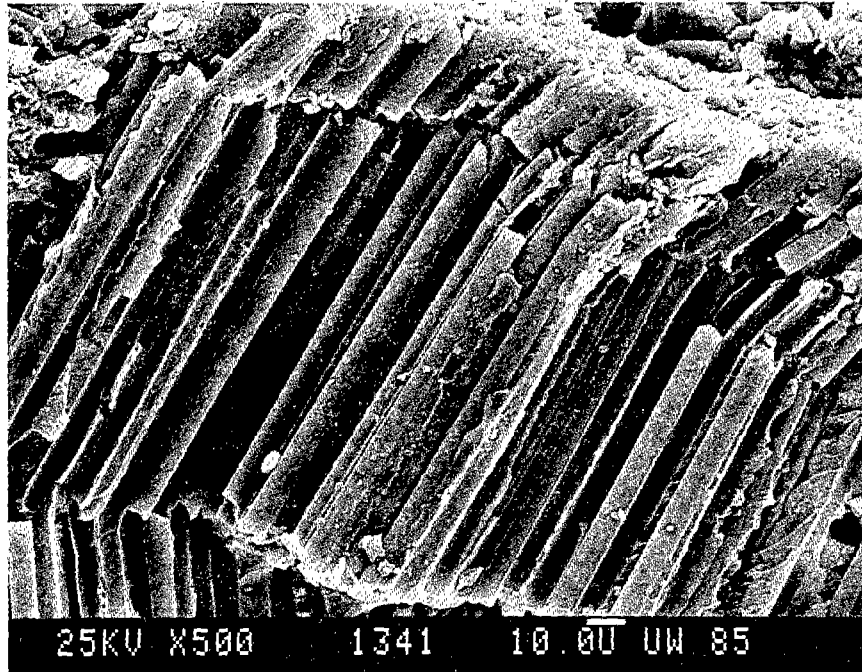


Figure 107. EPON 828-Sized AS4/Hexcel F155 Unidirectional Composite, Axial Compression Specimen AGEX11, 38°C, Moisture-Conditioned.

A buckled fiber length almost twice that of the unsized fiber composite of Figure 106 will be noted.

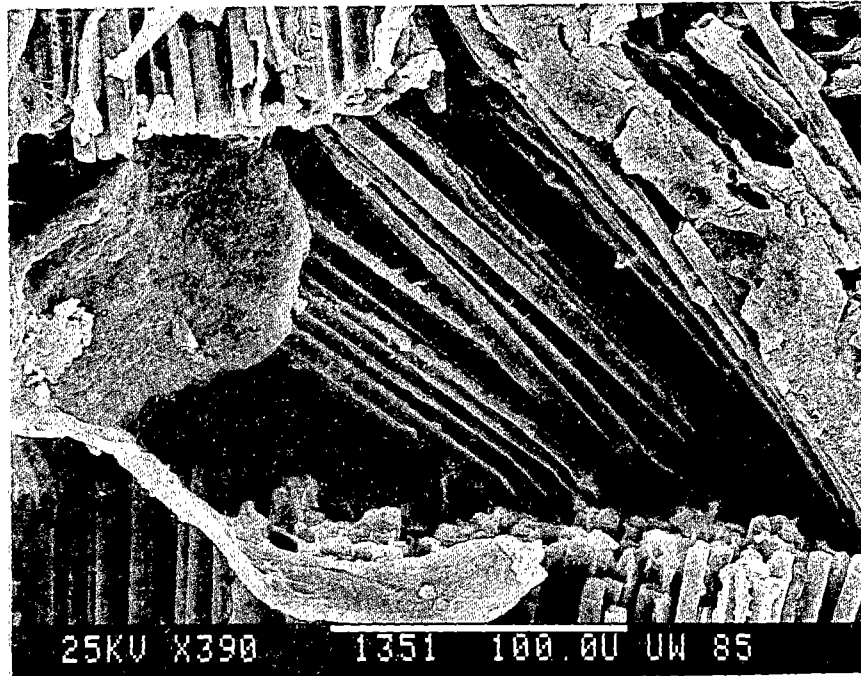


Figure 108. PVA-Sized AS4/Hexcel F155 Unidirectional Composite, Axial Compression Specimen AGEX28, 38°C, Moisture-Conditioned.

A greater fiber buckling length than for the EPON 828-sized fiber composite of Figure 107 is suggested.

ORIGINAL PAGE IS  
OF POOR QUALITY

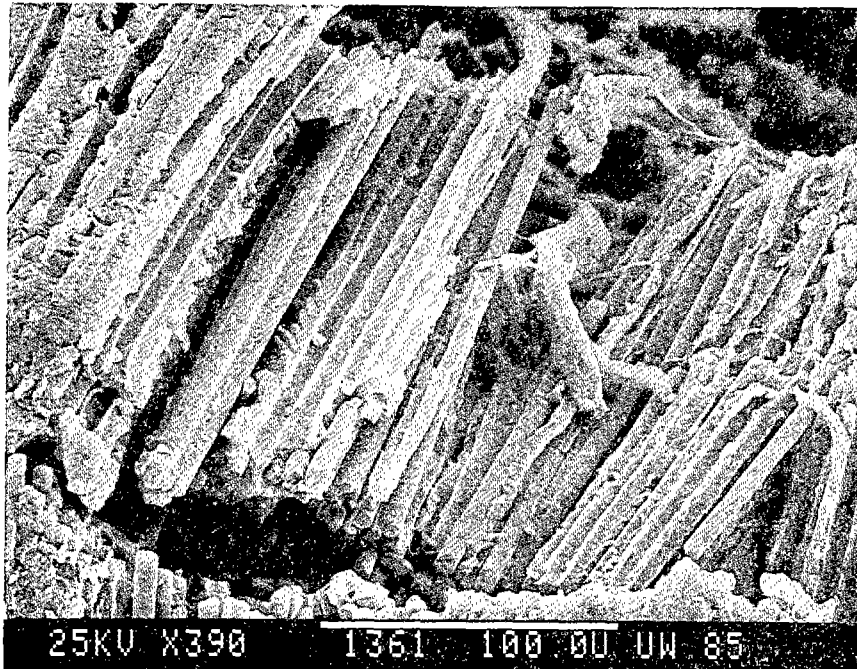


Figure 109. Polysulfone-Sized AS4/Hexcel F155 Unidirectional Composite, Axial Compression Specimen AGEX35, 38°C, Moisture-Conditioned.

Buckled fibers of lengths similar to those of the PVA-sized fiber composite shown in Figure 108 can be observed.



## SECTION 6

### ANALYTICAL/EXPERIMENTAL CORRELATIONS

The purpose of this section is to briefly describe a two-dimensional finite element micromechanics analysis which is available, and to apply it to the present study. The analysis is capable of predicting the complete response of a unidirectional composite to any combination of mechanical and hygrothermal loadings. These predictions will be correlated with the transverse tensile data experimentally measured as part of the present study.

#### 6.1 Micromechanics Analysis

The Composite Materials Research Group (CMRG) at the University of Wyoming has developed a numerical (finite element) micromechanics model to predict the loading response of a unidirectional fiber reinforced composite lamina [10]. This analysis allows for nonlinear stress-strain behavior in the constituent components of a composite system as well as for temperature- and moisture-dependent material properties. The analysis technique has been described in detail in Reference [10]; therefore, only a brief description will be included here. The computer program itself is called WYO2D, and is documented in Reference [31].

The model is based on a generalized plane strain finite element analysis of a typical repeating unit of matrix material containing a single fiber within a unidirectional continuous fiber composite. If a periodic fiber packing array is assumed, the region of interest can

- 195 -

Preceding Page Blank

ANK

be reduced, via periodicity arguments, to a single fiber surrounded by a block of matrix material. Then, by symmetry, this region to be analyzed can be reduced to a single quadrant. Other geometric arrays may be assumed, but previous work has shown that assuming a square array provides good correlation with experiment [27,28,32,33]. Further discussion of the rationale in choosing this model is contained in References [10,26]. The finite element grid used in the present micromechanics analysis is shown in Figure 110. By changing the radius of the fiber relative to the unit cell boundary, different fiber volumes within the composite material can be simulated. A typical grid is pictured in Figure 110.

Generalized plane strain, for purposes of this analysis, assumes displacements may occur in all three coordinate directions. Specifically, each displacement is dependent upon the x and y coordinates, and the displacement in the z-direction (fiber direction) has an additional linear dependence in the z-direction, the axial (fiber) coordinate of the composite ply. Including x and y dependence of the z-displacements allows a special form of axial (longitudinal) shear deformation corresponding to the generalized plane strain treatment. Therefore, although the analysis is basically two-dimensional in nature, five components of applied stress can be modeled, specifically  $\bar{\sigma}_x$ ,  $\bar{\sigma}_y$ ,  $\bar{\sigma}_z$ ,  $\bar{\tau}_{xz}$  and  $\bar{\tau}_{yz}$ . The model is therefore capable of predicting stress-strain response due to any one or any combination of these loading modes.

Material behavior of the fiber constituent is assumed to be transversely isotropic, in order to model anisotropic fibers such as graphite. The matrix material is assumed to be isotropic and elasto-

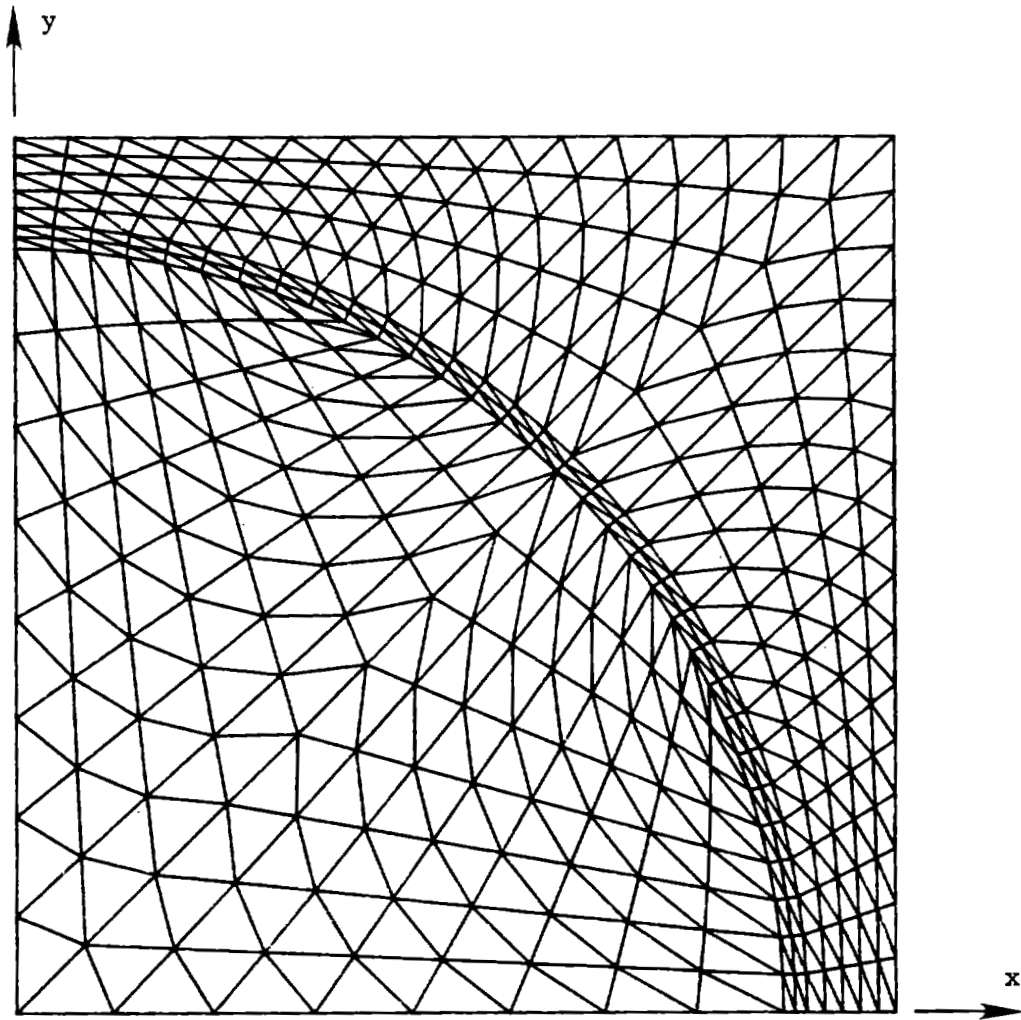


Figure 110. Typical Finite Element Model of One Quadrant of the Repeating Unit Cell of a Unidirectional Composite Material in a Square Fiber Packing Array.

plastic, the plastic response being modeled by the Prandtl-Reuss flow rule. As previously noted, temperature and moisture effects on the constituent material properties are also included.

The analysis includes a crack propagation capability also [25, 28,34], which is a recent addition to Computer Program WY02D [31]. Thus, it is now possible to study patterns of crack propagation induced under any combination of mechanical and hygrothermal loadings. This also extends the micromechanics analysis capability one step closer to the ultimate goal of being able to accurately predict unidirectional composite strength. Strengths can, in fact, be predicted now using the present analysis, as will be demonstrated in the next subsections. However, there is still insufficient unidirectional composite experimental data available covering enough different fiber/matrix material combinations and test conditions to permit an adequate correlation of micromechanics predictions with actual data. That is, to date, sufficient correlations have been attempted (see, for example, Reference [25]) to indicate significant promise, but not enough to be conclusive.

One recognized problem area is the selection or development of a suitable failure criterion. More composites test data must become available before much more is done in this area.

## 6.2 Constituent Properties

Constituent material properties for the Hercules AS4 fiber were obtained from Reference [2] where possible. Transverse fiber properties are very difficult to measure directly; therefore, it was necessary to estimate these values based on previous experience [18, 19]. The fiber properties used in the present analysis are listed in



Table 23.

The full experimental results for the three matrix materials characterized and utilized as part of the present study, viz, Hercules 3501-6, Hercules 4001, and Hexcel F155, were presented in detail in Section 4 of this report. For use in the micromechanics analysis, it is necessary to express these data in a form which can be input to the associated computer program. The experimental data could be input point by point, i.e., by expressing each stress-strain curve as a series of point values. This would be tedious. Also, since matrix tests were performed at discrete temperature and moisture conditions and the analysis is capable of predicting composite response for any combination of conditions, it is necessary to interpolate (and sometimes even to extrapolate) the available experimental data to other hygrothermal conditions. Thus, it is convenient to fit the temperature- and moisture-dependent data to an equation. This permits easy interpolation, and at the same time provides a means, by linear regression, of averaging the typically five individual stress-strain curves at each test condition together.

For the present predictions of composite response, only the neat resin stress-strain data generated from the shear tests were utilized. As the shear stress-strain response of the matrix materials is nonlinear, it is necessary to input the entire stress-strain curve into the micromechanics analysis. This is done by using a three-parameter experimental equation of the form first suggested by Richard and Blacklock [34], i.e.,

Table 23

## Hercules AS4 Graphite Fiber Properties [2]

Longitudinal Modulus, $E_{\ell}$	235 GPa	(34 Msi)
Transverse Modulus*, $E_t$	14 GPa	( 2 Msi)
Major Poisson's Ratio*, $\nu_{\ell t}$		0.20
In-Plane Poisson's Ratio*, $\nu_{tt}$		0.25
Longitudinal Shear Modulus*, $G_{\ell t}$	28 GPa	( 4 Msi)
In-Plane Shear Modulus**, $G_{tt}$	5.5 GPa	(0.8 Msi)
Coefficient of Longitudinal Thermal Expansion, $\alpha_{\ell}$		$-0.36 \times 10^{-6} / ^\circ\text{C}$
Coefficient of Transverse Thermal Expansion*, $\alpha_t$		$18 \times 10^{-6} / ^\circ\text{C}$
Longitudinal Tensile Strength, $\sigma_{\ell}^u$	3.59 GPa	(520 ksi)
Transverse Tensile Strength*, $\sigma_t^u$	0.35 GPa	(50 ksi)

---

\* Estimated (see References [18,19])

\*\* Calculated,  $G_{tt} = E_t / 2(1 + \nu_{tt})$

$$\tau = \frac{G \gamma}{\left[1 + \left|\frac{G\gamma}{\tau_0}\right|^n\right]^{\frac{1}{n}}}$$

where

G = initial shear modulus

n = curvature parameter

$\tau_0$  = asymptotic shear stress value

$\gamma$  = shear strain

The three parameters, G, n, and  $\tau_0$  describe the stress-strain response of the matrix in a particular temperature and moisture environment. By then using regression techniques, each parameter may be described as a polynomial function in temperature and moisture by using equations of the form

$$P = C_1 T^2 + C_2 T + C_3 M + C_4 TM + C_5$$

where

P = property of interest (e.g., G, n,  $\tau_0$ , etc.)

$C_1 - C_5$  = regression coefficients for that property

Therefore, the entire shear stress-strain response of the matrix is prescribed by three equations for G, n and  $\tau_0$ .

The coefficients describing the shear stress-strain behavior of the three matrix materials, along with the Poisson's ratios, yield and ultimate strengths, and thermal and moisture expansion coefficients, are presented in Tables 24 through 26. These are based upon the averaged test data presented in Section 4, and the

Table 24

Hercules 3501-6 Neat Resin Matrix Material Properties  
 Expressed as Functions of Temperature and Moisture  
 (T in °C, M in Wt. %)

$$\text{Property} = C_1 T^2 + C_2 T + C_3 M + C_4 TM + C_5$$

Property	$C_1$	$C_2$	$C_3$	$C_4$	$C_5$
----------	-------	-------	-------	-------	-------

Shear Data

G (psi)	0	$-1.14 \times 10^3$	$-2.49 \times 10^3$	0	$2.60 \times 10^5$
n	0	$2.56 \times 10^{-3}$	$2.78 \times 10^{-3}$	$1.65 \times 10^{-4}$	1.54
$\tau_o$ (psi)	0	$-1.50 \times 10^2$	$-1.36 \times 10^3$	0	$2.67 \times 10^4$
$\tau_y$ (psi)	0	$-3.19 \times 10^1$	$-3.94 \times 10^2$	0	$6.18 \times 10^3$
$\tau_u$ (psi)	0	$-8.73 \times 10^1$	$-6.03 \times 10^2$	0	$1.67 \times 10^4$

Tensile Data

$\sigma_u$ (psi)	0	$-3.47 \times 10^1$	$-1.48 \times 10^2$	0	$9.63 \times 10^3$
$\nu$	0	0	0	0	0.34

Temperature and Moisture Data

$\alpha$ (°C <sup>-1</sup> )	0	$1.22 \times 10^{-7}$	$1.04 \times 10^{-6}$	0	$3.83 \times 10^{-5}$
$\beta$ (%M <sup>-1</sup> )	0	0	0	0	$3.20 \times 10^{-3}$

Table 25

Hercules 4001 Neat Resin Matrix Material Properties  
Expressed as Functions of Temperature and Moisture  
(T in °C, M in Wt. %)

$$\text{Property} = C_1 T^2 + C_2 T + C_3 M + C_4 TM + C_5$$

Property	$C_1$	$C_2$	$C_3$	$C_4$	$C_5$
----------	-------	-------	-------	-------	-------

Shear Data

G (psi)	0	$-2.60 \times 10^2$	$-1.36 \times 10^3$	0	$1.86 \times 10^5$
n	0	0	0	0	3.00
$\tau_o$ (psi)	0	$-3.51 \times 10^1$	$-1.93 \times 10^6$	0	$9.81 \times 10^3$
$\tau_y$ (psi)	0	0	$2.56 \times 10^1$	0	$2.15 \times 10^3$
$\tau_u$ (psi)	0	$2.34 \times 10^1$	$4.56 \times 10^2$	0	$3.46 \times 10^3$

Tensile Data

$\sigma_u$ (psi)	0	0	$-4.33 \times 10^2$	0	$7.70 \times 10^3$
$\nu$	0	0	0	0	0.42

Temperature and Moisture Data

$\alpha$ (°C <sup>-1</sup> )	0	0	$-1.10 \times 10^{-6}$	0	$5.32 \times 10^{-5}$
$\beta$ (%M <sup>-1</sup> )	0	0	0	0	$4.67 \times 10^{-3}$

Table 26

Hexcel F155 Neat Resin Matrix Material Properties  
Expressed as Functions of Temperature and Moisture  
(T in °C, M in Wt. %)

$$\text{Property} = C_1 T^2 + C_2 T + C_3 M + C_4 TM + C_5$$

Property	$C_1$	$C_2$	$C_3$	$C_4$	$C_5$
G (psi)	0	$-3.84 \times 10^2$	$-3.74 \times 10^2$	0	$1.69 \times 10^5$
n	0	0	$8.88 \times 10^{-2}$	0	2.78
$\tau_o$ (psi)	0	0	$-2.63 \times 10^2$	0	$1.02 \times 10^4$
$\tau_y$ (psi)	0	0	$1.63 \times 10^2$	0	$2.00 \times 10^3$
$\tau_u$ (psi)	0	$-1.54 \times 10^1$	$9.36 \times 10^1$	0	$7.35 \times 10^3$

Tensile Data

$\sigma_u$ (psi)	0	$-4.67 \times 10^1$	$5.62 \times 10^2$	$-2.77 \times 10^1$	$1.23 \times 10^4$
$\nu$	0	0	0	0	0.40

Temperature and Moisture Data

$\alpha$ (°C <sup>-1</sup> )	0	0	$1.01 \times 10^{-6}$	0	$6.35 \times 10^{-5}$
$\beta$ (%M <sup>-1</sup> )	0	0	0	0	$3.12 \times 10^{-3}$

individual test specimen stress-strain curves included in Appendix B of this report.

These data are actually used in the form of octahedral shear stress-octahedral shear strain relations in the micromechanics analysis. Thus, it is necessary to convert the data to this form. These relations only differ from the relations given here in Tables 24 through 26 by appropriate constant factors. Thus, the general shapes of the stress-strain curves are unchanged.

### 6.3 Analysis Procedure

Although the WYO2D finite element analysis is capable of modeling any loading of a unidirectional composite, only transverse tensile and axial compressive loadings were utilized in the experimental portion of the present study. Axial compression failures were dominated by fiber microbuckling, as shown in the scanning electron microphotographs of Section 5. The test results did not indicate a strong dependence on interface bond strength, as summarized in Section 1, and discussed in detail in Section 4. Thus, only transverse tensile loadings were simulated in the present numerical analysis.

A typical finite element grid of the first quadrant of a typical repeating unit cell was previously shown in Figure 110. This represents the assumed square packing array of graphite fibers of circular cross section surrounded by matrix material. The actual fiber volume content modeled was varied as required to match the actual experimental data presented in Table 6 of Section 4.3.

In all computer simulations, the thermal stresses in the various composites due to cooldown from the cure temperature were included.

The specific cure temperatures for each matrix material were used, viz, 177°C (350°F) for the Hercules 3501-6, 204°C (400°F) for the Hercules 4001, and 127°C (260°F) for the Hexcel F155. The composites were assumed to be stress-free at the cure temperature.

After cooldown to room temperature, the moisture was added, if appropriate, and then the heat-up to the appropriate ETW test temperature was simulated. As discussed in Sections 3 and 4, the elevated test temperatures actually used in generating the unidirectional composite transverse tensile data were 93°C (200°F) for the AS4/3501-6 and AS4/4001 composites, and 38°C (100°F) for the AS4/F155 composites.

The transverse tensile loadings of the various unidirectional composites, at both the room temperature, dry (RTD) and the elevated temperature, wet (ETW) test conditions, were simulated numerically. As noted in the previous subsection, the neat resin shear test data were used to define the matrix stress-strain response. Although in theory the tensile test data and the shear test data should produce the same results, in fact they do not, as discussed in detail in References [10-12,18,19,25]. The shear data are much more nonlinear. That is, the inelastic response of the matrix is emphasized. The WY02D analysis is fully capable of modeling this inelastic response.

The matrix strength, as determined by a shear test, is also typically higher than the matrix strength as measured via a tensile test. Thus, use of shear strength (typically in octahedral shear stress form) as the criterion of failure will result in predictions of composite strength which are higher than those predicted using a maximum normal stress failure criterion. As for conventional metals



and other homogeneous materials also, a universal failure criterion for composite materials is not available. Preliminary prior studies [10,12,14,15,25] have indicated that the maximum normal stress criterion is preferable for transverse tensile loadings, and the octahedral shear stress (distortional energy) criterion provides more accurate predictions for shear loadings. This is intuitively logical, of course, although much more work needs to be done.

In the present study, both failure criteria were utilized. As will be shown, the maximum normal stress failure criterion did produce the better correlations with experimental data. Also, the fiber-matrix interfacial bond strength was degraded to varying degrees, as required to best simulate the unidirectional composite transverse tensile strengths produced by the four different fiber sizings. This was done for both the RTD and the ETW test conditions.

#### 6.4 AS4/3501-6 Correlations

##### 6.4.1 Thermal Residual Stresses

As previously discussed, significant thermal residual stresses are developed in graphite fiber/polymer matrix composites during cooldown from the cure temperature. These stresses are caused by a combination of coefficient of thermal expansion mismatch between the fibers and the matrix, and the stiffness mismatch. The process is complicated by the fact that the graphite fiber itself is highly anisotropic (see Table 23). However, the WYO2D analysis is fully capable of rigorously predicting these thermal residual stresses. In fact, any stress or strain component can be displayed in contour plot form, if desired. These plots are usually generated and studied as part of the data interpretation process. They may not be fully

reported, to save space, although a detailed presentation was included in Reference [11], for example.

In the present report, a detailed presentation of these thermal residual stresses will only be included for the AS4/3501-6 composite with a perfect interface. These plots are included in Figure 111. Contour plots of eight quantities are shown. Figures 111a through 111c represent the three principal stresses. The heading of each plot indicates the quantity being plotted, the current temperature and moisture content, the finite element solution increment number, the plot number, the current values of the six components of the applied mechanical loading, the minimum and maximum values of the quantity being plotted, and letters A through I representing nine successively increasing contour line values of the quantity of interest. As can be seen in Figure 111, the temperature is 21°C, the moisture content is 0%, and all of the externally applied mechanical loadings are zero. These possible loadings are as follows:

SXX = normal stress in the x-direction (the horizontal direction in these plots, as indicated in Figure 110)

SYY = normal stress in the y-direction (the vertical direction in these plots)

SZZ = normal stress in the z-direction (parallel to the fiber axis)

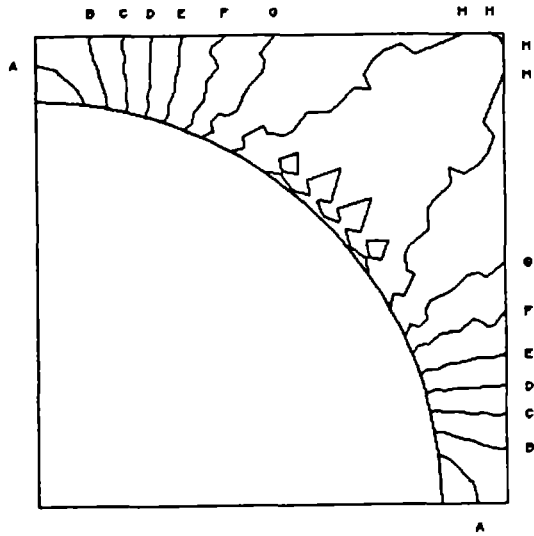
SYZ = shear stress along the horizontal boundaries, parallel to the fiber axis

SXZ = shear stress along the vertical boundaries, parallel to the fiber axis

ORIGINAL PAGE IS  
OF POOR QUALITY

3501-6 TRANS. TEN., PERFECT INT.

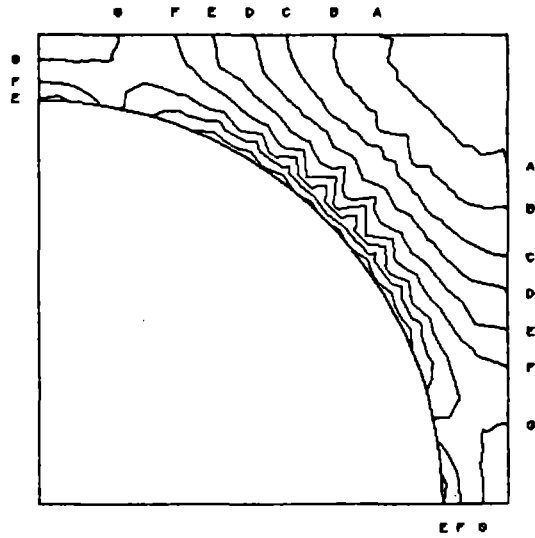
FIRST PRINCIPAL STRESS CONTOUR							
TEMP	INC	C	KSI	X	INCREMENT NO.	PLT NO.	
TEMP	-21.00	DEB	C	KSI	- .00 X	INCREMENT NO. - 17	PLT NO. - 1
OX	- .00	KSI	OY	- .00	KSI	OZ	- .00
OZ	- .00	KSI	MIN	- 2.00	KSI	MAX	- 1.00
B	- 0.00	KSI	C	- 0.00	KSI	D	- 0.00
F	- 0.00	KSI	G	- 0.00	KSI	H	- 0.00
			I	- 0.00	KSI		



a) first principal stress

3501-6 TRANS. TEN., PERFECT INT.

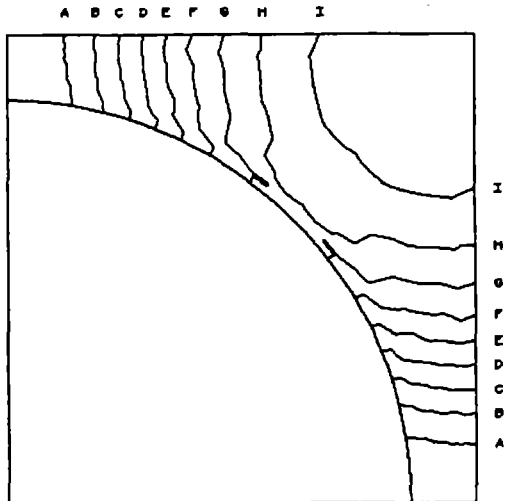
SECOND PRINCIPAL STRESS CONTOUR							
TEMP	INC	C	KSI	X	INCREMENT NO.	PLT NO.	
TEMP	-21.00	DEB	C	KSI	- .00 X	INCREMENT NO. - 17	PLT NO. - 2
OX	- .00	KSI	OY	- .00	KSI	OZ	- .00
OZ	- .00	KSI	MIN	- 1.00	KSI	MAX	- 0.00
B	- 1.00	KSI	C	- 1.00	KSI	D	- 2.00
F	- 2.00	KSI	G	- 2.00	KSI	H	- 2.77
			I	- 2.00	KSI		



b) second principal stress

3501-6 TRANS. TEN., PERFECT INT.

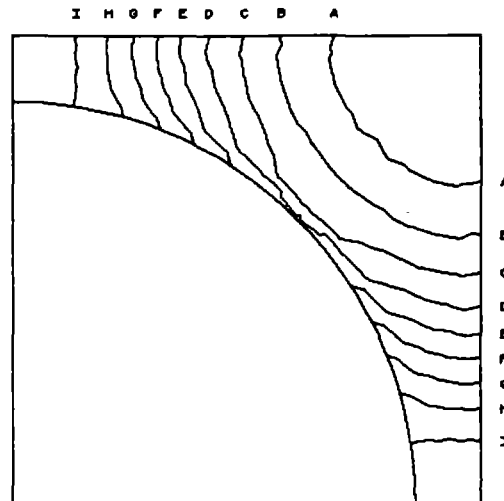
THIRD PRINCIPAL STRESS CONTOUR							
TEMP	INC	C	KSI	X	INCREMENT NO.	PLT NO.	
TEMP	-21.00	DEB	C	KSI	- .00 X	INCREMENT NO. - 17	PLT NO. - 3
OX	- .00	KSI	OY	- .00	KSI	OZ	- .00
OZ	- .00	KSI	MIN	- 1.00	KSI	MAX	- 1.00
B	- 1.00	KSI	C	- 1.00	KSI	D	- 1.00
F	- 1.00	KSI	G	- .00	KSI	H	- .00
			I	- 1.00	KSI		



c) third principal stress

3501-6 TRANS. TEN., PERFECT INT.

MAXIMUM SHEAR STRESS CONTOUR							
TEMP	INC	C	KSI	X	INCREMENT NO.	PLT NO.	
TEMP	-21.00	DEB	C	KSI	- .00 X	INCREMENT NO. - 17	PLT NO. - 4
OX	- .00	KSI	OY	- .00	KSI	OZ	- .00
OZ	- .00	KSI	MIN	- 1.00	KSI	MAX	- 2.00
B	- 1.00	KSI	C	- 1.00	KSI	D	- 1.00
F	- 2.00	KSI	G	- 2.00	KSI	H	- 2.00
			I	- 2.00	KSI		



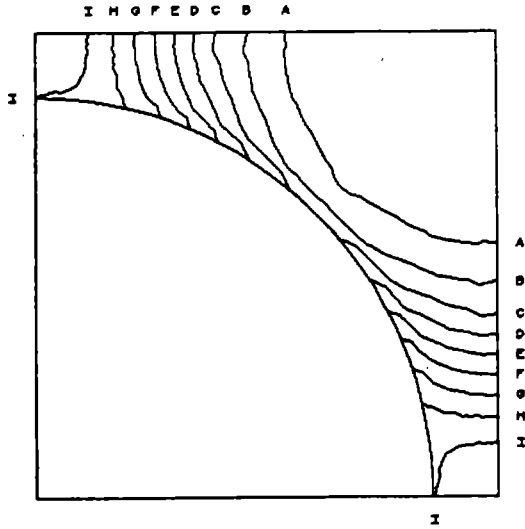
d) maximum shear stress

Figure 111. AS4/3501-6 Unidirectional Composite; Residual Thermal Stresses and Strains at Room Temperature after Cooldown from the 177°C (350°F) Cure Temperature. Fiber Volume = 59 Percent.

ORIGINAL PAGE IS  
OF POOR QUALITY

3881-6 TRANS. TEN., PERFECT INT.

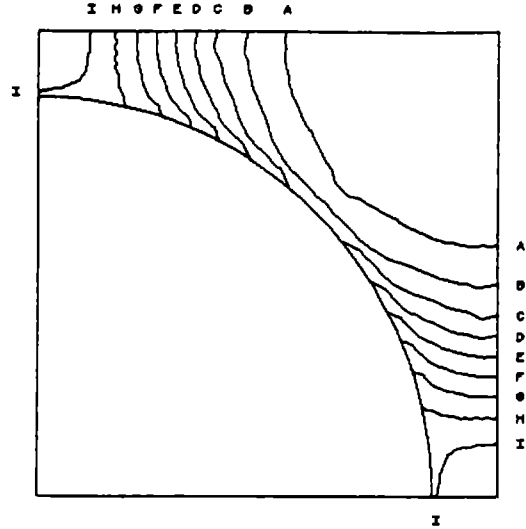
CIRCULAR SHEAR STRESS CONTROL  
 TEMP - 21.00 DEG. C KCBP - .00 X INCREMENT NO. - 17 PLOT NO. - 6  
 SXX - .00 KSI SYY - .00 KSI SZZ - .00 KSI SYZ - .00 KSI  
 SXY - .00 KSI SHX - 1.10 KSI SHY - 2.40 KSI A - 1.20 KSI  
 G - 1.40 KSI C - 1.00 KSI D - 1.00 KSI E - 1.04 KSI  
 F - 1.04 KSI G - 2.07 KSI H - 2.20 KSI I - 2.20 KSI



e) octahedral shear stress

3881-6 TRANS. TEN., PERFECT INT.

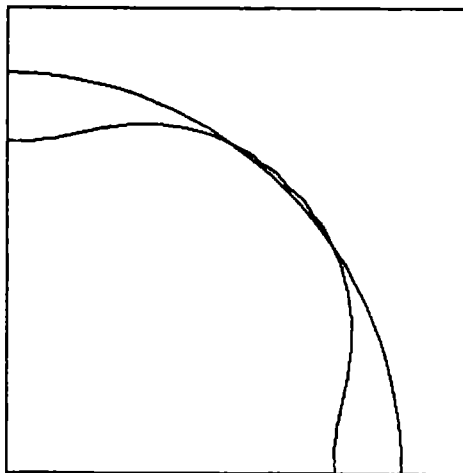
CIRCULAR SHEAR STRAIN CONTROL  
 TEMP - 21.00 DEG. C KCBP - .00 X INCREMENT NO. - 17 PLOT NO. - 6  
 SXX - .00 KSI SYY - .00 KSI SZZ - .00 KSI SYZ - .00 KSI  
 SXY - .00 KSI SHX - 0.44 SHY - 10.40 A - 0.44  
 G - 10.40 C - 11.40 D - 12.40 E - 13.40  
 F - 14.40 G - 15.40 H - 16.40 I - 17.40



f) octahedral shear strain

3881-6 TRANS. TEN., PERFECT INT.

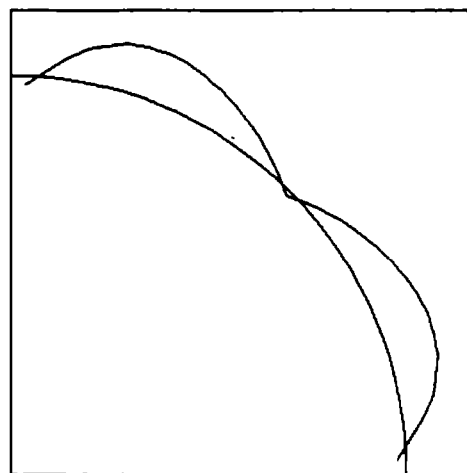
INTERFACE NORMAL STRESS  
 TEMP - 21.00 DEG. C KCBP - .00 X INCREMENT NO. - 17 PLOT NO. - 7  
 SXX - .00 KSI SYY - .00 KSI SZZ - .00 KSI SYZ - .00 KSI  
 SXY - .00 KSI SHX - -0.30 KSI SHY - 2.30 KSI



g) interface normal stress

3881-6 TRANS. TEN., PERFECT INT.

INTERFACE SHEAR STRESS  
 TEMP - 21.00 DEG. C KCBP - .00 X INCREMENT NO. - 17 PLOT NO. - 8  
 SXX - .00 KSI SYY - .00 KSI SZZ - .00 KSI SYZ - .00 KSI  
 SXY - .00 KSI SHX - -1.00 KSI SHY - 1.00 KSI



h) interface shear stress

Figure 111. AS4/3501-6 Unidirectional Composite; Residual Thermal (continued) Stresses and Strains at Room Temperature after Cooldown from the 177°C (350°F) Cure Temperature. Fiber Volume = 59 Percent.

In all of the present study, only a uniaxial, transverse tensile loading, i.e.,  $S_{XX} \neq 0$  only, will be modeled, as previously discussed. It will also be noted in Figure 111 that contours are plotted only in the matrix material, not in the fiber. This is to make viewing easier, the matrix stresses being of particular interest. The same data are available for the fiber, however, if desired.

The WY02D computer program was run using English rather than S.I. units. The input data of Tables 24 through 26 reflect these units also. Dual units will be used in all of the discussion to be included here, to avoid confusion with the plotted contour values.

Referring to Figure 111a, it will be noted that the highest cooldown-induced tensile stress was 28 MPa (4.0 ksi), and was highly concentrated at the fiber-matrix interface along the x and y axes, i.e., the axes of symmetry of the assumed square fiber packing array. The measured tensile strength of the Hercules 3501-6 epoxy matrix at the RTD condition was only 61 MPa (8.8 ksi), as indicated in Table 2 of Section 4. As shown in Figure 111d, the highest shear stress was only 19 MPa (2.7 ksi), the matrix shear strength being 101 MPa (14.7 ksi). Obviously, the tensile residual stress is more significant here.

Figures 111e and 111f are plots of the octahedral shear stresses and octahedral shear strains, respectively. As previously discussed, the former will also be used as a failure criterion in the present presentation.

Particularly in the present study of the influence of fiber sizings and the role of the fiber-matrix interface, it is important to be able to predict the stress distributions around the interface.

Figures 11lg and 11lh are plots of interface normal stress and interface shear stress, respectively. Values of normal stress plotted inside the quarter circle representing the fiber-matrix interface indicate compressive stresses. As shown in Figure 11lg, the interface normal residual stresses were primarily compressive here, due to the greater thermal contraction of the matrix relative to that of the fiber during cooldown. The headings in Figure 11lg indicate the maximum and minimum full scale range of the interface stress, zero stress being at the fiber-matrix interface line, and the positive full scale value being the right boundary of the region, at the x axis. Thus, the maximum compressive normal stresses, which occurred in Figure 11lg at the x and y axes, were equal to 16 MPa (2.4 ksi). This is about 25 percent of the tensile strength of the Hercules 3501-6 matrix (see Table 2), and is obviously a favorable stress state when interface failure under subsequent transverse tensile loading is of principal concern.

If matrix yielding had occurred during cooldown, an additional plot would have been included to show its extent, as local shaded areas. Also, if matrix or interface cracking had occurred, this would have been indicated by blackened areas on all of the plots, including the extent of yielding plot.

#### 6.4.2 Moisture-Induced Stresses

Since transverse tensile tests were also conducted at an elevated temperature, wet (93°C, 1%M) condition, the stresses induced by the matrix swelling associated with moisture absorption had to be included also. The resulting predicted stress state in the AS4/3501-6 unidirectional composite at room temperature, when the

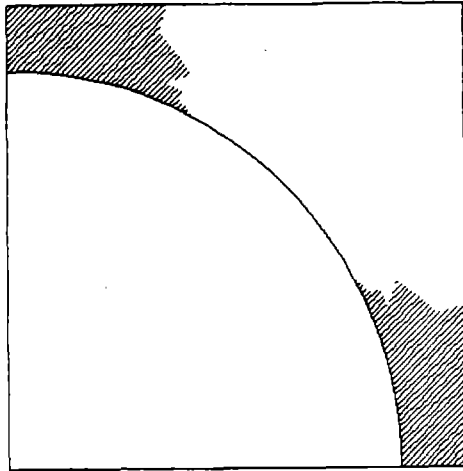
cooldown stresses and the moisture-induced stresses were both present, is indicated in Figures 112a and 112b. It will be recalled that the cooldown stresses alone did not cause any yielding. The addition of one weight percent moisture to the composite (which corresponded to a 2.9 weight percent moisture addition to the matrix since the graphite fibers were assumed to absorb no moisture) did induce yielding, as shown in Figure 112a. Also, the interface normal stress state was reversed. That is, the highest thermal residual stresses were compressive, viz, -17 MPa (-2.4 ksi), as previously indicated in Figure 111g. The highest stresses after the addition of moisture were tensile (Figure 112b), of 22 MPa (3.2 ksi) magnitude. That is, the addition of 2.9 weight percent moisture to the matrix induced residual stresses of magnitudes over 2.3 times those induced during cooldown. It will be further noted that the Hercules 3501-6 matrix is capable of absorbing over twice as much moisture as used in the present study, i.e., 6.0 weight percent (see Table 2 or 3 of Section 4). Thus, moisture-induced stresses are extremely important. The resulting tensile normal stresses at the interface are detrimental in terms of the subsequent transverse tensile loadings to be applied in the present study.

Figure 112c indicates the influence of a 50 percent degradation of interface strength. As compared to the perfect interface case (Figure 112a), the zone of yielding has spread almost completely around the interface.

Since the moisture-conditioned composites were tested at 93°C (200°F), the next step in the computer simulation was to increase the temperature. This caused the matrix to yield completely. The

3501-6 TRANS. TEN., PERFECT INT

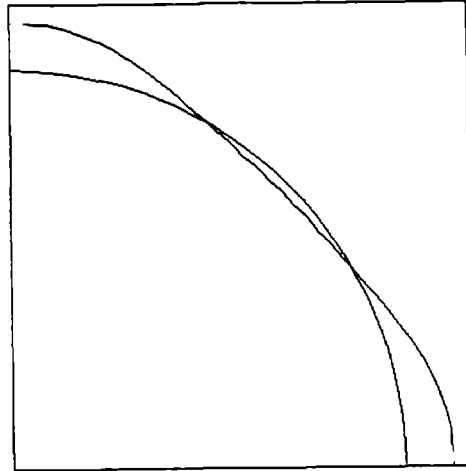
FINITE ELEMENT DISPLACEMENT GRID  
 TEMP - 21.00 DEG. C    MOD - 2.00 X    INCREMENT NO. - 21    PLOT NO. - 16  
 SX - .00 KSI    SY - .00 KSI    SZ - .00 KSI    SXZ - .00 KSI  
 ELASTIC ELEMENTS ARE    WHITE    PLASTIC ELEMENTS ARE    GRAY  
 FAILED ELEMENTS ARE    BLACK



a) extent of yielding, RTW

3501-6 TRANS. TEN., PERFECT INT

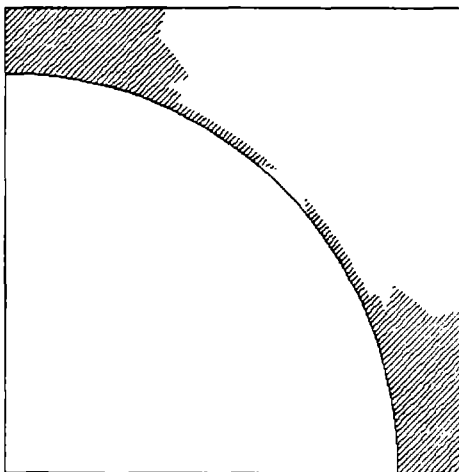
INTERFACE NORMAL STRESS  
 TEMP - 21.00 DEG. C    MOD - 2.00 X    INCREMENT NO. - 21    PLOT NO. - 7  
 SX - .00 KSI    SY - .00 KSI    SZ - .00 KSI    SXZ - .00 KSI  
 MIN - 0.20 KSI    MAX - 3.20 KSI



b) interface normal stress, RTW

3501-6 TRANS. TEN., 50% DEGRADED INT

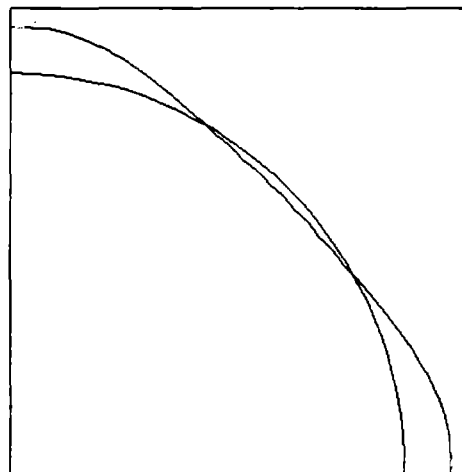
FINITE ELEMENT DISPLACEMENT GRID  
 TEMP - 21.00 DEG. C    MOD - 2.00 X    INCREMENT NO. - 21    PLOT NO. - 16  
 SX - .00 KSI    SY - .00 KSI    SZ - .00 KSI    SXZ - .00 KSI  
 ELASTIC ELEMENTS ARE    WHITE    PLASTIC ELEMENTS ARE    GRAY  
 FAILED ELEMENTS ARE    BLACK



c) extent of yielding, RTW,  
50% interface degradation

3501-6 TRANS. TEN., PERFECT INT.

INTERFACE NORMAL STRESS  
 TEMP - 00.00 DEG. C    MOD - 2.00 X    INCREMENT NO. - 20    PLOT NO. - 17  
 SX - .00 KSI    SY - .00 KSI    SZ - .00 KSI    SXZ - .00 KSI  
 MIN - 1.10 KSI    MAX - 1.10 KSI



d) interface normal stress, ETW

Figure 112. AS4/3501-6 Unidirectional Composite; Residual Hygro-thermal Stresses after Cooldown from the 177°C (350°F) Cure Temperature and the Addition of One Weight Percent Moisture to the Composite.



(compressive) thermal stresses decreased as the temperature was increased back up toward the 177°C (350°F) cure temperature, thus making the moisture-induced stresses even more dominate. The resulting interface normal stress distribution is indicated in Figure 112d. At 29 MPa (4.2 ksi), the maximum interface stress is about 30 percent higher than at room temperature (Figure 112b). This is particularly significant in that at 93°C, 2.9% M, the Hercules 3501-6 epoxy matrix material has a tensile strength of only 41 MPa (6.0 ksi), as indicated in Table 24. That is, the matrix tensile stress was 70 percent of ultimate before any transverse tensile loading was applied. This in itself explains why the ETW transverse tensile strengths of the AS4/3501-6 unidirectional composites were lower than at the RTD condition.

All of the predictions shown in Figure 112 are based on the assumption of an octahedral shear failure criterion. As long as no cracking occurs, this assumption is immaterial. Actually, some interface debonding (cracking) did occur during the heat-up to the test temperature when the maximum normal stress criterion was assumed, as will be discussed in Section 6.4.3.2.

The axial compressive strengths were lower at the ETW test condition than at the RTD condition for this reason also, combined with the lower matrix stiffness. The axial compressive loading induces transverse tensile stresses at the fiber-matrix interface, due to the Poisson effect. Combined with the preexisting moisture-induced tensile residual stresses (Figure 112d), the fibers debond from the surrounding matrix at lower axial compressive stress levels. This loss of lateral support, combined with the lower matrix

stiffness at the ETW condition, then leads to the fiber microbuckling clearly evident in the scanning electron microphotographs shown in Section 5.

#### 6.4.3 Transverse Tensile Loading

Both the room temperature, dry (RTD) and the elevated temperature, wet (ETW) experimental test conditions were simulated by the analysis. Correlations will be presented in separate subsections.

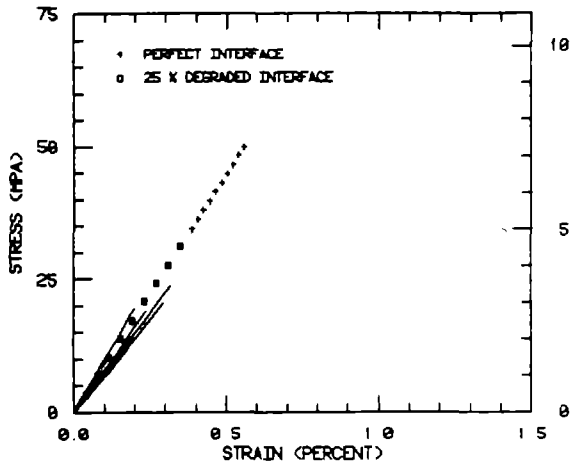
##### 6.4.3.1 Room Temperature, Dry

The WYO2D finite element analysis predictions of composite transverse tensile stress-strain response are correlated with the corresponding experimental data in Figure 113. A maximum normal stress failure criterion was utilized in generating these analytical results. The individual experimental curves, shown as solid lines, were taken directly from the test data presented in Appendices A and B. A single average curve of the experimental data could have been plotted (average data having been presented in Section 4). However, by plotting individual data curves, a good indication of the typical scatter in the experimental data is achieved. The four plots of Figure 113 represent the experimental data generated for the four different fiber sizings. The trends of these data were discussed in detail in Section 4.

The analytical results obtained assuming a perfect interface bond between the fibers and the matrix were generated directly, using the experimentally measured fiber and matrix constituent properties previously presented in Tables 23 and 24. No adjustments were made. All computer runs were performed using an average fiber volume, based

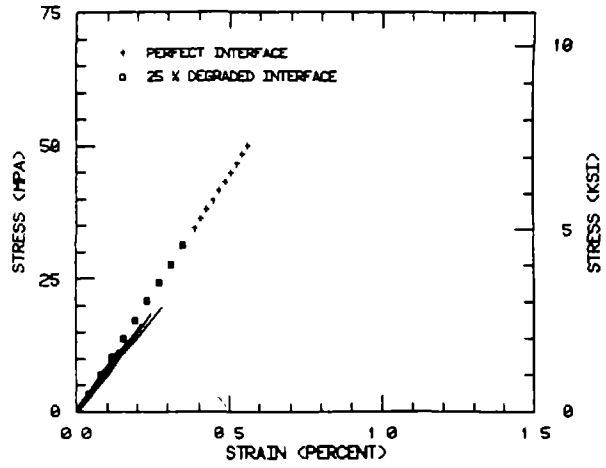
ORIGINAL PAGE IS  
OF POOR QUALITY

R T DRY, UNSIZED



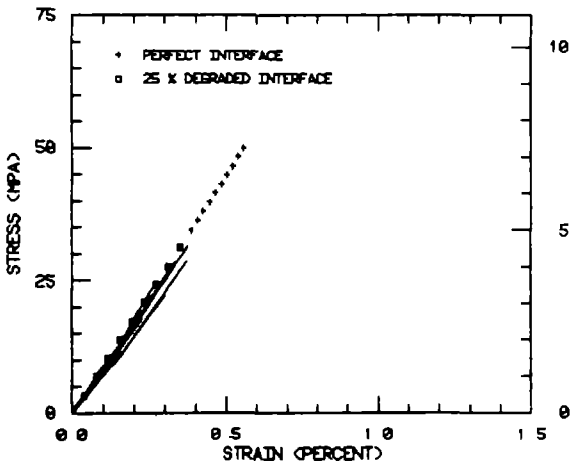
a) unsized

R.T DRY, 828 SIZED



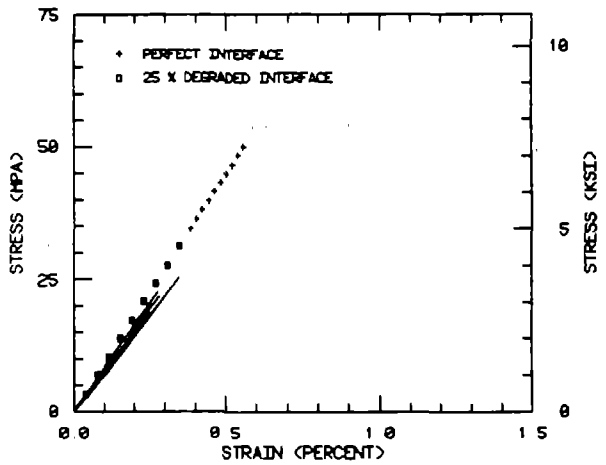
b) EPON 828 sized

R T DRY, PVA SIZED



c) PVA sized

R.T DRY, POLYSULFONE SIZED



d) polysulfone sized

Figure 113. AS4/3501-6 Unidirectional Composite, Room Temperature, Dry Condition, Transverse Tensile Loading. Correlations Between Predictions and Experimental Data for All Four Fiber Sizings, Using a Maximum Normal Stress Failure Criterion.

upon the individual measured values of Table 6, rather than to attempt to model each specific value. As discussed in Section 4, the experimental data did not indicate a strong sensitivity to these variations in fiber volume. Also plotted in Figure 113 are the analytical results predicted assuming a 25 percent strength degradation of the fiber-matrix interface. The finite elements around the interface can be assigned any properties desired. By simply reducing the strength properties as some percentage of the corresponding matrix properties, a degraded interface bond can be simulated. Thus, in Figure 113, the interface bond strength is simulated to be only 75 percent of the strength of the Hercules 3501-6 epoxy matrix itself.

As can be seen in Figure 113, the finite element analysis predicted the initial stiffnesses of all four composites well, particularly considering that no attempt was made to simulate the exact fiber volume variations. The predicted composite stress-strain curve for the perfect interface extends to 47 MPa (6.8 ksi). At that applied stress level, only limited matrix yielding had occurred, and no matrix cracking. Since this applied stress was already about twice that actually measured, this computer run was terminated. By assuming a 25 percent interface strength reduction, the predicted ultimate strength was reduced drastically. Complete composite fracture was predicted at the 31 MPa (4.5 ksi) stress level indicated in Figure 113. This value is in reasonable agreement with the experimentally measured strengths for all four fiber sizing conditions. As discussed in Section 4, it might have been expected that the EPON 828 and polysulfone sizings would have resulted in the

highest transverse tensile strengths, and the PVA sizing the lowest. As can be seen in Figure 113, almost the opposite was observed. Thus, no attempt was made to further refine the analysis to better fit the individual experimental data. In general, the agreement indicated in Figure 113 is good.

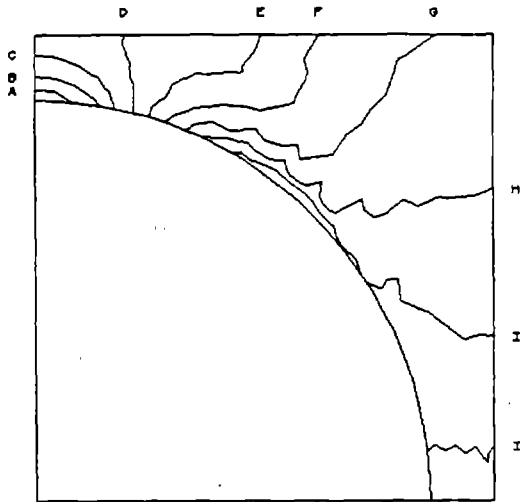
Examples of the internal stress states, extent of yielding, and crack patterns are included in Figure 114. Results for the 25 percent interface strength degradation are shown. Of course, results for each loading increment, for each of the eight stress and strain components presented in Figure 112, were available for study. That is, only four of the several hundred plots available are presented here, although many dozens of others were actually studied. Figure 114a shows that the maximum normal stress (the criterion for failure) occurred near the interface along the x axis. However, the maximum octahedral shear stress (the criterion for yield) occurred along the y axis, as shown in Figure 114b. Thus, first yielding occurred in the same region (Figure 114c). This yielding initiated at a low level of applied stress (less than 14 MPa), but did not spread rapidly. The extent of yielding at 28 MPa (4.0 ksi) is shown in Figure 114c. As previously indicated in Figure 113, full failure was predicted at 31 MPa (4.5 ksi). The extent of yielding at failure, and the crack pattern resulting in this failure, are shown in Figure 114d. As can be seen, the microcracking followed the interface up to the yield zone, and then across the thin web of yielded matrix, to result in a total fracture path.

As noted previously, an octahedral shear stress failure criterion was also tried. Since the stiffness properties were

ORIGINAL PAGE IS  
OF POOR QUALITY.

3581-6 TRANS. TEN., 25 X DEGRADED INT.

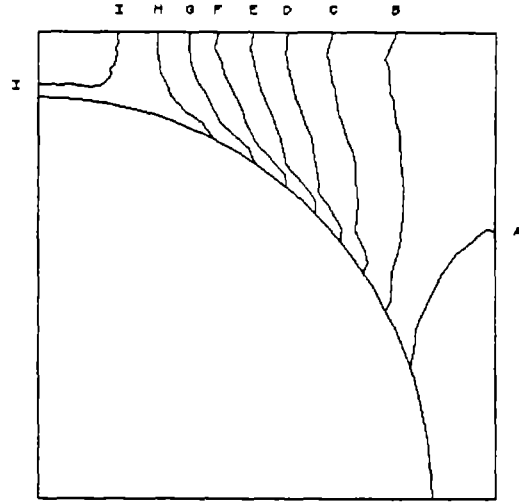
FINITE PRINCIPAL STRESS CONTOUR			
TEMP - 21.00 DEG. C	K002 - .00 N	INCREMENT NO. - 25	PLOT NO. - 11
SIX - 1.00 KSI	SYI - .00 KSI	SI2 - .00 KSI	SI2 - .00 KSI
SI2 - .00 KSI	MIN - 3.10 KSI	MAX - 5.70 KSI	A - 3.37 KSI
B - 3.05 KSI	C - 3.00 KSI	D - 4.17 KSI	E - 4.44 KSI
F - 4.71 KSI	G - 4.50 KSI	H - 0.24 KSI	I - 5.51 KSI



a) maximum principal stress

3581-6 TRANS. TEN., 25 X DEGRADED INT.

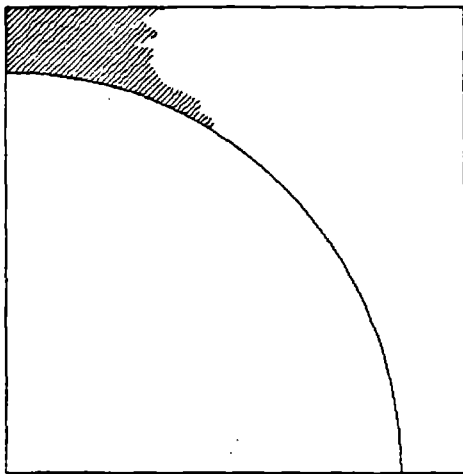
OCTAHEDRAL SHEAR STRESS CONTOUR			
TEMP - 21.00 DEG. C	K002 - .00 N	INCREMENT NO. - 25	PLOT NO. - 11
SIX - 1.00 KSI	SYI - .00 KSI	SI2 - .00 KSI	SI2 - .00 KSI
SI2 - .00 KSI	MIN - .70 KSI	MAX - 3.24 KSI	A - 1.01 KSI
B - 1.20 KSI	C - 1.51 KSI	D - 1.70 KSI	E - 2.00 KSI
F - 2.25 KSI	G - 2.50 KSI	H - 2.70 KSI	I - 2.00 KSI



b) octahedral shear stress

3581-6 TRANS. TEN., 25 X DEGRADED INT.

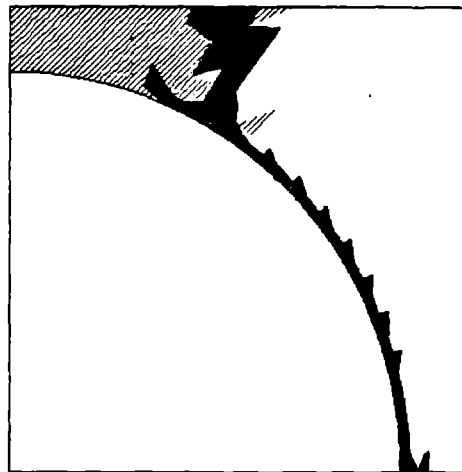
FINITE ELEMENT DISPLACEMENT GRID			
TEMP - 21.00 DEG. C	K002 - .00 N	INCREMENT NO. - 25	PLOT NO. - 20
SIX - 1.00 KSI	SYI - .00 KSI	SI2 - .00 KSI	SI2 - .00 KSI
SI2 - .00 KSI			
ELASTIC ELEMENTS ARE	WHITE	PLASTIC ELEMENTS ARE	GRAY
YIELD ELEMENTS ARE	BLACK		



c) extent of yielding

3581-6 TRANS. TEN., 25 X DEGRADED INT.

FINITE ELEMENT DISPLACEMENT GRID			
TEMP - 21.00 DEG. C	K002 - .00 N	INCREMENT NO. - 25	PLOT NO. - 30
SIX - 1.00 KSI	SYI - .00 KSI	SI2 - .00 KSI	SI2 - .00 KSI
SI2 - .00 KSI			
ELASTIC ELEMENTS ARE	WHITE	PLASTIC ELEMENTS ARE	GRAY
YIELD ELEMENTS ARE	BLACK		



d) crack pattern at failure

Figure 114. AS4/3501-6 Unidirectional Composite, Room Temperature, Dry Condition, Transverse Tensile Loading. Internal Stress States for the 25 Percent Degraded Interface Model, Using a Maximum Normal Stress Failure Criterion.

unchanged, the composite stress-strain curves up to first microcracking were the same as those shown in Figure 113 for the maximum normal stress failure criterion. That is, the stiffness was again adequately predicted. However, assuming a perfect interface, no microcracking had yet occurred at 103 MPa (15 ksi), the applied stress level at which the computer run was terminated. In fact, the matrix was not yet fully yielded. The extent of yielding at 34 MPa (5.0 ksi) and at 86 MPa (12.5 ksi) are indicated in Figures 115a and 115b, respectively. Assuming a 50 percent interface degradation resulted in early yielding at the fiber-matrix interface (Figure 115c), but still no failure at 69 MPa (10 ksi) applied stress, at which point the computer run was terminated. A similar result was obtained for a 75 percent interface strength degradation. At 14 MPa (2 ksi), the interface was fully yielded, as opposed to the almost full yielding for the 50 percent degradation shown in Figure 115c. However, again no failure had yet initiated at 69 MPa (10 ksi) and the analysis was terminated. The extent of yielding at 45 MPa (6.5 ksi) is shown in Figure 115d. It was the same for the 50 percent degradation case.

The conclusion must be that the octahedral shear stress failure criterion is not applicable to transverse tensile loading of the AS4/3501-6 unidirectional composite. On the other hand, the maximum normal stress failure criterion worked quite well, as demonstrated here.

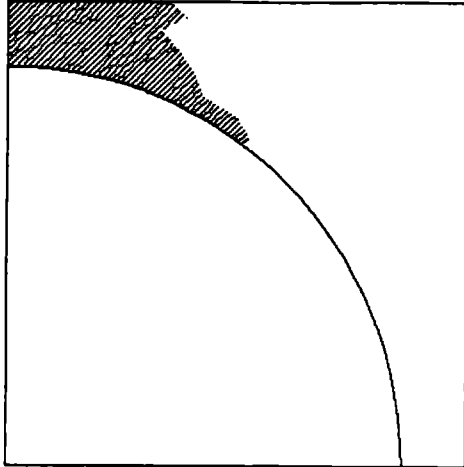
#### 6.4.3.2 Elevated Temperature, Wet (93°C, 1%M)

The experimentally determined individual transverse tensile stress-strain curves are plotted in Figure 116, for the four

ORIGINAL PAGE IS  
OF POOR QUALITY

3501-6 TRANS. TEN., PERFECT INT.

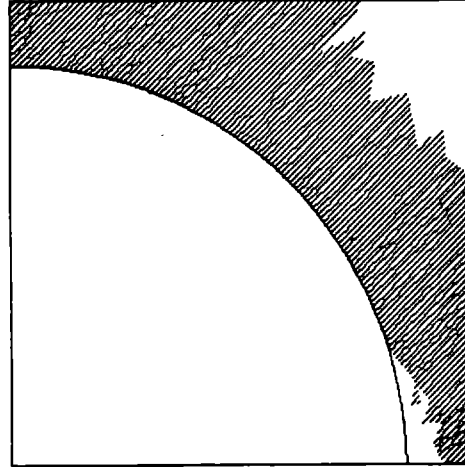
FINITE ELEMENT DISPLACEMENT GRID  
TEMP - 21.00 DEG C KCB - .00 X INCREMENT NO. - 02 PLOT NO. - 00  
SXX - 0.00 KSI SYY - .00 KSI SZZ - .00 KSI SXY - .00 KSI  
Sxz - .00 KSI  
ELASTIC ELEMENTS ARE WHITE PLASTIC ELEMENTS ARE GRAY  
FAILED ELEMENTS ARE BLACK



a) yielding at 34 MPa

3501-6 TRANS. TEN., PERFECT INT.

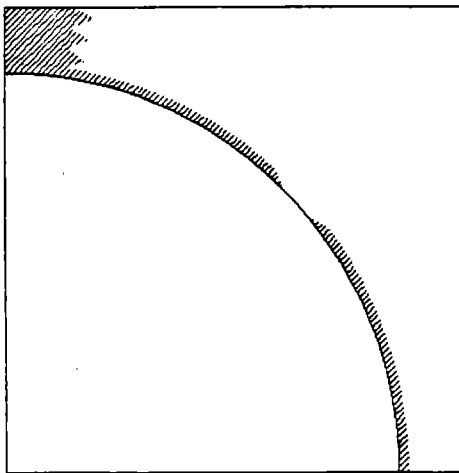
FINITE ELEMENT DISPLACEMENT GRID  
TEMP - 21.00 DEG C KCB - .00 X INCREMENT NO. - 02 PLOT NO. - 00  
SXX - 12.00 KSI SYY - .00 KSI SZZ - .00 KSI SXY - .00 KSI  
Sxz - .00 KSI  
ELASTIC ELEMENTS ARE WHITE PLASTIC ELEMENTS ARE GRAY  
FAILED ELEMENTS ARE BLACK



b) yielding at 86 MPa

3501-6 TRANS. TEN., 50% DEGRADED INT.

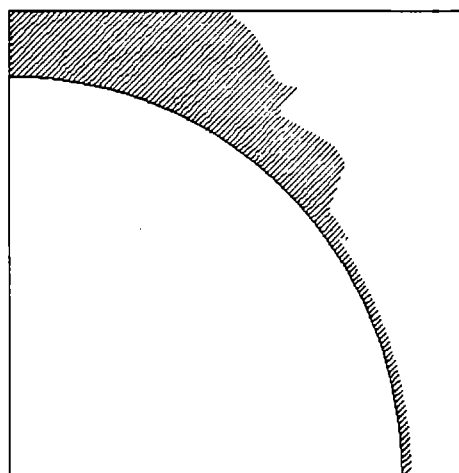
FINITE ELEMENT DISPLACEMENT GRID  
TEMP - 21.00 DEG C KCB - .00 X INCREMENT NO. - 21 PLOT NO. - 10  
SXX - 2.00 KSI SYY - .00 KSI SZZ - .00 KSI SXY - .00 KSI  
Sxz - .00 KSI  
ELASTIC ELEMENTS ARE WHITE PLASTIC ELEMENTS ARE GRAY  
FAILED ELEMENTS ARE BLACK



c) 50% interface degradation,  
yielding at 14 MPa

3501-6 TRANS. TEN., 75% DEGRADED INT.

FINITE ELEMENT DISPLACEMENT GRID  
TEMP - 21.00 DEG C KCB - .00 X INCREMENT NO. - 24 PLOT NO. - 10  
SXX - 6.00 KSI SYY - .00 KSI SZZ - .00 KSI SXY - .00 KSI  
Sxz - .00 KSI  
ELASTIC ELEMENTS ARE WHITE PLASTIC ELEMENTS ARE GRAY  
FAILED ELEMENTS ARE BLACK



d) 75% interface degradation,  
yielding at 45 MPa

Figure 115. AS4/3501-6 Unidirectional Composite, Room Temperature, Dry Condition, Transverse Tensile Loading. Extent of Yielding as a Function of Amount of Interface Degradation, Using an Octahedral Shear Stress Failure Criterion.

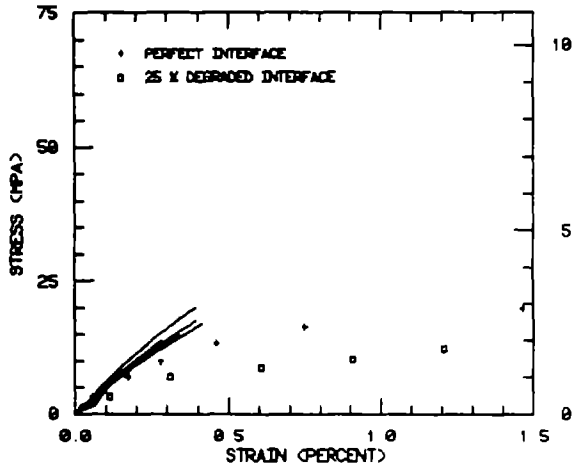


different fiber sizings. It will be noted that all results presented in this Section 6 have been plotted to the same scale, for ease in making comparisons. Also shown in Figure 116 are the WY02D micromechanics analysis predictions of the stress-strain response, for both a perfect interface and 25 percent degradation. The immediate conclusion might be that the ETW matrix modulus used in the analysis was not high enough. This is not the case, however. The low composite stiffness is due to the extensive matrix cracking predicted at very low applied stress levels. The first microcracking was predicted at at slightly less than 4 MPa (0.5 ksi), and full failure occurred at 23 MPa (3.4 ksi). This prediction was close to the experimentally measured strengths plotted in Figure 116. However, the predicted strains were much too high. Degrading the interface by 25 percent reduced the failure strains, by reducing the failure stress, but reduced the composite modulus even further below the experimental values.

Corresponding cracking patterns at selected load levels are shown in Figure 117. Figure 117a indicates the predicted crack pattern, which did follow the fiber-matrix interface even for this perfect interface case, at an applied stress level of 17 MPa (2.4 ksi). With increased loading, the crack then propagated across the thin web of matrix material at the y-axis leading to total fracture at 23 MPa (3.4 ksi), as indicated in Figure 116.

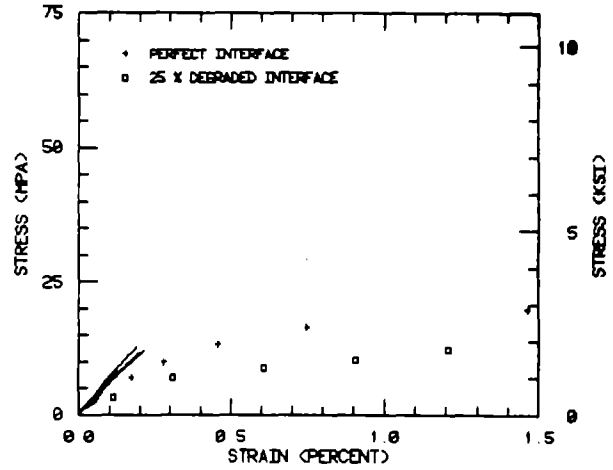
When the interface was degraded 25 percent, the interface was predicted to partially fail during heat-up to the 93°C test temperature, prior to any mechanical loading. This is shown in Figure 117b. At only 3.5 MPa (0.5 ksi) applied loading, the crack

93 DEG C., 1% M, UNSIZED



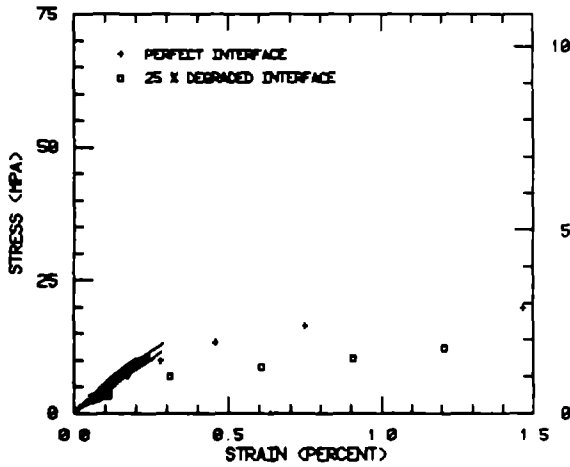
a) unsized

93 DEG C., 1% M, 828 SIZED



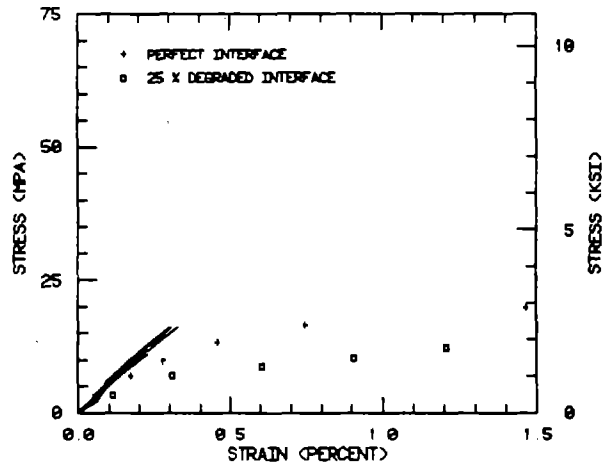
b) EPON 828 sized

93 DEG C., 1% M, PVA SIZED



c) PVA sized

93 DEG C., 1% M, POLYSULFONE SIZED



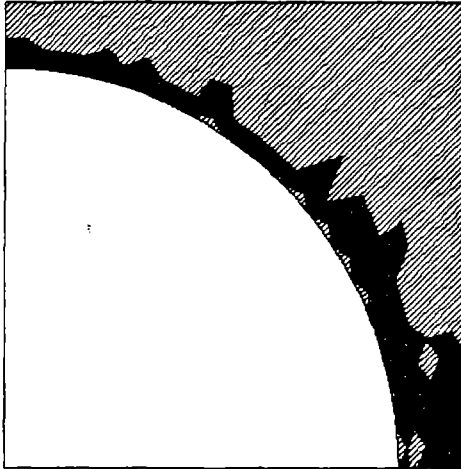
d) polysulfone sized

Figure 116. AS4/3501-6 Unidirectional Composite, Elevated Temperature, Wet Condition (93°C, 1% M), Transverse Tensile Loading. Correlations Between Predictions and Experimental Data for All Four Fiber Sizings, Using a Maximum Normal Stress Failure Criterion.

ORIGINAL PAGE IS  
OF POOR QUALITY

3501-6 TRANS. TEN., PERFECT INT.

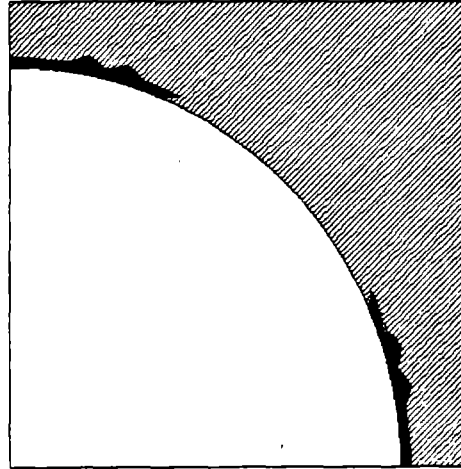
FINITE ELEMENT DISPLACEMENT GRID  
 TEMP - 99.99 DEG. C    MOD - 2.00 X    INCREMENT NO. - 34    PLOT NO. - 30  
 SXX - 2.57 KSI    SYY - .00 KSI    SZZ - .00 KSI    SYZ - .00 KSI  
 ELASTIC ELEMENTS ARE    WHITE    PLASTIC ELEMENTS ARE    GRAY



a) yielding at 17 MPa

3501-6 TRANS. TEN., 25 % DEGRADED INT.

FINITE ELEMENT DISPLACEMENT GRID  
 TEMP - 99.99 DEG. C    MOD - 2.00 X    INCREMENT NO. - 29    PLOT NO. - 29  
 SXX - .00 KSI    SYY - .00 KSI    SZZ - .00 KSI    SYZ - .00 KSI  
 ELASTIC ELEMENTS ARE    WHITE    PLASTIC ELEMENTS ARE    GRAY  
 FAILED ELEMENTS ARE    BLACK



b) 25% interface degradation, yielding prior to loading

3501-6 TRANS. TEN., 25 % DEGRADED INT.

FINITE ELEMENT DISPLACEMENT GRID  
 TEMP - 99.99 DEG. C    MOD - 2.00 X    INCREMENT NO. - 34    PLOT NO. - 30  
 SXX - .00 KSI    SYY - .00 KSI    SZZ - .00 KSI    SYZ - .00 KSI  
 ELASTIC ELEMENTS ARE    WHITE    PLASTIC ELEMENTS ARE    GRAY  
 FAILED ELEMENTS ARE    BLACK



c) 25% interface degradation, yielding at 3.5 MPa

3501-6 TRANS. TEN., 25 % DEGRADED INT.

FINITE ELEMENT DISPLACEMENT GRID  
 TEMP - 99.99 DEG. C    MOD - 2.00 X    INCREMENT NO. - 34    PLOT NO. - 30  
 SXX - 2.00 KSI    SYY - .00 KSI    SZZ - .00 KSI    SYZ - .00 KSI  
 ELASTIC ELEMENTS ARE    WHITE    PLASTIC ELEMENTS ARE    GRAY  
 FAILED ELEMENTS ARE    BLACK



d) 25% interface degradation, yielding at 14 MPa

Figure 117. AS4/3501-6 Unidirectional Composite, Elevated Temperature, Wet Condition (93°C, 1% M), Transverse Tensile Loading. Extent of Interface and Matrix Cracking, Based Upon a Maximum Normal Stress Failure Criterion.

had spread as indicated in Figure 117c. At 14 MPa (2.0 ksi), it extended completely around the interface (Figure 117d). Total fracture then occurred at 16 MPa (2.3 ksi). This early cracking produced the low composite modulus and high strain to failure. It appears that modeling a higher matrix tensile strength for this ETW condition would have produced better agreement with the experimental data.

Using an octahedral shear stress failure criterion resulted in no matrix cracking up to 69 MPa (10 ksi) for the perfect interface model, at which point the analysis was terminated. Degrading the interface 50 percent still resulted in no matrix or interface failure up to 69 MPa (10 ksi). However, the predicted composite modulus was in good agreement with the measured values. This further supports the statement made earlier that it was the extensive matrix cracking when using the maximum normal stress criterion that caused the apparent low composite modulus indicated in Figure 116.

A suitable failure criterion appears to be one somewhere between the two considered here.

## 6.5 AS4/4001 Correlations

The Hercules 4001 bismaleimide matrix was cured at a higher temperature than the Hercules 3501-6 epoxy, i.e., 204°C (400°F) rather than 177°C (350°F). This was taken into account in modeling the AS4/4001 composite. Yet, as will be shown, the hygrothermal stresses in this composite were actually lower than for the AS4/3501-6 composite, due to the influence of other factors.

### 6.5.1 Thermal Residual Stresses

As indicated in Table 3 of Section 4, the shear strength of the

Hercules 4001 at the RTD condition was measured to be quite low, viz, 17 MPa (2.4 ksi). Thus, the shear yield stress was correspondingly low. These low values may have been associated with the use of the Iosipescu shear test method on this relatively brittle resin system, as discussed in Section 3. Nevertheless, the actual measured values were used in the present analysis. This resulted in complete yielding of the matrix material during cooldown from the 204°C (400°F) cure temperature. This did not significantly influence the subsequent mechanical loading, however, if a maximum normal stress failure criterion was used. The measured tensile strength of the Hercules 4001 bismaleimide matrix was 53 MPa (7.7 ksi), i.e., over three times its shear strength.

#### 6.5.2 Moisture-Induced Stresses

As noted in the previous subsection, the matrix had already fully yielded during cooldown after curing the composite. The addition of one weight percent moisture to the AS4/4001 composite (corresponding to 2.7% M in the matrix itself, the matrix saturation level being 7.0% M) resulted in a net interface normal hygrothermal residual stress of almost exactly zero. That is, the tensile normal stress induced by moisture absorption almost exactly offset the cooldown-induced compressive normal stress at the interface. All other stress components were also very low, of course.

Heating the moisture-conditioned composite up to the 93°C (200°F) ETW test temperature increased the interface normal stress to coefficient of thermal expansion (Table 4) and a lower coefficient of moisture expansion (Table 5). The present predictions demonstrate the power of the micromechanics analysis to quantify the influences of

such variables.

Because of these relatively low hygrothermal stresses, no matrix cracking was predicted, even for a 25 percent degraded interface.

### 6.5.3 Transverse Tensile Loading

#### 6.5.3.1 Room Temperature, Dry

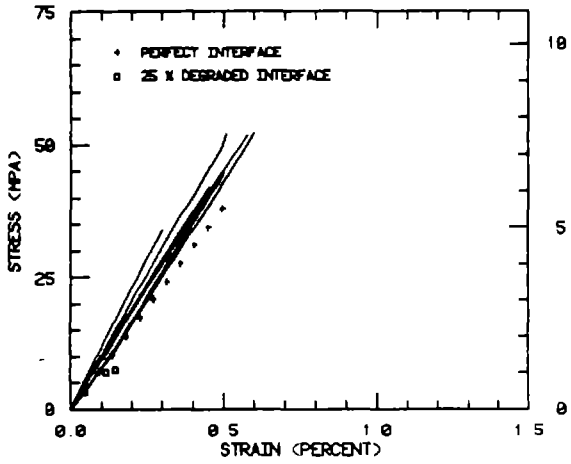
The predicted stress-strain curves, assuming a maximum normal stress failure criterion, are presented in Figure 118, along with the individual stress-strain curves for all four fiber sizing composites. The perfect interface results correlated very well with the experimental data, tending to slightly underpredict ultimate strengths and moduli except for the PVA-sized fiber composite. The underprediction of moduli was again undoubtedly due to slightly premature matrix cracking, associated with the maximum normal stress failure criterion used. The PVA-sized fibers would be expected to result in the poorest interface bonding, and hence, the earliest matrix cracking. As seen in Figure 118, the strengths of these specimens were the lowest.

For the perfect interface bond, no matrix cracking was predicted up to almost 38 MPa (5.5 ksi). However, a crack then initiated at the interface, at about 45° from the loading axis (the x-axis), and spread rapidly in both directions, causing immediate failure. The 9 MPa (1.3 ksi), still a relatively low level. The reason for this more favorable residual stress state relative to that in the AS4/3501-6 composite discussed in Section 6.4.2, was a higher resultant fracture is shown in Figure 119a.

Assuming a 25 percent interface degradation caused interface cracking to occur at only 3.5 MPa (0.5 ksi), as shown in Figure 119b.

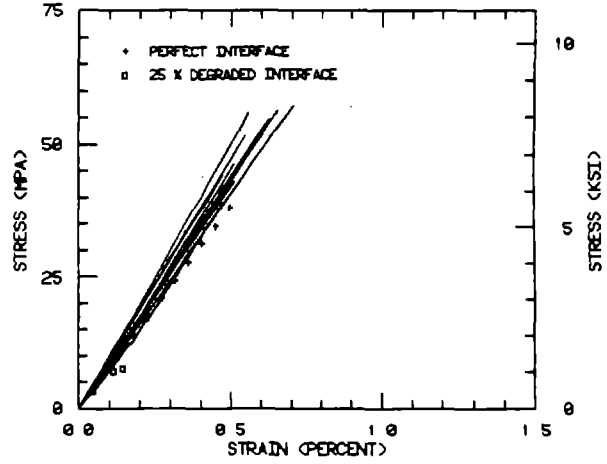
ORIGINAL PAGE IS  
OF POOR QUALITY

R. T. DRY, UNSIZED



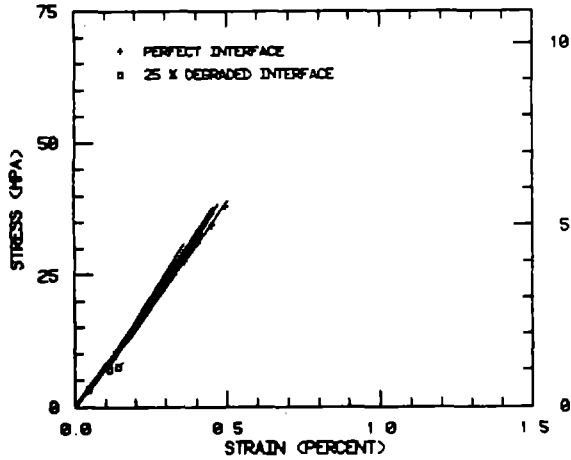
a) unsized

R. T. DRY, 828 SIZED



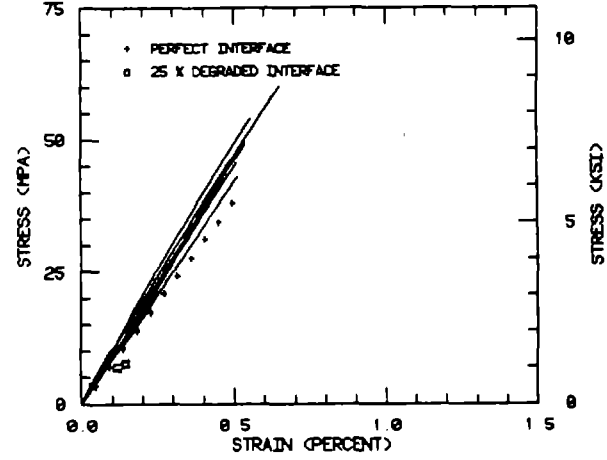
b) EPON 828 sized

R. T. DRY, PVA SIZED



c) PVA sized

R. T. DRY, POLYSULFONE SIZED



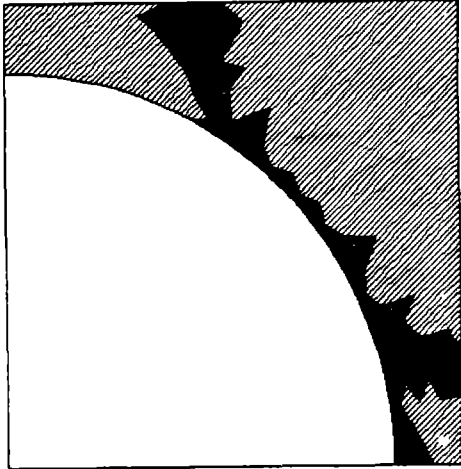
d) polysulfone sized

Figure 118. AS4/4001 Unidirectional Composite, Room Temperature, Dry Condition, Transverse Tensile Loading. Correlations Between Predictions and Experimental Data for All Four Fiber Sizings, Using a Maximum Normal Stress Failure Criterion.

ORIGINAL PAGE IS  
OF POOR QUALITY

4001 TRANS. TEN., PERFECT INT.

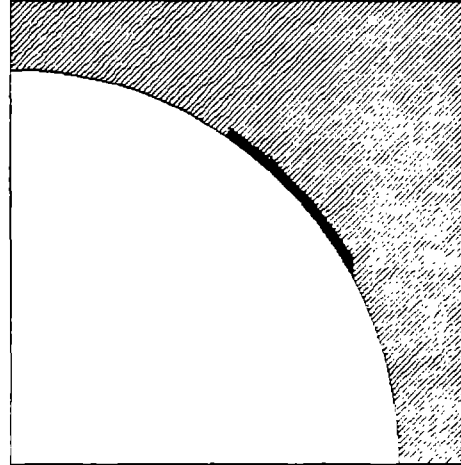
FINITE ELEMENT DEFORMATION GRID  
TEMP - 20.000 C KED - 00 X INCREMENT NO - 31 PLOT NO - 30  
SX - 0.000 X SY - 00 KSI SZ - 00 KSI SZ - 00 KSI  
SX - 0.000 X SY - 00 KSI SZ - 00 KSI



a) crack pattern at failure

4001 TRANS. TEN., 25% DEGRADED INT

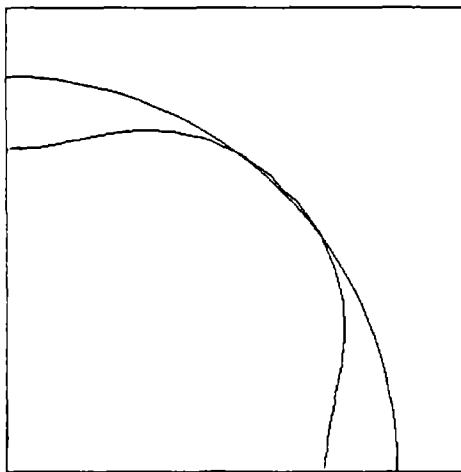
FINITE ELEMENT DEFORMATION GRID  
TEMP - 20.000 C KED - 00 X INCREMENT NO - 29 PLOT NO - 28  
SX - 00 KSI SY - 00 KSI SZ - 00 KSI SZ - 00 KSI  
SX - 00 KSI SY - 00 KSI SZ - 00 KSI  
PLATED ELEMENTS ARE WHITE  
FILLED ELEMENTS ARE BLACK



b) 25% interface degradation,  
yielding at 3.5 MPa

4001 TRANS. TEN., 25% DEGRADED INT

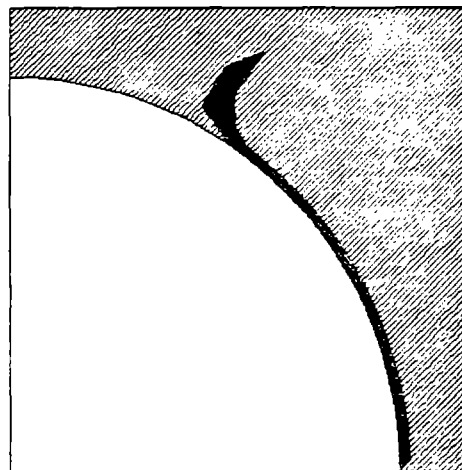
INTERFACE NORMAL STRESS  
TEMP - 20.000 C KED - 00 X INCREMENT NO - 18 PLOT NO - 7  
SX - 0.000 X SY - 00 KSI SZ - 00 KSI SZ - 00 KSI  
SX - 0.000 X SY - 00 KSI SZ - 00 KSI  
SX - 0.000 X SY - 00 KSI SZ - 00 KSI



c) interface normal stress,  
prior to loading, RTD

4001 TRANS. TEN., 25% DEGRADED INT

FINITE ELEMENT DEFORMATION GRID  
TEMP - 20.000 C KED - 00 X INCREMENT NO - 31 PLOT NO - 30  
SX - 1.000 X SY - 00 KSI SZ - 00 KSI SZ - 00 KSI  
SX - 00 KSI SY - 00 KSI SZ - 00 KSI  
PLATED ELEMENTS ARE WHITE



d) 25% interface degradation,  
yielding at 7 MPa

Figure 119. AS4/4001 Unidirectional Composite, Room Temperature, Dry Condition, Transverse Tensile Loading. Extent of Interface and Matrix Cracking, Based Upon a Maximum Normal Stress Failure Criterion.



As for the perfect interface case, debonding occurred first at 45° to the loading axis because of the very favorable compressive residual stress at the interface along the x and y axes. This preexisting stress state is shown in Figure 119c. This interface debond quickly spread to the x axis, and then propagated up into the bulk matrix at 6.9 MPa (1.0 ksi), as shown in Figure 119d. Full fracture occurred at 7.6 MPa (1.1 ksi), as indicated by the stress-strain curve of Figure 118.

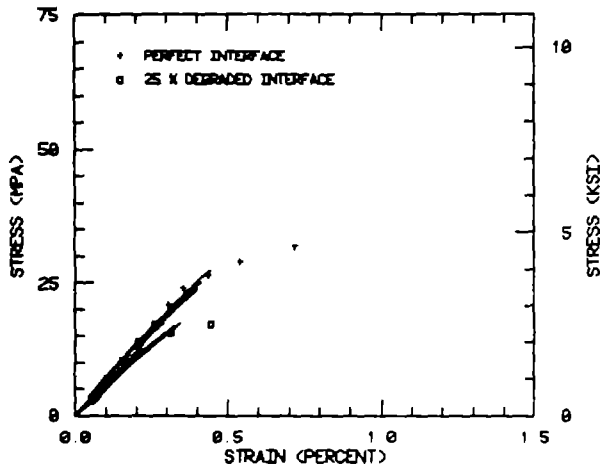
These results suggest that the interface bond for the various AS4/4001 composites was not degraded significantly at the RTD condition.

Use of the octahedral shear failure criterion resulted in extensive matrix cracking at low applied stress levels, and hence, composite moduli which were too low, combined with high apparent strains to failure. As previously discussed, this was due to the low measured shear strength of the Hercules 4001 matrix at room temperature. Use of a more typical shear strength would have undoubtedly resulted in good modulus predictions, but composite strengths which were much too high.

#### 6.5.3.2 Elevated Temperature, Wet

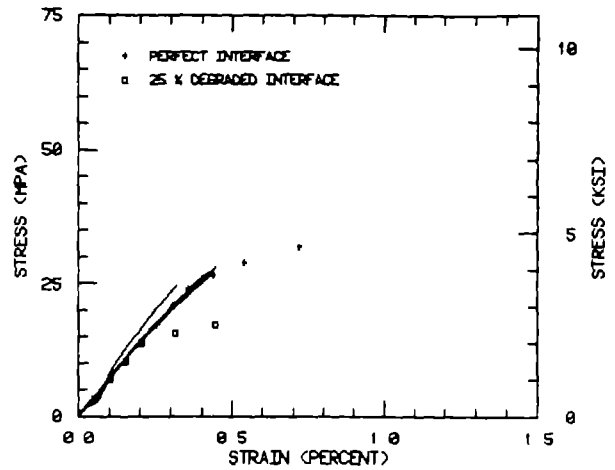
The ETW predicted transverse tensile loading stress-strain curves are shown in Figure 120, for both a perfect interface and a 25 percent degraded interface, assuming a maximum normal stress failure criterion. The experimental data for the four fiber surface treatments are also plotted. As can be seen, the assumption of a perfect interface resulted in good general agreement with the nonlinearity of the experimentally determined stress-strain response.

93 DEG. C., 1% M, UNSIZED



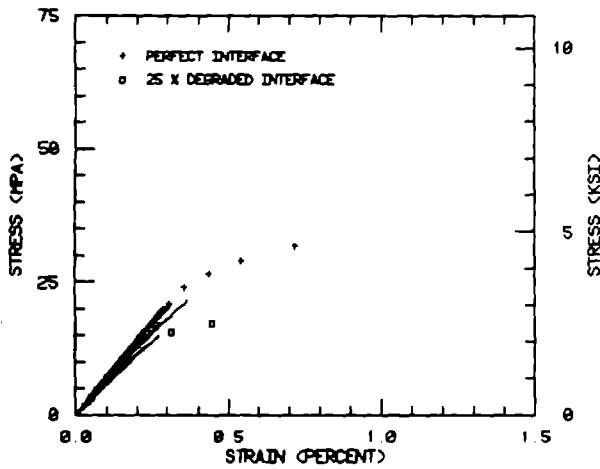
a) unsized

93 DEG. C., 1% M, 828 SIZED



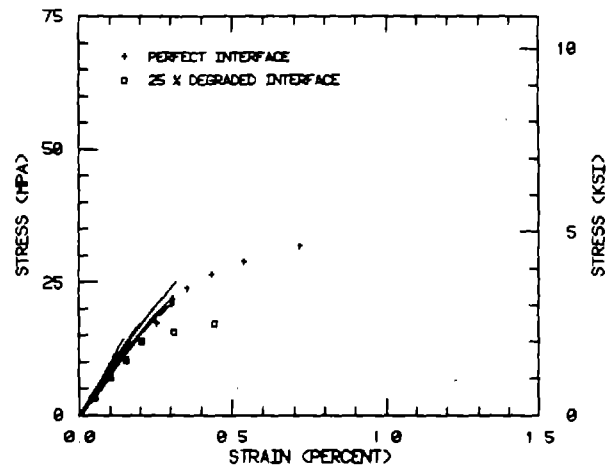
b) EPON 828 sized

93 DEG. C., 1% M, PVA SIZED



c) PVA sized

93 DEG. C., 1% M, POLYSULFONE SIZED



d) polysulfone sized

Figure 120. AS4/4001 Unidirectional Composite, Elevated Temperature, Wet Condition (93°C, 1% M), Transverse Tensile Loading. Correlations Between Predictions and Experimental Data for All Four Fiber Sizings, Using a Maximum Normal Stress Failure Criterion.

The predicted strengths were slightly high, although closer control of the allowable matrix strain at assumed failure would probably adjust this difference. The assumption of a 25 percent interface degradation was obviously too severe, as indicated in Figure 120.

The failure mode predicted assuming a perfect interface is shown in Figure 121a. The fracture is in the bulk matrix, rather than at the interface. This is quite unlike that predicted for the AS4/3501-6 composite at the same ETW condition (see Figure 117a), which was primarily an interface failure. The reason for this distinct difference is related to the differences in coefficients of thermal expansion and moisture expansion between the two matrix materials, as already discussed in Section 6.5.2. The interface normal hygrothermal stresses prior to loading, although still tensile, were much lower for the AS4/4001 composite. This stress distribution is shown in Figure 121b.

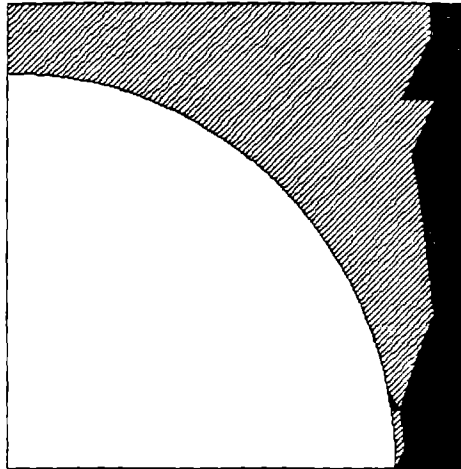
Degrading the interface strength by 25 percent was sufficient, however, to shift the failure back to the interface, as indicated in Figures 121c and 121d. First cracking also occurred earlier in the loading, accounting for the reduced apparent composite modulus indicated in Figure 120. Likewise, total fracture occurred earlier. That is, the predicted composite strength was only slightly greater than 17 MPa (2.5 ksi), whereas for the perfect interface it was 32 MPa (4.6 ksi).

As for the RTD condition, degradation effects due to fiber sizing variations appeared to be minimal. Also, the interfaces of the composites incorporating the Hercules 4001 bismaleimide matrix did not appear to be degraded by the elevated temperature and

ORIGINAL PAGE IS  
OF POOR QUALITY

4001 TRANS. TEN., PERFECT INT.

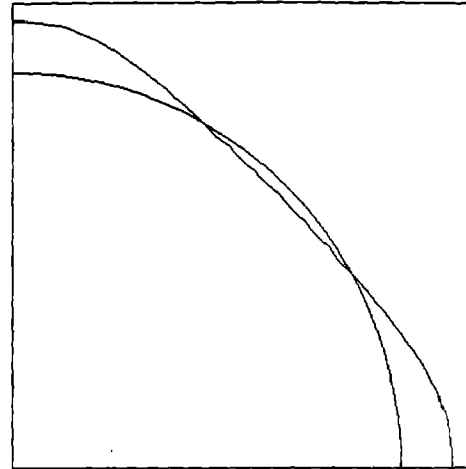
FINITE ELEMENT DISPLACEMENT GRID  
 TEMP - 93.00 DEG. C    MOD - 2.70 N    INCREMENT NO. - 41    PLOT NO. - 00  
 SXX - 4.61 KSI    SYY - 00 KSI    SZZ - 00 KSI    SYZ - 00 KSI  
 SXX - 00 KSI  
 SYY - 00 KSI  
 SZZ - 00 KSI  
 ELASTIC ELEMENTS ARE    WHITE  
 PLASTIC ELEMENTS ARE    WHITE



a) crack pattern at failure

4001 TRANS. TEN., PERFECT INT.

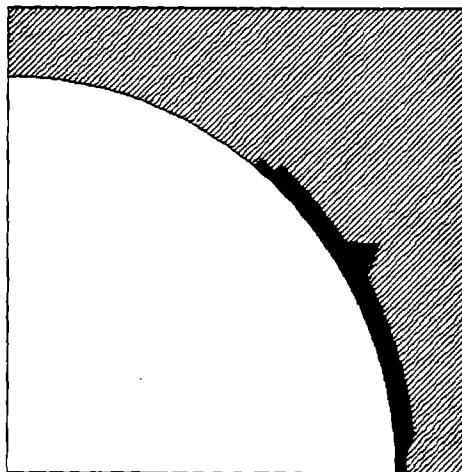
INTERFACE NORMAL STRESS  
 TEMP - 93.00 DEG. C    MOD - 2.70 N    INCREMENT NO. - 31    PLOT NO. - 27  
 SXX - 00 KSI    SYY - 00 KSI    SZZ - 00 KSI    SYZ - 00 KSI  
 SXX - 00 KSI  
 SYY - 00 KSI  
 SZZ - 00 KSI  
 SXX - -1.32 KSI    SYY - 1.32 KSI



b) interface normal stress, ETW, prior to loading

4001 TRANS. TEN., 25 % DEGRADED INT.

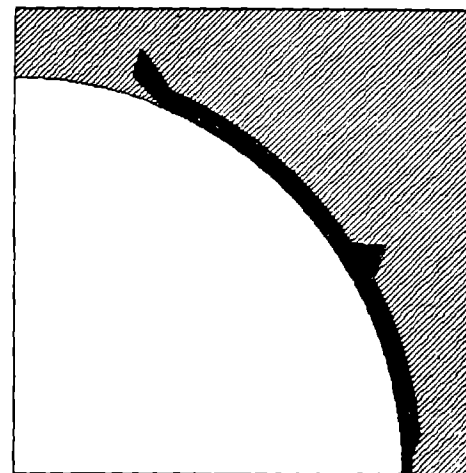
FINITE ELEMENT DISPLACEMENT GRID  
 TEMP - 93.00 DEG. C    MOD - 2.70 N    INCREMENT NO. - 41    PLOT NO. - 00  
 SXX - 2.68 KSI    SYY - 00 KSI    SZZ - 00 KSI    SYZ - 00 KSI  
 SXX - 00 KSI  
 SYY - 00 KSI  
 SZZ - 00 KSI  
 ELASTIC ELEMENTS ARE    WHITE    PLASTIC ELEMENTS ARE    GRAY  
 FAILED ELEMENTS ARE    BLACK



c) 25% interface degradation, cracking at 14 MPa

4001 TRANS. TEN., 25 % DEGRADED INT.

FINITE ELEMENT DISPLACEMENT GRID  
 TEMP - 93.00 DEG. C    MOD - 2.70 N    INCREMENT NO. - 51    PLOT NO. - 70  
 SXX - 2.58 KSI    SYY - 00 KSI    SZZ - 00 KSI    SYZ - 00 KSI  
 SXX - 00 KSI  
 SYY - 00 KSI  
 SZZ - 00 KSI  
 ELASTIC ELEMENTS ARE    WHITE    PLASTIC ELEMENTS ARE    GRAY  
 FAILED ELEMENTS ARE    BLACK



d) 25% interface degradation, cracking at 17 MPa

Figure 121. AS4/4001 Unidirectional Composite, Elevated Temperature, Wet Condition (93°C, 1% M), Transverse Tensile Loading. Extent of Interface and Matrix Cracking, Based Upon a Maximum Normal Stress Failure Criterion.

presence of moisture. The AS4/3501-6 composites indicated greater influences, as previously shown.

Although no results will be presented here, the use of an octahedral shear stress failure criterion again did not produce good correlations with the experimental data. Assuming a perfect interface resulted in a good prediction of modulus as would be expected, but the strength was much too high. First cracking, which as for the maximum normal stress failure criterion (see Figure 121a) occurred in the bulk matrix rather than at the interface, initiated at 55 MPa (7.9 ksi), total fracture being predicted at 68 MPa (9.8 ksi). The experimentally measured composite strengths were only on the order of 25 MPa (3.6 ksi), as shown previously in Figure 121.

Assuming a 25 percent interface degradation resulted in a predicted composite modulus which was much too low, because of the excessive interface cracking which occurred. Correspondingly, the composite strength prediction was too low, and the strain to failure too great.

#### 6.6 AS4/F155 Correlations

As discussed in detail in Sections 3 and 4, the Hexcel F155 is advertised as a rubber-toughened 121°C (250°F) cure epoxy. The actual cure temperature of 127°C (260°F) recommended by the manufacturer was used in fabricating the composites tested here, as discussed in Section 3. Thus, this 127°C (260°F) cure temperature was also modeled here. It will be noted that the other two matrix systems were cured or postcured at higher temperatures, the Hercules 3501-6 epoxy at 177°C (350°F) and the Hercules 4001 bismaleimide at 204°C (400°F).

#### 6.6.1 Thermal Residual Stresses

The coefficient of thermal expansion of the Hexcel F155 rubber-toughened epoxy was higher than those of the two other matrix systems, as might be expected (see Table 4). However, because of the lower cure temperature, and hence the smaller temperature decrease when cooling down to room temperature, the thermal residual stresses in the AS4/F155 composites were predicted to be significantly lower than in the other two composite systems. For example, the highest interface normal stress in the AS4/F155 composite was -10 MPa (-1.4 ksi). The corresponding stresses in the AS4/4001 and AS4/3501-6 composites were -21 MPa (-3.0 ksi) and -31 MPa (-4.5 ksi), respectively. Unfortunately, since these are compressive stresses at the interface, higher stresses are favorable if a transverse tensile loading is to be applied, as being considered here.

#### 6.6.2 Moisture-Induced Stresses

The coefficient of moisture expansion of the Hexcel F155 matrix was comparable to that of the Hercules 3501-6 epoxy, and lower than that of the Hercules 4001 bismaleimide (see Table 5). It will also be recalled that the average fiber volumes of the AS4/F155 composites were lower than for the other two composite systems (see Table 6). An average fiber volume of 40 percent was modeled in the present micromechanics analyses. As a result of these various factors, the maximum interface normal residual stress at the ETW test condition, although tensile, was only 4 MPa (0.6 ksi). The corresponding stresses in the AS4/4001 and AS4/3501-6 composites were 9 MPa (1.3 ksi) and 29 MPa (4.2 ksi), respectively. This lower tensile residual stress is favorable in terms of subsequent transverse tensile

loadings.

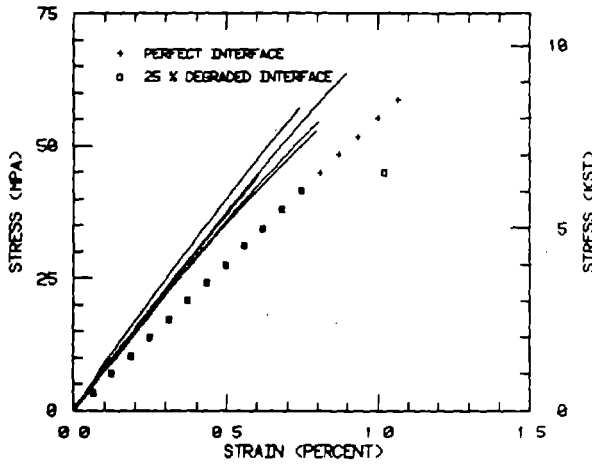
### 6.6.3 Transverse Tensile Loading

#### 6.6.3.1 Room Temperature, Dry

The micromechanics analysis consistently underpredicted the RTD transverse tensile stiffness of the AS4/F155 unidirectional composites, as can be seen in Figure 122. These particular plots are for the maximum normal stress failure criterion. But since matrix cracking did not initiate at low stress levels, the low moduli predicted cannot be attributed to this effect, as was the case in prior discussions. The measured moduli of the Hexcel F155 matrix were lower than for the other two resin systems (see Tables 2 and 3), but this was not unexpected and there is no reason to suspect these experimental data. Variations in fiber volume do not appear to be an explanation either. A fiber volume of 40 percent was modeled and, as indicated in Table 6, this is a representative average value for the various AS4/F155 unidirectional composites.

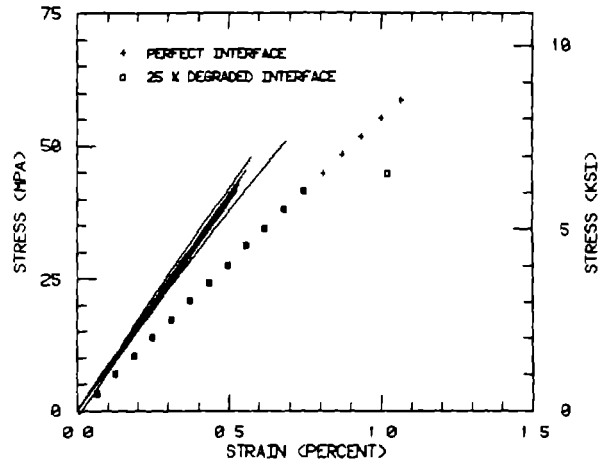
For the perfect interface assumption, first failure did not occur until a stress level of 59 MPa (8.5 ksi) was attained. This first crack initiated in the matrix at the x axis (the axis of loading), and immediately spread to the interface and across the matrix again, to the upper boundary of the region being modeled. Full failure was at 62 MPa (9.0 ksi), as indicated in Figure 122. That is, once a crack initiated, complete fracture followed quickly. Similar results were obtained for the 25 percent degraded interface case, but at lower stress levels, as indicated in Figure 122. Also, the crack did tend to follow the interface more closely for the degraded interface model, as might be expected.

R T DRY, UNSIZED



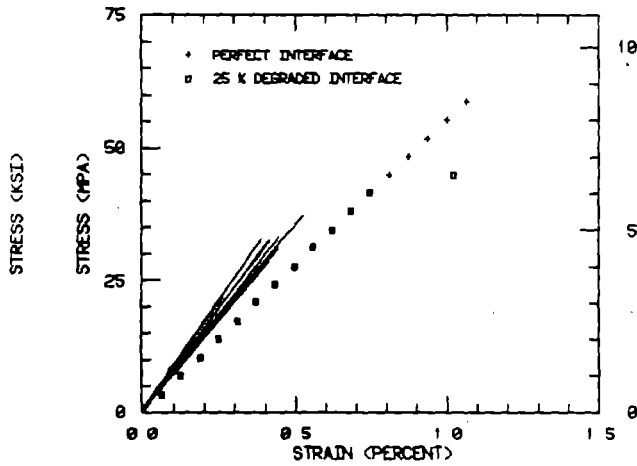
a) unsized

R T DRY, 828 SIZED



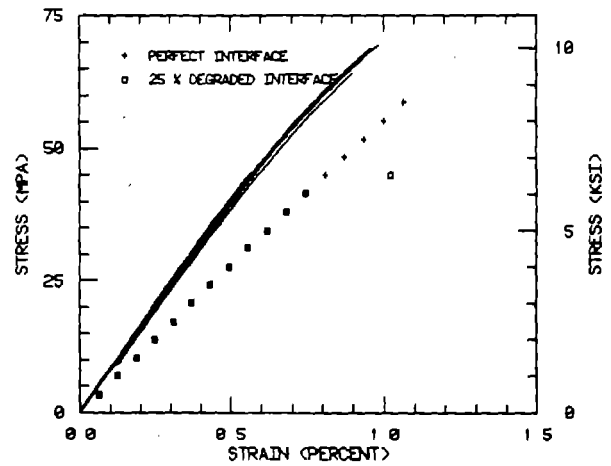
b) EPON 828 sized

R.T DRY, PVA SIZED



c) PVA sized

R T DRY, POLYSULFONE SIZED



d) polysulfone sized

Figure 122. AS4/F155 Unidirectional Composite, Room Temperature, Dry, Transverse Tensile Loading. Correlations Between Predictions and Experimental Data for All Four Fiber Sizings, Using a Maximum Normal Stress Failure Criterion.



Figures 123a through 123c indicate the internal stress states in the perfect interface model composite at an applied stress level of 41 MPa (6 ksi), i.e., before any local failures had occurred. Figure 123a indicates the interface normal tensile stresses which had developed, the maximum value being quite high at 69 MPa (10 ksi). However, as indicated in Figure 123b, the maximum principal stress away from the interface was even slightly higher, i.e., 74 MPa (10.7 ksi), in the matrix along the x axis between fibers. This explains why the initial failure eventually occurred away from the interface.

It will also be noted that the RTD tensile strength of the Hexcel F155 matrix was measured to be considerably higher than that of the other two matrix materials. As indicated in Table 2, the tensile strength of the Hexcel F155 matrix was 77 MPa (11.2 ksi), which was about 25 percent higher than that of the Hercules 3501-6, and almost 50 percent higher than that of the Hercules 4001.

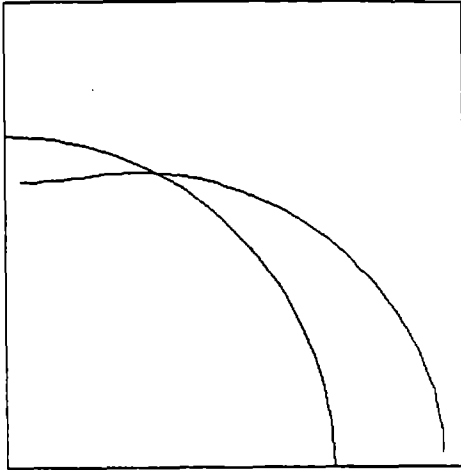
On the other hand, the shear strength of the Hexcel F155 was not so high. At 48 MPa (7.0 ksi), as indicated in Table 3, it was only about 50 percent that of the Hercules 3501-6 epoxy. Of course, as previously discussed in Section 6.5, the shear strength of the Hercules 4001, at only 2.4 MPa (17 ksi), was questionably low and thus cannot be compared.

While these variations in neat resin tensile and shear strengths may be explained in large part by the difficulties in performing neat resin testing, use of these results in the micromechanics analysis obviously has a strong influence on the predicted results. For example, use of the octahedral shear stress failure criterion, which is based upon the shear test data, would be expected to lead to

ORIGINAL PAGE IS  
OF POOR QUALITY

F155 TRANS. TEN., PERFECT INT.

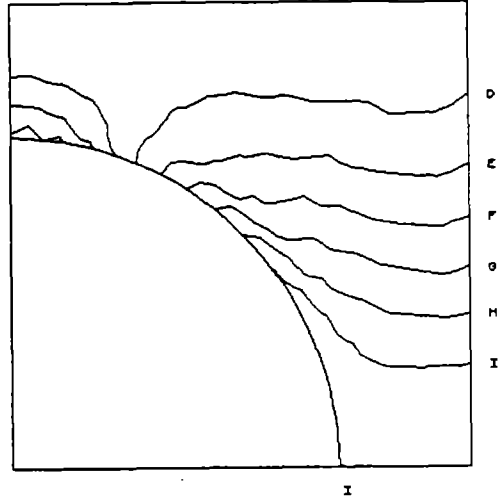
INTERFACE NORMAL STRESS  
 TEMP = 29.00 DEG. C    MOD = 00 X    INCREMENT NO = 20    PLOT NO = 47  
 SX = 0.00 KSI    SY = 00 KSI    SZ = 00 KSI    S12 = 00 KSI  
 TX = 4.00 KSI    TXZ = 0.00 KSI



a) interface normal stress at 41 MPa

F155 TRANS. TEN., PERFECT INT.

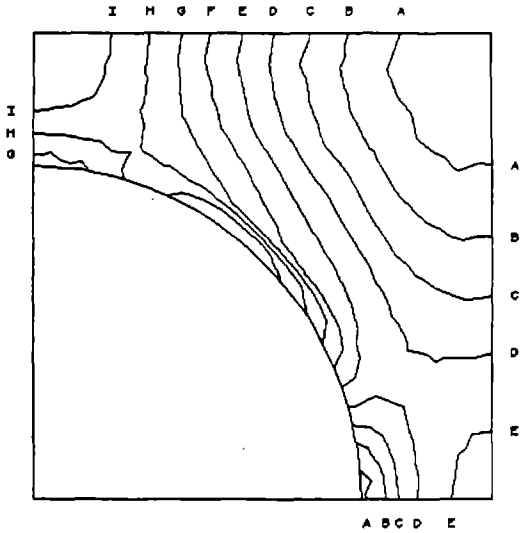
FIRST PRINCIPAL STRESS CONTOUR  
 TEMP = 29.00 DEG. C    MOD = 00 X    INCREMENT NO = 20    PLOT NO = 48  
 SX = 0.00 KSI    SY = 00 KSI    SZ = 00 KSI    S12 = 00 KSI  
 TX = 0.00 KSI    TXZ = 0.20 KSI    TY = 10.70 KSI    A = 4.00 KSI  
 B = 4.74 KSI    C = 0.40 KSI    D = 0.20 KSI    E = 0.00 KSI  
 F = 7.70 KSI    G = 0.40 KSI    H = 0.21 KSI    I = 0.00 KSI



b) first principal stress at 41 MPa

F155 TRANS. TEN., PERFECT INT.

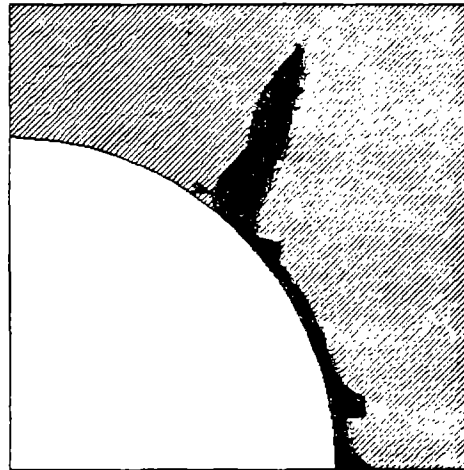
OCTAHEDRAL SHEAR STRESS CONTOUR  
 TEMP = 29.00 DEG. C    MOD = 00 X    INCREMENT NO = 20    PLOT NO = 49  
 SX = 0.00 KSI    SY = 00 KSI    SZ = 00 KSI    S12 = 00 KSI  
 TX = 0.00 KSI    TXZ = 1.17 KSI    TY = 4.00 KSI    A = 1.00 KSI  
 B = 1.70 KSI    C = 2.00 KSI    D = 2.00 KSI    E = 2.00 KSI  
 F = 2.00 KSI    G = 3.00 KSI    H = 3.47 KSI    I = 3.70 KSI



c) octahedral shear stress at 41 MPa

F155 TRANS. TEN., 25% DEGRADED INT.

FINITE ELEMENT DEFORMATION GRID  
 TEMP = 29.00 DEG. C    MOD = 00 X    INCREMENT NO = 20    PLOT NO = 50  
 SX = 0.00 KSI    SY = 00 KSI    SZ = 00 KSI    S12 = 00 KSI  
 TX = 0.00 KSI    TXZ = 0.00 KSI    TY = 0.00 KSI    A = 0.00 KSI  
 B = 0.00 KSI    C = 0.00 KSI    D = 0.00 KSI    E = 0.00 KSI  
 F = 0.00 KSI    G = 0.00 KSI    H = 0.00 KSI    I = 0.00 KSI



d) 25% interface degradation, cracking at 45 MPa

Figure 123. AS4/F155 Unidirectional Composite, Room Temperature, Dry, Transverse Tensile Loading. Stress Contours and Extent of Matrix Cracking, Based Upon a Maximum Normal Stress Failure Criterion.

earlier cracking, due to the lower measured shear strength of the Hexcel F155 matrix material. Figure 123c is a plot of the octahedral shear stress distribution at an applied stress of 41 MPa (6.0 ksi), i.e., prior to any failure. It will be noted that the highest stresses occurred at the interface, about 50° above the loading axis, and also along the y axis away from the interface.

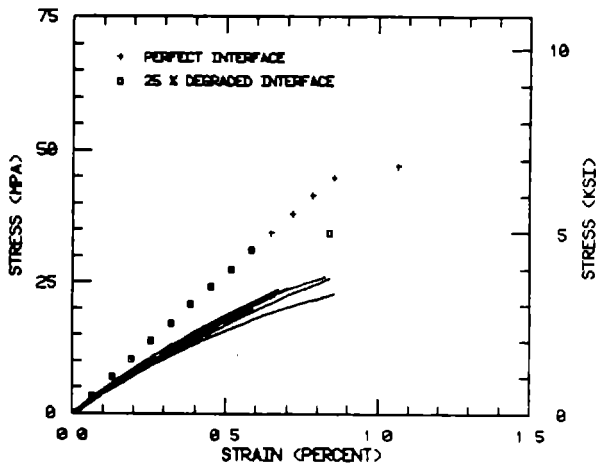
Assuming a 25 percent interface strength degradation caused first failure to occur earlier in the loading, as expected. Again, however, total failure followed initial failure very closely. The respective values were 41 MPa (6.0 ksi) and 45 MPa (6.5 ksi). These values were in reasonable agreement with the experimental data, as indicated in Figure 122.

Use of the octahedral shear stress failure theory resulted in a composite strength prediction of 80 MPa (12.4 ksi) for the perfect interface assumption, and an only slightly lower value for a 25 percent degraded interface model. That is, once again the predicted strengths were too high using this failure criterion.

#### 6.6.3.2 Elevated Temperature, Wet

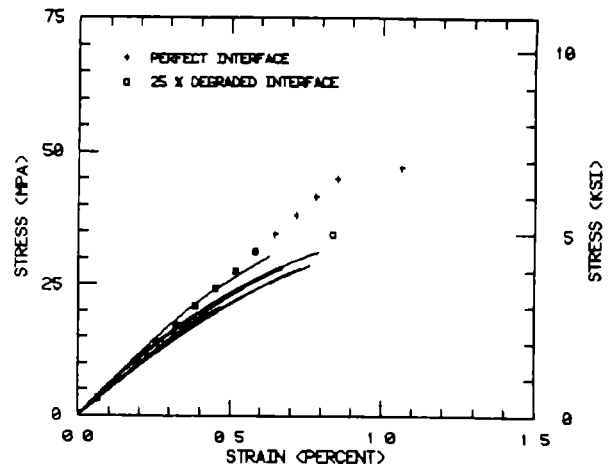
Correlations between the analytically predicted transverse tensile stress-strain curves for the unidirectional AS4/F155 composite, based upon a maximum normal stress failure criterion, and the experimental data are plotted in Figure 124. The assumption of a perfect interface resulted in a predicted composite modulus which was too high in general. First failure was predicted at 45 MPa (6.5 ksi), with complete fracture following almost immediately at 47 MPa (6.8 ksi). Assuming a 25 percent degraded interface lowered the onset of cracking to 31 MPa (4.5 ksi), and full failure to 35 MPa (5.0 ksi).

38 DEG. C , 1% M, UNSIZED



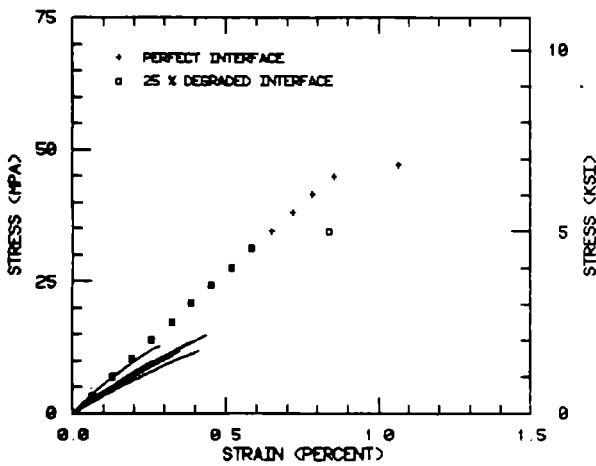
a) unsized

38 DEG C , 1% M, 820 SIZED



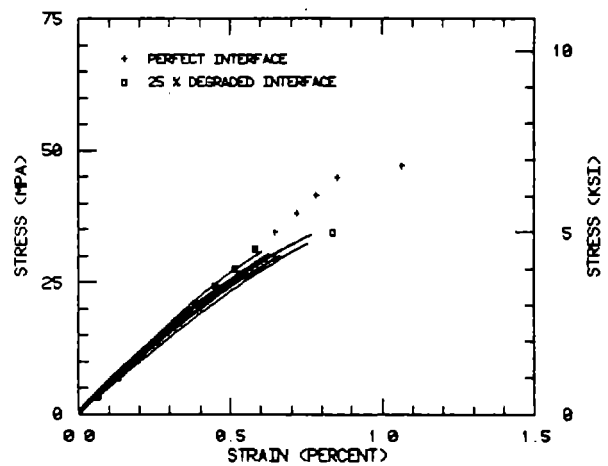
b) EPON 828 sized

38 DEG C , 1% M, PVA SIZED



c) PVA sized

38 DEG C , 1% M, POLYSULFONE SIZED



d) polysulfone sized

Figure 124. AS4/F155 Unidirectional Composite , Elevated Temperature, Wet Condition (38°C, 1% M), Transverse Tensile Loading. Correlations Between Predictions and Experimental Data for All Four Fiber Sizings, Using a Maximum Normal Stress Failure Criterion.

There was some concern in the experimental portion of the program that, because of the ability of the Hexcel F155 matrix to absorb moisture rapidly (see Table 5 for moisture saturation levels), the AS4/F155 composites may have absorbed additional moisture while waiting to be tested. To assess the potential influences of this possibility, the computer simulations of Figure 124 were repeated assuming a 2% M (i.e., a two weight percent moisture weight gain) in these composites. The additional moisture would be expected to increase the unfavorable tensile residual hygrothermal stresses in the matrix, and thus, presumably promote matrix cracking and lower composite strengths. This would also decrease the apparent modulus and increase the strain to failure.

While the actual predictions did indicate these expected trends, the magnitudes of the changes were relatively small. The matrix did begin to crack at slightly lower levels of applied stress, but the cracks did not grow to total failure as rapidly. This was associated with the lower modulus and greater failure strain of the Hexcel F155 epoxy at the higher moisture level (see Table 3).

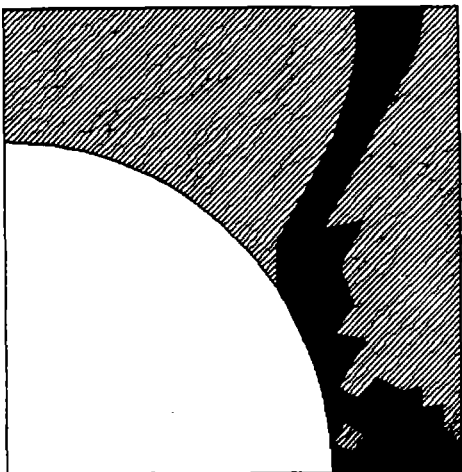
The crack patterns at total failure for the four computer simulations, i.e., perfect and 25 percent degraded interfaces, and 1% M and 2% M, are shown in Figure 125. While there were differences, they were not great. As expected, the crack followed the degraded interface more closely.

This type of analysis again points out the value of having a predictive tool available. It was relatively simple to assess the influence of a possible abnormal amount of moisture absorption, and to demonstrate that even if it had occurred, it would not have

ORIGINAL PAGE IS  
OF POOR QUALITY

F155 TRANS. TEN., PERFECT INT.

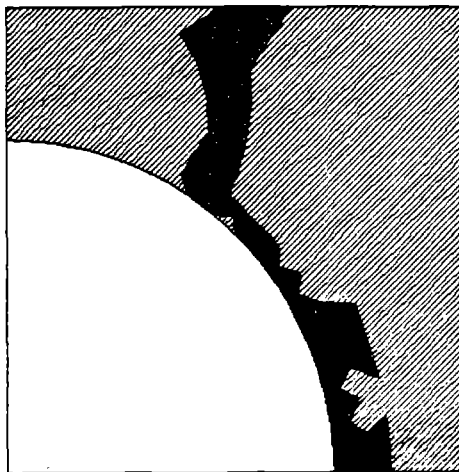
FINITE ELEMENT DISPLACEMENT GRID			
TEMP - 30.00 DEG. C	MOD - 1.00 X	INCREMENT NO. - 30	PLOT NO. - 00
SM - 7.50 KSI	SY - .00 KSI	SZ - .00 KSI	SIZ - .00 KSI
SE - .00 KSI			
ELASTIC ELEMENTS ARE	WHITE	PLASTIC ELEMENTS ARE	GRAY
PROLED ELEMENTS ARE	BLACK		



a) perfect interface, 1%M

F155 TRANS. TEN., PERFECT INT.

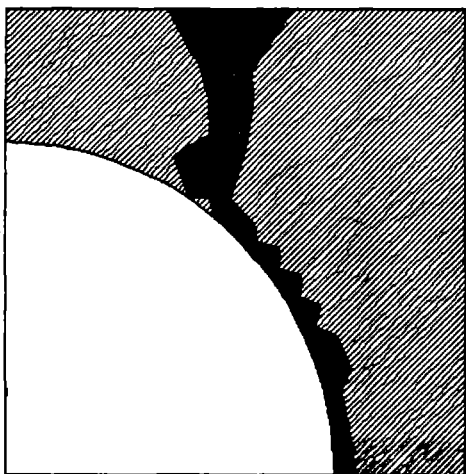
FINITE ELEMENT DISPLACEMENT GRID			
TEMP - 30.00 DEG. C	MOD - 3.00 X	INCREMENT NO. - 30	PLOT NO. - 00
SM - 0.75 KSI	SY - .00 KSI	SZ - .00 KSI	SIZ - .00 KSI
SE - .00 KSI			
ELASTIC ELEMENTS ARE	WHITE	PLASTIC ELEMENTS ARE	GRAY
PROLED ELEMENTS ARE	BLACK		



b) perfect interface, 2%M

F155 TRANS. TEN., 25 X DEGRADED INT.

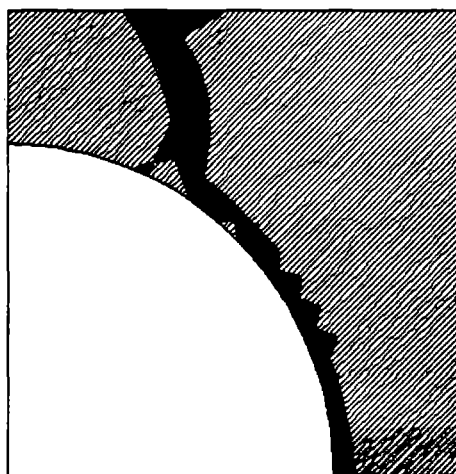
FINITE ELEMENT DISPLACEMENT GRID			
TEMP - 30.00 DEG. C	MOD - 1.00 X	INCREMENT NO. - 30	PLOT NO. - 70
SM - 0.00 KSI	SY - .00 KSI	SZ - .00 KSI	SIZ - .00 KSI
SE - .00 KSI			
ELASTIC ELEMENTS ARE	WHITE	PLASTIC ELEMENTS ARE	GRAY
PROLED ELEMENTS ARE	BLACK		



c) 25% interface degradation, 1%M

F155 TRANS. TEN., 25 X DEGRADED INT.

FINITE ELEMENT DISPLACEMENT GRID			
TEMP - 30.00 DEG. C	MOD - 3.00 X	INCREMENT NO. - 30	PLOT NO. - 70
SM - 4.00 KSI	SY - .00 KSI	SZ - .00 KSI	SIZ - .00 KSI
SE - .00 KSI			
ELASTIC ELEMENTS ARE	WHITE	PLASTIC ELEMENTS ARE	GRAY
PROLED ELEMENTS ARE	BLACK		



d) 25% interface degradation, 2%M

Figure 125. AS4/F155 Unidirectional Composite, Elevated Temperature, Wet Condition, Transverse Tensile Loading. Influence of Composite Moisture Content and Interface Bond Strength on Predicted Crack Patterns, Using a Maximum Normal Stress Failure Criterion.

drastically altered the experimental results obtained.

#### 6.7 Summary of Results

It has been demonstrated that the WYO2D finite element micromechanics analysis can predict unidirectional composite transverse tensile properties with reasonable accuracy. The analysis can be used to show the influences of selected variables such as fiber volume, interface bond strength, test temperature, moisture content, etc., without the necessity of performing a full test program. In future work, it will hopefully also be used to help design the original test matrix, so that the parameters which are indicated to be particularly important can be tested, and others neglected or only included to the extent necessary to show that they are negligible.





## SECTION 7

### CONCLUSIONS AND RECOMMENDATIONS

This study demonstrated that other factors such as the type of matrix and the specific loading mode have greater influences on composite performance than any one of the four different composite sizings utilized here. This is, of course, a very positive finding in that it suggests the latitude which is permissible in selecting a fiber sizing.

It was demonstrated that a unidirectional composite is still the most desirable composite form for performance evaluations. The quasi-isotropic laminates produced complex failure modes, which tended to obscure the role of the fiber-matrix interface in the fracture. Even the simple interlaminar (short beam) shear tests of the quasi-isotropic laminates were not as useful as shear tests of the unidirectional composites would have been.

The two single fiber composite test methods used were too dependent on the testing technique, and too time consuming to be practical screening tests. The single fiber pullout test requires the formation of a very thin fiber disk of matrix around a single graphite fiber. This is a very delicate fabrication procedure, and if not done exactly right, will not produce valid results. In fact, even if done properly, the results are often in wide variance with those obtained using other test methods. This was discussed in detail in Section 4.6. The second single fiber test method used, a dogboned tensile coupon of neat resin with a single graphite fiber

247

Preceding Page Blank

ANK 100-111-111-111

embedded in it along its axis, also proved to be difficult to use with normal structural resins such as those of the present study. The test method was originally developed using model resin systems, capable of being cured at low temperatures and exhibiting high strains to failure. The present resins were not in this category.

To summarize the test procedures, much was learned, and is carefully documented in this report, about the ability of various test configurations to serve as sensitive indicators of fiber-matrix interface performance. Complex laminates, such as the quasi-isotropic laminates specified for use in the present study, are not good choices; and model composites such as the single fiber test specimens are not sufficiently representative of actual, high fiber volume composites. A simple unidirectional composite, tested in the fundamental loading modes, viz, axial tension, axial compression, transverse tension, transverse compression, and in-plane (longitudinal) shear, is clearly the proper choice. Even of these tests, those which emphasize the role of the interface are the logical loading modes to use if it is the effectiveness of the interface which is to be evaluated. The first choice would thus be an Iosipescu shear test of the unidirectional composite, followed by transverse tensile and axial compression tests.

Along with the positive fact that there was no strong distinction in the performance of the four different fiber sizings in so many different loading modes, vast amounts of useful design data were generated. These data are fully presented and documented in this report and its appendices. Properties such as neat resin stress-strain curves to failure, and coefficients of thermal and

moisture expansion, are not normally available. Likewise, the influences of elevated temperature and moisture on both the neat resin and the corresponding composites are included. Failure modes are documented in the form of an extensive collection of scanning electron microphotographs of composite fracture surfaces. These hopefully will be very useful to future investigators, for comparison purposes as new fiber sizings are developed.

A finite element micromechanics analysis and related computer program, WY02D, only recently developed and therefore not yet used extensively, was also introduced. Only the unidirectional composite transverse tensile data were analyzed here. However, the results presented in Section 6, and their correlations with the actual experimental data, demonstrate the great potential of such a tool. Not only was it shown that the analysis can predict actual unidirectional composite response, it was demonstrated that it can be used to estimate the influence of potential variables. In fact, it is this capability that is of particular significance. If the actual testing has already been done, an analysis to predict these measured properties is superfluous. However, testing is both extremely time consuming and expensive; and if it does not lead to useful results, it is also wasteful of resources. The micromechanics analysis can be used to screen candidate material combinations under various loading and environmental conditions, including those which would be difficult to achieve in the laboratory. Only those most promising combinations then need be actually fabricated and tested.

The present study was designed by NASA-Ames to generate data on actual composite material systems and fiber sizings in current use.

This was achieved, as fully documented in this report. It is recommended that in any future study, model systems also be included. For example, the present study would have benefited from the inclusion of a fiber surface treatment or fiber sizing which resulted in little or no interface bonding. This would have provided a strong baseline for comparisons. Likewise, focusing on fewer test methods is strongly recommended. This will permit a more in-depth evaluation, by permitting more combinations of materials and environments. For example, as extensive as the present study was, only the room temperature, dry and one elevated temperature, wet environmental condition were studied. Thus, it was not possible to separate temperature effects from moisture effects. Nor was it possible to identify the temperature or moisture level at which significant losses of critical composite properties would have occurred. The use of only two or three basic test methods, rather than the eight different methods called for in the present study, will permit these additional determinations.

In conclusion, it is recommended that additional studies be conducted, using additional matrix materials, other fibers, and a wider range of fiber sizings. The generation of complete stress-strain curves to failure, and the careful documentation of composite fabrication and test conditions, is extremely important. Details, such as the recording of fiber volumes, fracture surface characteristics, and the quality of the materials used should not be overlooked. In this way, a complete and therefore useful data base can gradually be assembled. It is hoped that the present work meets these requirements.

#### REFERENCES

1. "Vitrex PEEK/Carbon Fibre," Data Sheet APC PD3, Imperial Chemical Industries, ICI Americas, Inc., Wilmington, Delaware, 1983.
2. "Hercules Product Data Sheet No. 847-3: Magnamite Graphite Fiber Type AS4," Hercules, Inc., Magna, Utah, August 1981.
3. "EPON 828 Epoxy Resin," Shell Data Sheets, Shell Development Company, Houston, Texas, 1984.
4. "Udell P1700 Polysulfone Resin," General Electric Data Sheets, Plastics Operations, General Electric Company, Pittsfield, Massachusetts, 1982.
5. "Hercules 3501-6 Epoxy Resin," Hercules Specification HS-SG-560, Revision A, Hercules, Inc., Magna, Utah, November 1983.
6. "Hercules 4001 Bismaleimide Resin," Hercules Data Sheets, Hercules, Inc., Magna, Utah, 1983.
7. "Hexcel F155 - A Controlled Flow Epoxy Resin for Laminating and Co-Curing at 250°F Cure," Product Data Sheet, Hexcel Corporation, Dublin, California, March 1982.
8. "Techkits Epoxy Adhesive A-12," Techkits, Inc., Demarest, New Jersey, 1984.
9. D. F. Adams and D. E. Walrath, "Hygrothermal Response of Polymer Matrix Composite Materials," Report UWME-DR-901-102-1, Department of Mechanical Engineering, University of Wyoming, September 1979.
10. D. A. Crane and D. F. Adams, "Finite Element Micromechanical Analysis of a Unidirectional Composite Including Longitudinal Shear Loading," Report UWME-DR-101-101-1, Department of Mechanical Engineering, University of Wyoming, February 1981.
11. R. S. Zimmerman, D. F. Adams, and D. E. Walrath, "Investigation of the Relations Between Neat Resin and Advanced Composite Mechanical Properties," Report UWME-DR-301-101-1: Volume I - Results, Volume II - Appendices, Department of Mechanical Engineering, University of Wyoming, May 1983.
12. R. S. Zimmerman, D. F. Adams, "Mechanical Properties Testing of Candidate Polymer Matrix Materials for Use in High Performance Composites," Report UWME-DR-401-104-1, Department of Mechanical Engineering, University of Wyoming, August 1984.
13. E. M. Odom and D. F. Adams, "A Study of Polymer Matrix Fatigue Properties," Report UWME-DR-301-103-1, Department of Mechanical

Engineering, University of Wyoming, June 1983.

14. D. E. Walrath and D. F. Adams, "Analysis of the Stress State in an Iosipescu Shear Test Specimen," Report UWME-DR-301-102-1, Department of Mechanical Engineering, University of Wyoming, June 1983.
15. D. E. Walrath and D. F. Adams, "Verification and Application of the Iosipescu Shear Test Method," Report UWME-DR-401-103-1, Department of Mechanical Engineering, University of Wyoming, June 1984.
16. D. F. Adams and D. E. Walrath, "Iosipescu Shear Properties of SMC Composite Materials," Proceedings of the Sixth Conference on Composite Materials: Testing and Design, ASTM STP 787, Phoenix, Arizona, May 1981, pp. 19-33.
17. D. E. Walrath and D. F. Adams, "The Iosipescu Shear Test as Applied to Composite Materials," Experimental Mechanics, Vol. 23, No. 1, March 1983, pp. 105-110.
18. D. S. Cairns and D. F. Adams, "Moisture and Thermal Expansion of Composite Materials," Report UWME-DR-101-104-1, Department of Mechanical Engineering, University of Wyoming, November 1981.
19. D. S. Cairns and D. F. Adams, "Moisture and Thermal Expansion Properties of Unidirectional Composite Materials and the Epoxy Matrix," Journal of Reinforced Plastics and Composites, Vol. 2, No. 4, October 1983, pp. 239-255.
20. S. V. Hayes, "Rate Sensitive Tensile Impact Properties of Fully and Partially Loaded Unidirectional Composites," M.S. Thesis, Department of Mechanical Engineering, University of Wyoming, Laramie, Wyoming, May 1980.
21. S. V. Hayes and D. F. Adams, "Rate Sensitive Tensile Impact Properties of Fully and Partially Loaded Unidirectional Composites," Journal of Testing and Evaluation, Vol. 10, No. 2, March 1982, pp. 61-68.
22. M. N. Irion, D. F. Adams and D. E. Walrath, "Compression Creep Behavior of SMC Composite Materials," Report UWME-DR-004-104-1, Department of Mechanical Engineering, University of Wyoming, March 1980.
23. M. N. Irion and D. F. Adams, "Compression Creep Testing of Unidirectional Composite Materials," Composites, Vol. 12, No. 2, April 1981, pp. 117-123.
24. L. Penn, F. Bystry, W. Karp and S. Lee, "Aramid/Epoxy vs. Graphite/Epoxy: Origin of the Difference in Strength at the Interface," Proceedings of the 185th National Meeting

- of the American Chemical Society, Seattle, Washington, March 1983.
25. D. F. Adams, R. L. Ramkumar, and D. E. Walrath, "Analysis of Porous Laminates in the Presence of Ply Drop-Offs and Fastener Holes," Northrop Technical Report NOR 84-10, Naval Air Systems Command Contract N00019-82-C-0063, May 1984.
  26. D. F. Adams and D. R. Doner, "Transverse Normal Loading of a Unidirectional Composite," Journal of Composite Materials, Vol. 1, No. 2, April 1967, pp. 152-164.
  27. D. F. Adams, "Inelastic Analysis of a Unidirectional Composite Subjected to Transverse Normal Loading," Journal of Composite Materials, Vol. 4, No. 3, July 1970, pp. 310-318.
  28. D. F. Adams, "Elastoplastic Crack Propagation in a Transversely Loaded Unidirectional Composite," Journal of Composite Materials, Vol. 8, No. 1, January 1974, pp. 38-54.
  29. B. D. Agarwal and L. J. Broutman, Analysis and Performance of Fiber Composites, John Wiley & Sons, New York, N.Y., 1980.
  30. L. T. Drzal, M. J. Rich, J. D. Camping and W. J. Park, "Interfacial Shear Strength and Failure Mechanisms in Graphite Fiber Composites," Proceedings of the 35th Annual Technical Conference, The Society of the Plastics Industry, 1980, Paper 20-C.
  31. R. F. Cilensek, "WY02D Finite Element Analysis Computer Program User Instructions and Documentation," Composite Materials Research Group, University of Wyoming, Laramie, Wyoming, August 1984.
  32. D. F. Adams, "Inelastic Analysis of a Unidirectional Composite Subjected to Transverse Normal Loading," Report RM-6245-PR, The Rand Corporation, May 1970.
  33. D. F. Adams and S. W. Tsai, "The Influence of Random Filament Packing on the Transverse Stiffness of Unidirectional Composites," Journal of Composite Materials, Vol. 3, No. 3, July 1969, pp. 368-381.
  34. D. F. Adams and D. P. Murphy, "Analysis of Crack Propagation as an Energy Absorption Mechanism in Metal Matrix Composites," Report UWME-DR-101-102-1, Department of Mechanical Engineering, University of Wyoming, February 1981.
  35. R. M. Richard and J. M. Blacklock, "Finite Element Analysis of Inelastic Structures," AIAA Journal, Vol. 7, No. 3, March 1969, pp. 432-438.





APPENDIX A

TABLES OF INDIVIDUAL SPECIMEN TEST RESULTS

Preceding Page Blank

ANY



Table A1

## Individual Hercules 4001 Neat Resin Tensile Test Results

Specimen No.	Tensile Strength (MPa)	Tensile Strength (ksi)	Tensile Modulus (GPa)	Tensile Modulus (Msi)	Ultimate Strain (percent)	Poisson's Ratio
<u>Room Temperature, Dry</u>						
AARZ 01	45	6.5	3.5	0.51	1.3	0.44
2	28*	4.1*	3.7	0.53	-	0.43
3	52	7.6	3.6	0.52	1.5	0.43
4	52	7.6	3.7	0.53	1.5	0.46
5	61	8.9	3.6	0.52	1.9	0.43
Average	53	7.7	3.6	0.52	1.6	0.44
Std. Dev.	7	1.0	0.1	0.01	0.3	0.01
<u>38°C, 7.0%M</u>						
AAEZ 00	35	5.1	2.3	0.34	2.2	0.38
1	-	-	-	-	1.6	0.36
2	30	4.4	2.3	0.34	1.4	0.38
3	30	4.3	2.5	0.36	-	0.39
4	-	-	-	-	-	0.40
5	34	5.0	2.4	0.35	2.0	0.35
6	27	3.9	2.3	0.34	1.3	0.45
7	32	4.6	2.3	0.34	1.6	0.34
8	-	-	-	-	1.8	0.41
9	-	-	-	-	1.4	-
Average	32	4.6	2.4	0.35	1.4	0.38
Std. Dev.	3	0.4	0.1	0.01	0.1	0.03

\*Not included in average

Preceding Page Blank

Table A2

## Individual Hexcel F155 Neat Resin Tensile Test Results

Specimen No.	Tensile Strength (MPa)	Tensile Strength (ksi)	Tensile Modulus (GPa)	Tensile Modulus (Msi)	Ultimate Strain (percent)	Poisson's Ratio
<u>Room Temperature, Dry</u>						
AARX 01	76	11.0	3.0	0.44	3.5	0.42
2	80	11.6	3.1	0.45	3.9	0.40
3	80	11.6	3.1	0.45	3.7	0.40
4	80	11.6	3.1	0.45	3.8	0.44
5	71	10.3	3.0	0.44	3.0	0.40
Average	77	11.2	3.1	0.45	3.6	0.41
Std. Dev.	4	0.6	0.0	0.01	0.4	0.02
<u>38°C, 9.6%M</u>						
AAEX 00	-	-	-	-	2.9	-
1	44	6.4	2.3	0.33	1.4	0.38
2	30	4.3	2.2	0.32	1.4	0.36
3	39	5.6	2.1	0.30	3.0	0.38
4	39	5.7	2.3	0.33	3.5	0.39
5	39	5.7	2.0	0.29	3.5	0.40
6	37	5.3	1.9	0.28	2.7	0.35
7	39	5.7	2.3	0.33	4.1	0.45
8	44	6.4	1.9	0.28	3.8	0.34
9	44	6.4	2.2	0.32	4.0	0.41
Average	41	5.9	2.1	0.30	3.5	0.38
Std. Dev.	1	0.1	0.1	0.02	0.5	0.03

Table A3

## Individual Hercules 4001 Neat Resin Iosipescu Shear Test Results

Specimen No.	Shear Strength		Shear Modulus		Shear Strain
	(MPa)	(ksi)	(GPa)	(Msi)	(percent)
<u>Room Temperature, Dry</u>					
ABRZ 01	28	4.0	1.3	0.19	2.1
2	16	2.3	1.2	0.18	1.3
3	10	1.5	1.2	0.18	0.8
4	12	1.8	1.1	0.16	1.1
5	8*	1.1*	1.2	0.17	0.7
Average	17	2.4	1.2	0.18	1.2
Std. Dev.	8	1.1	0.1	0.01	0.6
<u>100°C, Dry</u>					
ABRZ 10	37	5.3	1.0	0.15	4.4
11	59	8.5	1.1	0.16	5.5
13	36	5.2	1.1	0.16	3.8
14	28	4.1	1.0	0.15	3.0*
Average	40	5.8	1.1	0.16	4.6
Std. Dev.	13	1.9	0.0	0.01	0.8
<u>Room Temperature, 7.0%M</u>					
ABEZ 10	43	6.2	1.4*	0.20*	2.2
11	43	6.2	1.0	0.14	4.9
12	37	5.4	1.0	0.15	3.8
13	23*	3.3*	1.3	0.19	1.8
14	-	-	1.2	0.17	-
Average	41	5.9	1.1	0.16	3.2
Std. Dev.	3	0.5	0.2	0.02	1.4
<u>93°C, 7.0%M</u>					
ABEZ 01	12	1.8	0.8	0.11	1.7
2	10*	1.5*	0.9	0.13	-
3	17	2.5	0.6	0.09	5.7*
4	15	2.2	0.7	0.10	2.3
5	19	2.7	0.8	0.11	2.7
Average	16	2.3	0.7	0.11	2.2
Std. Dev.	3	0.4	0.1	0.01	0.5

\*Not included in average

Table A4

## Individual Hexcel F155 Neat Resin Iosipescu Shear Test Results

Specimen No.	Shear Strength (MPa)	Shear Strength (ksi)	Shear Modulus (GPa)	Shear Modulus (Msi)	Shear Strain (percent)
<u>Room Temperature, Dry</u>					
ABRX 01	48	7.0	1.1	0.16	5.3
02	39	5.7	1.0	0.14	4.7
03	50	7.3	1.1	0.16	5.6
04	56	8.1	1.0	0.15	5.8
05	35*	5.1*	1.0	0.15	3.6*
Average	48	7.0	1.1	0.15	5.4
Std. Dev.	7	1.0	0.1	0.01	0.5
<u>75°C, Dry</u>					
ABRX 10	43	6.3	1.1	0.16	5.8*
11	43	6.2	1.0	0.15	8.8
12	41	6.0	0.8	0.12	8.8
14	43	6.2	1.0	0.14	11.6*
Average	43	6.2	1.0	0.14	8.8
Std. Dev.	1	0.1	0.1	0.02	-
<u>Room Temperature, 9.6%M</u>					
ABEX 10	48	7.0	1.0	0.14	5.8
11	43	6.2	1.0	0.14	5.8
12	46	6.6	1.0	0.15	5.8
13	48	6.9	1.1	0.16	5.8
14	-	-	-	-	-
Average	46	6.7	1.0	0.15	5.8
Std. Dev.	3	0.4	0.1	0.01	-
<u>38°C, 9.6%M</u>					
ABEX 00	35	5.0	1.0	0.16	5.3
01	34	4.9	1.0	0.14	5.7
02	33	4.8	0.9	0.13	5.7
03	33	4.8	0.8	0.12	5.7
04	34	4.9	0.9	0.13	5.7
Average	34	4.9	0.9	0.14	5.6
Std. Dev.	1	0.1	0.1	0.02	0.2

\*Not included in average

Table A5

Individual Fiber Volumes  
for the Various AS4 Graphite/Hercules 3501-6 Epoxy Composite Panels

Fiber Sizing	Unidirectional Panels (percent)		Quasi-Isotropic Panels (percent)	
Unsize		47.4		53.9
		47.0		54.3
		<u>47.6</u>		<u>55.2</u>
	Average	47.3	Average	54.5
	Std. Dev.	0.3	Std. Dev.	0.7
EPON 828		58.9		59.5
		58.6		58.9
		<u>59.2</u>		<u>57.9</u>
	Average	58.9	Average	58.8
	Std. Dev.	0.3	Std. Dev.	0.8
PVA		56.4		64.5
		56.6		64.9
		<u>57.1</u>		<u>62.8</u>
	Average	56.7	Average	64.1
	Std. Dev.	0.4	Std. Dev.	1.1
Polysulfone		52.4		52.4
		52.1		51.7
		<u>52.8</u>		<u>51.9</u>
	Average	52.4	Average	52.0
	Std. Dev.	0.4	Std. Dev.	0.4

Table A6

Individual Fiber Volumes for the Various  
AS4 Graphite/Hercules 4001 Bismaleimide Composite Panels

Fiber Sizing	Unidirectional Panels (percent)		Quasi-Isotropic Panels (percent)	
Unsize		51.2		53.0
		52.1		55.4
		<u>54.1</u>		<u>55.1</u>
	Average	52.5	Average	54.5
	Std. Dev.	1.5	Std. Dev.	1.3
EPON 828		57.1		49.6
		55.9		55.6
		<u>57.2</u>		<u>51.4</u>
	Average	56.7	Average	52.2
	Std. Dev.	0.7	Std. Dev.	3.1
PVA		57.1		51.4
		55.7		50.7
		<u>55.8</u>		<u>58.5</u>
	Average	56.2	Average	53.5
	Std. Dev.	0.8	Std. Dev.	4.3
Polysulfone		65.4		52.3
		61.2		60.0
		<u>61.7</u>		<u>59.4</u>
	Average	62.8	Average	57.2
	Std. Dev.	2.3	Std. Dev.	4.3



Table A7

Individual Fiber Volumes for the Various  
AS4 Graphite/Hexcel F155 Epoxy Composite Panels

Fiber Sizing	Unidirectional Panels (percent)		Quasi-Isotropic Panels (percent)	
Unsize		38.7		26.3
		35.6		28.8
		<u>38.8</u>		<u>30.1</u>
	Average	37.7	Average	28.4
	Std. Dev.	1.8	Std. Dev.	1.9
EPON 828		39.4		44.4
		39.8		41.5
		<u>40.7</u>		<u>45.4</u>
	Average	40.0	Average	43.8
	Std. Dev.	0.7	Std. Dev.	2.0
PVA		40.0		48.2
		39.6		47.1
		<u>39.6</u>		<u>47.0</u>
	Average	39.7	Average	47.4
	Std. Dev.	0.2	Std. Dev.	0.7
Polysulfone		41.6		42.8
		42.5		44.4
		<u>47.8</u>		<u>39.4</u>
	Average	44.0	Average	42.2
	Std. Dev.	3.4	Std. Dev.	2.6

Table A8

Individual AS4/3501-6 Unidirectional Composite  
 Transverse Tensile Test Results at the Room Temperature, Dry Condition

Fiber Sizing	Specimen No.	Tensile Strength (MPa)	Tensile Strength (ksi)	Tensile Modulus (GPa)	Tensile Modulus (Msi)	Ultimate Strain (percent)	
Unsize	AFRY 00	10*	1.5*	8.8	1.28	0.11*	
	1	21	3.0	9.7*	1.40*	0.21	
	2	28	4.0	7.1	1.03	0.39	
	3	17	2.5	7.2	1.04	0.24	
	4	19	2.7	7.0	1.01	0.27	
	5	31*	4.5*	7.6	1.10	0.42*	
	6	27	3.9	8.0	1.16	0.33	
	Average		22	3.2	7.6	1.10	0.29
	Std. Dev.		5	0.7	0.7	0.10	0.07
EPON 828	AFRY 10	-	-	8.0	1.16	-	
	11	20	2.9	7.2	1.04	0.28	
	12	13*	1.9*	7.7	1.11	0.16*	
	13	26	3.7	7.7	1.11	0.33	
	14	20	2.9	-	-	0.25	
	15	19	2.8	7.8	1.13	0.25	
	16	26*	3.8*	7.5	1.09	0.34*	
	Average		21	3.1	7.7	1.11	0.28
	Std. Dev.		3	0.4	0.3	0.04	0.04
PVA	AFRY 20	19*	2.8*	8.0	1.16	0.22*	
	21	23	3.4	8.0	1.16	0.30	

Table A8

- Continued -

Fiber Sizing	Specimen No.	Tensile Strength (MPa)	Tensile Strength (ksi)	Tensile Modulus (GPa)	Tensile Modulus (Msi)	Ultimate Strain (percent)
PVA	AFRY 22	32	4.6	8.3	1.20	0.35
	23	24	3.5	7.0*	1.01*	0.32
	24	32	4.6	7.1*	1.03*	0.41*
	25	21*	3.0*	8.1	1.18	0.25*
	26	32	4.7	8.4	1.22	0.38
	27	34*	5.0*	8.3	1.21	0.42*
	Average	29	4.2	8.2	1.19	0.34
Std. Dev.	5	0.7	0.2	0.03	0.04	
Polysulfone	AFRY 30	25	3.6	7.2	1.04	0.32
	31	28	4.1.	7.4	1.07	0.39
	32	23	3.4	7.2	1.04	0.32
	33	21	3.1	7.7	1.12	0.28
	34	21	3.1	7.7	1.11	0.28
	35	22	3.2	8.0	1.16	0.27
	36	26	3.8	8.2	1.19	0.32
	37	19	2.8	7.2	1.05	0.27
	Average	24	3.5	7.6	1.10	0.29
	Std. Dev.	3	0.4	0.4	0.06	0.02

\*Not included in average

Table A9

Individual AS4/3501-6 Unidirectional Composite Transverse Tensile  
Test Results at the Elevated Temperature, Wet Condition  
(93°C, 1%M)

Fiber Sizing	Specimen No.	Tensile Strength (MPa)	Tensile Strength (ksi)	Tensile Modulus (GPa)	Tensile Modulus (Msi)	Ultimate Strain (percent)
Unsize	AFEY 00	13	1.9	5.2	0.75	0.28*
	01	21*	3.0*	5.9	0.85	0.41
	02	18	2.6	4.6	0.66	0.41
	03	17	2.5	4.8	0.69	0.43*
	04	15	2.2	5.2	0.75	0.35
	05	14	2.1	5.6	0.81	0.30
	06	14	2.0	5.9	0.85	0.25
	07	14	2.1	5.0	0.73	0.33
	Average	15	2.2	5.2	0.76	0.34
	Std. Dev.	2	0.3	0.5	0.07	0.06
EPON 828	AFEY 10	12	1.8	5.7	0.82	0.22
	11	12	1.7	5.9	0.86	0.20
	12	12	1.8	6.1	0.89	0.23
	13	10	1.5	6.1	0.88	0.10*
	14	14*	2.0*	6.8	0.99	0.20
	15	12	1.8	5.9	0.85	0.21
	16	9*	1.3	6.4	0.93	0.14*
	17	10*	1.4*	5.2	0.75	-
	Average	12	1.7	6.0	0.87	0.21
Std. Dev.	1	0.1	0.5	0.07	0.01	

Table A9

- Continued -

Fiber Sizing	Specimen No.	Tensile Strength (MPa)	Tensile Strength (ksi)	Tensile Modulus (GPa)	Tensile Modulus (Msi)	Ultimate Strain (percent)	
PVA	AFEY 20	12	1.7	3.4	0.50	0.29*	
	21	10	1.4	5.5*	0.80*	0.18	
	22	10	1.5	3.4	0.49	0.22	
	23	7*	1.0*	5.2*	0.76*	0.13*	
	24	11	1.6	2.3*	0.33*	0.27	
	25	11	1.6	3.6	0.52	0.23	
	26	10	1.5	5.0	0.73	0.21	
	27	11	1.6	3.1	0.45	0.25	
	28	10	1.5	2.8	0.41	0.21	
	29	13*	1.9*	5.4*	0.79*	0.29*	
		Average	11	1.6	3.6	0.52	0.22
	Std. Dev.	1	0.1	0.8	0.11	0.03	
Polysulfone	AFEY 30	11*	1.6*	5.5	0.80	0.23*	
	31	12*	1.7*	3.9*	0.56*	0.22*	
	32	17	2.4	5.4	0.78	0.33	
	33	16	2.3	5.7	0.82	0.30	
	34	17	2.4	5.8	0.84	0.31	
	35	14	2.1	4.9	0.71	0.27	
	36	17	2.4	5.9	0.85	0.32	
	37	17	2.4	6.2*	0.90*	0.31	
		Average	16	2.3	5.5	0.80	0.31
		Std. Dev.	1	0.1	0.3	0.05	0.02

\*Not included in average

Table A10

Individual AS4/4001 Unidirectional Composite Transverse Tensile Test  
Results at the Room Temperature, Dry Condition

Fiber Sizing	Specimen No.	Tensile Strength (MPa)	Tensile Strength (ksi)	Tensile Modulus (GPa)	Tensile Modulus (Msi)	Ultimate Strain (percent)
Unsize	AFRZ 00	59*	8.5*	10.1	1.47	0.51
	01	48	7.0	9.2	1.33	0.52
	02	55	8.0	9.0	1.30	0.62
	03	48	6.9	8.8	1.28	0.54
	04	39*	5.7*	11.2	1.62	0.35*
	05	50	7.3	9.0	1.31	1.02*
	06	54	7.9	8.9	1.29	0.62
	07	50	7.2	9.2	1.33	0.55
	Average	51	7.4	9.4	1.37	0.56
	Std. Dev.	3	0.5	0.8	0.11	0.05
EPON 828	AFRZ 10	62*	9.0*	10.1	1.46	0.62
	11	57	8.2	8.6	1.25	0.66
	12	58	8.4	9.4	1.37	0.62
	13	50	7.2	9.4	1.36	0.53*
	14	61	8.8	8.7	1.26	0.71*
	15	48	6.9	8.5	1.23	0.56
	16	58	8.4	8.9	1.29	0.66
	17	42*	6.1*	7.3	1.06	0.51*
	18	60	8.7	8.3	1.20	0.74*
		19	50	7.2	9.2	1.34
	Average	55	8.0	8.8	1.28	0.61
	Std. Dev.	6	0.8	0.8	0.11	0.05

Table A10

- Continued -

Fiber Sizing	Specimen No.	Tensile Strength (MPa)	Tensile Strength (ksi)	Tensile Modulus (GPa)	Tensile Modulus (Msi)	Ultimate Strain (percent)
PVA	AFRZ 20	41	6.0	8.2	1.19	0.51
	21	34	5.0	8.3	1.20	0.42
	22	34	4.9	7.9	1.14	0.44
	23	39	5.6	8.1	1.18	0.48
	24	34	5.0	8.1	1.17	0.44
	25	40	5.8	8.3	1.21	0.48
	26	33	4.8	7.9	1.15	0.38*
	27	42	6.1	7.9	1.14	0.54*
	Average	37	5.4	8.1	1.17	0.46
	Std. Dev.	3	0.5	0.2	0.03	0.03
Polysulfone	AFRZ 30	53	7.7	9.3	1.35	0.58
	31	62*	9.0*	9.3	1.35	0.67*
	32	45	6.5	8.4	1.22	0.54
	33	40*	5.8*	9.2	1.34	0.43*
	34	48	7.0	9.0	1.30	0.43*
	35	46	6.6	8.6	1.25	0.49
	36	49	7.1	9.1	1.32	0.55
	37	57	8.3	9.8	1.42	0.59
	Average	50	7.2	9.1	1.32	0.55
	Std. Dev.	1	0.7	0.4	0.06	0.04

\*Not included in average

Table All

Individual AS4/4001 Unidirectional Composite Transverse Tensile  
 Test Results at the Elevated Temperature, Wet Condition  
 (93°C, 1%M)

Fiber Sizing	Specimen No.	Tensile Strength (MPa)	Tensile Strength (ksi)	Tensile Modulus (GPa)	Tensile Modulus (Msi)	Ultimate Strain (percent)
Unsize	AFEZ 00	26	3.7	6.8	0.99	0.42
	01	25	3.6	6.5	0.94	0.41
	02	17	2.5	6.1	0.89	0.34
	03	26	3.8	7.0	1.02	0.43
	04	28*	4.1*	7.3	1.06	0.46*
	05	18	2.6	5.4*	0.78*	0.36
	06	18	2.6	5.7*	0.82*	0.36
	07	18	2.6	7.3	1.06	0.30*
Average		21	3.1	6.8	0.99	0.39
	Std. Dev.	4	0.6	0.5	0.07	0.04
EPON 828	AFEZ 10	28	4.0	7.1	1.03	0.45
	11	27	3.9	7.1	1.03	0.43
	12	28	4.0	4.9*	0.71*	0.43
	13	28	4.0	6.9	1.00	0.42
	14	26	3.7	4.3*	0.63*	0.40
	15	29	4.2	6.8	0.98	0.47
	16	26	3.7	8.2*	1.19*	0.33
	Average	27	3.9	7.0	1.01	0.42
Std. Dev.	1	0.2	0.1	0.02	0.04	



Table All

- Continued -

Fiber Sizing	Specimen No.	Tensile Strength (MPa)	Tensile Strength (ksi)	Tensile Modulus (GPa)	Tensile Modulus (Msi)	Ultimate Strain (percent)
PVA	AFEZ 20	17	2.5	9.1	1.32	0.21
	21	23	3.3	8.3	1.20	0.32
	22	15*	2.2*	10.2*	1.48*	0.15*
	23	19	2.7	7.7	1.12	0.26
	24	26*	3.7*	8.4	1.22	0.33*
	25	21	3.0	8.6	1.25	0.25
	26	19	2.8	7.8	1.13	0.25
	27	22	3.2	7.5*	1.09*	0.32
	Average	20	2.9	8.3	1.21	0.27
	Std. Dev.	2	0.3	0.6	0.08	0.04
Polysulfone	AFEZ 30	17	2.5	9.1	1.32	0.21
	31	23	3.3	8.3	1.20	0.32
	32	15*	2.2*	10.2*	1.48*	0.15*
	33	19	2.7	7.7	1.12	0.26
	34	26*	3.7*	8.4	1.22	0.33*
	35	21	3.0	8.6	1.25	0.25
	36	19	2.8	7.8	1.13	0.25
	37	22	3.2	7.5*	1.09*	0.32
	Average	20	2.9	8.3	1.21	0.27
	Std. Dev.	2	0.3	0.6	0.08	0.04

\*Not included in average

Table A12

Individual AS4/F155 Unidirectional Composite Transverse Tensile  
Test Results at the Room Temperature, Dry Condition

Fiber Sizing	Specimen No.	Tensile Strength (MPa)	Tensile Strength (ksi)	Tensile Modulus (GPa)	Tensile Modulus (Msi)	Ultimate Strain (percent)
Unsize	AFRX 00	40*	5.8*	6.3	0.91	0.51*
	01	59	8.6	13.4*	1.94*	0.46*
	02	61	8.9	7.7	1.11	0.80
	03	60	8.7	6.9	1.00	0.90
	04	56	8.1	6.9	1.00	0.86
	05	50	7.3	7.2	1.05	0.69
	06	-	-	-	-	-
	07	68*	9.8*	7.1	1.03	0.96
	Average	57	8.3	7.0	1.02	0.84
	Std. Dev.	4	0.6	0.5	0.07	0.10
EPON 828	AFRX 10	49	7.1	7.9	1.15	0.61
	11	50	7.3	8.1	1.17	0.62
	12	49	7.1	7.9	1.15	0.62
	13	49	7.1	7.9	1.15	0.61
	14	44	6.4	8.1	1.17	0.57
	15	56	8.2	7.3	1.06	0.78*
	16	54	7.9	8.3	1.20	0.67
	Average	50	7.3	7.9	1.15	0.62
	Std. Dev.	4	0.6	0.3	0.04	0.03

Table A12

- Continued -

Fiber Sizing	Specimen No.	Tensile Strength (MPa)	Tensile Strength (ksi)	Tensile Modulus (GPa)	Tensile Modulus (Msi)	Ultimate Strain (percent)
PVA	AFRX 20	37	5.4	6.9	1.00	0.54
	21	40	5.8	7.3	1.06	0.54
	22	39	5.7	7.7	1.12	0.50
	23	30*	4.3*	8.0	1.16	0.36*
	24	39	5.7	7.7	1.11	0.52
	25	41	6.0	7.0	1.01	0.59*
	26	33	4.8	6.8	0.99	0.49
	27	39	5.7	8.3	1.20	0.47
	Average	39	5.6	7.4	1.08	0.51
	Std. Dev.	3	0.4	0.6	0.08	0.03
Polysulfone	AFRX 30	67	9.7	7.7	1.12	0.93
	31	77*	11.2*	7.7	1.11	0.28*
	32	57*	8.3*	7.8	1.13	0.75
	33	52*	7.5*	8.0	1.16	0.66*
	34	68	9.9	7.4	1.07	0.98
	35	72	10.5	7.7	1.11	1.02
	36	61	8.9	7.9	1.15	0.82
	37	72	10.5	7.9	1.14	1.02
	Average	68	9.9	7.7	1.12	0.92
	Std. Dev.	5	0.7	0.2	0.03	0.11

\*Not included in average

Table A13

Individual AS4/F155 Unidirectional Composite Transverse Tensile  
Test Results at the Elevated Temperature, Wet Condition  
(38°C, 1%M)

Fiber Sizing	Specimen No.	Tensile Strength (MPa)	Tensile Strength (ksi)	Tensile Modulus (GPa)	Tensile Modulus (Msi)	Ultimate Strain (percent)	
Unsize	AFEX 01	23	3.4	3.8	0.55	0.91*	
	02	23	3.4	4.2	0.61	0.70	
	03	24	3.5	4.7*	0.68*	0.70	
	04	27	3.9	3.8	0.55	0.90	
	05	27	3.9	3.5	0.51	0.88	
	06	21	3.0	3.7	0.53	0.62*	
	07	25	3.6	3.7	0.54	0.74	
Average		24	3.5	3.8	0.55	0.78	
	Std. Dev.	2	0.3	0.2	0.03	0.10	
EPON 828	AFEX 10	32	4.6	6.0*	0.87*	0.84	
	11	21*	3.1*	5.4	0.78	0.49*	
	12	30	4.3	4.6*	0.66*	0.81	
	13	29	4.2	5.3	0.77	0.71	
	14	30	4.3	5.8	0.84	0.74	
	15	25	3.6	4.8	0.69	0.57*	
	16	28	4.1	4.5*	0.65*	0.76	
	17	31	4.5	5.7	0.82	0.93*	
	Average		29	4.2	5.4	0.78	0.77
		Std. Dev.	2	0.3	0.4	0.06	0.05

Table A13

- Continued -

Fiber Sizing	Specimen No.	Tensile Strength (MPa)	Tensile Strength (ksi)	Tensile Modulus (GPa)	Tensile Modulus (Msi)	Ultimate Strain (percent)
PVA	AFEX 20	13	1.9	3.6	0.52	0.38
	21	10*	1.5*	3.8	0.55	0.27*
	22	14	2.0	3.6	0.52	0.40
	23	13	1.9	5.4*	0.78*	0.30*
	24	15*	2.2*	3.4	0.49	0.46*
	25	12	1.8	3.4	0.50	0.36
	26	11	1.6	3.4	0.50	0.33
	27	12	1.8	3.3	0.48	0.43
	Average	12	1.8	3.5	0.51	0.38
	Std. Dev.	1	0.1	0.2	0.02	0.04
Polysulfone	AFEX 30	32	4.6	6.1*	0.88*	0.48*
	31	32	4.6	5.4	0.79	0.66
	32	35	5.1	5.2	0.76	0.81*
	33	31	4.5	5.2	0.76	0.70
	34	31	4.5	4.8	0.69	0.69
	35	34	4.9	4.5*	0.65*	0.80*
	36	32	4.6	5.8*	0.84*	0.63
	37	34	4.9	5.0	0.72	0.75
	Average	33	4.7	5.1	0.74	0.69
	Std. Dev.	2	0.2	0.3	0.04	0.05

\*Not included in average

Table A14

Individual AS4/3501-6 Unidirectional Axial Compression Test Results  
at the Room Temperature, Dry Condition

Fiber Sizing	Specimen No.	Compressive Strength		Compressive Modulus		Ultimate Strain (percent)
		(MPa)	(ksi)	(GPa)	(Msi)	
Unsize	AGRY 00	774	112	96	13.9	-
	01	869*	126*	105	15.2	-
	02	627*	91*	144*	20.9*	1.15
	03	669	97	97	14.1	0.69*
	04	703	102	99	14.3	1.12
	05	621	90	97	14.1	1.31
	06	745	108	104	15.1	1.75
	07	621*	90*	110	16.0	-
	08	724	105	86*	12.5*	2.59
	09	800	116	90	13.1	3.54*
	Average	717	104	100	14.5	1.58
	Std. Dev.	62	9	6	0.9	0.62
EPON 828	AGRY 10	634*	92*	99	14.3	0.68
	11	827*	120*	117	16.9	0.74
	12	827*	120*	-	-	-
	13	731	106	104	15.1	-
	14	669	97	121	17.6	-
	15	738	107	141	20.4	0.67
	16	641*	93*	105	15.3	0.46
	17	696	101	174*	25.3	0.34*
	18	814	118	123	17.8	0.52
	19	821*	119*	106	15.4	1.02*
	Average	731	106	114	16.6	0.62
	Std. Dev.	55	8	14	2.0	0.12
PVA	AGRY 20	752	109	121	17.5	0.74
	21	883	128	111	16.1	1.08*
	22	703	102	141	20.5	0.51
	23	821	119	126	18.3	0.64
	24	876	127	119	17.2	0.92
	25	752	109	113	16.4	0.58
		Average	800	116	122	17.7
	Std. Dev.	71	11	11	1.6	0.10

Table A14

- Continued -

Fiber Sizing	Specimen No.	Compressive Strength		Compressive Modulus		Ultimate Strain (percent)
		(MPa)	(ksi)	(GPa)	(Msi)	
Polysulfone	AGRY 30	855	124	97*	14.0*	0.98
	31	883	128	99*	14.4*	0.93
	32	938	136	152*	22.0*	0.59*
	33	738	107	111	16.1	1.08
	34	765	111	-	-	-
	35	834	121	120	17.4	0.67*
	36	883	128	120	17.4	0.90
	37	958	139	105	15.2	0.91
	38	786	114	125	18.2	1.01
	39	752	109	117	17.0	1.10*
		Average	841	122	117	16.9
	Std. Dev.	76	11	8	1.1	0.07

---

\*Not included in average

Table A15

Individual AS4/3501-6 Unidirectional Composite Axial Compression  
Test Results at the Elevated Temperature, Wet Condition  
(93°C, 1%M)

Fiber Sizing	Specimen No.	Compressive Strength		Compressive Modulus		Ultimate Strain (percent)
		(MPa)	(ksi)	(GPa)	(Msi)	
Unsize	AGEY 00	504	73.1	88	12.7	0.53
	01	354*	51.3*	85	12.4	0.43
	02	529	76.7	99*	14.3*	0.66
	03	392	56.9	68	9.8	0.44
	04	365	53.0	105*	15.3*	0.36*
	05	305*	44.3*	68	9.9	0.31*
	06	535	77.6	47*	6.8*	0.59
	07	474	68.7	82	11.9	0.57
	08	483	70.1	78	11.3	0.59
	09	589*	85.4*	85	12.3	0.77*
	Average	469	68.0	79	11.5	0.55
	Std. Dev.	66	9.5	8	1.2	0.08
EPON 828	AGEY 10	541	78.5	83	12.1	0.57
	11	532	77.1	95	13.8	0.67
	12	512	74.3	58*	8.4*	0.92*
	13	474	68.8	82	11.9	0.90*
	14	547	79.3	97	14.0	0.50
	15	467	67.7	74	10.7	0.42
	16	650	94.2	117*	16.9*	0.43
	17	530	76.9	-	-	0.32*
	18	538	78.0	103	14.9	0.56
	19	566	82.1	77	11.2	0.64
	Average	536	77.7	87	12.7	0.54
	Std. Dev.	51	7.4	11	1.6	0.10
PVA	AGEY 20	517	75.0	91	13.2	0.58
	21	510	73.9	61*	8.9*	0.47
	22	479	69.5	113*	16.4*	0.45
	23	549	79.6	83	12.1	0.65
	24	456	66.2	-	-	1.31*
	25	543	78.8	105	15.2	0.69
	26	531	77.0	93	13.5	0.53
		Average	512	74.3	93	13.5
	Std. Dev.	34	4.9	9	1.3	0.10



Table A15

- Continued -

Fiber Sizing	Specimen No.	Compressive Strength		Compressive Modulus		Ultimate Strain (percent)	
		(MPa)	(ksi)	(GPa)	(Msi)		
Polysulfone	AGEY 30	589	85.4	99	14.4	0.67	
	31	396*	57.4*	54*	7.9*	0.66	
	32	534	77.4	77	11.1	0.81	
	33	525	76.2	110*	16.0*	0.46	
	34	580	84.1	80	11.6	0.71	
	35	534	77.4	60*	8.7*	1.36*	
	36	-	-	-	-	-	
	37	558	80.9	108	15.7	0.51	
	38	650*	94.2*	103	15.0	1.67*	
	39	<u>536</u>	<u>77.7</u>	<u>99</u>	<u>14.4</u>	<u>0.57</u>	
	Average		551	79.9	95	13.7	0.63
	Std. Dev.		25	3.6	13	1.9	0.12

---

\*Not included in average

Table A16

Individual AS4/4001 Unidirectional Axial Compression Test Results  
at the Room Temperature, Dry Condition

Fiber Sizing	Specimen No.	Compressive Strength		Compressive Modulus		Ultimate Strain (percent)
		(MPa)	(ksi)	(GPa)	(Msi)	
Unsize	AGRZ 00	883	128	134*	19.4*	1.66*
	01	876	127	138*	20.0*	1.15
	02	1007	146	108	15.6	1.00
	03	800	116	111	16.1	0.71*
	04	993	144	97	14.1	1.09
	05	841	122	105	15.2	0.80
	06	910	132	100	14.5	1.33
	07	993	144	105	15.2	0.97
	08	945	137	103	15.0	0.68*
	09	986	143	108	15.7	1.02
	Average		924	134	105	15.2
Std. Dev.		76	11	4	0.6	0.16
EPON 828	AGRZ 10	1083*	157*	157*	22.7*	0.86
	11	917	133	122	17.7	0.87
	12	883	128	122	17.7	0.71*
	13	821	119	127	18.4	0.70*
	14	862	125	98*	14.2*	0.92*
	Average	869	126	123	17.9	0.87
	Std. Dev.	41	6	3	0.4	0.06
PVA	AGRZ 20	655*	95*	98	14.2	0.79
	21	869	126	105	15.3	0.90
	22	862	125	134	19.5*	0.66*
	23	876	127	112	16.3	0.82
	24	752	109	-	-	-
	25	931*	135*	147*	21.3*	0.91
	26	814	118	116	16.8	0.75
	27	807	117	72*	10.4*	-
	28	938*	136*	97	14.0	0.99*
	29	821	119	119	17.3	0.83
	Average	827	120	108	15.6	0.84
Std. Dev.	41	6	10	1.4	0.06	

Table A16

- Continued -

Fiber Sizing	Specimen No.	Compressive Strength		Compressive Modulus		Ultimate Strain (percent)
		(MPa)	(ksi)	(GPa)	(Msi)	
Polysulfone	AGRZ 30	1020*	148*	129	18.7	-
	31	1000*	145*	136	19.7	-
	32	800	116	120	17.4	0.73*
	33	676*	98*	74*	10.8*	-
	34	690*	100*	157*	22.7*	0.59
	35	924	134	-	-	-
	36	965	140	130	18.8	-
	37	834	121	159*	23.0*	0.43*
	38	924	134	71*	10.3*	-
	39	876	127	125	18.2	0.63
		Average	889	129	128	18.6
	Std. Dev.	62	9	6	0.8	0.13

\*Not included in average

Table A17

Individual AS4/4001 Unidirectional Axial Compression Test Results  
At the Elevated Temperature, Wet Condition  
(93°C, 1%M)

Fiber Sizing	Specimen No.	Compressive Strength		Compressive Modulus		Ultimate Strain (percent)
		(MPa)	(ksi)	(GPa)	(Msi)	
Unsize	AGEZ 00	496	72	81	11.8	0.76
	01	572	83	96	13.9	0.61
	02	531	77	92	13.4	0.56
	03	621	90	94	13.6	0.72
	04	579	84	61*	8.8*	0.86
	05	614	89	99	14.3	0.87
	06	579	84	74	10.7	1.04
	07	552	80	87	12.6	0.75
	08	648	94	112*	16.3*	1.73*
	09	579	84	68*	9.9*	1.21
	AL	614	89	104	15.1	0.61
		Average	579	84	91	13.2
	Std. Dev.	41	6	10	1.4	0.20
EPON 828	AGEZ 10	607	88	82*	11.9*	1.81*
	11	365*	53*	157	22.8	0.25*
	12	703	102	87	12.6	0.90
	13	600	87	106	15.4	0.60
	14	710	103	141	20.5	0.77
	15	662	96	110	16.0	0.77
	16	648	94	112	16.3	0.61
	17	717	104	127	18.4	0.89
	18	703	102	136	19.7	0.56
		Average	669	97	122	17.7
	Std. Dev.	48	7	14	2.1	0.14
PVA	AGEZ 20	490*	71*	105	15.2	0.47
	21	614	89	92*	13.3*	0.92*
	22	593	86	109	15.8	0.56
	23	552	80	110	15.9	0.29*
	24	690*	100*	128*	18.6*	0.59
	25	614	89	119*	17.3*	0.56
	26	510*	74*	96*	13.9*	0.57
	27	579	84	107	15.5	0.46
	28	614	89	93*	13.5*	0.85*

Table A17

- Continued -

Fiber Sizing	Specimen No.	Compressive Strength		Compressive Modulus		Ultimate Strain (percent)
		(MPa)	(ksi)	(GPa)	(Msi)	
PVA	AGEZ 29	710*	103*	142	20.6*	0.58
	AL	614	89	104	15.1	0.61
	Average	600	87	107	15.5	0.55
	Std. Dev.	24	4	7	0.4	0.06
Polysulfone	AGEZ 30	634	92	-	-	0.30*
	31	579	84	129	18.7	0.51
	32	593	86	118	17.1	0.33*
	33	614	89	75*	10.9*	0.56
	34	800*	116*	123	17.8	0.68*
	35	786*	114*	141*	20.5*	0.42
	36	752*	109*	119	17.2	0.78*
	37	579	84	128	18.5	0.46
	38	690	100	91*	13.2*	0.49
	39	607	88	123	17.8	0.50
	Average	621	90	123	17.9	0.49
Std. Dev.	34	5	4	0.6	0.04	

\*Not included in average

Table A18

Individual AS4/F155 Unidirectional Composite Axial Compression  
Test Results at the Room Temperature, Dry Condition

Fiber Sizing	Specimen No.	Compressive Strength		Compressive Modulus		Ultimate Strain (percent)
		(MPa)	(ksi)	(GPa)	(Msi)	
Unsize	AGR 00	538	78	72	10.4	0.74*
	01	614*	89*	70	10.1	0.89
	02	627*	91*	72	10.5	1.52*
	03	503	73	54	7.9	1.06
	04	441*	64*	46*	6.7*	1.05
	05	607	88	68	9.8	0.96
	06	579	84	70	10.1	-
	07	469	68	65	9.4	1.01
	08	586	85	74	10.7	-
	09	421*	61*	52*	7.5*	0.83
	Average	545	79	68	9.9	0.97
	Std. Dev.	55	8	6	0.9	0.09
EPON 828	AGR 10	752*	109*	83	12.1	1.06
	11	676	98	94	13.7	0.87
	12	690	100	94	13.6	0.93
	13	683	99	80	11.6	0.93
	14	662	96	81	11.8	0.92
	15	683	99	74*	10.8*	0.98
	16	621	90	74*	10.7*	0.95
	17	572*	83*	80	11.3	0.77
	18	572*	83*	89	12.9	0.82
	19	703	102	108*	15.6*	0.85
	Average	676	98	85	12.4	0.91
	Std. Dev.	28	4	7	1.0	0.08
PVA	AGR 20	462	67	107*	15.5*	0.50*
	21	552	80	75	10.8	0.80
	22	572	83	76	11.0	0.78
	23	524	76	77	11.2	0.71
	24	565	82	97*	14.0*	0.72
	25	593	86	72	10.5	0.86*
	26	621	90	91	13.2	0.80
	27	524	76	70	10.1	0.75
	28	496	72	66*	9.6*	0.79
	29	586	85	93	13.5	0.66
	Average	552	80	79	11.5	0.75
	Std. Dev.	48	7	9	1.3	0.05

Table A18

- Continued -

Fiber Sizing	Specimen No.	Compressive Strength		Compressive Modulus		Ultimate Strain (percent)	
		(MPa)	(ksi)	(GPa)	(Msi)		
Polysulfone	AGRX 30	600	87	81*	11.7*	0.79	
	31	634	92	84	12.2	0.75	
	32	641	93	93	13.5	0.72	
	33	600	87	84	12.7	0.73	
	34	621	90	85	12.4	0.78	
	35	552	80	109*	15.8*	0.63	
	36	565	82	92	13.4	0.65	
	37	627	91	101	14.6	0.61	
	38	648	94	97	14.0	0.69	
	39	600	87	117*	16.9*	0.59	
	Average		607	88	91	13.2	0.69
	Std. Dev.		34	5	7	1.0	0.07

---

\*Not included in average

Table A19

Individual AS4/F155 Unidirectional Composite Axial Compression  
Test Results at the Elevated Temperature, Wet Condition  
(38°C, 1%M)

Fiber Sizing	Specimen No.	Compressive Strength		Compressive Modulus		Ultimate Strain
		(MPa)	(ksi)	(GPa)	(Msi)	(percent)
Unsize	AGEX 00	365	53	66*	9.5*	0.55
	01	359*	52*	57	8.2	0.60
	02	324*	47*	52	7.5	0.71
	03	386	56	43*	6.2*	0.96*
	04	448*	65*	61	8.8	0.71
	05	462*	67*	54	7.8	0.81
	06	441	64	66*	9.6*	0.67
	07	434	63	50	7.3	0.77
	08	414	60	46	6.6	0.76
	09	393	57	39*	5.7*	0.41*
		Average	406	59	53	7.7
	Std. Dev.	30	4	5	0.8	0.09
EPON 828	AGEX 10	517	75	72	10.5	0.67
	11	448	65	69	10.0	0.64*
	12	483	70	67	9.7	0.72*
	13	490	71	67	9.7	0.71
	14	496	72	64	9.3	0.71
	15	531*	77*	75	10.9	0.70
	16	517	75	71	10.3	0.69
	17	462	67	83*	12.0*	0.70
	18	400*	58*	64	9.3	0.62*
	19	483	70	52*	7.5*	0.66
	Average	486	71	69	10.0	0.69
	Std. Dev.	24	4	4	0.6	0.02
PVA	AGEX 20	359	52	77	11.1	0.72
	21	303*	44*	79	11.4	0.58
	22	338	49	74	10.7	0.67
	23	386	56	86*	12.5*	0.85*
	24	310*	45*	60*	8.7*	0.72
	25	345	50	81	11.8	0.14*
	26	345	50	56*	8.1*	0.19
	27	421*	61*	85*	12.4*	0.11*
	28	359	52	66	9.5	0.13*



Table A19

- Continued -

Fiber Sizing	Specimen No.	Compressive Strength		Compressive Modulus		Ultimate Strain (percent)
		(MPa)	(ksi)	(GPa)	(Msi)	
PVA	AGEX 29	<u>352</u>	<u>51</u>	<u>69</u>	<u>10.0</u>	<u>0.66</u>
	Average	354	51	74	10.8	0.59
	Std. Dev.	16	2	6	0.9	0.20
Polysulfone	AGEX 30	552*	80*	94	13.6	0.57
	31	476	69	71	10.3	0.66
	32	359*	52*	92	13.4	0.40*
	33	531	77	89	12.9	0.88*
	34	462	67	86	12.5	0.56
	35	455	66	90	13.0	0.56
	36	503	73	90	13.0	0.55
	37	483	70	92	13.3	0.52
	38	455	66	77	11.2	0.61
	39	<u>545*</u>	<u>79*</u>	<u>83</u>	<u>12.1</u>	<u>0.69</u>
	Average	482	70	86	12.5	0.59
Std. Dev.	29	4	7	1.1	0.06	

\*Not included in average

Table A20

Individual AS4/3501-6 Quasi-Isotropic Laminate Axial Tensile  
Test Results at the Room Temperature, Dry Condition

Fiber Sizing	Specimen No.	Tensile Strength		Tensile Modulus		Ultimate Strain (percent)
		(MPa)	(ksi)	(GPa)	(Msi)	
Unsize	AIRY 00	405	59	41	5.9	0.99*
	01	376*	55*	36	5.3	1.04
	02	510*	74	42	6.2	1.21
	03	492	71	42	6.1	1.27*
	04	476	69	43	6.2	1.16
	Average	471	68	41	5.9	1.14
	Std. Dev.	46	7	3	0.4	0.09
EPON 828	AIRY 10	469	68	43	6.3	1.09
	11	427	62	40	5.8	1.89*
	12	416	60	42	6.0	1.01
	13	416	60	42	6.1	1.01
	14	425	62	41	5.9	1.05
	Average	430	62	42	6.0	1.21
	Std. Dev.	22	3	1	0.2	0.38
PVA	AIRY 20	162*	24*	15*	2.2*	1.09
	21	430	62	34	5.0	1.25
	22	399	58	34	4.9	1.20
	23	410	59	34	5.0	1.19
	24	438	64	37	5.3	1.19
	Average	421	61	35	5.1	1.18
	Std. Dev.	21	3	1	0.2	0.06
Polysulfone	AIRY 30	467	68	41	6.0	1.15
	31	389*	56*	41	5.9	0.96*
	32	512	74	39	5.7	1.31
	33	410	60	38	5.5	1.11
	34	483	70	37	5.4	1.30
	35	564*	82*	42	6.0	1.37*
	Average	469	68	40	5.8	1.22
Std. Dev.	41	6	2	0.3	0.10	

\*Not included in average

Table A21

Individual AS4/3501-6 Quasi-Isotropic Laminate Axial Tensile  
Test Results at the Elevated Temperature, Wet Condition  
(93°C, 1%M)

Fiber Sizing	Specimen No.	Tensile Strength		Tensile Modulus		Ultimate Strain (percent)
		(MPa)	(ksi)	(GPa)	(Msi)	
Unsize	AIEY 00	197*	29*	42	6.1	0.47*
	01	463	67	39	5.7	1.21
	02	350*	51*	-	-	-
	03	442	64	44	6.4	1.06
	04	448	65	43	6.2	1.21
	Average	451	65	42	6.1	1.16
	Std. Dev.	11	2	2	0.3	0.08
EPON 828	AIEY 10	467	68	41	5.9	1.30
	11	494	72	44	6.3	1.18
	12	343*	50*	57*	8.2*	-
	13	475	69	43	6.3	1.46*
	14	487	71	41	6.0	0.98
	15	-	-	-	-	1.02
	Average	481	70	42	6.1	1.12
Std. Dev.	12	2	1	0.2	0.15	
PVA	AIEY 20	436	63	34	5.0	1.36
	21	263*	38*	39	5.6	-
	22	121*	18*	40	5.8	-
	23	414	60	37	5.4	1.32
	24	423	61	37	5.3	1.43
	Average	424	62	37	5.4	1.37
	Std. Dev.	11	2	2	0.3	0.06
Polysulfone	AIEY 30	447	65	43	6.2	1.38
	31	515	75	43	6.2	1.27
	32	477	69	42	6.1	1.15
	33	466	68	41	6.0	1.16
	34	450	65	43	6.2	1.09
	35	488	71	42	6.2	1.19
	Average	474	69	42	6.2	1.21
Std. Dev.	25	4	1	0.1	0.10	

\*Not included in average

Table A22

Individual AS4/4001 Quasi-Isotropic Laminate Axial Tensile  
Test Results at the Room Temperature, Dry Condition

Fiber Sizing	Specimen No.	Tensile Strength		Tensile Modulus		Ultimate Strain (percent)
		(MPa)	(ksi)	(GPa)	(Msi)	
Unsize	AIRZ 00	440*	64*	42*	6.0*	1.06
	01	398	58	40	5.7	1.03
	02	370	54	32	4.7	1.18*
	03	339	49	32	4.6	1.07
	04	<u>308*</u>	<u>45*</u>	<u>33</u>	<u>4.8</u>	<u>0.94</u>
	Average	369	54	34	5.0	1.03
	Std. Dev.	30	5	4	0.5	0.06
EPON 828	AIRZ 10	312	45	27	4.0	1.15
	11	305	44	28	4.1	1.10
	12	319	46	30	4.4	1.07
	13	342	50	32	4.6	1.08
	14	<u>309</u>	<u>45</u>	<u>30</u>	<u>4.3</u>	<u>1.05</u>
	Average	317	46	29	4.3	1.09
	Std. Dev.	15	2	2	0.3	0.04
PVA	AIRZ 20	293	43	27	3.9	1.09
	21	293	43	28	4.0	1.01
	22	314	46	27	3.9	1.16
	23	301	44	28	4.0	1.08
	24	<u>315</u>	<u>46</u>	<u>25</u>	<u>3.7</u>	<u>1.24</u>
	Average	303	44	27	3.9	1.11
	Std. Dev.	11	2	1	0.2	0.09
Polysulfone	AIRZ 30	404	59	38	5.5	1.11
	31	448	65	37	5.3	1.20
	32	425	62	35	5.1	1.26
	33	445	65	36	5.2	1.27
	34	<u>436</u>	<u>63</u>	<u>36</u>	<u>5.3</u>	<u>1.21</u>
	Average	432	63	36	5.3	1.21
	Std. Dev.	18	3	1	0.1	0.06

\*Not included in average

Table A23

Individual AS4/4001 Quasi-Isotropic Laminate Axial Tensile  
Test Results at the Elevated Temperature, Wet Condition  
(93°C, 1%M)

Fiber Sizing	Specimen No.	Tensile Strength		Tensile Modulus		Ultimate Strain (percent)
		(MPa)	(ksi)	(GPa)	(Msi)	
Unsize	AIEZ 00	178*	26*	22*	3.2*	0.33*
	01	532	77	45	6.6	1.20
	02	485	70	44	6.4	1.13
	03	442	64	41	6.0	1.14
	04	418	61	41	5.9	1.06
	05	<u>447</u>	<u>65</u>	<u>45</u>	<u>6.5</u>	<u>1.05</u>
	Average	465	67	43	6.2	1.12
Std. Dev.	44	6	2	0.3	0.06	
EPON 828	AIEZ 10	445	65	39	5.7	1.15
	11	518	75	44	6.3	1.15
	12	485	70	41	6.0	1.24
	13	401	58	38	5.5	1.07
	14	452	66	39	5.7	1.17
	15	<u>436</u>	<u>63</u>	<u>39</u>	<u>5.7</u>	<u>1.15</u>
	Average	456	66	40	5.8	1.16
Std. Dev.	41	6	2	0.3	0.05	
PVA	AIEZ 20	160*	23*	14*	2.0*	2.05*
	21	408	59	36	5.2	1.18
	22	441	64	37	5.4	1.24
	23	487	71	37	5.4	1.39
	24	471	68	39	5.7	1.27
	25	<u>341*</u>	<u>50</u>	<u>37</u>	<u>5.3</u>	<u>0.97*</u>
	Average	452	66	37	5.4	1.27
Std. Dev.	35	50	1	0.2	0.09	
Polysulfone	AIEZ 30	596	86	46	6.6	1.44
	31	618	89	49	7.0	1.33
	32	603	88	48	7.0	1.34
	33	598	89	48	7.0	1.40
	34	613	87	48	7.0	1.27

Table A23

- Continued -

Fiber Sizing	Specimen No.	Tensile Strength		Tensile Modulus		Ultimate Strain
		(MPa)	(ksi)	(GPa)	(Msi)	(percent)
Polysulfone	AIEZ 35	<u>563</u>	<u>82</u>	<u>44</u>	<u>6.4</u>	<u>1.39</u>
	Average	598	87	47	6.8	1.36
	Std. Dev.	19	3	2	0.3	0.06

---

\*Not included in average

Table A24

Individual AS4/F155 Quasi-Isotropic Laminate Axial Tensile  
Test Results at the Room Temperature, Dry Condition

Fiber Sizing	Specimen No.	Tensile Strength		Tensile Modulus		Ultimate Strain (percent)
		(MPa)	(ksi)	(GPa)	(Msi)	
Unsize	AIRX 00	333	48.3	23	3.4	1.44
	01	294	42.7	22	3.2	1.35
	02	305	44.2	23	3.3	1.36
	03	335	48.6	24	3.5	1.42
	Average	317	46.0	23	3.3	1.39
	Std. Dev.	20	3.0	1	0.1	0.05
EPON 828	AIRX 10	473	68.7	32	4.70	1.52
	11	465	67.5	31	4.55	1.50
	12	432	62.6	33	4.72	1.34
	13	447	64.9	33	4.72	1.39
	14	430	62.3	31	4.55	1.47
	Average	449	65.2	32	4.65	1.44
Std. Dev.	19	2.9	1	0.09	0.09	
PVA	AIRX 20	451	65.4	33	4.81	1.37
	21	473	68.6	32	4.67	1.50
	22	457	66.3	32	4.66	1.44
	23	428	62.1	32	4.66	1.35
	24	450	65.3	33	4.79	1.39
	Average	452	65.5	33	4.72	1.41
Std. Dev.	16	2.3	1	0.08	0.06	
Polysulfone	AIRX 30	394	57.2	31	4.55	1.26
	31	313	45.4	31	4.56	1.00
	32	372	54.0	32	4.63	1.18
	33	363	52.6	30	4.35	1.22
	34	402	58.3	31	4.46	1.32
	Average	369	53.5	31	4.51	1.20
Std. Dev.	35	5.1	1	0.11	0.12	

Table A25

Individual AS4/F155 Quasi-Isotropic Laminate Axial Tensile  
Test Results at the Elevated Temperature, Wet Condition  
(38°C, 1%M)

Fiber Sizing	Specimen No.	Tensile Strength		Tensile Modulus		Ultimate Strain (percent)
		(MPa)	(ksi)	(GPa)	(Msi)	
Unsize	ALEX 00	95*	14*	8*	1.2*	1.13
	01	195	43	21	3.0	1.41
	02	268	39	20	2.9	1.28
	03	306	44	23	3.3	1.37
	04	<u>274</u>	<u>40</u>	<u>21</u>	<u>3.0</u>	<u>1.32</u>
	Average	286	42	21	3.1	1.30
	Std. Dev.	18	3	1	0.2	0.11
EPON 828	ALEX 10	370	54	30	4.3	1.16
	11	403	58	31	4.5	1.23
	12	351	51	28	4.1	1.24
	13	382	55	28	4.1	1.34
	14	<u>389</u>	<u>56</u>	<u>32</u>	<u>4.6</u>	<u>1.18</u>
	Average	379	55	30	4.3	1.23
	Std. Dev.	20	3	2	0.2	0.07
PVA	ALEX 20	376	55	28	4.0	1.27
	21	390	57	29	4.2	1.32
	22	353	51	31	4.6	1.01*
	23	350	51	30	4.3	1.21
	24	<u>377</u>	<u>55</u>	<u>29</u>	<u>4.2</u>	<u>1.34</u>
	Average	369	54	29	4.3	1.29
	Std. Dev.	17	3	1	0.2	0.06
Polysulfone	ALEX 30	303*	44*	29	4.1	1.06
	31	345	50	26	3.8	1.31
	32	372	54	30	4.3	1.23
	33	399	58	31	4.6	1.28
	34	<u>405</u>	<u>59</u>	<u>28</u>	<u>4.1</u>	<u>1.39</u>
	Average	380	55	29	4.2	1.25
	Std. Dev.	28	4	2	0.3	0.12

\*Not included in average



Table A26

Individual AS4/3501-6 Quasi-Isotropic Laminate Axial Compression  
Test Results at the Room Temperature, Dry Condition

Fiber Sizing	Specimen No.	Compressive Strength		Compressive Modulus		Ultimate Strain (percent)	
		(MPa)	(ksi)	(GPa)	(Msi)		
Unsize	AHRY 00	102*	15*	37	5.3	0.90	
	01	313	45	33	4.7	2.90*	
	02	290	42	39	5.7	1.19	
	03	354	51	60*	8.7*	0.75*	
	04	414*	60*	44*	6.4*	1.74	
	05	252*	37*	35	5.1	1.45	
	Average		319	46	38	5.5	1.32
Std. Dev.		32	5	5	0.7	0.35	
EPON 828	AHRY 10	323	47	54	7.9	1.45	
	11	346	50	60	8.8	0.70	
	12	396	58	56	8.2	2.85*	
	13	409	59	53	7.7	1.45	
	14	365	53	40*	5.8*	0.67	
	Average		368	53	56	8.1	1.07
	Std. Dev.		35	5	3	0.5	0.44
PVA	AHRY 20	324	47	49	7.0	1.30*	
	21	363	53	35*	5.1*	1.15	
	22	363	53	52*	7.5*	0.68*	
	23	332	48	35*	5.1*	1.07	
	24	401	58	47	6.8	1.05	
	Average		356	52	48	6.9	1.09
	Std. Dev.		30	4	1	0.2	0.06
Polysulfone	AHRY 30	359	52	42	6.1	1.31	
	31	394	57	56	8.1	1.28	
	32	375	54	49	7.1	0.75*	
	33	408	59	-	-	3.09*	
	34	376	55	72*	10.4*	-	
	Average		383	56	49	7.1	1.30
	Std. Dev.		19	3	7	1.0	0.21

\*Not included in average

Table A27

Individual AS4/3501-6 Quasi-Isotropic Laminate Axial Compression  
Test Results at the Elevated Temperature, Wet Condition  
(93°C, 1%M)

Fiber Sizing	Specimen No.	Compressive Strength		Compressive Modulus		Ultimate Strain (percent)
		(MPa)	(ksi)	(GPa)	(Msi)	
Unsize	AHEY 00	294	43	32*	4.7*	0.79
	01	306	44	37	5.4	1.03
	02	299	43	42	6.1	1.05*
	03	285	41	-	-	0.67*
	04	297	43	42	6.1	0.80
	Average	296	43	40	5.9	0.87
	Std. Dev.	8	1	3	0.4	0.14
EPON 828	AHEY 10	299	43	43	6.2	1.01
	11	312	45	40	5.7	1.09
	12	290	42	42	6.1	0.92
	13	291	42	35	5.1	0.98
	14	295	43	28*	4.1*	1.37*
	15	289	42	38	5.6	0.10
	Average	296	43	40	5.7	0.96
Std. Dev.	9	1	3	0.5	0.09	
PVA	AHEY 20	233	34	31	4.5	0.92
	21	206	30	36*	5.3*	0.75
	22	184*	27*	34	4.9	0.71
	23	265*	39*	21*	3.1*	1.39*
	24	199	29	25	3.6	0.83
	Average	213	31	30	4.3	0.80
Std. Dev.	18	3	5	0.7	0.09	
Polysulfone	AHEY 30	282	41	40	5.9	0.82
	31	278	40	32	4.6	1.02
	32	300	44	35	5.0	1.11
	33	305	44	36	5.2	0.78
	34	303	44	35	5.0	0.96
	Average	294	43	35	5.1	0.93
Std. Dev.	13	2	3	0.5	0.10	

\*Not included in average

Table A28

Individual AS4/4001 Quasi-Isotropic Laminate Axial Compression  
Test Results at the Room Temperature, Dry Condition

Fiber Sizing	Specimen No.	Compressive Strength		Compressive Modulus		Ultimate Strain (percent)
		(MPa)	(ksi)	(GPa)	(Msi)	
Unsize	AHRZ 00	440	64	28	4.0	3.10
	01	452	66	36	5.2	3.74
	02	416	60	40	5.8	3.00
	03	350	51	37	5.4	1.32
	04	471	68	-	-	-
	05	481	70	-	-	1.69
	Average	452	65	38	5.5	2.59
Std. Dev.	26	4	2.2	0.3	0.78	
EPON 828	AHRZ 10	369	54	35	5.1	1.08*
	11	441	64	58*	8.4*	1.84
	12	399	58	45	6.5	2.30
	13	392	57	39	5.6	1.51
	14	414	60	35	5.1	2.27
	15	441	64	45	6.5	3.68*
	Average	468	59	39	5.8	1.98
Std. Dev.	29	4	5	0.7	0.38	
PVA	AHRZ 20	327*	47*	49	7.2	1.55
	21	413*	60*	45	6.6	2.93
	22	376	55	55*	8.0*	2.90
	23	423*	61*	9*	1.3*	-
	24	368	53	38*	5.5*	1.20*
	Average	386	56	47	6.9	2.46
Std. Dev.	24	4	3	0.4	0.79	
Polysulfone	AHRZ 30	474	69	45	6.5	-
	31	403	59	43	6.3	-
	32	392	57	46	6.7	-
	33	474	69	69*	10.0*	2.65
	34	481	70	46	6.6	-
	Average	445	65	45	6.5	-
Std. Dev.	43	6	1	0.2	-	

\*Not included in average

Table A29

Individual AS4/4001 Quasi-Isotropic Laminate Axial Compression  
Test Results at the Elevated Temperature, Wet Condition  
(93°C, 1%M)

Fiber Sizing	Specimen No.	Compressive Strength		Compressive Modulus		Ultimate Strain
		(MPa)	(ksi)	(GPa)	(Msi)	(percent)
Unsize	AHEZ 00	332	48	27	3.9	1.30
	01	341	49	31	4.6	1.48
	02	352	51	35	5.1	1.61
	03	330	48	34	4.9	0.89*
	04	332	48	33	4.8	1.24
	Average	337	49	32	4.7	1.41
	Std. Dev.	9	1	3	0.5	0.17
EPON 828	AHEZ 10	352	51	27*	4.0*	1.15
	11	359	52	46	6.6	0.91
	12	374	54	35	5.1	1.40
	13	325	47	51*	7.3*	0.70
	14	367	53	35	5.0	1.24
	Average	356	52	38	5.6	1.10
	Std. Dev.	19	3	6	0.9	0.17
PVA	AHEZ 20	297	43	28	4.1	1.16
	21	312	45	29	4.2	2.24*
	22	268	39	44	6.4	1.26
	23	354	51	54*	7.8*	1.03
	24	285	41	38	5.5	0.98
	25	314	46	33	4.8	1.05
	Average	305	44	34	5.0	1.09
Std. Dev.	30	4	7	1.0	0.12	
Polysulfone	AHEZ 30	348	51	-	-	1.02
	31	397	58	-	-	0.96
	32	407	59	46	6.7	1.04
	33	368	53	47	6.8	0.83*
	34	379	55	59*	8.5*	1.26*
	35	410	59	70*	5.1*	1.13
	Average	385	56	47	6.8	1.04
Std. Dev.	24	4	1	0.1	0.07	

\*Not included in average

Table A30

Individual AS4/F155 Quasi-Isotropic Laminate Axial Compression  
Test Results at the Room Temperature, Dry Condition

Fiber Sizing	Specimen No.	Compressive Strength		Compressive Modulus		Ultimate Strain (percent)
		(MPa)	(ksi)	(GPa)	(Msi)	
Unsize	AHRX 00	221	32	19	2.8	1.26
	01	223	32	22	3.2	1.25
	02	234	34	20	3.0	1.23
	03	167*	24*	18*	2.6*	1.07
	04	200	29	34*	5.0*	1.20
	05	<u>240</u>	<u>35</u>	<u>33</u>	<u>4.7</u>	<u>1.10</u>
	Average	224	32	26	3.7	1.19
Std. Dev.	15	2	6	0.8	0.08	
EPON 828	AHRX 10	261	38	36	5.3	0.71*
	11	285	41	44*	6.4*	0.85
	12	300	44	32	4.7	0.86
	13	302	44	29*	4.2*	0.97*
	14	252	37	35	5.1	0.95
	15	<u>284</u>	<u>41</u>	<u>33</u>	<u>4.7</u>	<u>0.86</u>
	Average	281	41	34	4.9	0.88
Std. Dev.	20	3	2	0.3	0.04	
PVA	AHRX 20	305	44	32	4.6	1.02
	21	264	38	44	6.3	0.98
	22	265	39	27	4.0	1.27*
	23	282	41	34	4.9	0.89
	24	289	42	32	4.7	0.85
	25	<u>294</u>	<u>43</u>	<u>62*</u>	<u>9.0*</u>	<u>1.18</u>
	Average	283	41	34	4.9	1.02
Std. Dev.	16	2	6	0.9	0.12	
Polysulfone	AHRX 30	224	33	25	3.6	1.13
	31	265	38	27	3.9	0.99
	32	262	38	34*	4.9*	0.99
	33	259	38	26	3.7	-
	34	<u>268</u>	<u>39</u>	<u>18</u>	<u>4.2</u>	<u>1.01</u>
	Average	256	37	27	3.9	1.03
	Std. Dev.	18	3	2	0.3	0.07

\*Not included in average

Table A31

Individual AS4/F155 Quasi-Isotropic Laminate Axial Compression  
Test Results at the Elevated Temperature, Wet Condition  
(38°C, 1%M)

Fiber Sizing	Specimen No.	Compressive Strength (MPa) (ksi)		Compressive Modulus (GPa) (Msi)		Ultimate Strain (percent)
Unsize	AHEX 00	123	18	16	2.4	1.46
	01	139	20	16	2.4	2.39*
	02	136	20	17	2.4	0.89*
	03	142	21	18	2.5	1.84
	04	136	20	14	2.1	1.48
	05	-	-	-	-	1.81
	Average	135	20	16	2.4	1.65
Std. Dev.	7	1	1	0.2	0.21	
EPON 828	AHEX 10	181	26	24	3.5	1.26
	11	173	25	24	3.5	1.09
	12	173	25	28*	4.1*	1.15
	13	199	29	25	3.6	0.83*
	14	199	29	20	3.0	1.38
	15	169	25	18*	2.6*	1.42*
	Average	182	27	23	3.4	1.22
Std. Dev.	13	2	2	0.3	0.13	
PVA	AHEX 20	118*	17*	29	4.2	0.66
	21	146	21	23*	3.4*	0.64
	22	148	22	28	4.1	0.57
	23	166	24	22*	3.2*	0.82
	24	152	22	29	4.2	0.93
	25	159	23	29	4.3	0.64
	Average	154	22	29	4.2	0.69
Std. Dev.	8	1	1	0.1	0.09	
Polysulfone	AHEX 30	159	23	24	3.5	0.84
	31	154	22	16*	2.3*	1.52
	32	163	24	39*	5.7*	0.74*
	33	165	24	25	3.6	1.90*

Table A31

- Continued -

Fiber Sizing	Specimen No.	Compressive Strength		Compressive Modulus		Ultimate Strain (percent)
		(MPa)	(ksi)	(GPa)	(Msi)	
Polysulfone	AHEX 34	172	25	26	3.8	1.00
	35	<u>168</u>	<u>24</u>	<u>20</u>	<u>2.9</u>	<u>1.68</u>
	Average	163	24	24	3.5	1.26
	Std. Dev.	7	1	3	0.4	0.40

---

\*Not included in average

Table A32

Individual AS4/3501-6 Quasi-Isotropic Laminate Flexural Test  
Results at the Room Temperature, Dry Condition

Fiber Sizing	Specimen No.	Flexural Strength		Flexural Modulus		Flexural Strain (percent)
		(MPa)	(ksi)	(GPa)	(Msi)	
Unsize	AJRY 00	934	136	56.4	8.19	1.66
	01	894	130	56.3	8.16	1.59
	02	863	125	56.6	8.21	1.52
	03	851	123	58.4	8.47	1.46
	04	<u>757</u>	<u>110</u>	<u>46.0</u>	<u>6.68</u>	<u>1.64</u>
	Average	860	125	54.7	7.94	1.57
	Std. Dev.	69	10	5.0	0.72	0.08
EPON 828	AJRY 10	909	132	56.7	8.22	1.60
	11	881	128	63.5	9.21	1.39
	12	970	141	62.0	8.99	1.56
	13	761	110	55.5	8.05	1.37
	14	<u>887</u>	<u>129</u>	<u>62.8</u>	<u>9.11</u>	<u>1.41</u>
	Average	882	128	60.1	8.72	1.47
	Std. Dev.	76	11	3.7	0.54	0.11
PVA	AJRY 20	762	111	47.0	6.82	1.62
	21	818	119	52.5	7.62	1.56
	22	820	119	48.8	7.08	1.68
	23	812	118	47.8	6.93	1.70
	24	<u>881</u>	<u>128</u>	<u>53.1</u>	<u>7.71</u>	<u>1.66</u>
	Average	818	119	49.8	7.23	1.64
	Std. Dev.	42	6	2.8	0.41	0.06
Polysulfone	AJRY 30	1003	145	64.7	9.38	1.55
	31	904	131	56.7	8.23	1.59
	32	852	124	54.0	7.83	1.58
	33	956	139	59.2	8.58	1.62
	34	<u>999</u>	<u>145</u>	<u>61.5</u>	<u>8.92</u>	<u>1.62</u>
	Average	943	137	59.2	8.59	1.59
	Std. Dev.	65	9	4.1	0.60	0.03



Table A33

Individual AS4/3501-6 Quasi-Isotropic Laminate Flexural Test Results  
at the Elevated Temperature, Wet Condition  
(93°C, 1%M)

Fiber Sizing	Specimen No.	Flexural Strength (MPa)	Flexural Strength (ksi)	Flexural Modulus (GPa)	Flexural Modulus (Msi)	Flexural Strain (percent)
Unsize	AJEY 00	827*	120*	98.6*	14.30*	0.84*
	01	625	91	54.7	7.93	1.14*
	02	534	77	51.2	7.43	1.04
	03	509	74	50.5	7.32	1.01
	04	<u>526</u>	<u>76</u>	<u>60.7</u>	<u>8.81</u>	<u>0.87</u>
	Average	548	80	54.3	7.87	0.97
	Std. Dev.	52	8	4.7	0.68	0.09
EPON 828	AJEY 10	480*	70*	61.4	8.90	0.78*
	11	636	92	60.1	8.71	1.06
	12	679	99	58.5	8.48	1.16
	13	452*	66*	44.8*	6.50*	1.01
	14	<u>636</u>	<u>92</u>	<u>55.8</u>	<u>8.09</u>	<u>1.14</u>
	Average	651	94	59.0	8.55	1.09
	Std. Dev.	25	4	2.4	0.35	0.07
PVA	AJEY 20	383*	56*	33.7*	4.89*	1.13
	21	517	75	45.8	6.64	1.13
	22	570	83	49.5	7.18	1.15
	23	519	75	46.4	6.73	1.12
	24	<u>515</u>	<u>75</u>	<u>46.7</u>	<u>6.77</u>	<u>1.10</u>
	Average	530	77	47.1	6.83	1.13
	Std. Dev.	27	4	1.7	0.24	0.02
Polysulfone	AJEY 30	712	103	62.3*	9.03*	1.14
	31	598	87	51.6	7.48	1.16
	32	599	87	53.6	7.77	1.12
	33	590	86	54.1	7.85	1.10
	34	<u>625</u>	<u>91</u>	<u>52.2</u>	<u>7.57</u>	<u>1.20</u>
	Average	625	91	52.9	7.67	1.14
	Std. Dev.	50	7	1.2	0.17	0.04

\*Not included in average

Table A34

Individual AS4/4001 Quasi-Isotropic Laminate Flexural Test Results  
at the Room Temperature, Dry Condition

Fiber Sizing	Specimen No.	Flexural Strength		Flexural Modulus		Flexural Strain (percent)
		(MPa)	(ksi)	(GPa)	(Msi)	
Unsize	AJRZ 00	967	140	60.0	8.70	1.61
	01	1019	148	68.9	9.99	1.48
	02	971	141	65.7	9.53	1.48
	03	885	128	72.7	10.55	1.22
	04	970	141	68.8	9.98	1.41
	Average	963	140	67.2	9.75	1.44
	Std. Dev.	48	7	4.7	0.69	0.14
EPON 828	AJRZ 10	973	141	70.0	10.15	1.39
	11	1060*	154*	73.5	10.66	1.44
	12	783*	114*	47.4*	6.88*	1.65
	13	990	144	66.2	9.61	1.49
	14	927	134	60.1	8.72	1.54
	Average	963	140	67.5	9.78	1.50
	Std. Dev.	33	5	5.7	0.83	0.10
PVA	AJRZ 20	851	123	56.1	8.14	1.52
	21	810	117	50.7	7.36	1.60
	22	834	121	53.6	7.78	1.55
	23	866	126	53.0	7.68	1.63
	24	814	118	52.0	7.54	1.56
	Average	835	121	53.1	7.70	1.57
	Std. Dev.	21	3	2.0	0.29	0.04
Polysulfone	AJRZ 30	1114	162	69.5	10.08	1.60
	31	996	145	65.0	9.42	1.53
	32	1044	152	67.1	9.73	1.56
	33	1032	150	67.1	9.10	1.64
	34	992	144	65.6	9.52	1.51
	Average	1035	150	66.0	9.57	1.57
	Std. Dev.	49	7	2.5	0.36	0.05

\*Not included in average

Table A35

Individual AS4/4001 Quasi-Isotropic Laminate Flexural Test Results  
at the Elevated Temperature, Wet Condition  
(93°C, 1%M)

Fiber Sizing	Specimen No.	Flexural Strength (MPa)	Flexural Strength (ksi)	Flexural Modulus (GPa)	Flexural Modulus (Msi)	Flexural Strain (percent)
Unsize	AJEZ 00	475*	69*	39.7*	5.76*	1.20
	01	711	103	57.8	8.39	1.23
	02	734	107	67.2	9.75	1.09
	03	743	108	72.5	10.52	1.02
	04	<u>683</u>	<u>99</u>	<u>67.2</u>	<u>9.75</u>	<u>1.01</u>
	Average	718	104	66.2	9.60	1.11
	Std. Dev.	28	4	6.1	0.89	0.10
EPON 828	AJEZ 10	645	94	51.7	7.50	1.25
	11	622	90	48.0	6.96	1.30
	12	704	102	54.1	7.84	1.30
	13	714	104	53.2	7.71	1.34
	14	<u>770</u>	<u>112</u>	<u>56.9</u>	<u>8.25</u>	<u>1.35</u>
	Average	691	100	52.8	7.65	1.31
	Std. Dev.	62	9	3.3	0.47	0.04
PVA	AJEZ 20	709	103	59.4	8.62	1.19
	21	670	97	59.4	8.62	1.13
	22	668	97	53.7	7.79	1.24
	23	620	90	53.9	7.82	1.15
	24	<u>675</u>	<u>98</u>	<u>60.1</u>	<u>8.71</u>	<u>1.12</u>
	Average	668	97	57.3	8.31	1.17
	Std. Dev.	35	5	3.2	0.46	0.05
Polysulfone	AJEZ 30	827	120	69.2	10.03	1.20
	31	785	114	70.9	10.28	1.11
	32	892	129	80.6	11.69	1.11
	33	881	128	74.8	10.85	1.18
	34	<u>884</u>	<u>128</u>	<u>78.8</u>	<u>11.43</u>	<u>1.12</u>
	Average	854	124	74.9	10.86	1.14
	Std. Dev.	48	7	4.9	0.71	0.04

\*Not included in average

Table A36

Individual AS4/F155 Quasi-Isotropic Laminate Flexural Test Results  
at the Room Temperature, Dry Condition

Fiber Sizing	Specimen No.	Flexural Strength		Flexural Modulus		Flexural Strain (percent)
		(MPa)	(ksi)	(GPa)	(Msi)	
Unsize	AJRX 00	548	79	30.4	4.42	1.80
	01	592	86	31.9	4.63	1.85
	02	613	89	34.7	5.03	1.77
	03	548	80	23.5*	3.41*	2.33*
	04	615	89	32.5	4.71	1.89
	Average	583	85	32.4	4.70	1.83
	Std. Dev.	34	5	1.8	0.25	0.05
EPON 828	AJRX 10	719	104	47.7	6.91	1.51
	11	609	88	37.0	5.37	1.64
	12	654	95	35.4	5.13	1.85*
	13	693	101	50.7*	7.36*	1.37*
	Average	669	97	40.0	5.80	1.58
	Std. Dev.	48	7	6.7	0.97	0.09
	PVA	AJRX 20	654	95	44.2	6.41
21		643	93	39.6	5.74	1.62
22		703	102	41.8	6.06	1.68
23		602	87	32.0*	4.64*	1.88
24		684	99	43.6	6.32	1.57
Average		658	95	42.3	6.13	1.65
Std. Dev.		38	6	2.1	0.30	0.15
Polysulfone	AJRX 30	577	84	29.8*	4.33*	1.93
	31	688	100	40.6	5.90	1.69
	32	665	97	40.8	5.92	1.63
	33	649	94	34.6	5.02	1.87
	34	678	98	41.7	6.05	1.62
	Average	651	94	39.4	5.71	1.75
	Std. Dev.	44	6	3.3	0.47	0.14

---

\*Not included in average

Table A37

Individual AS4/F155 Quasi-Isotropic Laminate Flexural Test Results  
at the Elevated Temperature, Wet Condition  
(38°C, 1%M)

Fiber Sizing	Specimen No.	Flexural Strength (MPa) (ksi)		Flexural Modulus (GPa) (Msi)		Flexural Strain (percent)
Unsize	AJEX 01	87*	13*	-	-	-
	02	369	54	26.3	3.82	1.40
	03	374	54	22.8	3.30	1.65
	04	<u>371</u>	<u>54</u>	<u>27.2</u>	<u>3.95</u>	<u>1.36</u>
	Average	371	54	25.4	3.69	1.47
	Std. Dev.	3	0	2.0	0.34	0.16
EPON 828	AJEX 10	482	70	41.5	6.02	1.16
	11	446	65	37.7	5.47	1.18
	12	494	72	42.5	6.17	1.16
	13	471	68	42.7	6.19	1.10
	14	<u>467</u>	<u>68</u>	<u>40.9</u>	<u>5.93</u>	<u>1.15</u>
	Average	472	69	41.1	5.96	1.15
Std. Dev.	18	3	2.0	0.29	0.03	
PVA	AJEX 20	365	53	35.5	5.15	1.03
	21	348	50	29.3	4.25	1.19
	22	401	58	34.5	5.01	1.16
	23	320	46	33.0	4.79	0.97
	24	<u>386</u>	<u>56</u>	<u>34.3</u>	<u>4.97</u>	<u>1.12</u>
	Average	364	53	33.3	4.83	1.09
Std. Dev.	32	5	2.4	0.35	0.09	
Polysulfone	AJEX 30	390	57	42.0	6.09	0.93*
	31	426	62	33.1	4.80	1.29*
	32	440	64	39.6	5.74	1.11
	33	364	53	34.7	5.03	1.05
	34	<u>416</u>	<u>60</u>	<u>37.0</u>	<u>5.36</u>	<u>1.13</u>
	Average	407	59	37.2	5.40	1.10
Std. Dev.	30	4	3.6	0.52	0.04	

\*Not included in average

Table A38

Individual AS4/3501-6 Quasi-Isotropic Laminate Interlaminar  
Shear Test Results at the Room Temperature, Dry Condition

Fiber Sizing	Specimen No.	Shear Strength (MPa)	Shear Strength (ksi)
Unsize	AKRY 00	30	4.3
	01	29	4.2
	02	29	4.2
	03	33	4.8
	04	<u>28</u>	<u>4.1</u>
	Average	30	4.3
	Std. Dev.	2	0.3
EPON 828	AKRY 10	29	4.3
	11	30	4.3
	12	31	4.5
	13	28	4.0
	14	<u>38</u>	<u>5.5</u>
	Average	31	4.5
	Std. Dev.	4	0.6
PVA	AKRY 20	27	3.9
	21	32	4.6
	22	28	4.0
	23	26	3.7
	24	<u>32</u>	<u>4.6</u>
	Average	29	4.2
	Std. Dev.	3	0.4
Polysulfone	AKRY 30	30	4.3
	31	30	4.3
	32	31	4.5
	33	31	4.5
	34	<u>31</u>	<u>4.4</u>
	Average	30	4.4
	Std. Dev.	1	0.1

Table A39

Individual AS4/3501-6 Quasi-Isotropic Laminate Interlaminar Shear  
Test Results at the Elevated Temperature, Wet Condition  
(93°C, 1%M)

Fiber Sizing	Specimen No.	Shear Strength	
		(MPa)	(ksi)
Unsize	AKEY 00	26	3.8
	01	24	3.5
	02	29	4.2
	03	26	3.8
	04	<u>24</u>	<u>3.5</u>
	Average	26	3.8
	Std. Dev.	2	0.3
EPON 828	AKEY 10	40*	5.8*
	11	23	3.3
	12	23	3.3
	13	24	3.4
	14	<u>24</u>	<u>3.4</u>
	Average	23	3.4
	Std. Dev.	0	0.1
PVA	AKEY 20	29	4.2
	21	25	3.6
	22	23	3.3
	23	21	3.1
	24	<u>21</u>	<u>3.0</u>
	Average	24	3.4
	Std. Dev.	3	0.5
Polysulfone	AKEY 30	-	-
	31	24	3.5
	32	26	3.7
	33	25	3.7
	34	<u>25</u>	<u>3.6</u>
	Average	25	3.6
	Std. Dev.	1	0.1

---

\*Not included in average

Table A40

Individual AS4/4001 Quasi-Isotropic Laminate Interlaminar Shear  
Test Results at the Room Temperature, Dry Condition

Fiber Sizing	Specimen No.	Shear Strength (MPa)	Shear Strength (ksi)
Unsize	AKRZ 00	40	5.7
	01	33	4.8
	02	51	7.4
	03	67	9.7
	04	39	5.7
	05	<u>67</u>	<u>9.7</u>
	Average	50	7.2
Std. Dev.	15	2.1	
EPON 828	AKRZ 10	75	10.8
	11	57	8.3
	12	45	6.5
	13	57	8.3
	14	<u>53</u>	<u>7.8</u>
	Average	57	8.3
Std. Dev.	11	1.6	
PVA	AKRZ 20	40	5.8
	21	42	6.1
	22	37	5.4
	23	45	6.5
	24	<u>45</u>	<u>6.5</u>
	Average	42	6.1
Std. Dev.	3	0.5	
Polysulfone	AKRZ 30	59	8.6
	31	53	7.4
	32	49	7.1
	33	50	7.2
	34	<u>48</u>	<u>7.0</u>
	Average	52	7.5
Std. Dev.	5	0.7	

---

\*Not included in average



Table A41

Individual AS4/4001 Quasi-Isotropic Laminate Interlaminar Shear  
 Test Results at the Elevated Temperature, Wet Condition  
 (93°C, 1%M)

Fiber Sizing	Specimen No.	Shear Strength (MPa)	Shear Strength (ksi)
Unsize	AKEZ 00	42	6.1
	01	45	6.5
	02	49	7.1
	03	44	6.4
	04	<u>40</u>	<u>5.7</u>
	Average	44	6.4
	Std. Dev.	4	0.5
EPON 828	AKEZ 10	43	6.2
	11	44	6.4
	12	39	5.6
	13	<u>43</u>	<u>6.2</u>
	Average	42	6.1
	Std. Dev.	2	0.4
PVA	AKEZ 20	38	5.4
	21	32	4.7
	22	37	5.4
	23	<u>34</u>	<u>4.9</u>
	Average	35	5.1
	Std. Dev.	3	0.4
Polysulfone	AKEZ 30	51	7.4
	31	51	7.4
	32	53	7.7
	33	44	6.4
	34	<u>45</u>	<u>6.5</u>
	Average	49	7.1
	Std. Dev.	4	0.6

Table A42

Individual AS4/F155 Quasi-Isotropic Laminate Interlaminar Shear  
Test Results at the Room Temperature, Dry Condition

Fiber Sizing	Specimen No.	Shear Strength (MPa)	Shear Strength (ksi)
Unsize	AKRX 00	59	8.6
	01	53	7.7
	02	57	8.3
	03	63	9.2
	04	<u>62</u>	<u>9.0</u>
	Average	59	8.6
	Std. Dev.	4	0.6
EPON 828	AKRX 10	71	10.3
	11	79	11.5
	12	75	10.8
	13	78	11.4
	14	<u>80</u>	<u>11.6</u>
	Average	77	11.1
	Std. Dev.	4	0.6
PVA	AKRX 20	54	7.9
	21	66	9.6
	22	60	8.8
	23	68	9.9
	24	<u>67</u>	<u>9.7</u>
	Average	63	9.2
	Std. Dev.	6	0.8
Polysulfone	AKRX 30	68	9.9
	31	73	10.5
	32	58	8.5
	33	53	7.7
	34	<u>62</u>	<u>8.9</u>
	Average	63	9.1
	Std. Dev.	8	1.1

Table A43

Individual AS4/F155 Quasi-Isotropic Laminate Interlaminar Shear  
 Test Results at the Elevated Temperature, Wet Condition  
 (38°C, 1%M)

Fiber Sizing	Specimen No.	Shear Strength (MPa)	Shear Strength (ksi)
Unsize	AKEX 01	15	2.1
	02	16	2.3
	03	16	2.2
	04	<u>14</u>	<u>2.1</u>
	Average	15	2.2
	Std. Dev.	1	0.1
EPON 828	AKEX 10	26*	3.7*
	11	22*	3.2*
	12	51	7.5
	13	51	7.4
	14	<u>50</u>	<u>7.2</u>
	Average	51	7.4
Std. Dev.	1	0.1	
PVA	AKEX 20	26	3.8
	21	<u>26</u>	<u>3.8</u>
	Average	26	3.8
Std. Dev.	0	0	
Polysulfone	AKEX 30	42	6.1
	31	46	6.7
	32	45	6.5
	33	51	7.3
	34	<u>48</u>	<u>7.0</u>
	Average	46	6.7
Std. Dev.	3	0.5	

\*Not included in average

Table A44

Individual AS4/3501-6 Quasi-Isotropic Laminate Instrumented Tensile  
Impact Test Results at the Room Temperature, Dry Condition

Fiber Sizing	Specimen No.	Ultimate Strength		Dynamic Modulus		Total Energy	
		(MPa)	(ksi)	(GPa)	(Msi)	(kJ/m <sup>3</sup> )	(ft-lb/in <sup>3</sup> )
Unsize	ALRY 00	297	43.0	35	5.1	765	17.0
	02	462	67.0	37	5.4	1484	33.0
	03	483	70.0	37	5.4	1574	35.0
	Average	414	60.0	37	5.3	1259	28.0
	Std. Dev.	102	14.8	1	0.2	450	10.0
EPON 828	ALRY 10	469	68.0	43	6.2	1394	31.0
	11	428	62.0	37	5.3	1574	35.0
	12	352	51.0	40	5.8	675	15.0
	13	400	58.0	40	5.8	989	22.0
	Average	412	59.8	40	5.8	1169	26.0
Std. Dev.	49	7.1	3	0.4	405	9.0	
PVA	ALRY 20	379	55.0	32	4.6	1259	28.0
	21	386	56.0	37	5.3	1124	25.0
	22	414	60.0	35	5.0	1394	31.0
	23	358	52.0	38	5.5	945	21.0
	24	414	60.0	36	5.2	1169	26.0
Average	390	56.6	35	5.1	1178	26.2	
Std. Dev.	23	3.4	2	0.3	166	3.7	

Table A44

- Continued -

Fiber Sizing	Specimen No.	Ultimate Strength		Dynamic Modulus		Total Energy	
		(MPa)	(ksi)	(GPa)	(Msi)	(kJ/m <sup>3</sup> )	(ft-lb/in <sup>3</sup> )
Polysulfone	ALRY 30	441	64.0	32	4.7	1889	42.0
	31	400	58.0	35	5.1	1124	25.0
	32	414	60.0	38	5.5	1259	28.0
	33	358	52.0	35	5.0	1034	23.0
	34	421	61.0	35	5.0	1304	29.0
	Average	407	59.0	35	5.1	1322	29.4
	Std. Dev.	31	4.5	2	0.3	328	7.3

Table A45

Individual AS4/3501-6 Quasi-Isotropic Laminate Instrumented Tensile Impact  
 Test Results at the Elevated Temperature, Wet Condition  
 (93°C, 1%M)

Fiber Sizing	Specimen No.	Ultimate Strength		Dynamic Modulus		Total Energy	
		(MPa)	(ksi)	(GPa)	(Msi)	(kJ/m <sup>3</sup> )	(ft-lb/in <sup>3</sup> )
Unsize	ALEY 00	379	55.0	-	-	1304	29.0
	01	386	56.0	40	5.8	1079	24.0
	02	379	55.0	39	5.7	1619	36.0
	03	-	-	40	5.8	-	-
	Average	381	55.3	40	5.8	1349	30.0
	Std. Dev.	4	0.6	0	0.1	270	6.0
EPON 828	ALEY 12	531	77.0	39	5.6	1844	41.0
	13	483	70.0	41	5.9	1214	27.0
	Average	507	73.5	40	5.8	1529	34.0
	Std. Dev.	35	5.0	1	0.2	445	9.9
PVA	ALEY 20	234	34.0	20*	2.9*	1124	25.0
	21	393	57.0	32	4.6	1124	25.0
	22	496	72.0	31	4.5	2159	48.0
	Average	374	54.3	31	4.6	1484	33.0
	Std. Dev.	132	19.1	-	-	585	3.0

Table A45

- Continued -

Fiber Sizing	Specimen No.	Ultimate Strength		Dynamic Modulus	Total Energy		
		(MPa)	(ksi)		(kJ/m <sup>3</sup> )	(ft-lb/in <sup>3</sup> )	
Polysulfone	ALEY 31	503	73.0	37	5.4	1709	38.0
	32	531	77.0	41	5.9	1934	43.0
	33	441	64.0	39	5.6	1619	36.0
	34	490	71.0	35	5.1	1709	38.0
	Average	492	71.3	38	5.5	1754	39.0
	Std. Dev.	37	5.4	2	0.3	135	3.0

\*Not included in average

Table A46

Individual AS4/4001 Quasi-Isotropic Laminate Instrumented Tensile Impact  
Test Results at the Room Temperature, Dry Condition

Fiber Sizing	Specimen No.	Ultimate Strength		Dynamic Modulus		Total Energy	
		(MPa)	(ksi)	(GPa)	(Msi)	(kJ/m <sup>3</sup> )	(ft-lb/in <sup>3</sup> )
EPON 828	ALRZ 10	352	51.0	35	5.1	-	-
	11	414	60.0	32	4.6	1259	28.0
	12	393	57.0	39	5.6	1439	32.0
	13	400	58.0	32	4.7	1124	25.0
	14	365	53.0	32	4.7	1034	23.0
	Average	385	55.8	34	4.9	1214	27.0
	Std. Dev.	26	3.7	3	0.4	175	3.9
Polysulfone	ALRZ 30	428	62.0	37	5.4	1394	31.0
	31	421	61.0	42	6.1	1079	24.0
	32	469	68.0	32	4.7	1709	38.0
	33	428	62.0	38	5.5	1214	27.0
	34	393	57.0	51	7.4	-	-
	Average	428	62.0	40	5.8	1349	30.0
	Std. Dev.	27	3.9	7	1.0	270	6.0



Table A47

Individual AS4/F155 Quasi-Isotropic Laminate Instrumented Tensile Impact  
Test Results at the Room Temperature, Dry Condition

Fiber Sizing	Specimen No.	Ultimate Strength		Dynamic Modulus		Total Energy	
		(MPa)	(ksi)	(GPa)	(Msi)	(kJ/m <sup>3</sup> )	(ft-lb/in <sup>3</sup> )
Unsize	ALRX 01	253	36.6	21	3.0	765	17.0
	02	232	33.7	19	2.7	945	21.0
	03	317	46.0	24	3.5	1214	27.0
	04	297	43.0	22	3.2	1079	24.0
	Average	276	40.0	21	3.0	989	22.0
	Std. Dev.	39	5.7	3	0.4	180	4.0
EPON 828	ALRX 10	379	55.0	26	3.8	1304	29.0
	11	379	55.0	37	5.4	1349	30.0
	12	352	51.0	32	4.6	945	21.0
	13	310	45.0	32	4.7	720	16.0
	14	221	32.0	30	4.4	495*	11.0*
	15	365	53.0	26	3.8	1349	30.0
	Average	334	48.5	30	4.4	1133	25.2
	Std. Dev.	61	8.9	4	0.6	287	6.4
PVA	ALRX 20	359	52.0	37	5.3	1034	23.0
	21	359	52.0	20	2.9	1484	33.0
	22	372	54.0	35	5.1	1259	28.0
	23	352	51.0	38	5.5	1079	24.0
	24	365	53.0	35	5.0	989	22.0
	Average	361	52.4	33	4.8	1169	26.0
	Std. Dev.	8	1.1	8	1.1	225	5.0

Table A47

- Continued -

Fiber Sizing	Specimen No.	Ultimate Strength		Dynamic Modulus	Total Energy	
		(MPa)	(ksi)			
Polysulfone	ALRX 30	386	56.0	31	1259	28.0
	31	352	51.0	32	855	19.0
	32	365	53.0	35	945	21.0
	33	365	53.0	37	989	22.0
	34	379	55.0	40	945	21.0
	Average	370	53.6	35	989	22.0
	Std. Dev.	13	1.9	3	135	3.0

\*Not included in average

Table A48

Individual AS4/F155 Quasi-Isotropic Laminate Instrumented Tensile  
 Test Results at the Elevated Temperature, Wet Condition  
 (38°C, 1%M)

Fiber Sizing	Specimen No.	Ultimate Strength (MPa)	Ultimate Strength (ksi)	Dynamic Modulus (GPa)	Dynamic Modulus (Msi)	Total Energy (kJ/m <sup>3</sup> )	Total Energy (ft-lb/in <sup>3</sup> )	
Unsize	ALEX 00	-	-	15	2.1	-	-	
	01	207	30.0	16	2.3	-	-	
	02	228	33.0	18	2.6	1034	23.0	
	03	269	39.0	20	2.9	1169	26.0	
	Average	234	34.0	17	2.5	1102	24.5	
	Std. Dev.	32	4.6	3	0.4	94	2.1	
EPON 828	ALEX 10	386	56.0	28	4.1	1934	43.0	
	11	-	-	-	-	-	-	
	12	-	-	30	4.4	2294	51.0	
	13	407	59.0	28	4.0	1754	39.0	
	14	359	52.0	32	4.6	-	-	
	Average	384	55.7	30	4.3	1979	44.0	
	Std. Dev.	24	3.5	2	0.3	270	6.0	
PVA	ALEX 20	359	52.0	25	3.6	1934	43.0	
	23	352	51.0	32	4.6	-	-	
	24	379	55.0	25	3.6	2069	46.0	
		Average	363	52.7	27	3.9	2001	44.5
		Std. Dev.	15	2.1	4	0.6	94	2.1

Table A48

- Continued -

Fiber Sizing	Specimen No.	Ultimate Strength (MPa)	Ultimate Strength (ksi)	Dynamic Modulus (GPa)	Dynamic Modulus (Msi)	Total Energy (kJ/m <sup>3</sup> )	Total Energy (ft-lb/in <sup>3</sup> )
Polysulfone	ALEX 30	352	51.0	35	5.1	1619	36.0
	31	365	53.0	30	4.4	1574	35.0
	32	359	52.0	34	4.9	1034	23.0
	33	317	46.0	28	4.1	-	-
	Average	348	50.5	34	4.6	1408	31.3
	Std. Dev.	21	3.1	3	0.5	324	7.2

Table A49

## Individual AS4/3501-6 Single Fiber Pullout Test Results

Fiber Sizing	Specimen No.	Fiber Diameter		Embedded Length		Interfacial Shear Strength	
		( $\mu\text{m}$ )	( $10^{-4}$ in)	(mm)	( $10^{-3}$ in)	(MPa)	(ksi)
Unsize	AFRY 01	7.4	2.9	94	3.7	55*	7.9*
	02	8.6	3.4	91	3.6	36	5.2
	03	7.9	3.1	-	-	-	-
	04	8.6	3.4	109	4.3	26	3.7
	05	8.6	3.4	89	3.5	37	5.3
	06	8.6	3.4	91	3.6	21*	3.1*
	Average		8.4	3.3	94	3.7	33
Std. Dev.		0.5	0.2	8	0.3	6	0.9
PVA	AERY 20	7.9	3.1	130	5.1	36	5.2
	21	9.7*	3.8*	173*	6.8*	19*	2.7*
	22	6.9	2.7	104*	4.1*	34	4.9
	23	7.4	2.9	135	5.3	28	4.0
	Average		7.4	2.9	132	5.2	32
Std. Dev.		0.5	0.2	4	0.1	4	0.6
Polysulfone	AERY 30	8.6	3.4	58*	2.3*	45	6.5
	31	7.4	2.9	97	3.8	43	6.3
	32	8.6	3.4	71	2.8	41	5.9
	33	8.6	3.4	84	3.3	37	5.4
	Average		8.3	3.3	84	3.3	42
Std. Dev.		0.6	0.3	13	0.5	3	0.5

---

\*Not included in average

Table A50

## Individual AS4/4001 Single Fiber Pullout Test Results

Fiber Sizing	Specimen No.	Fiber Diameter		Embedded Length		Interfacial Shear Strength	
		( $\mu\text{m}$ )	( $10^{-4}\text{in}$ )	(mm)	( $10^{-3}\text{in}$ )	(MPa)	(ksi)
Unsize	AERZ 00	10.2*	4.0*	173	6.8	18	2.6
	01	8.6	3.4	218	8.6	19	2.7
	02	8.6	3.4	86*	3.4*	37*	5.3
	03	7.9	3.1	211	8.3	24	3.5
	Average	8.4	3.3	201	7.9	20	2.9
	Std. Dev.	0.4	0.2	24	1.0	3	0.5
PVA	AERZ 20	8.6	3.4	196	7.7	17	2.5
	21	9.7	3.8	185	7.3	16	2.3
	22	9.7	3.8	66*	2.6*	31*	4.5*
	23	7.4*	2.9*	127	5.0	16	2.3
	Average	9.3	3.7	169	6.7	16	2.4
	Std. Dev.	0.6	0.2	37	1.5	1	0.1
Polysulfone	AERZ 33	9.7	3.8	81	3.2	48	6.9
	34	7.9	3.1	122	4.8	33	4.8
	Average	8.9	3.5	102	4.0	40	5.9
	Std. Dev.	-	-	-	-	-	-

---

\*Not included in average

Table A51

## Individual AS4/F155 Single Fiber Pullout Test Results

Fiber Sizing	Specimen No.	Fiber Diameter		Embedded Length		Interfacial Shear Strength	
		( $\mu\text{m}$ )	( $10^{-4}\text{in}$ )	(mm)	( $10^{-3}\text{in}$ )	(MPa)	(ksi)
Polysulfone	AERX 30	8.6	3.4	89	3.5	54*	7.8*
	31	8.6	3.4	178	7.0	23	3.3
	32	8.6	3.4	79	3.1	23	3.4
	33	8.6	3.4	170	6.7	17	2.5
	Average	8.6	3.4	130	5.1	21	3.1
	Std. Dev.	0.0	0.0	52	2.1	3	0.5

---

\*Not included in average





APPENDIX B

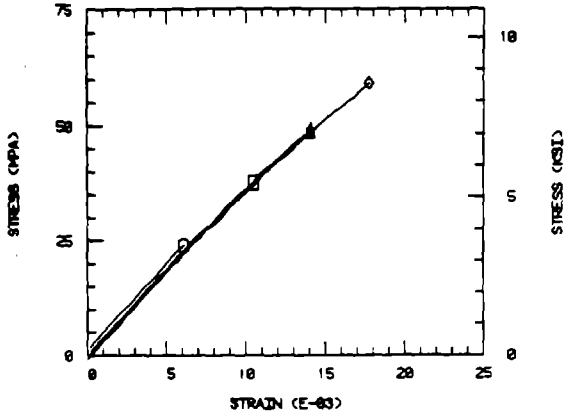
INDIVIDUAL DATA PLOTS

Preceding Page Blank

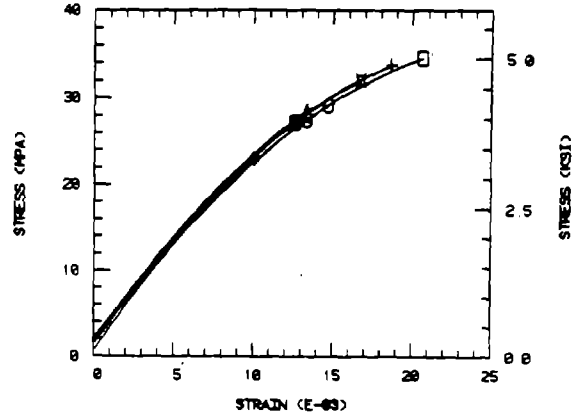
ANK NOT



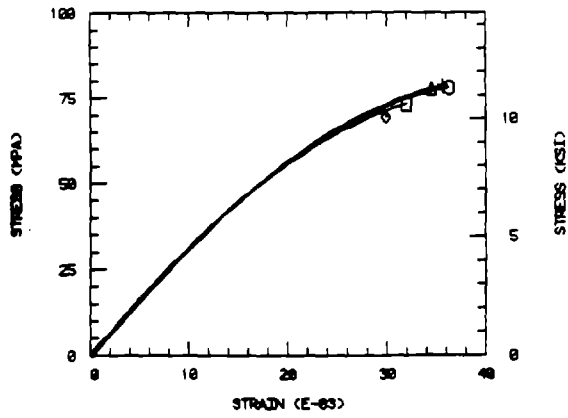
N. RESIN TEN. R. T., DRY 4001



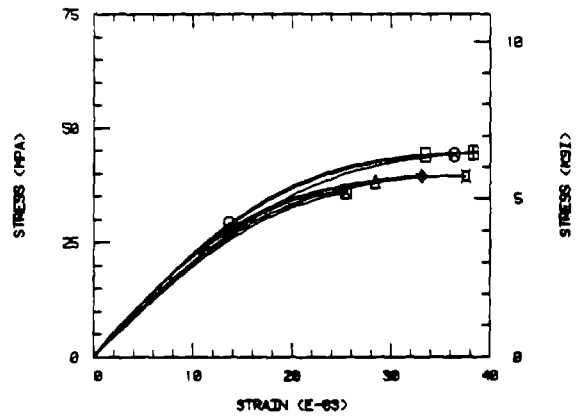
N RESIN TENSION ELV TEMP 4001



N RESIN TENSION R T F155



N RESIN TENSION ELV TEMP F155

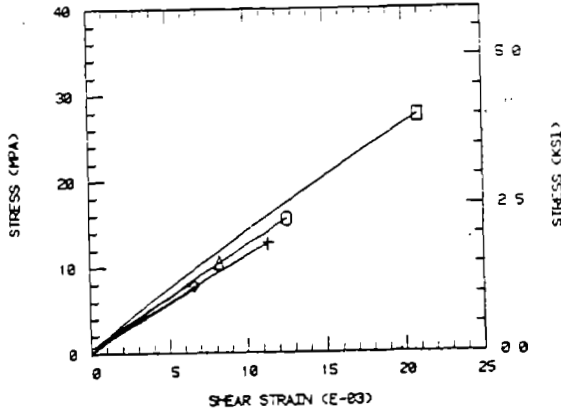


Neat Resin Uniaxial Tension

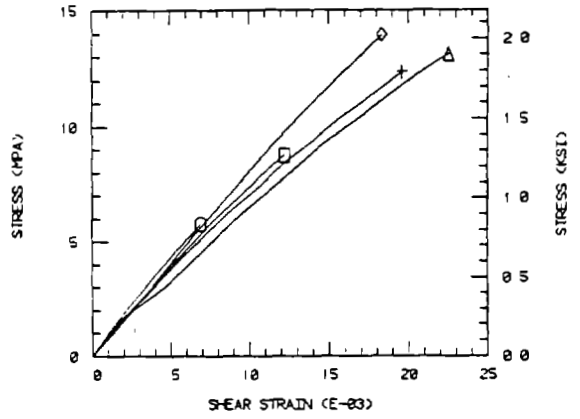
Preceding Page Blank

ORIGINAL PAGE IS  
OF POOR QUALITY

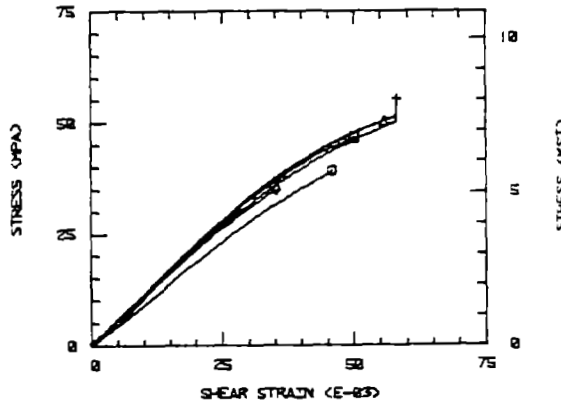
IOSIPESCU SHEAR R T DRY 4001



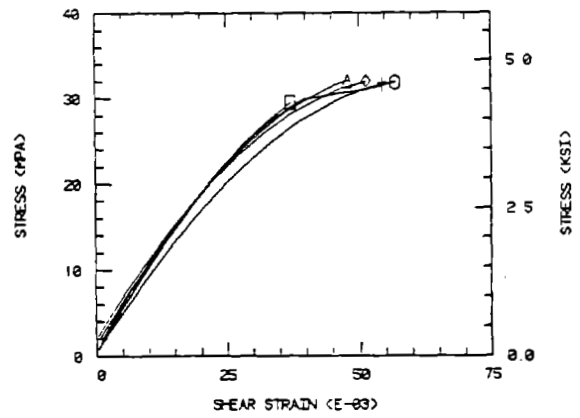
IOSIPESCU SHEAR ELV TEMP, WET 4001



F155 IOSIPESCU SHEAR ROOM TEMP, DRY

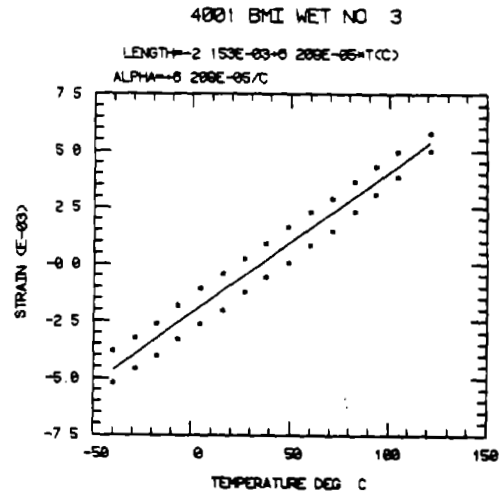
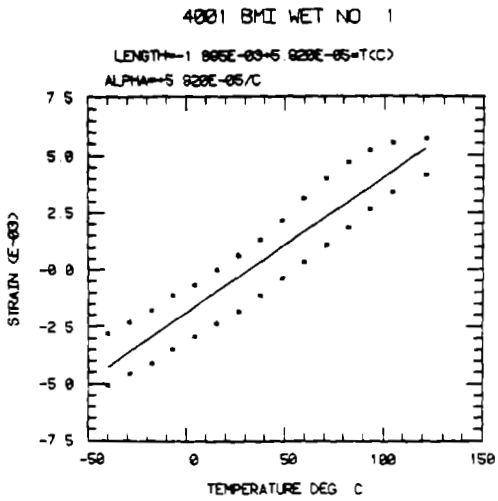
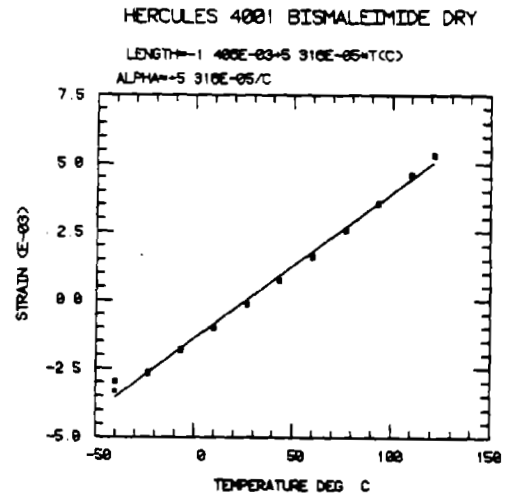
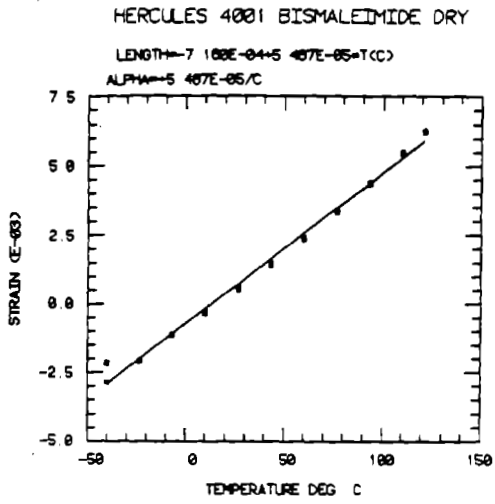


IOSIPESCU SHEAR ELV TEMP, WET F155

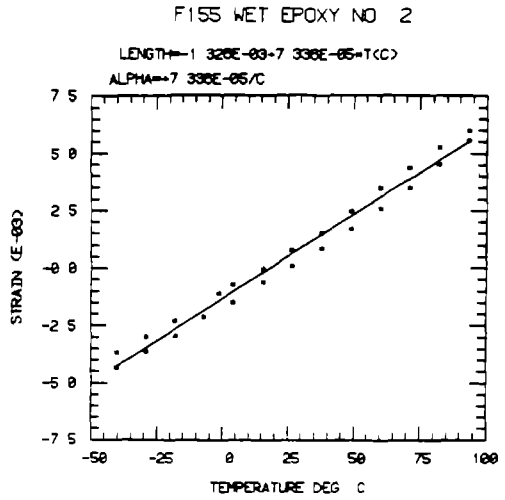
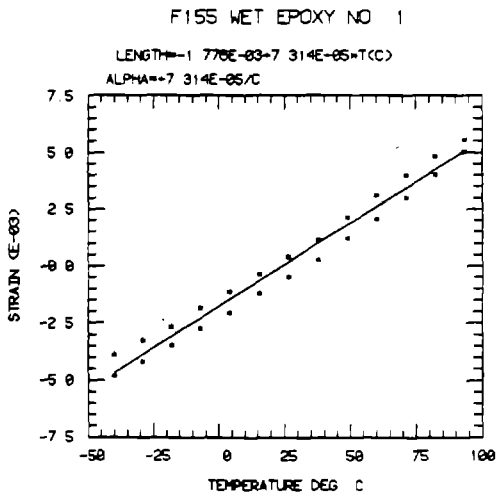
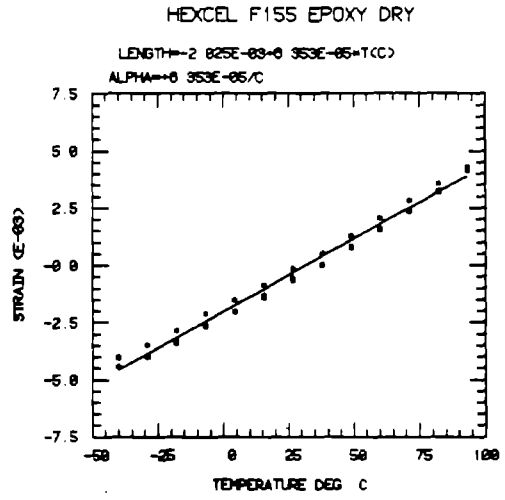
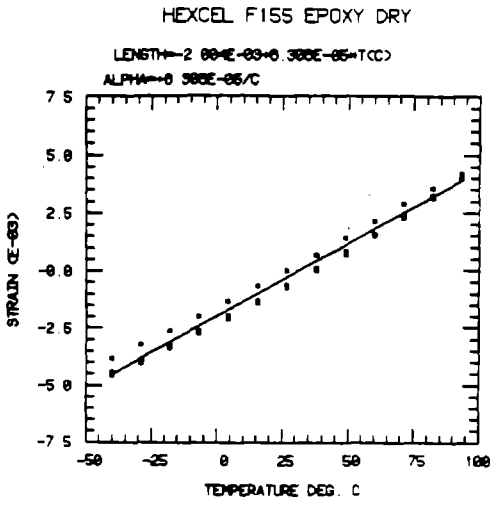


Neat Resin Iosipescu Shear

ORIGINAL PAGE IS  
OF POOR QUALITY

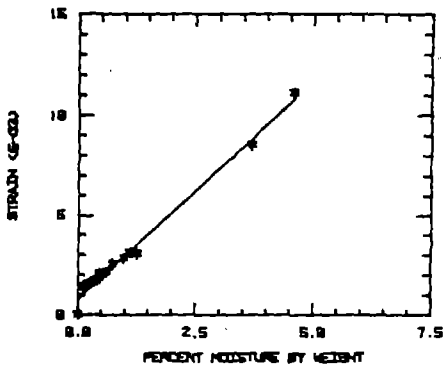


Hercules 4001 Bismaleimide Neat Resin Thermal Expansion

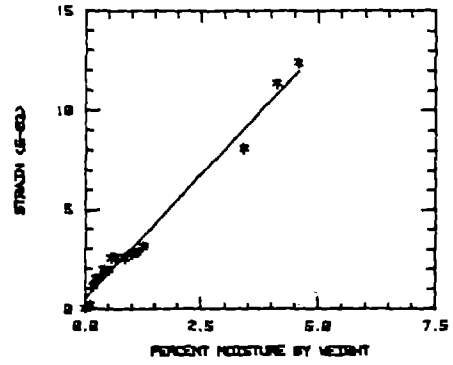


Hexcel F155 Rubber-Toughened Epoxy Neat Resin Thermal Expansion

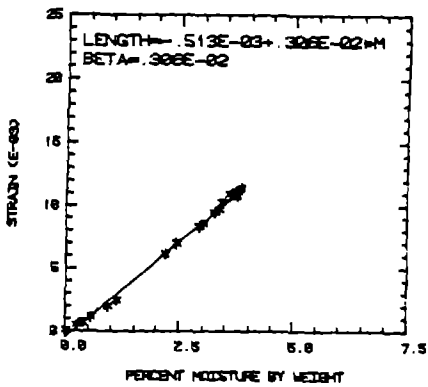
HERCULES 4001 BISMALTIMIDE NO. 1



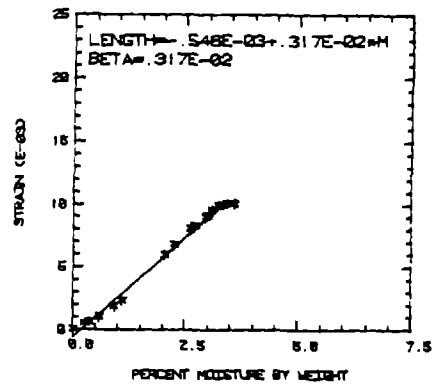
HERCULES 4001 BISMALTIMIDE NO. 2



SPECIMEN-1 FISS

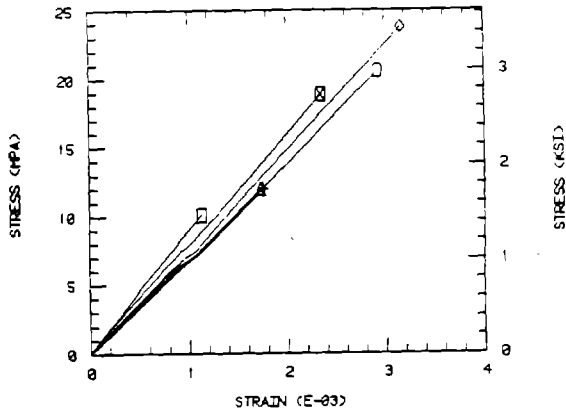


SPECIMEN-2 FISS

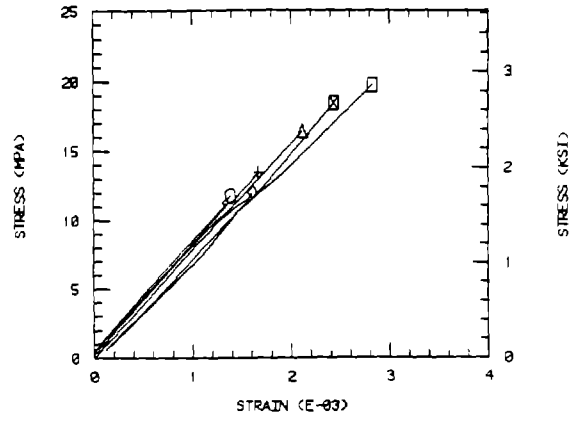


Neat Resin Moisture Expansion

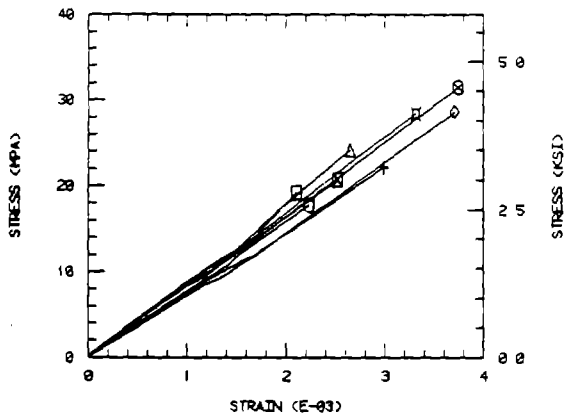
TRAN TENSION TENSILE, DRY 3501-6 UNSIZED



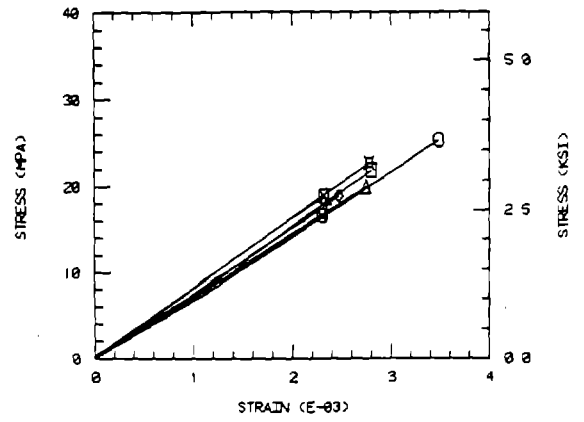
TRAN TENSION TENSILE, DRY 3501-6 828



TRAN TENSION TENSILE, DRY 3501-6 PVA



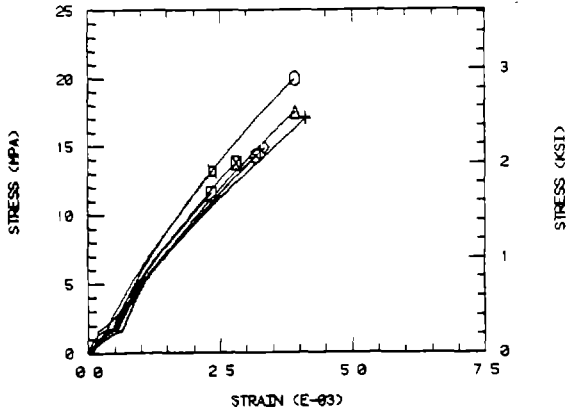
TRAN TENSION TENSILE, DRY 3501-6 P-SULFON



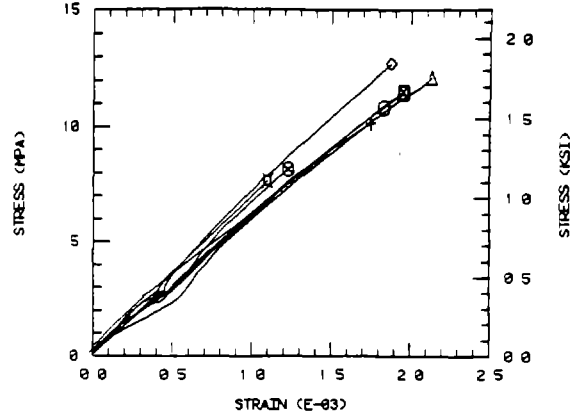
Unidirectional Composite Transverse Tension



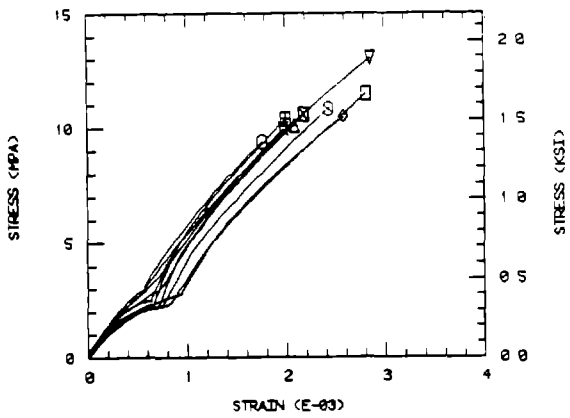
TRAN TEN ELV TEMP, WET 3501-6 UNSIZED



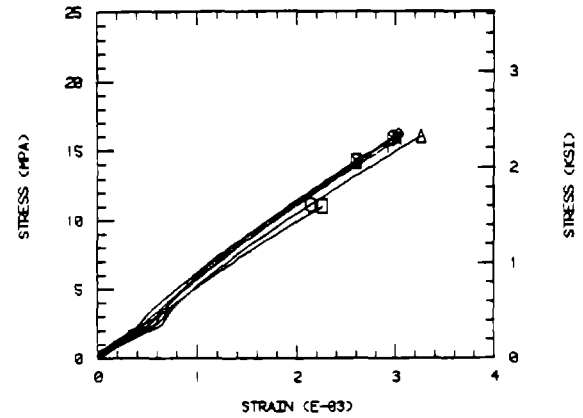
TRAN TEN ELV TEMP, WET 3501-6 828



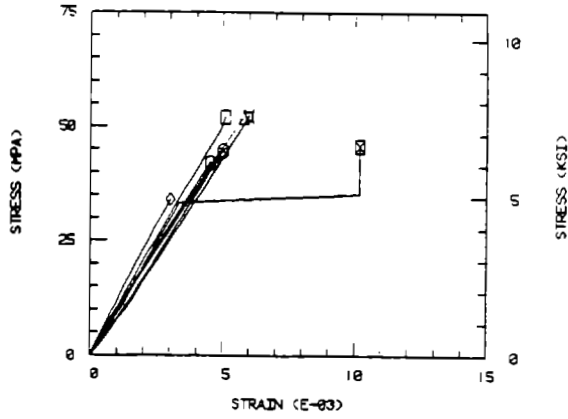
TRAN TEN ELV TEMP, WET 3501-6 PVA



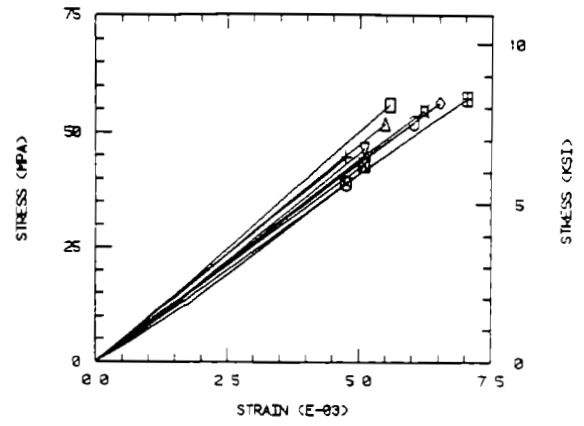
TRAN TEN ELV TEMP, WET 3501-6 P-SULFONE



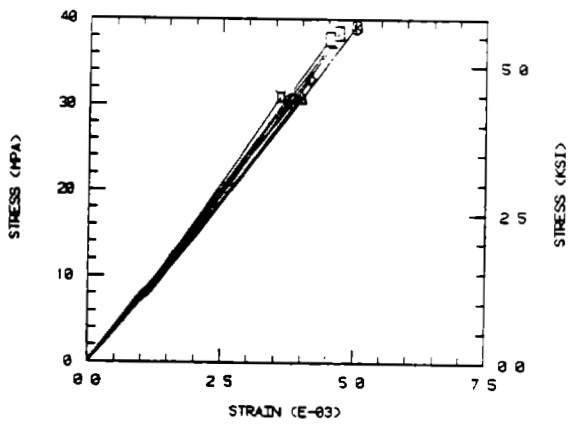
TRAN TEN R T , DRY 4001 UNSIZED



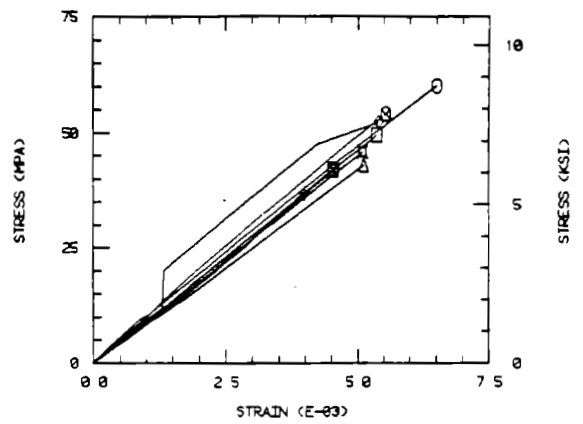
TRAN TEN R T , DRY 4001 828



TRAN TEN R T , DRY 4001 PVA

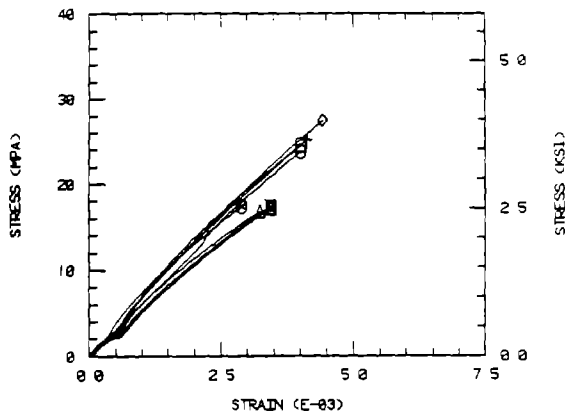


TRAN TEN R T , DRY 4001 P-SULFON

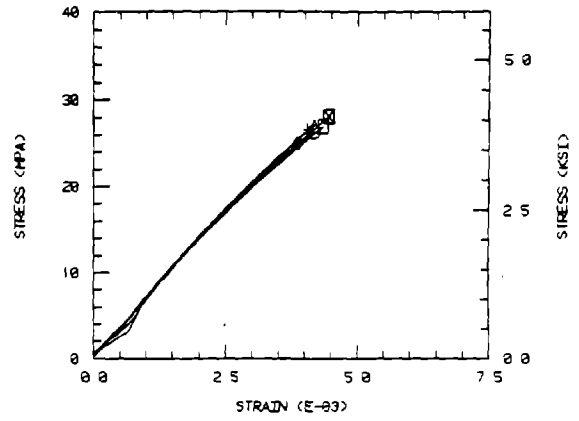


ORIGINAL PAGE IS  
OF POOR QUALITY

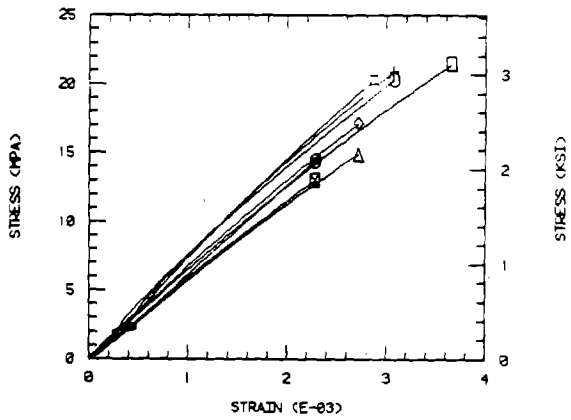
TRAN TEN ELV TEMP, WET 4001 UNSIZED



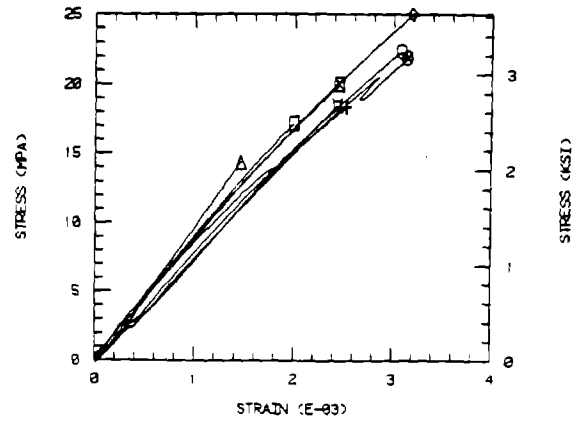
TRAN TEN ELV TEMP, WET 4001 SLS



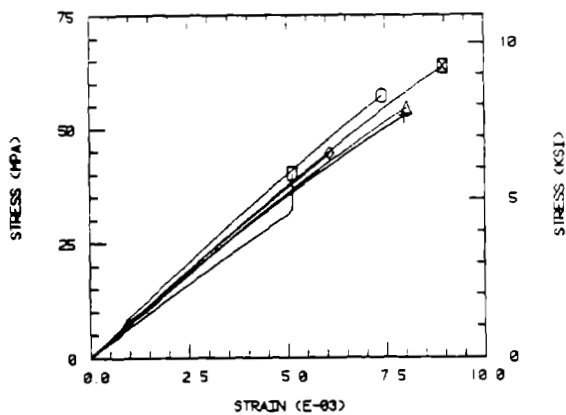
TRAN TEN ELV TEMP, WET 4001 PVA



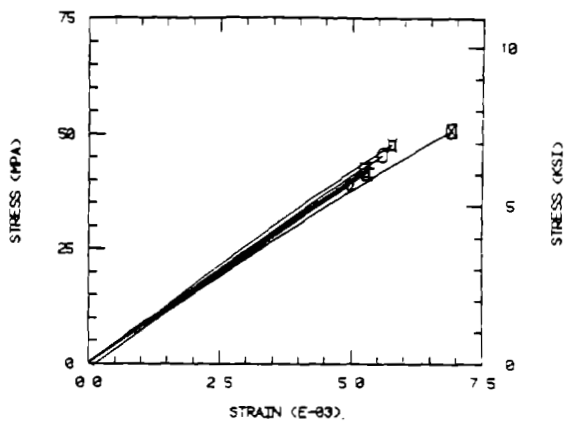
TRAN TEN ELV TEMP, WET 4001 P-SULFONE



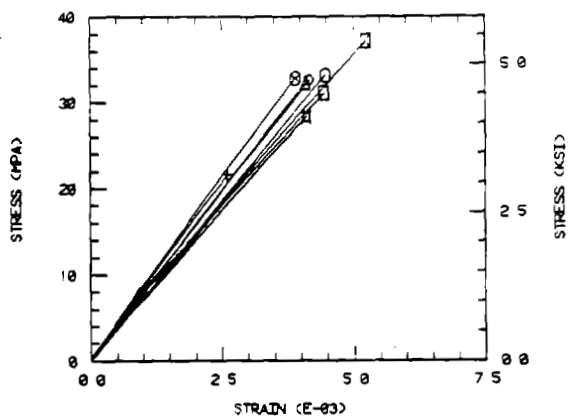
TRAN TEN R T , DRY FISS UNSIZED



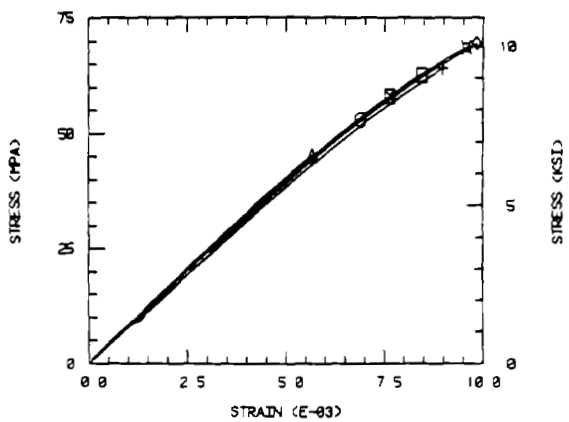
TRAN TEN R T , DRY FISS 828



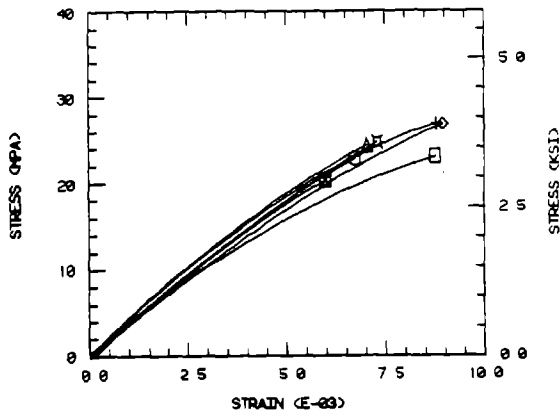
TRAN TEN R T , DRY FISS PVA



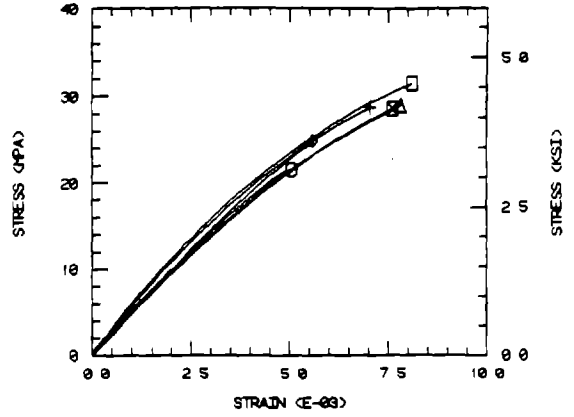
TRAN TEN R T , DRY FISS P-SULFON



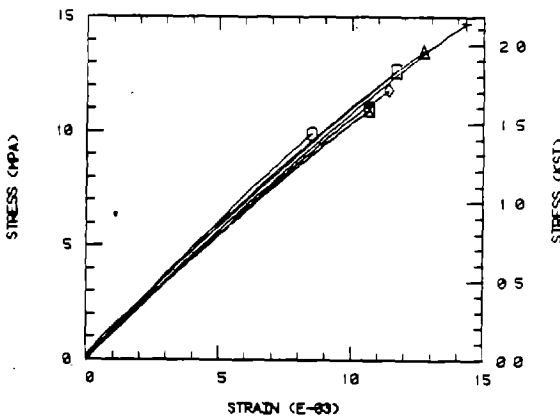
TRAN TEN ELV TEMP, WET FISS UNSIZED



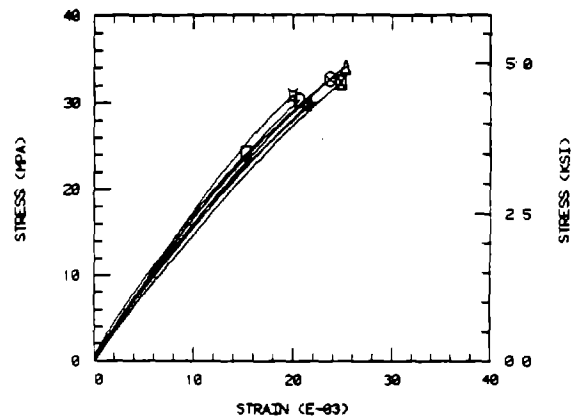
TRAN TEN ELV TEMP, WET FISS 828



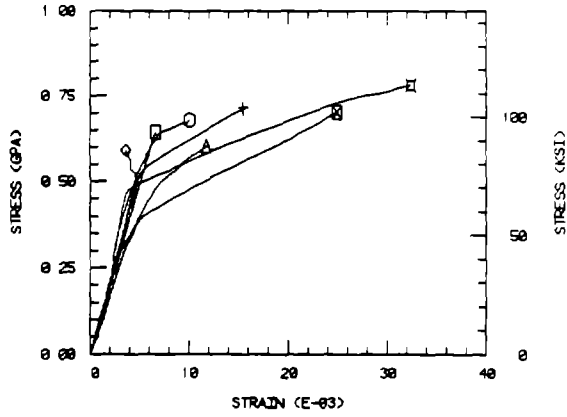
TRAN TEN ELV TEMP FISS PVA



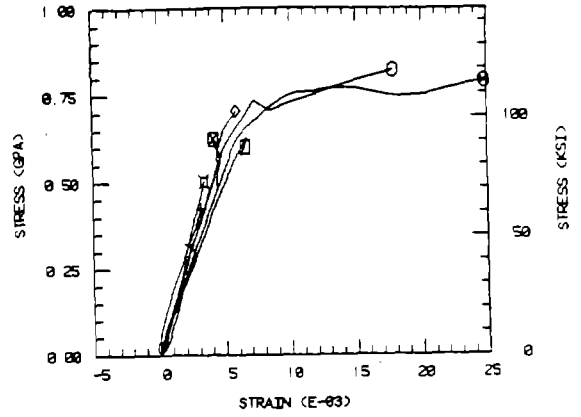
TRAN TEN ELV TEMP, WET FISS P-SULFONE



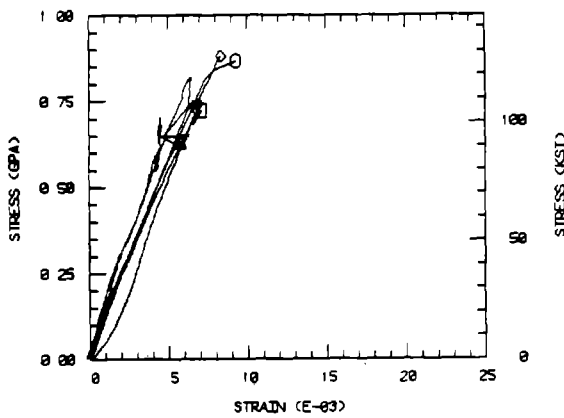
AXIAL COMP R T , DRY, 3501-6, UNSIZED



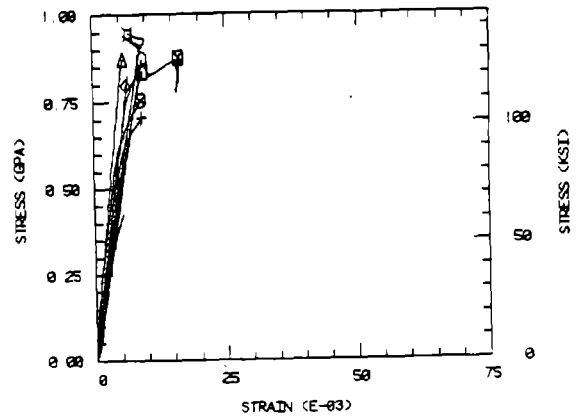
AXIAL COMP R T , DRY, 3501-6, 828



AXIAL COMP R T , DRY, 3501-6, PVA



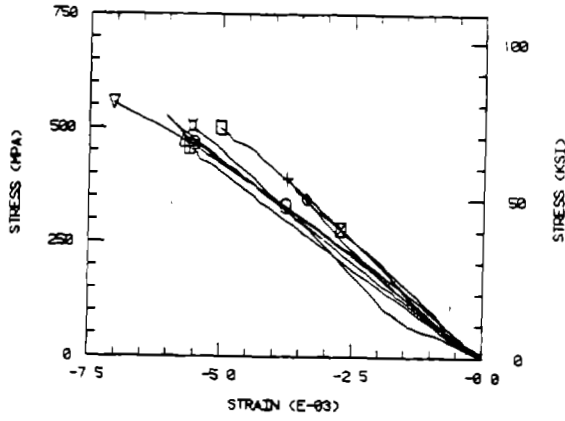
AXIAL COMP R T , DRY, 3501-6, P-SULFON



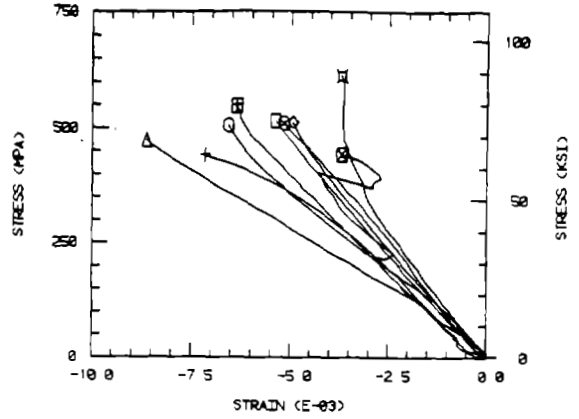
Unidirectional Composite Axial Compression

ORIGINAL PAGE IS  
OF POOR QUALITY

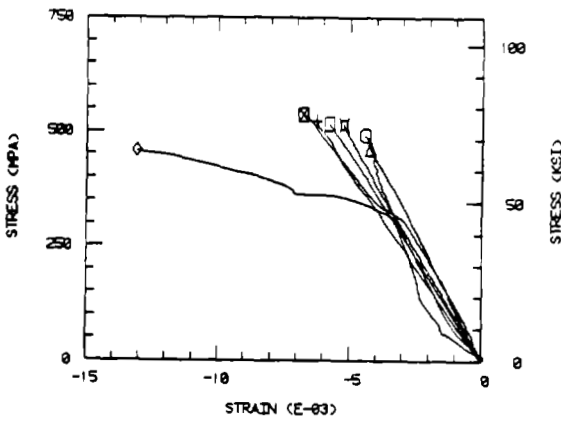
AXIAL COMP ELV TEMP ,WET 3501-6 UNSIZE



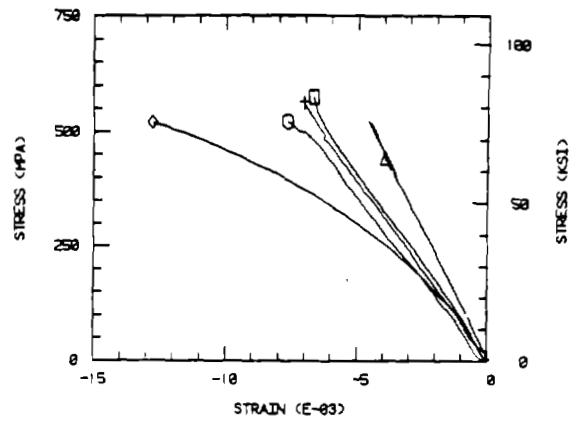
AXIAL COMP ELV TEMP ,WET 3501-6 828



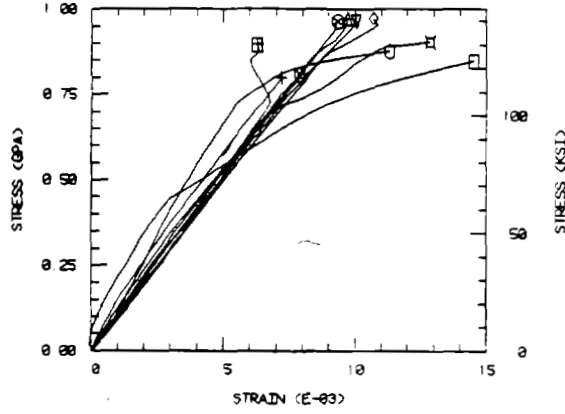
AXIAL COMP ELV TEMP ,WET 3501-6 PVA



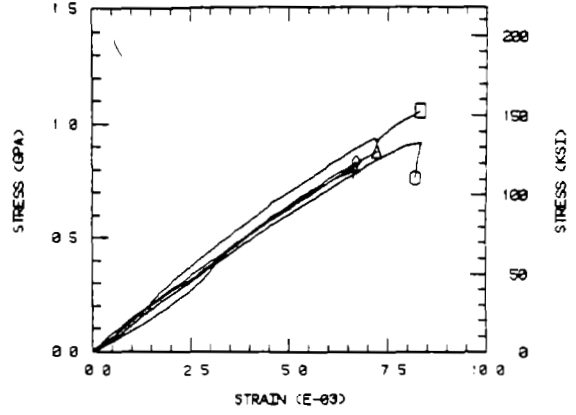
AXIAL COMP ELV TEMP WET 3501-6 P-SULFO



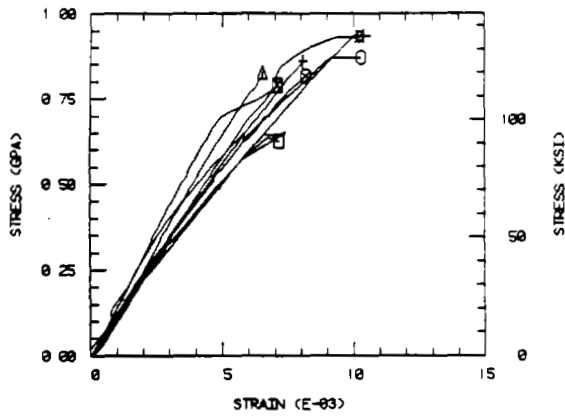
AXIAL COMP R T , DRY, 4001, UNSIZED



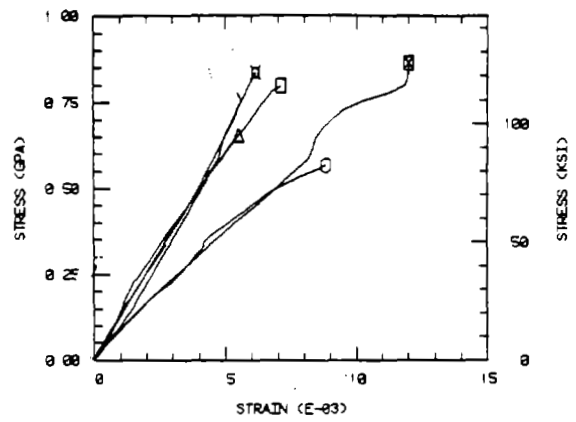
AXIAL COMP R T , DRY, 4001, 828



AXIAL COMP R T , DRY, 4001, PVA

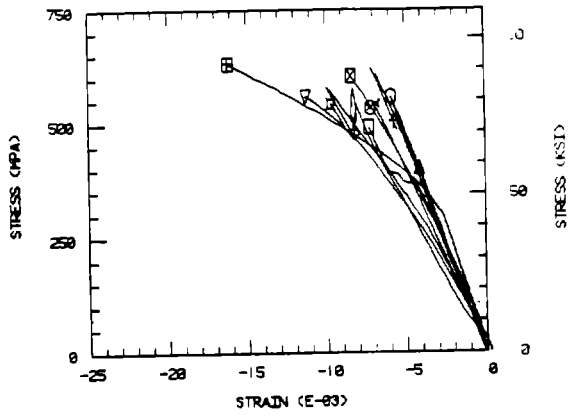


AXIAL COMP R T , DRY, 4001, P-SULFON

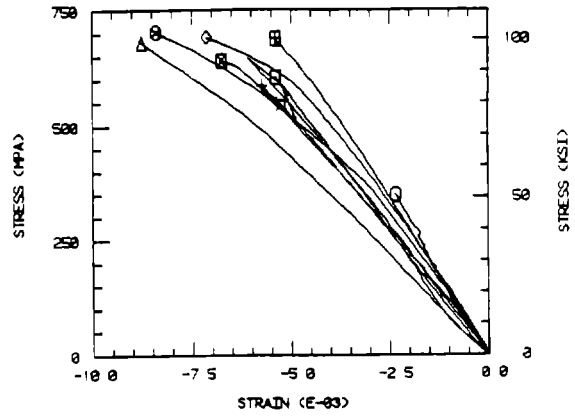




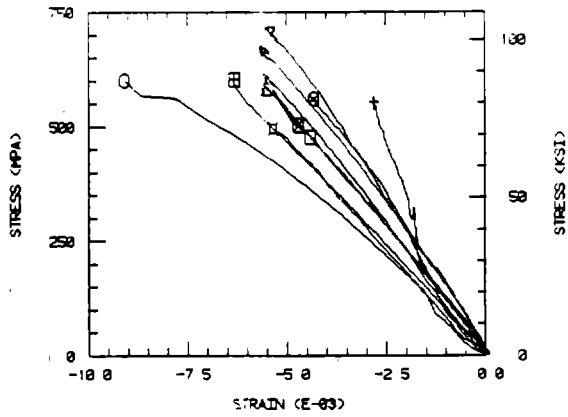
AXIAL COMP ELV TEMP ,WET 4001 UNSIZED



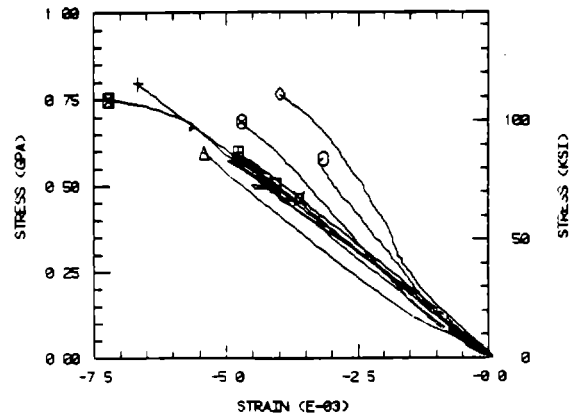
AXIAL COMP ELV TEMP ,WET 4001 828



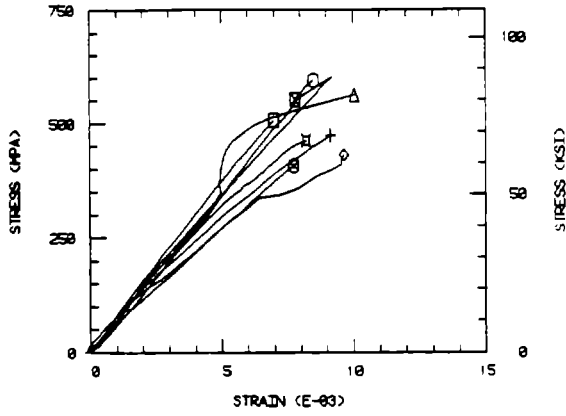
AXIAL COMP ELV TEMP ,WET 4001 PVA



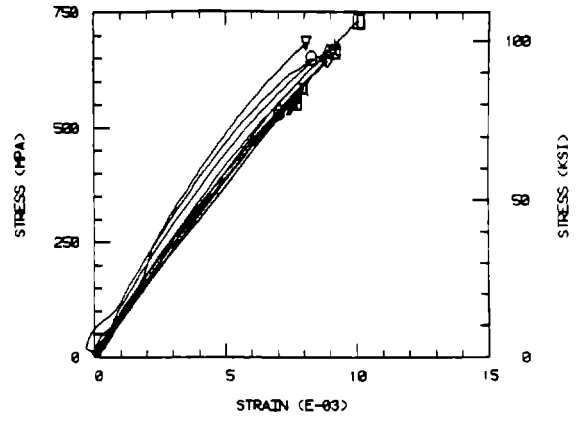
AXIAL COMP ELV TEMP ,WET 4001 P-SULFON



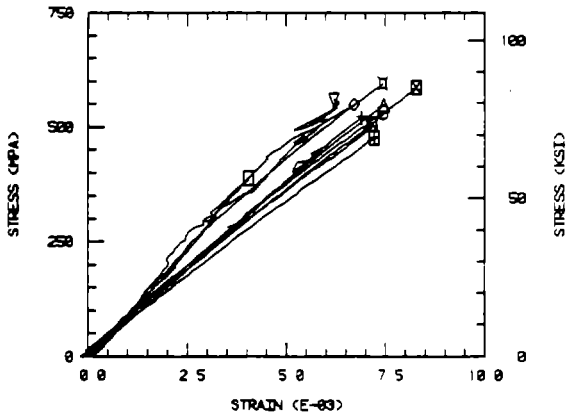
AXIAL COMP R T , DRY, F155 UNSIZED



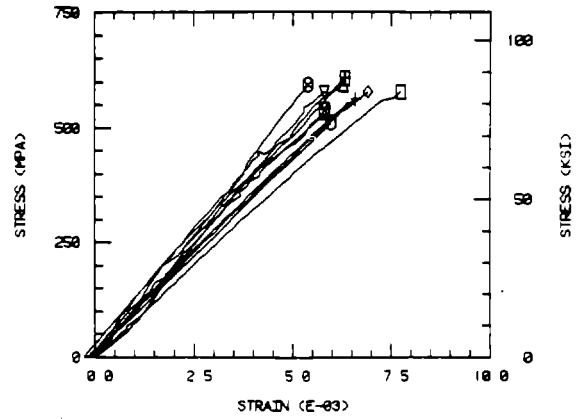
AXIAL COMP R T , DRY, F155, 828



AXIAL COMP R T , DRY, F155, PVA

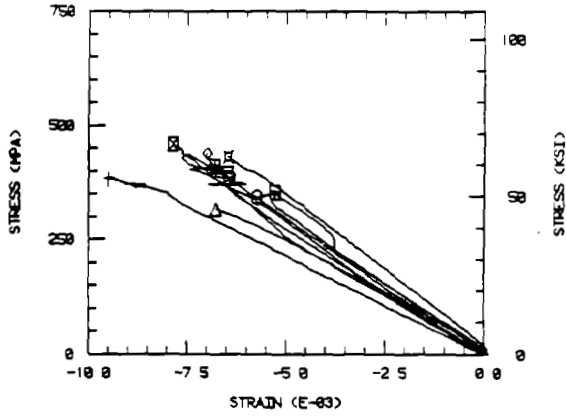


AXIAL COMP R T , DRY, F155, P-SULFON

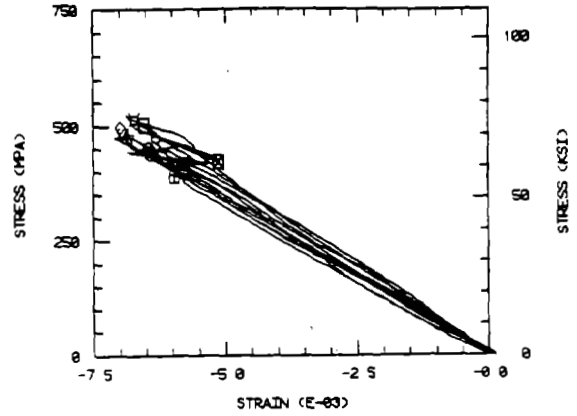


ORIGINAL PAGE IS  
OF POOR QUALITY

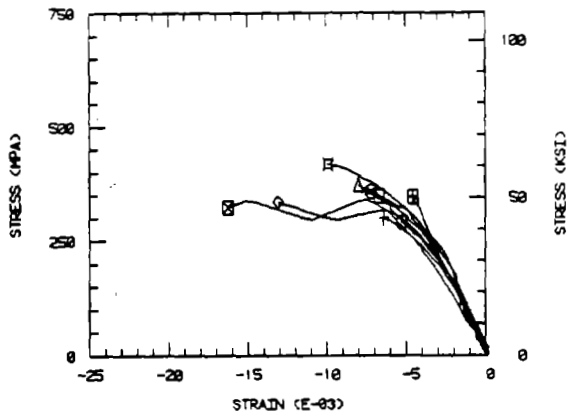
AXIAL COMP ELV TEMP ,WET F155 UNSIZED



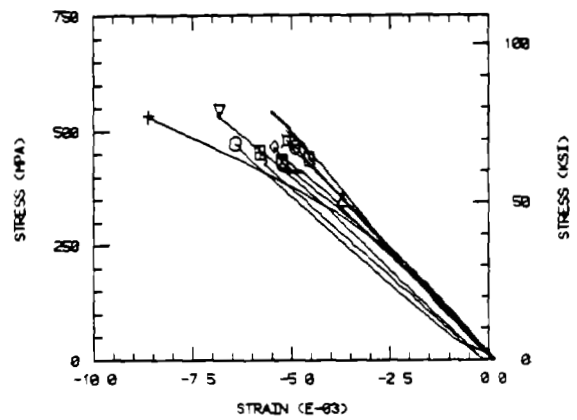
AXIAL COMP ELV TEMP ,WET F155 828



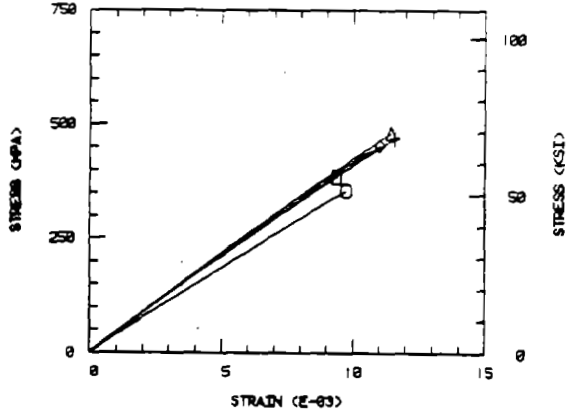
AXIAL COMP ELV TEMP ,WET F155 PVA



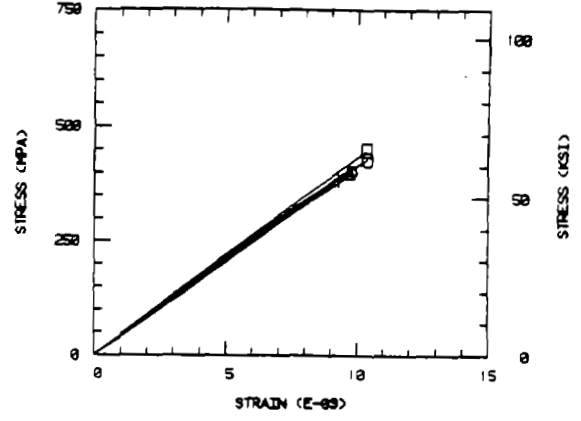
AXIAL COMP ELV TEMP ,WET F155 P-SULFON



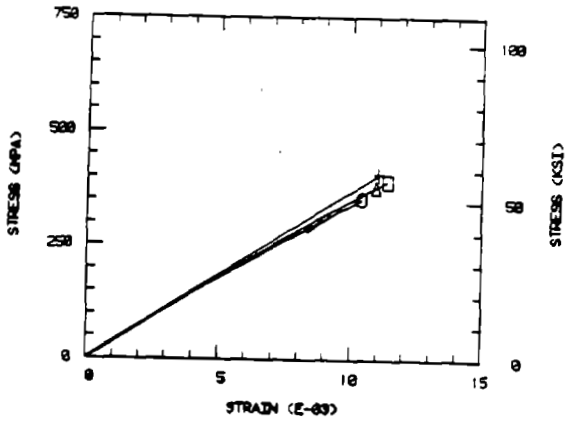
LAM TEN R T , DRY 3501-6 UNSIZED



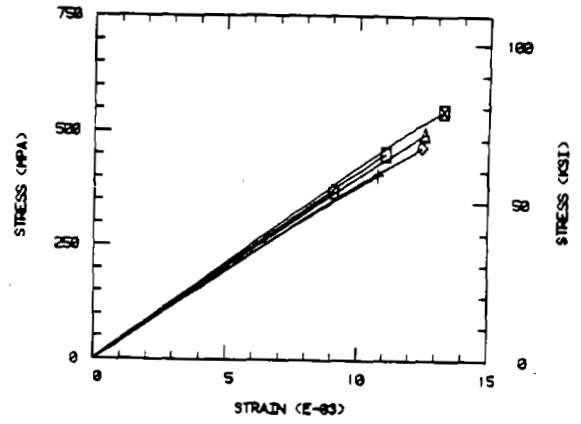
LAM TEN R T , DRY 3501-6 828



LAM TEN R T , DRY 3501-6 PVA



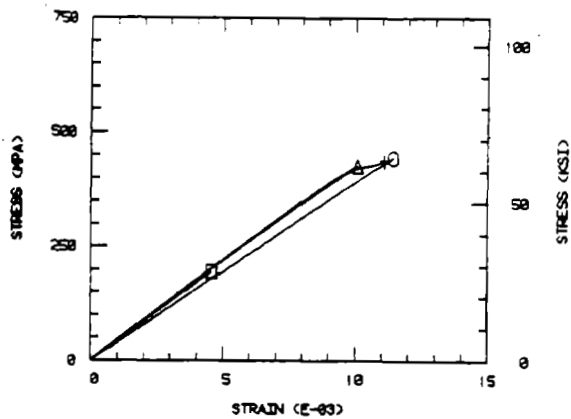
LAM TEN R T , DRY 3501-6 P-SULFON



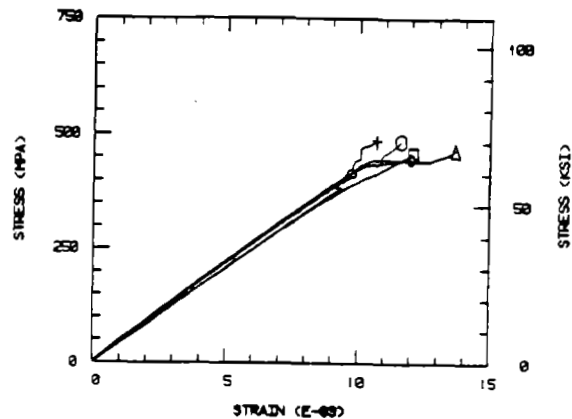
Quasi-Isotropic Laminate Axial Tension

ORIGINAL PAGE IS  
OF POOR QUALITY.

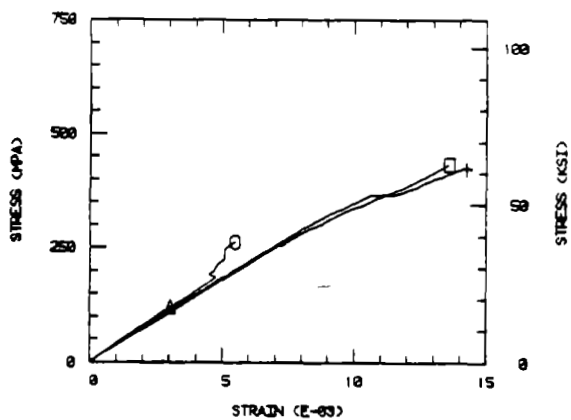
LAM TEN ELV TEMP ,WET 3501-6 UNSIZED



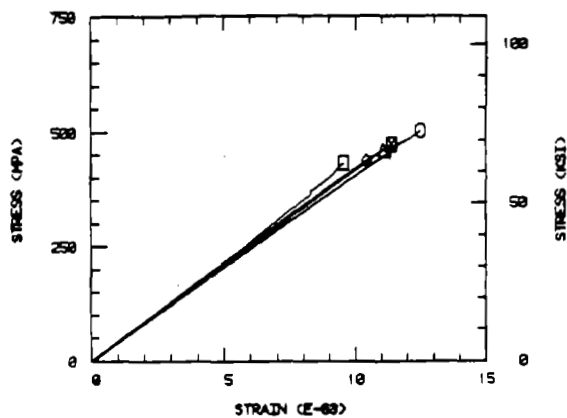
LAM TEN ELV TEMP ,WET 3501-6 828



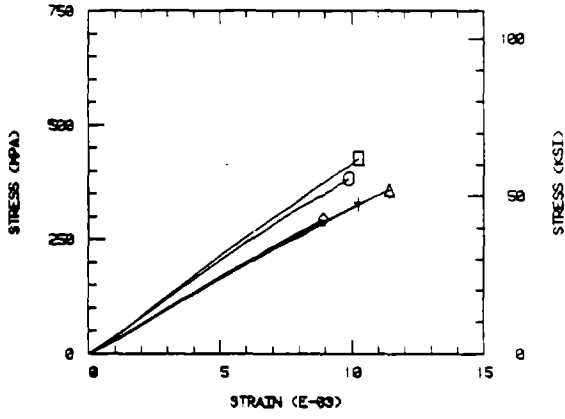
LAM TEN ELV TEMP ,WET 3501-6 PVA



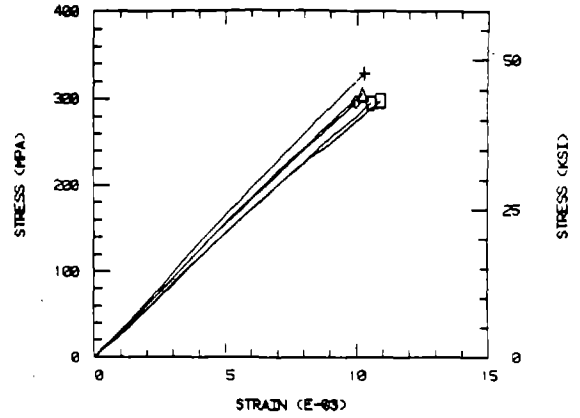
LAM TEN ELV TEMP ,WET 3501-6 P-SULFON



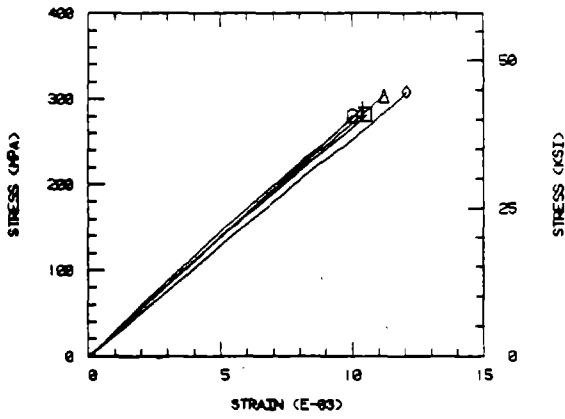
LAM TEN R T , DRY 4001 UNSIZED



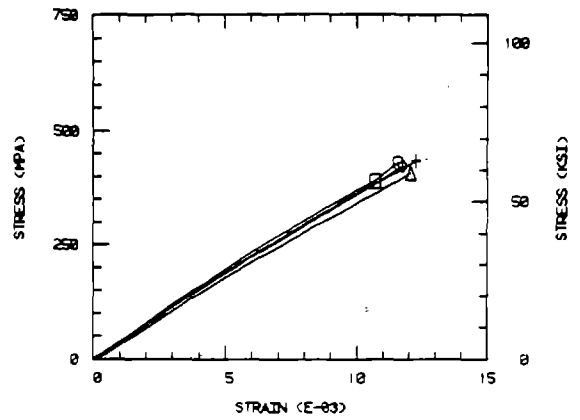
LAM TEN R T , DRY 4001 828



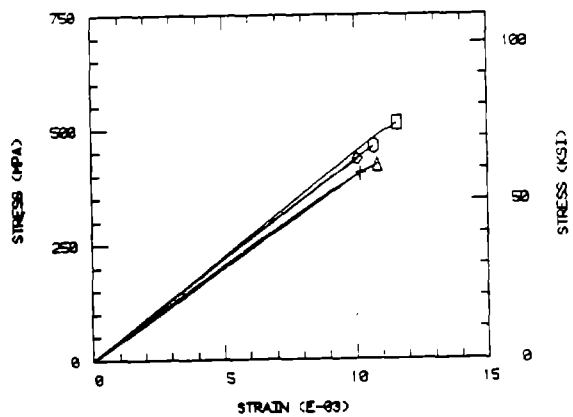
LAM TEN R T , DRY 4001 PVA



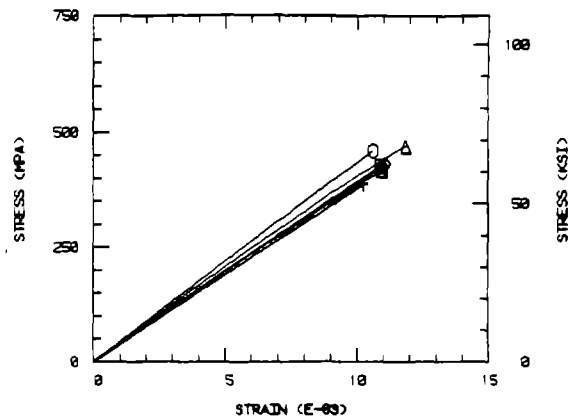
LAM TEN R T , DRY 4001 P-SULFON



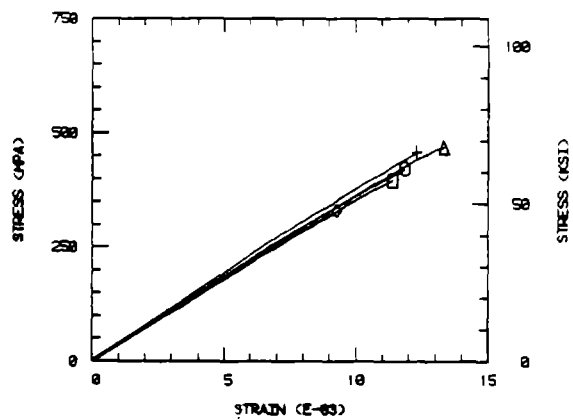
LAM TEN ELV TEMP ,WET 4001 UNSIZED



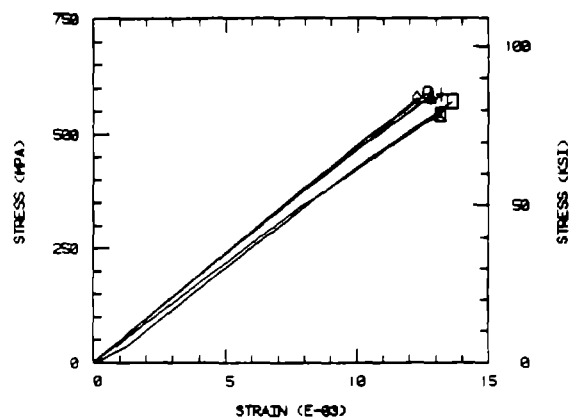
LAM TEN ELV TEMP ,WET 4001 828



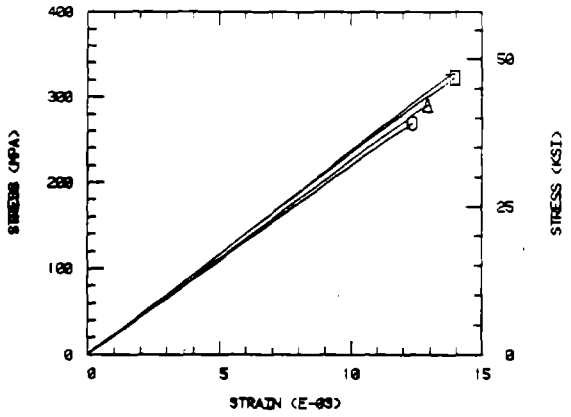
LAM TEN ELV TEMP ,WET 4001 PVA



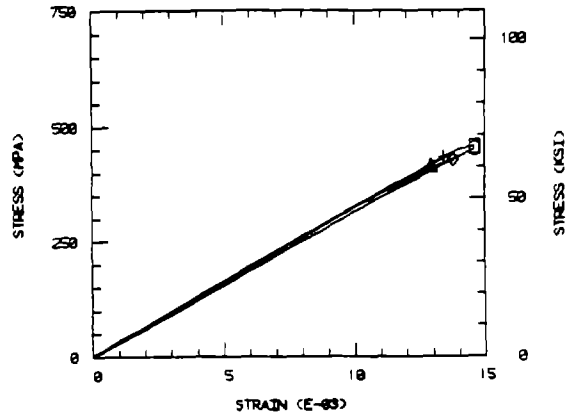
LAM TEN ELV TEMP ,WET 4001 P-SULFON



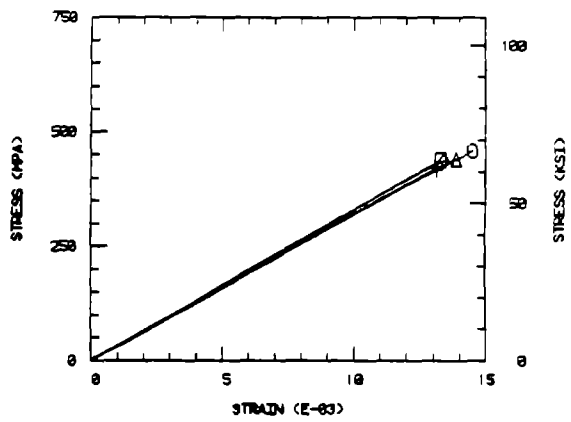
LAM TEN R T , DRY F155 UNSIZED



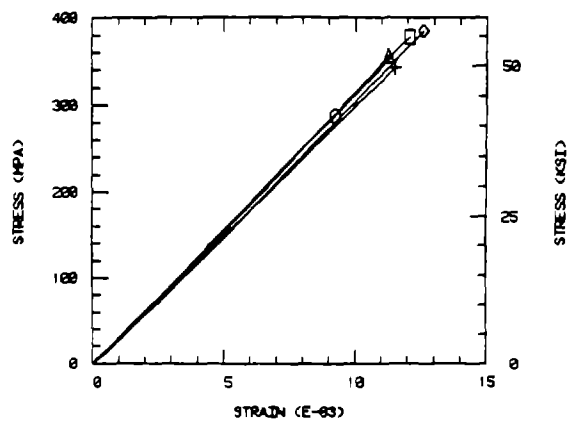
LAM TEN R T , DRY F155 828



LAM TEN R T , DRY F155 PVA



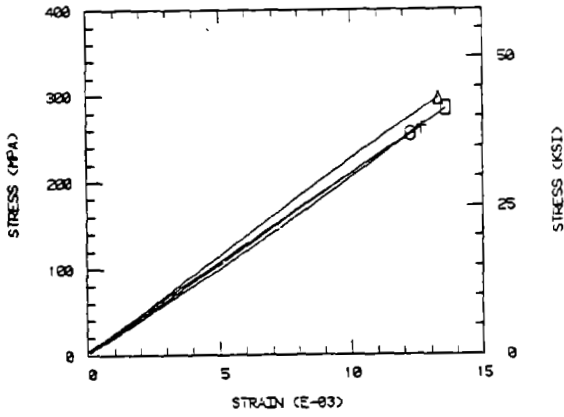
LAM TEN R T , DRY F155 P-SULFON



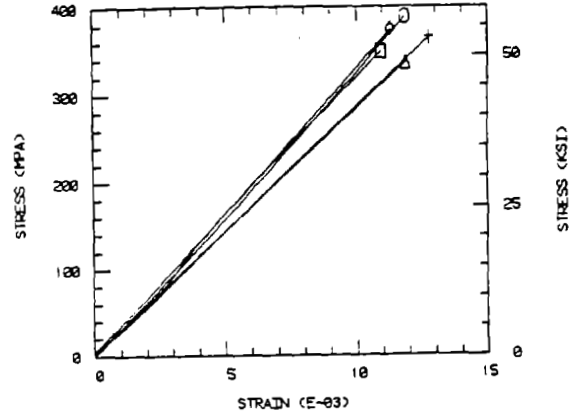


ORIGINAL PAGE IS  
OF POOR QUALITY

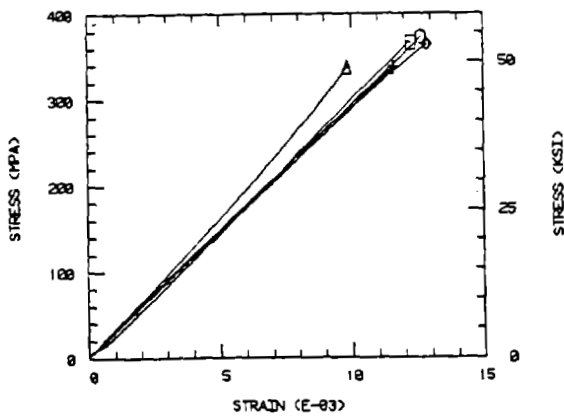
LAM TEN ELV TEMP WET F155 UNSIZED



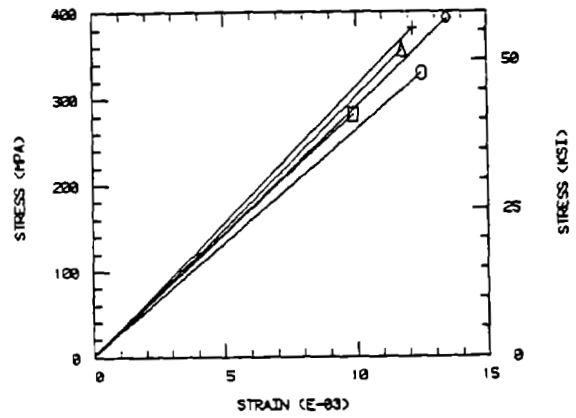
LAM TEN. ELV. WET F155 828



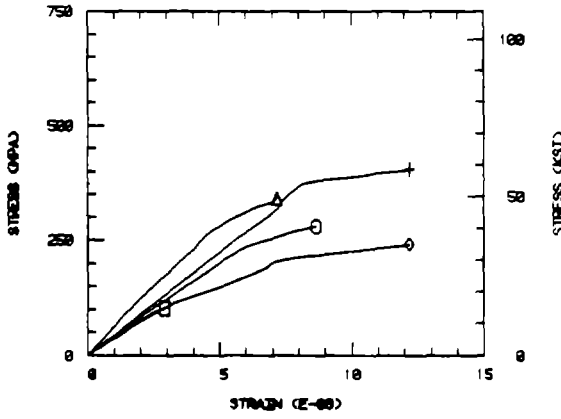
LAM TEN ELV TEMP WET F155 PVA



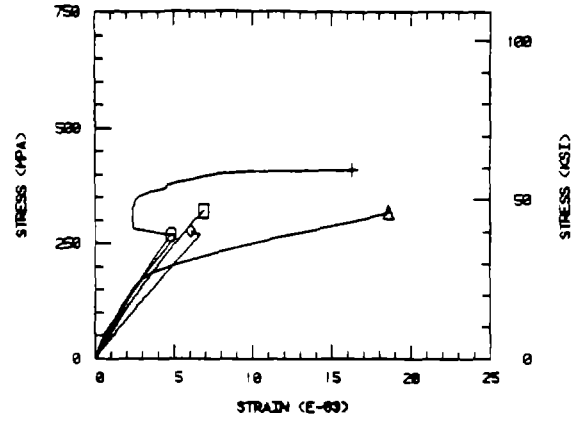
LAM TEN. ELV. TEMP. WET F155 P-SULFON



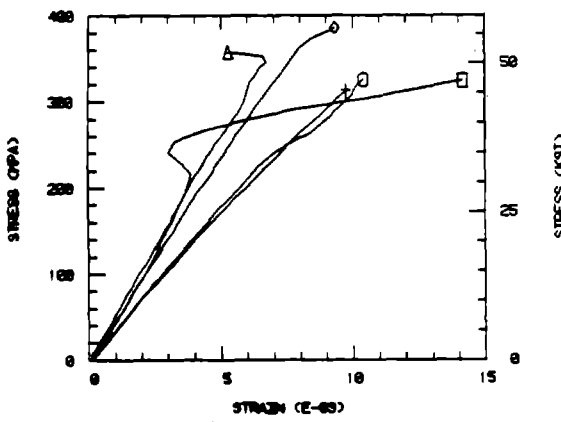
LAM COMP R T , DRY, 3501-6, UNSIZED



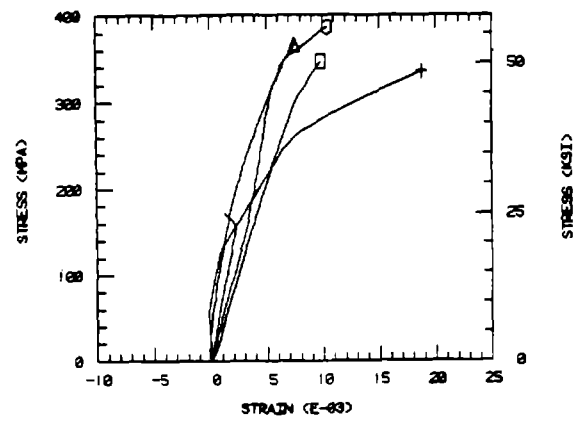
LAM COMP R T , DRY, 3501-6, 828



LAM COMP R T , DRY, 3501-6, PVA



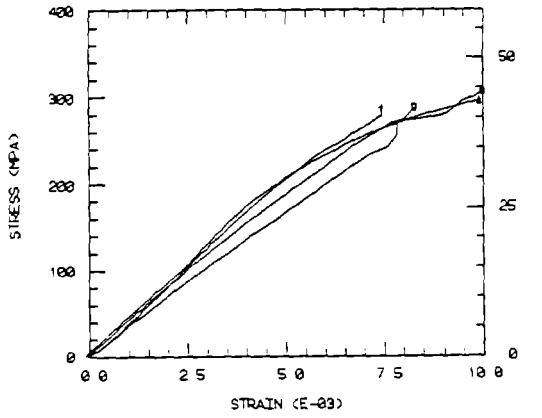
LAM COMP R T , DRY, 3501-6, P-SULFON



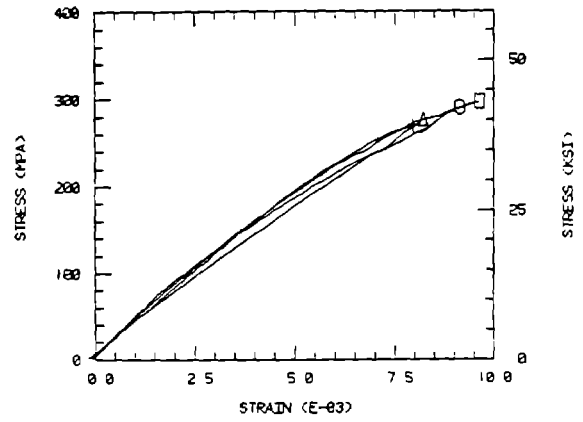
Quasi-Isotropic Laminate Axial Compression

ORIGINAL PAGE IS  
OF POOR QUALITY

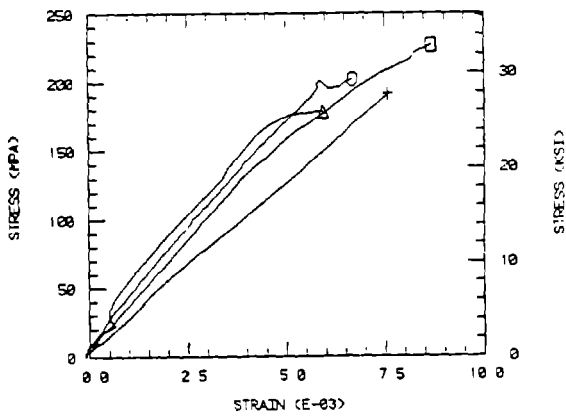
LAM COMP 3501-6 UNSIZED, ELV TEMP, WET



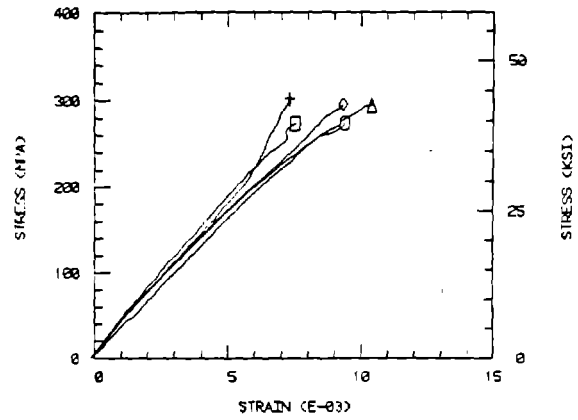
LAM COMP ELV TEMP ,WET 3501-6 828



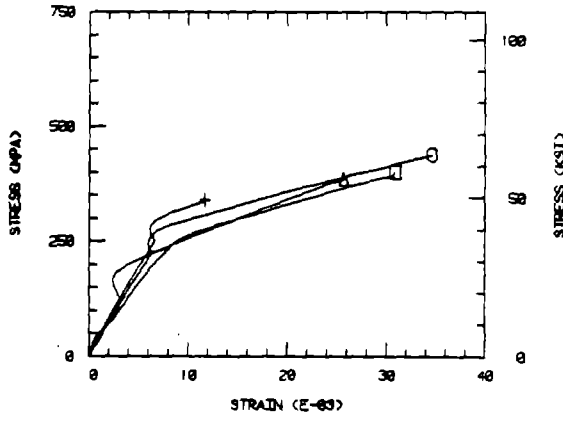
LAM COMP ELV TEMP ,WET 3501-6 PVA



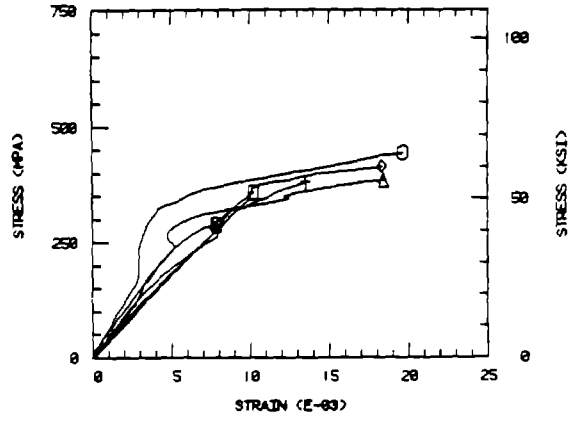
LAM COMP ELV TEMP ,WET 3501-6 P-SULFON



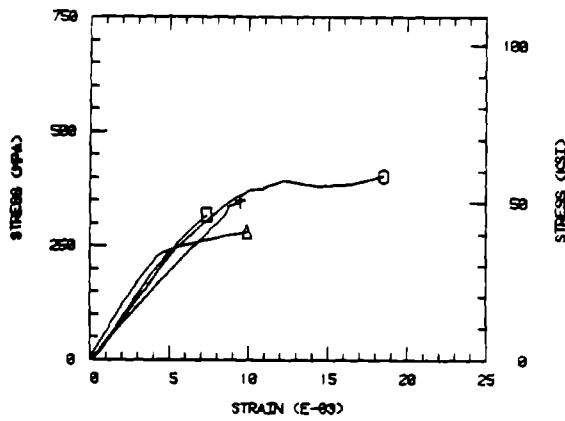
LAM COMP R T , DRY, 4001, UNSIZED



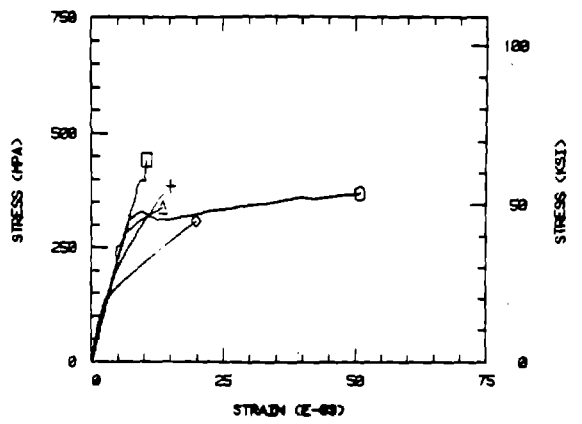
LAM COMP R T , DRY, 4001, 820



LAM COMP R T , DRY, 4001, PVA

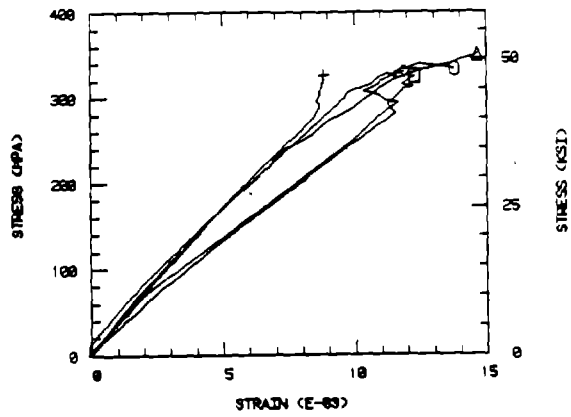


LAM COMP R T , DRY, 4001, P-SULFON

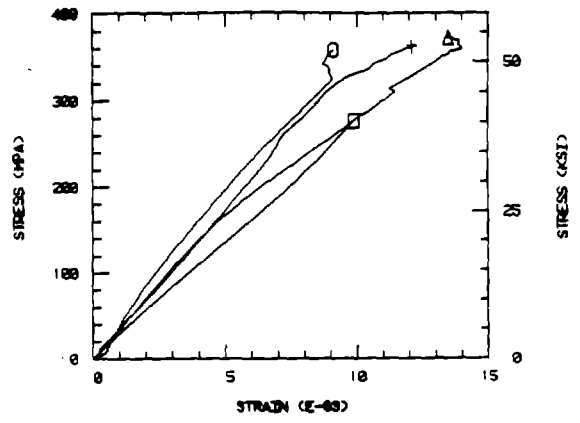


ORIGINAL PAGE IS  
OF POOR QUALITY

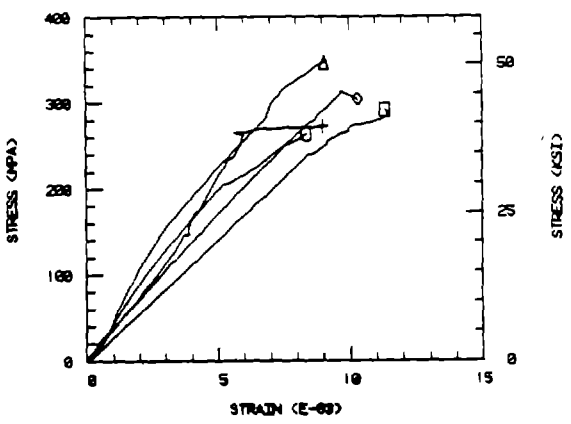
LAM COMP ELV TEMP ,WET 4001 UNSIZED



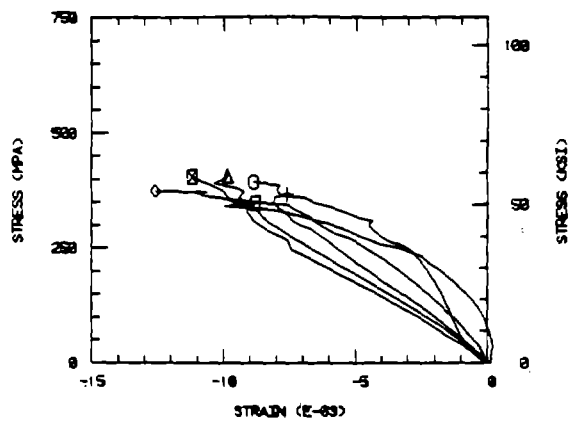
LAM COMP ELV TEMP ,WET 4001 828



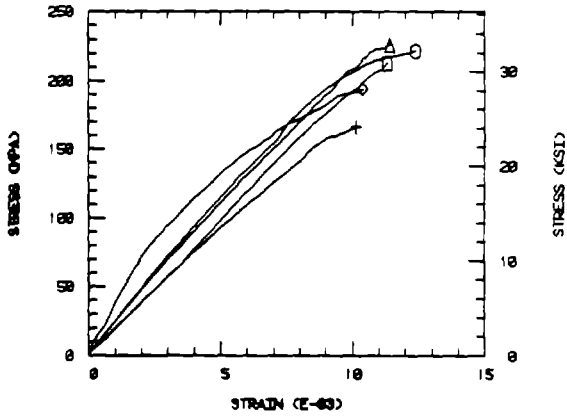
LAM COMP ELV TEMP ,WET 4001 PVA



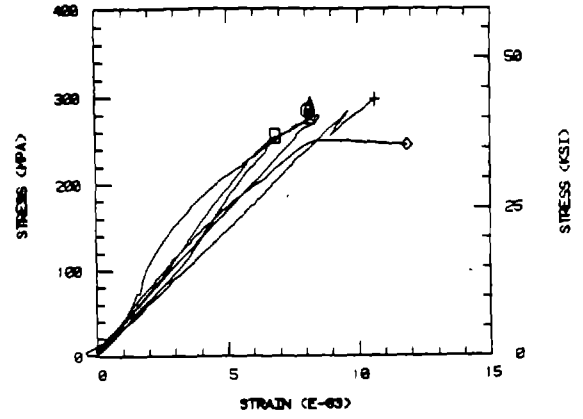
LAM COMP ELV TEMP ,WET 4001 P-SULFON



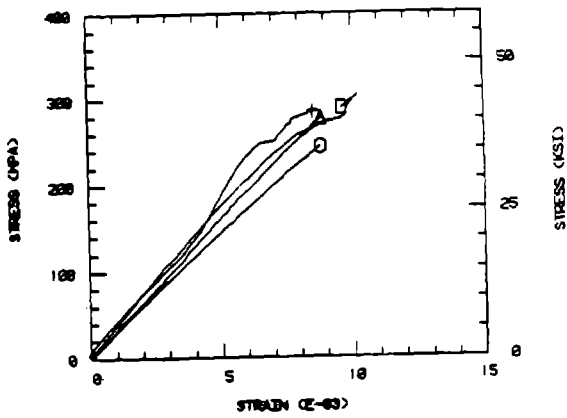
LAM COMP R T , DRY, FISS., UNSIZED



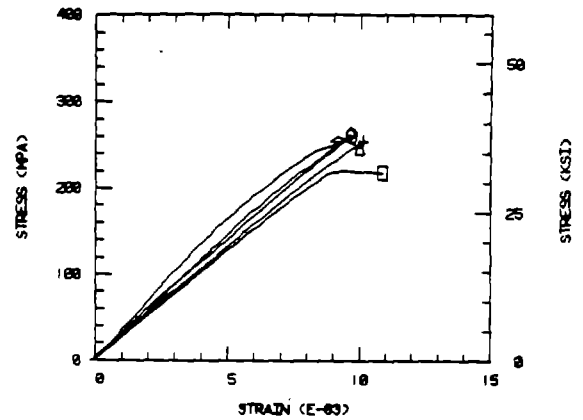
LAM COMP R T , DRY, FISS., 828



LAM COMP R T , DRY, FISS., PVA

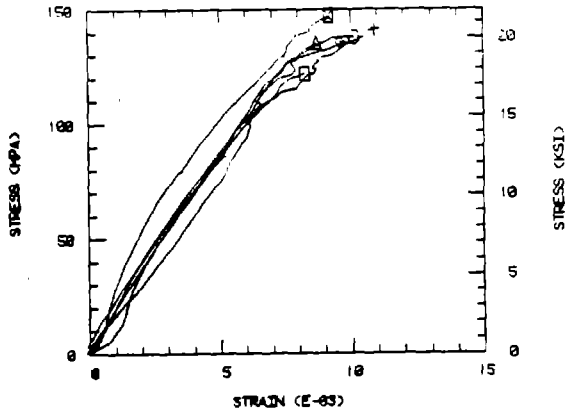


LAM COMP R T , DRY, FISS., P-SULFON

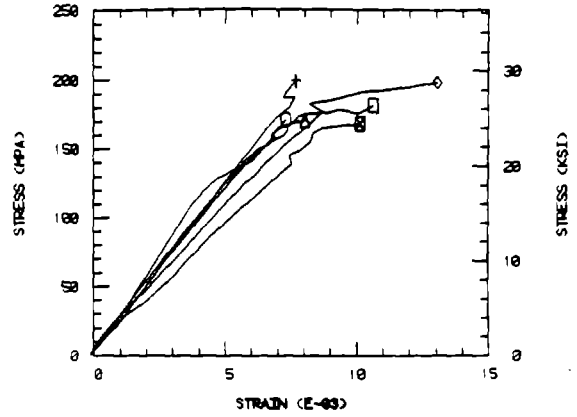


ORIGINAL PAGE IS  
OF POOR QUALITY

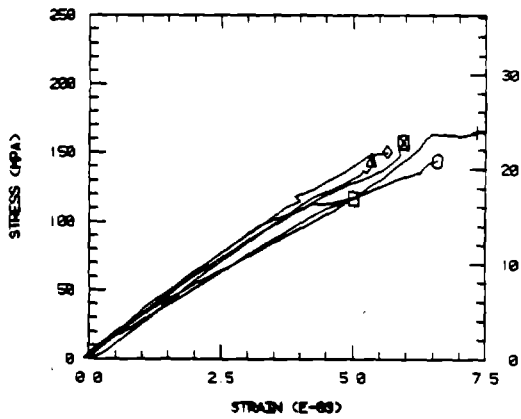
LAM COMP ELV TEMP ,WET F155 UNSIZED



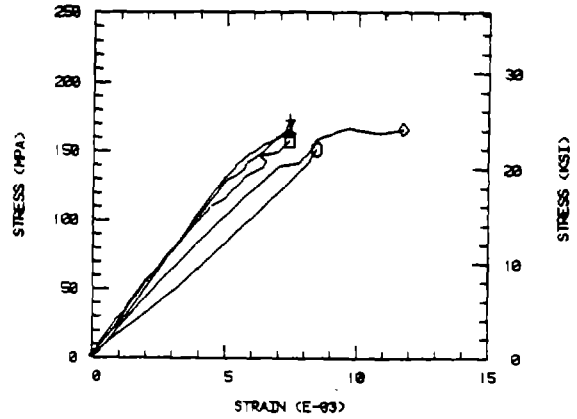
LAM COMP ELV TEMP ,WET F155 828



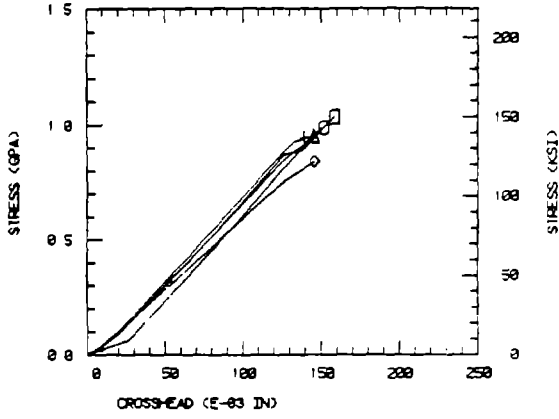
LAM COMP ELV TEMP ,WET F155 PVA



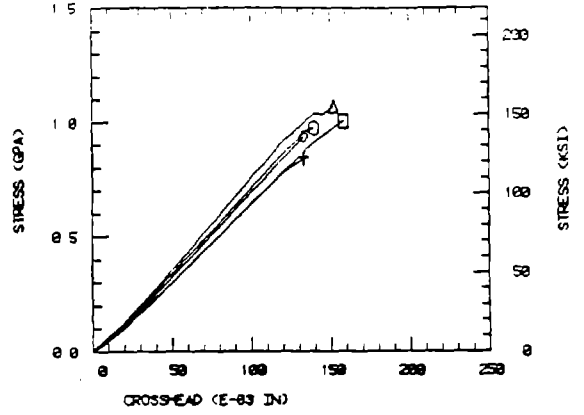
LAM COMP ELV TEMP ,WET F155 P-SULFON



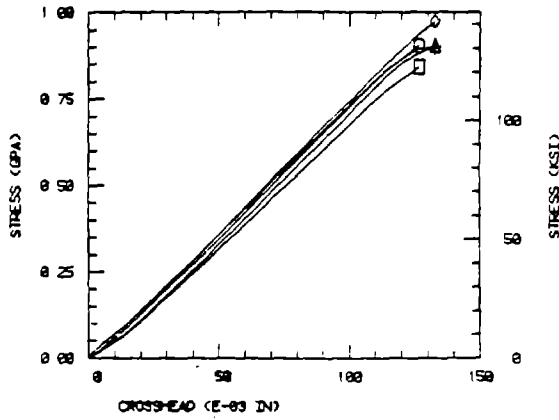
LAM FLEX R T , DRY 3501-6 UNSIZED



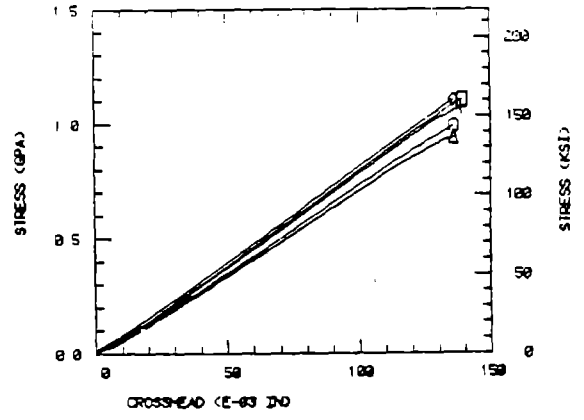
LAM FLEX R T , DRY 3501-6 828



LAM FLEX R T , DRY 3501-6 PVA



LAM FLEX R T , DRY 3501-6 P-SULFON

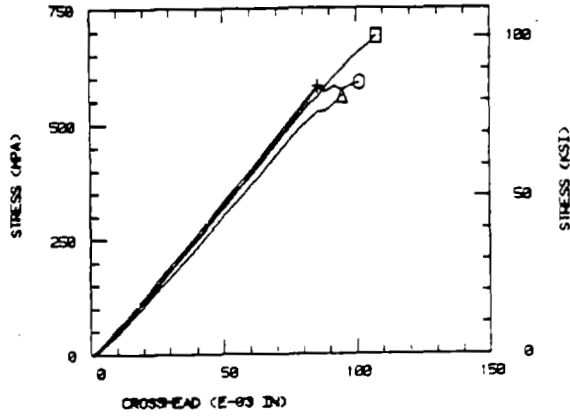


Quasi-Isotropic Laminate Flexure

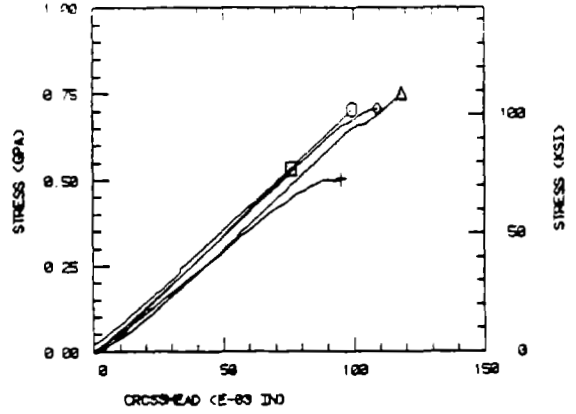


ORIGINAL PAGE IS  
OF POOR QUALITY

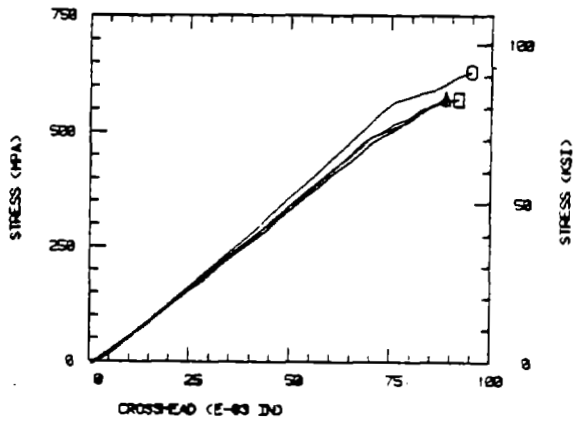
LAM FLEX ELV TEMP ,WET 3501-6 UNSIZED



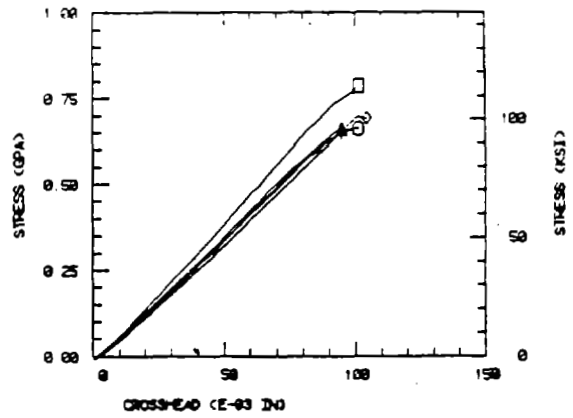
LAM FLEX ELV TEMP ,WET 3501-6 828



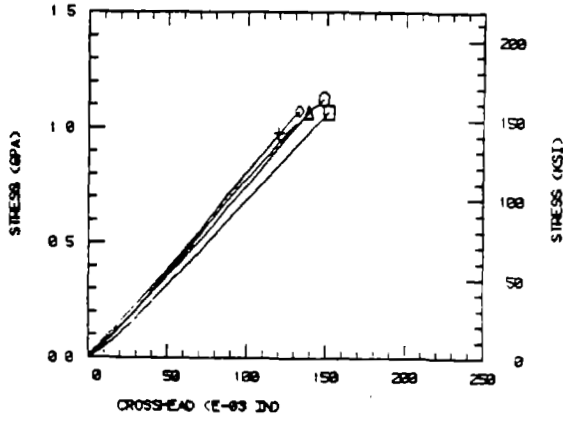
LAM FLEX ELV TEMP ,WET 3501-6 PVA



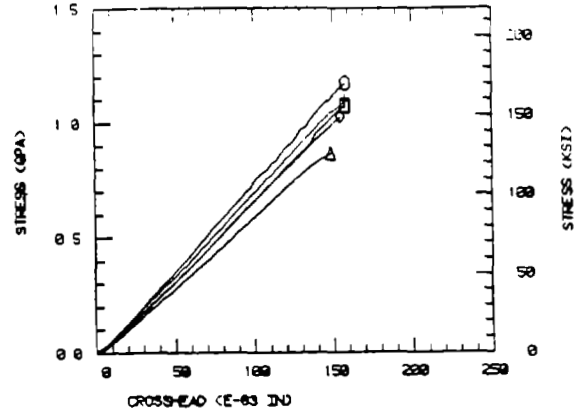
LAM FLEX ELV TEMP ,WET 3501-6 P-SULFON



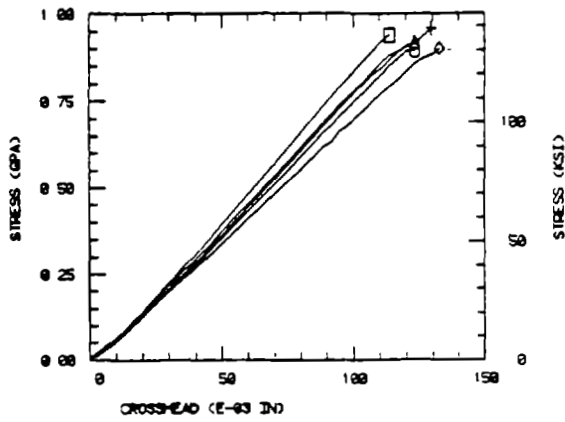
LAM.FLEX. R T , DRY 4001 UNSIZED



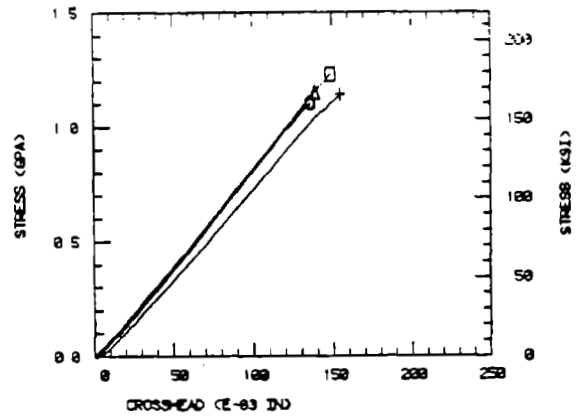
LAM.FLEX. R T , DRY 4001 828



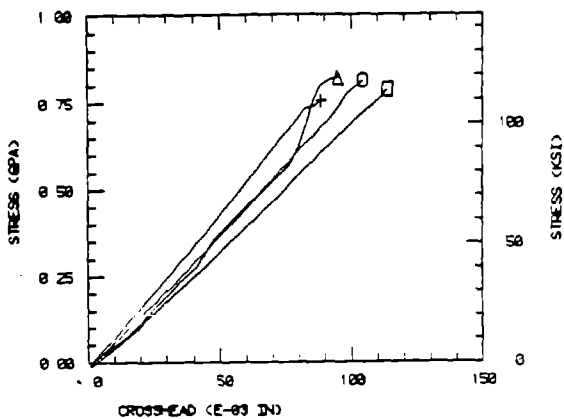
LAM.FLEX. R T , DRY 4001 PVA



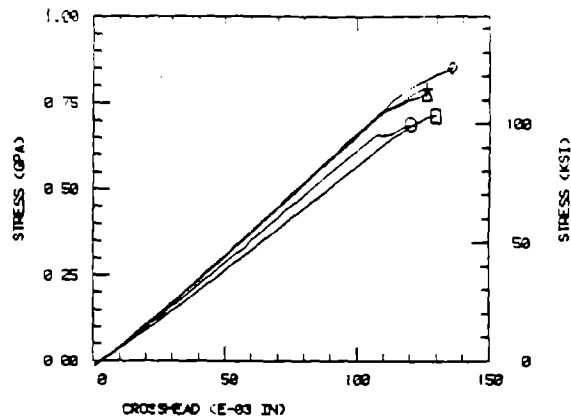
LAM.FLEX. R T , DRY 4001 P-SULFON



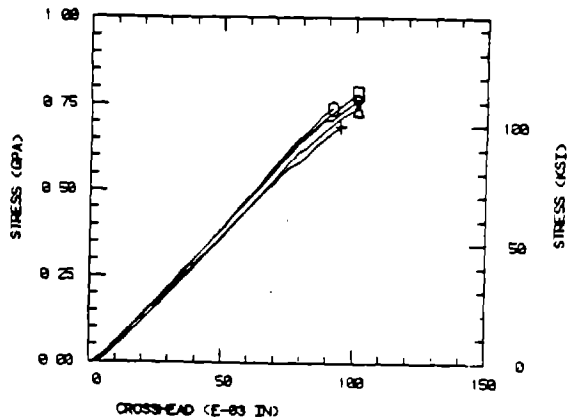
LAM FLEX ELV TEMP ,WET 4001 UNSIZED



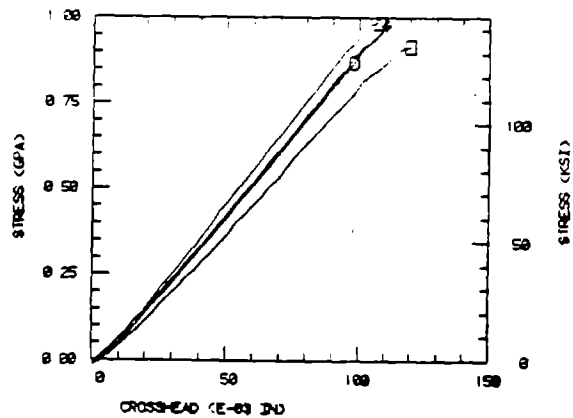
LAM FLEX ELV TEMP ,WET 4001 828



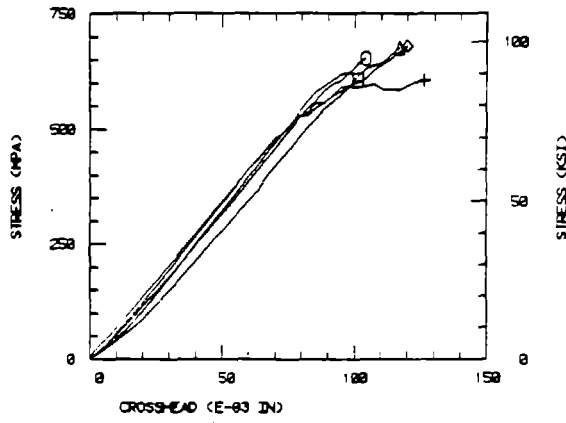
LAM FLEX ELV TEMP ,WET 4001 PVA



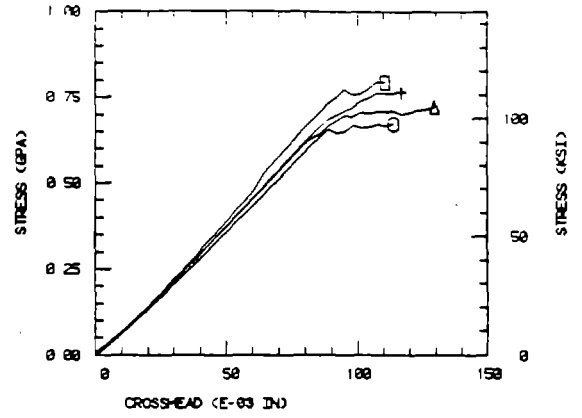
LAM FLEX ELV TEMP ,WET 4001 P-SULFON



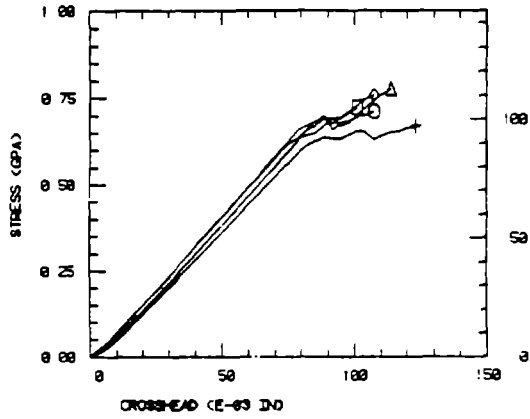
LAM FLEX. R T , DRY F155 UNSIZED



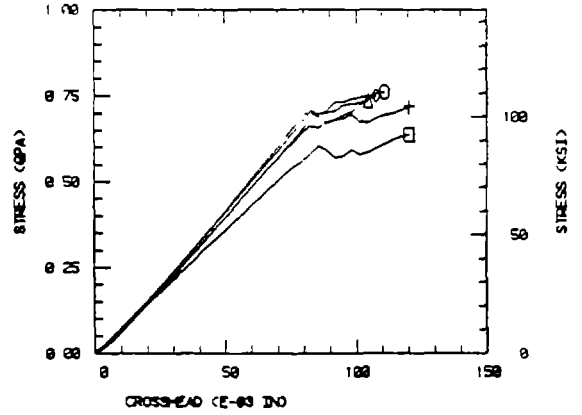
LAM FLEX. R T , DRY F155 828



LAM FLEX. R T , DRY F155 PVA

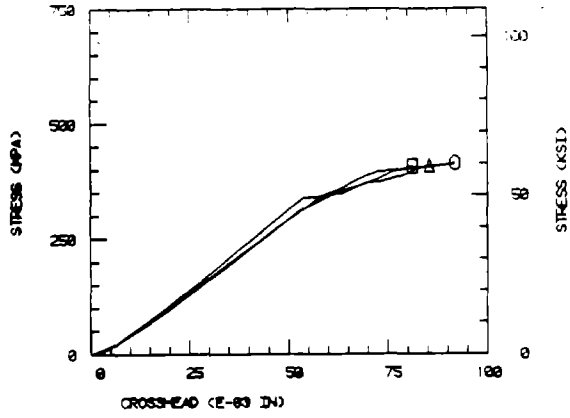


LAM FLEX. R T , DRY F155 P-SULFON

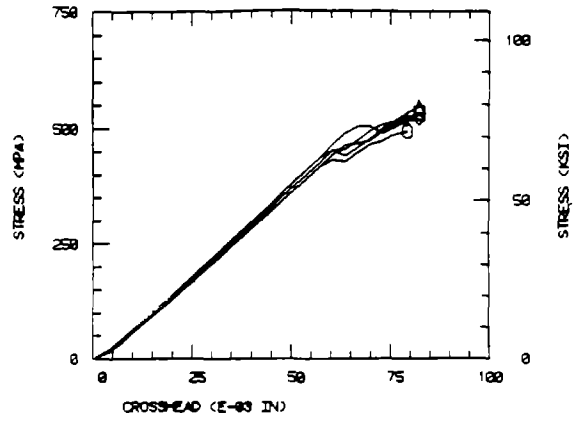


ORIGINAL PAGE IS  
OF POOR QUALITY

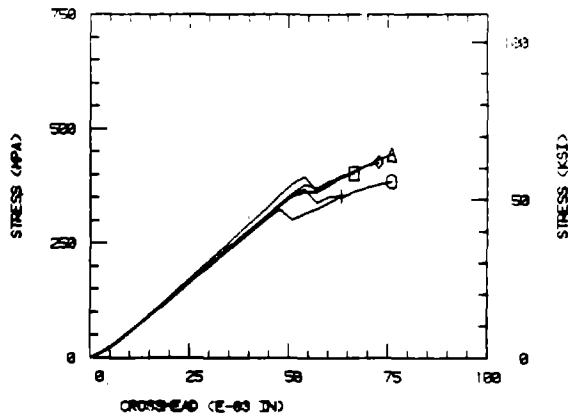
LAM FLEX ELV TEMP ,WET F155 UNSIZED



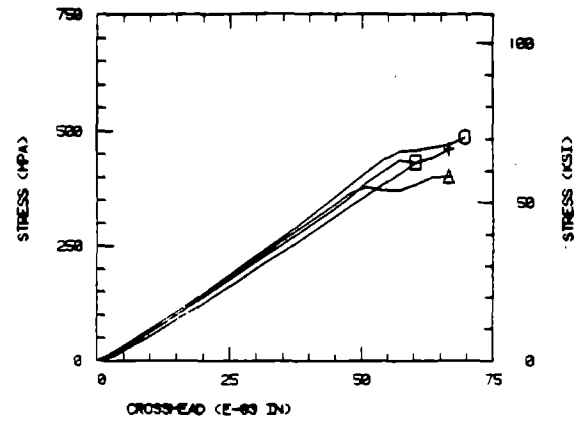
LAM FLEX ELV TEMP ,WET F155 828



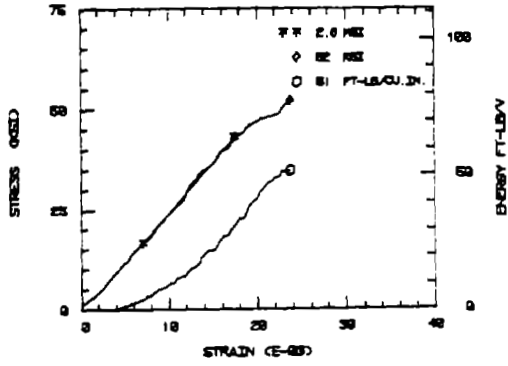
LAM FLEX ELV TEMP ,WET F155 PVA



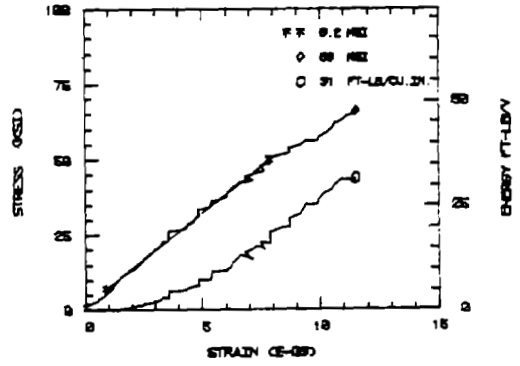
LAM FLEX ELV TEMP ,WET F155 P-SULFON



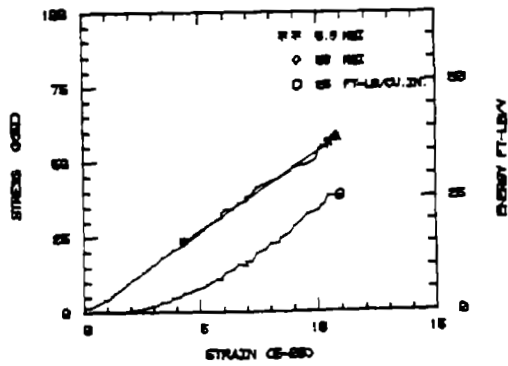
ALRY22



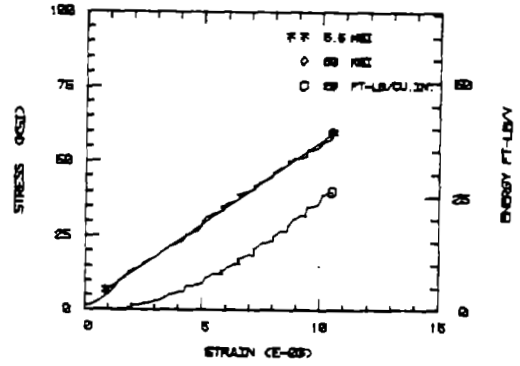
ALRY18



ALRY21

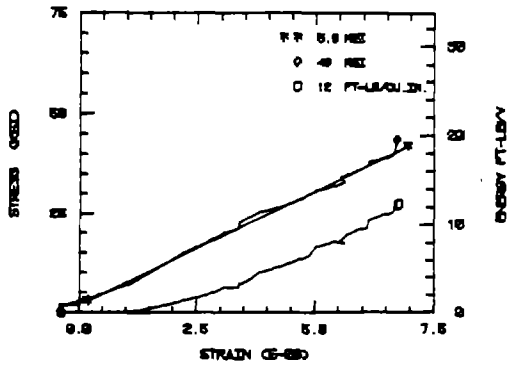


ALRY32

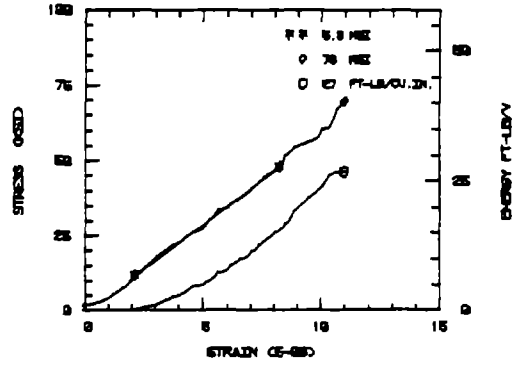


Quasi-Isotropic Laminate Tensile Impact

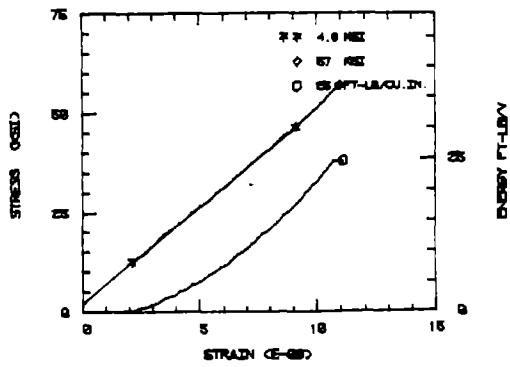
ALEY23



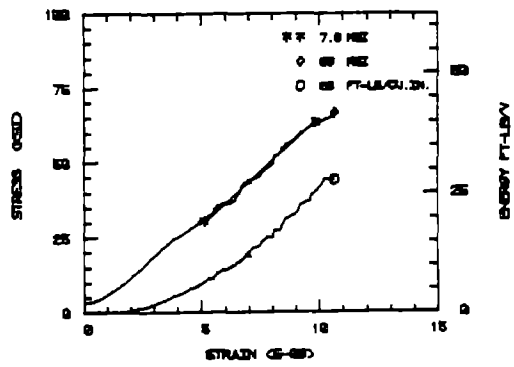
ALEY13



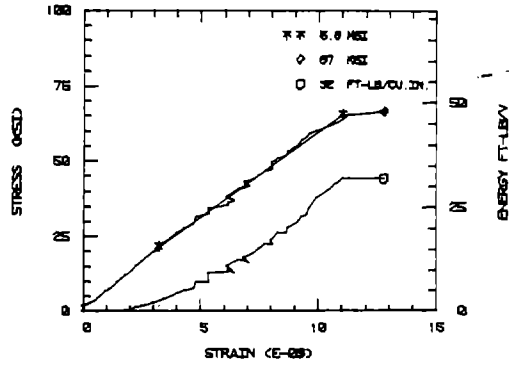
ALEY21



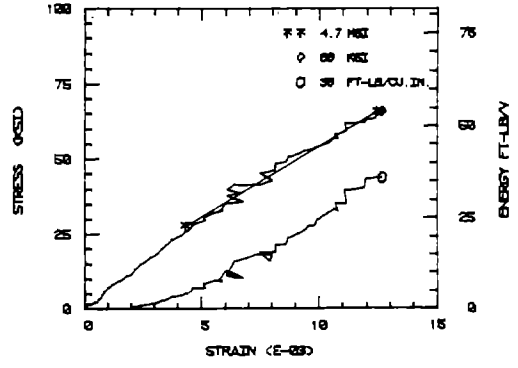
ALEY34



ALRZ12

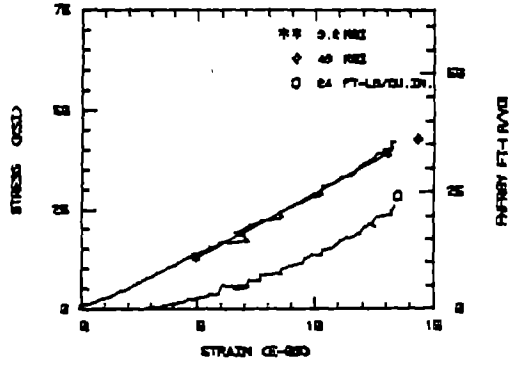


ALRZ32

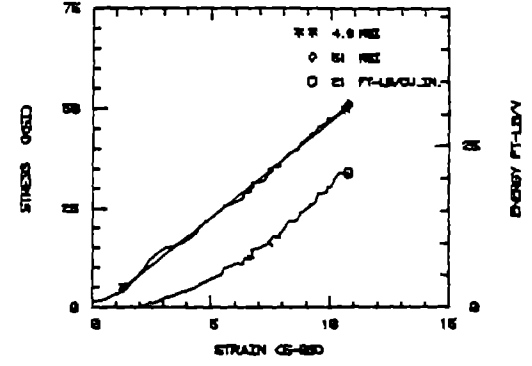




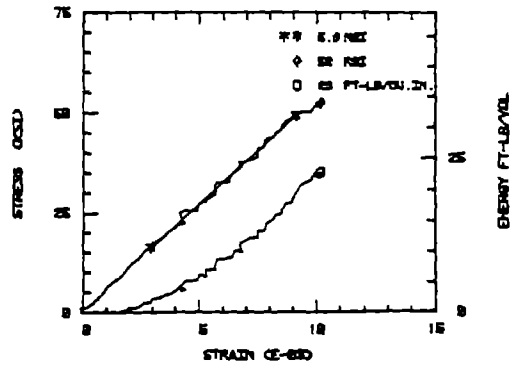
ALRX04



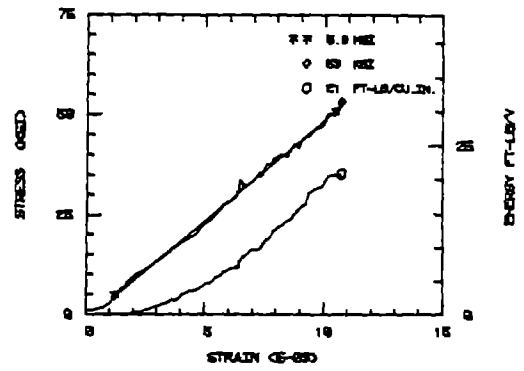
ALRX12



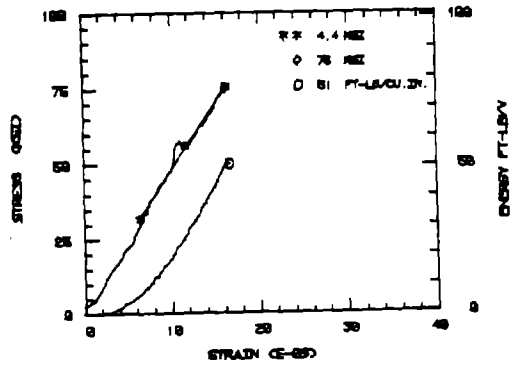
ALRX28



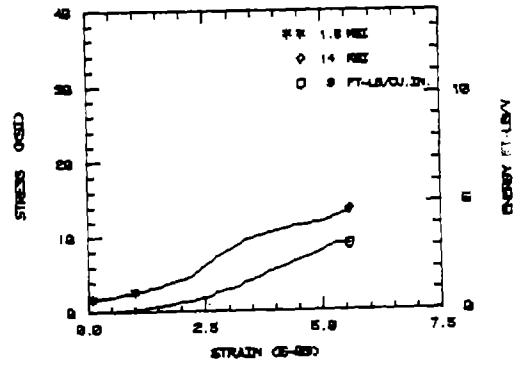
ALRX32



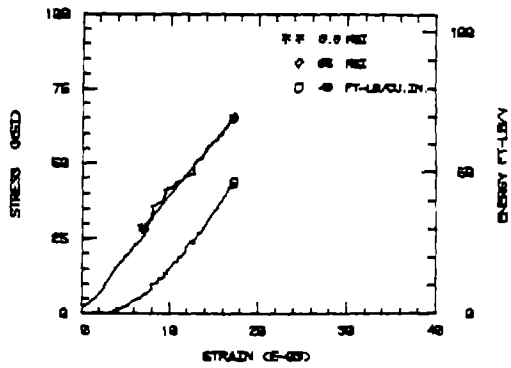
ALEX22



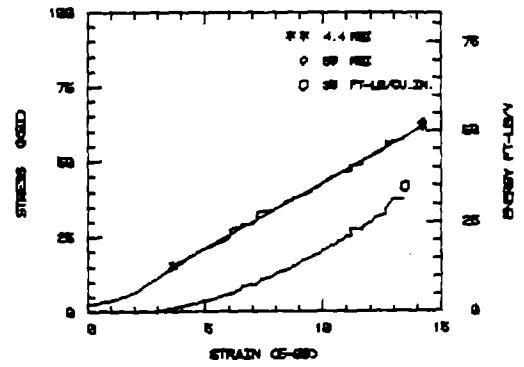
ALEX14



ALEX24



ALEX31

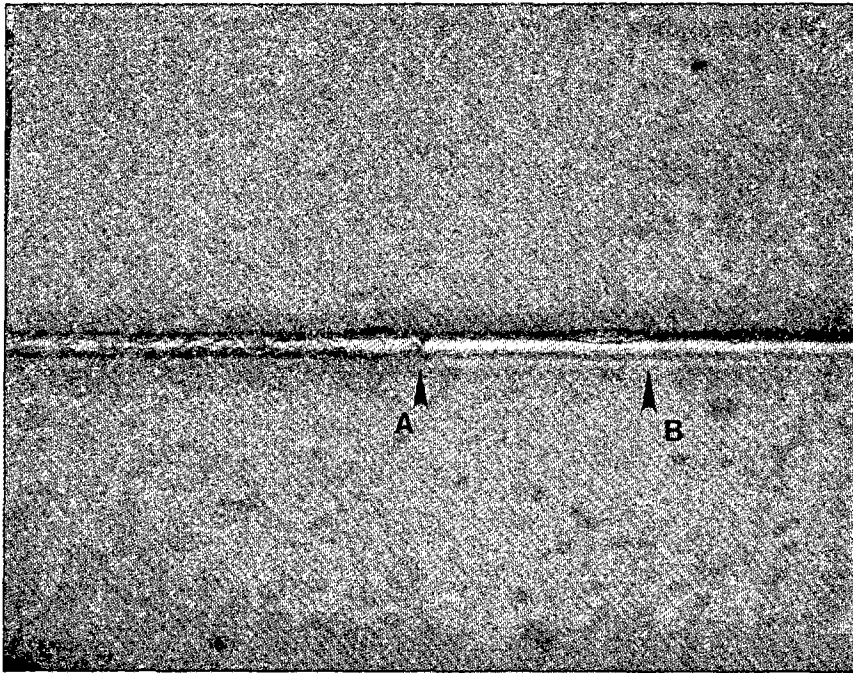


APPENDIX C

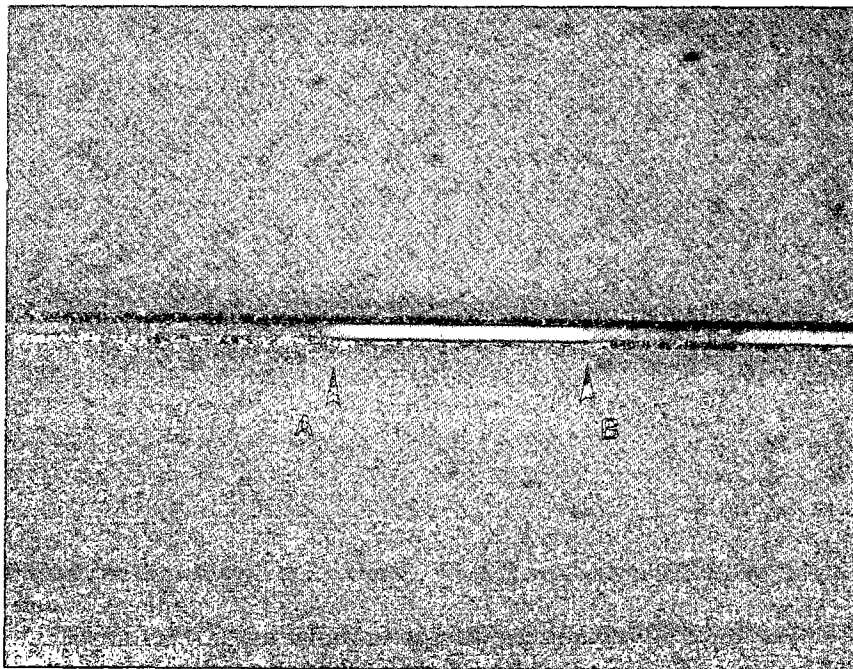
ADDITIONAL PHOTOGRAPHS OF  
SINGLE FIBER PULLOUT SPECIMEN FRACTURE SURFACES



ORIGINAL PAGE IS  
OF POOR QUALITY

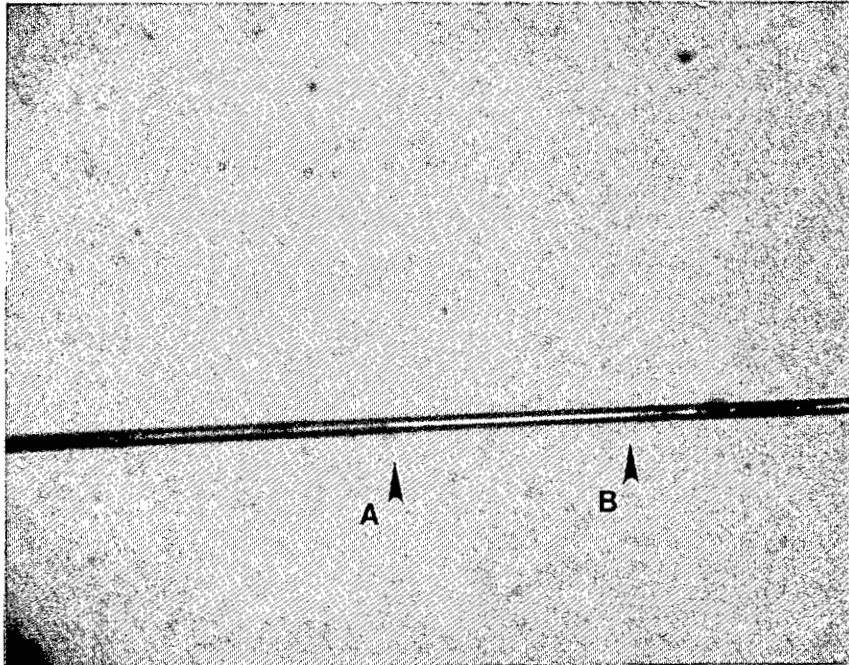


Specimen AERY01: Unsized AS4/3501-6 (320X)

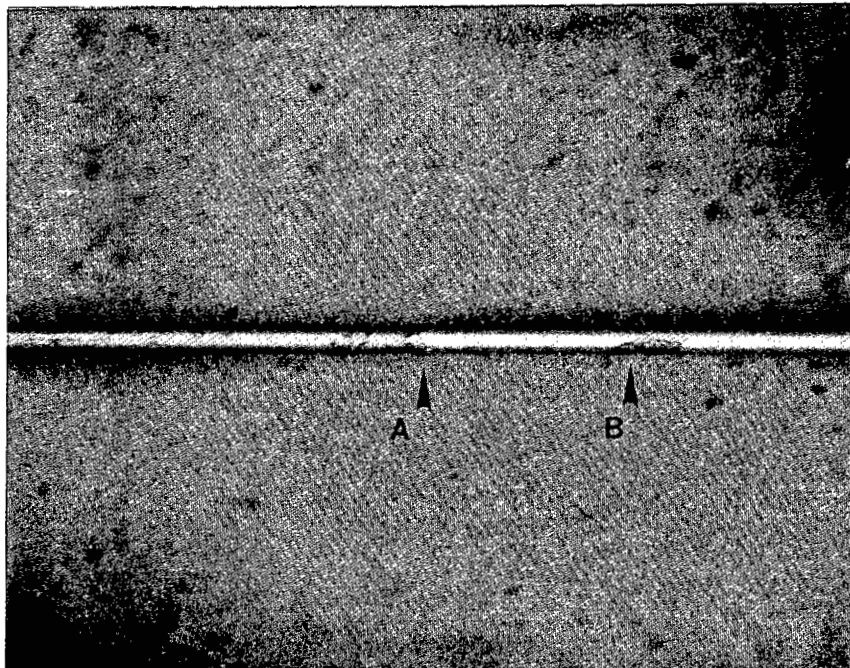


Specimen AERY02: Unsized AS4/3501-6 (320X)

Preceding Page Blank AND NOT FOUND

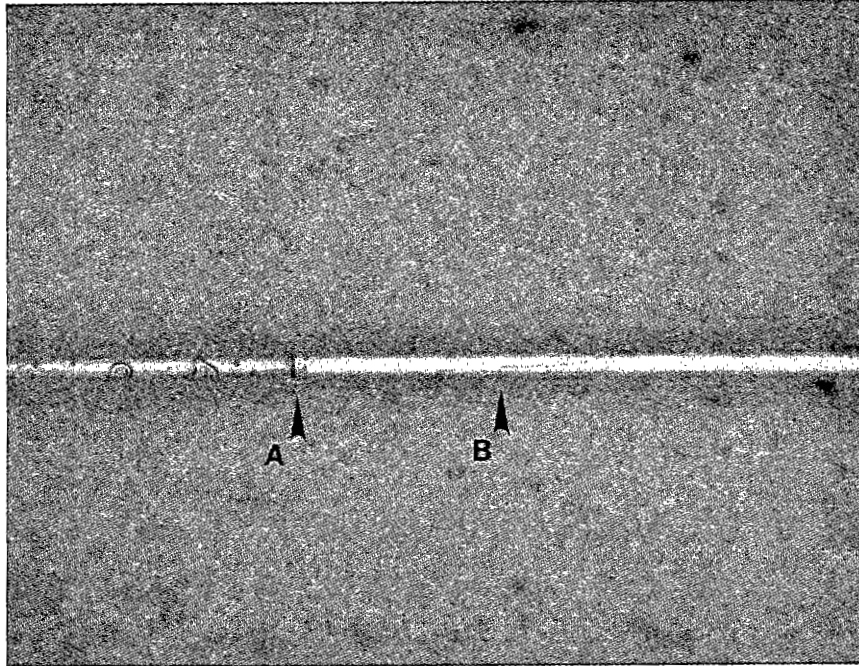


Specimen AERY03: Unsized AS4/3501-6 (160X)

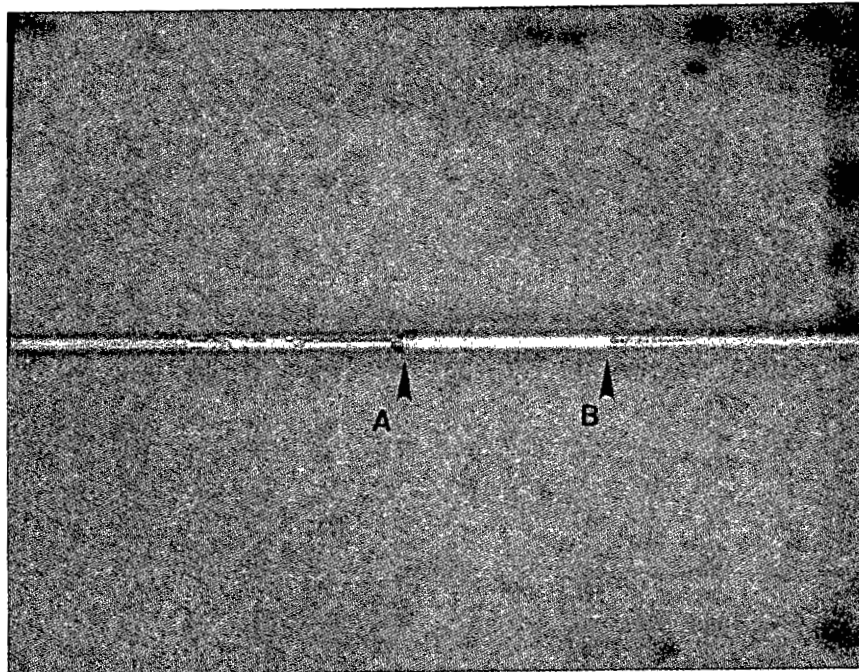


Specimen AERY05: Unsized AS4/3501-6 (320X)

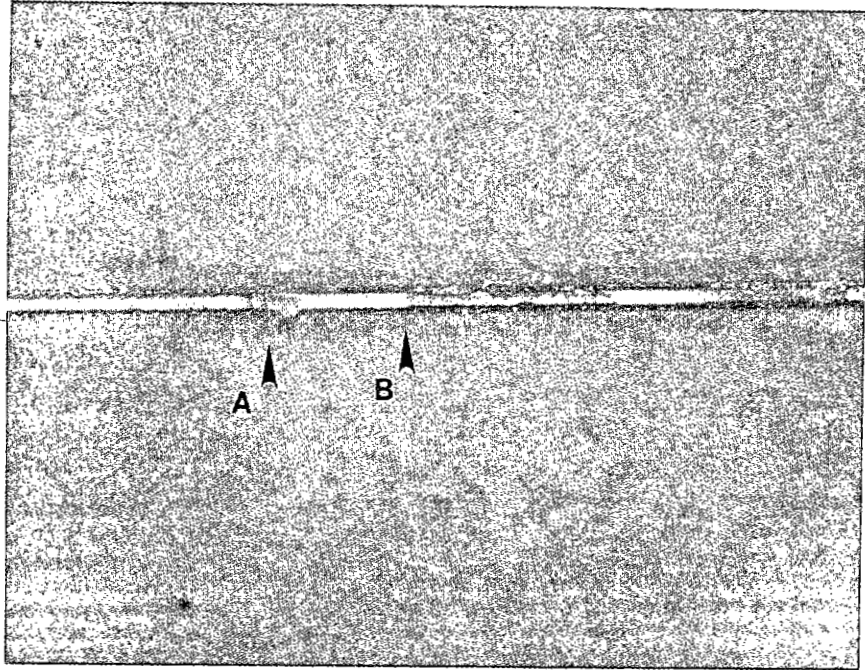
ORIGINAL PAGE IS  
OF POOR QUALITY



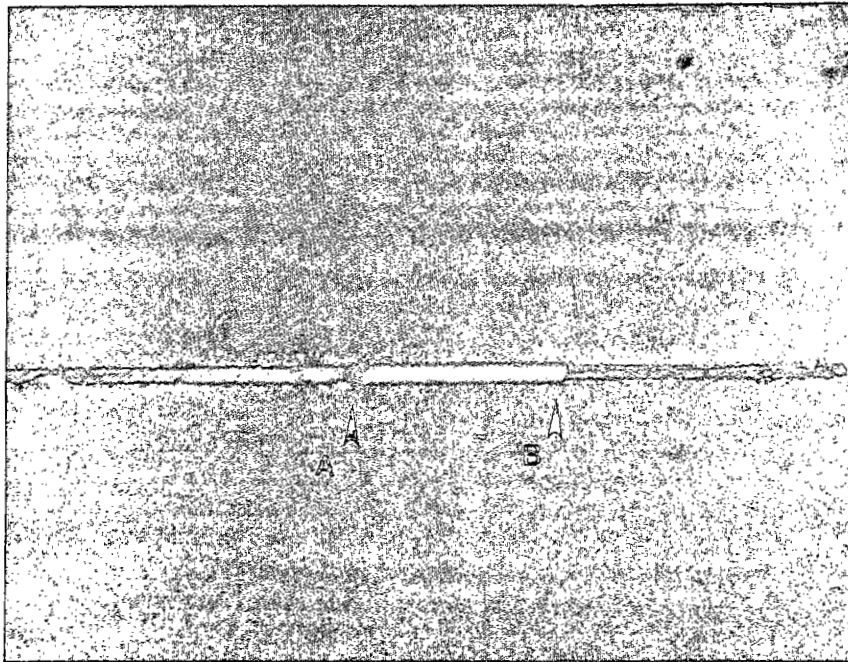
Specimen AERY06: Unsized AS4/3501-6 (320X)



Specimen AERY22: PVA-Sized AS4/3501-6 (250X)



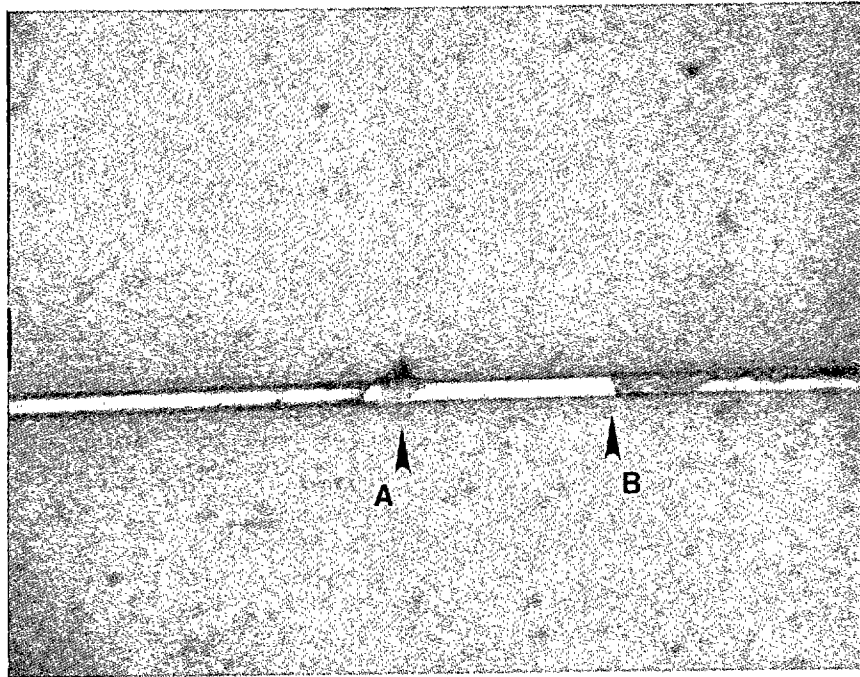
Specimen AERY30: Polysulfone-Sized AS4/3501-6 (320X)



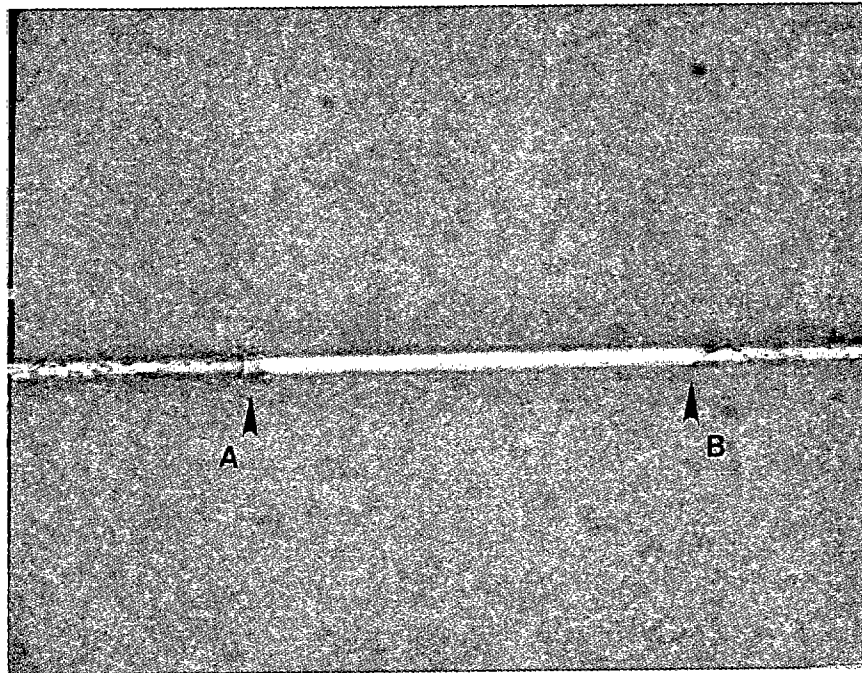
Specimen AERY33: Polysulfone-Sized AS4/3501-6 (320X)



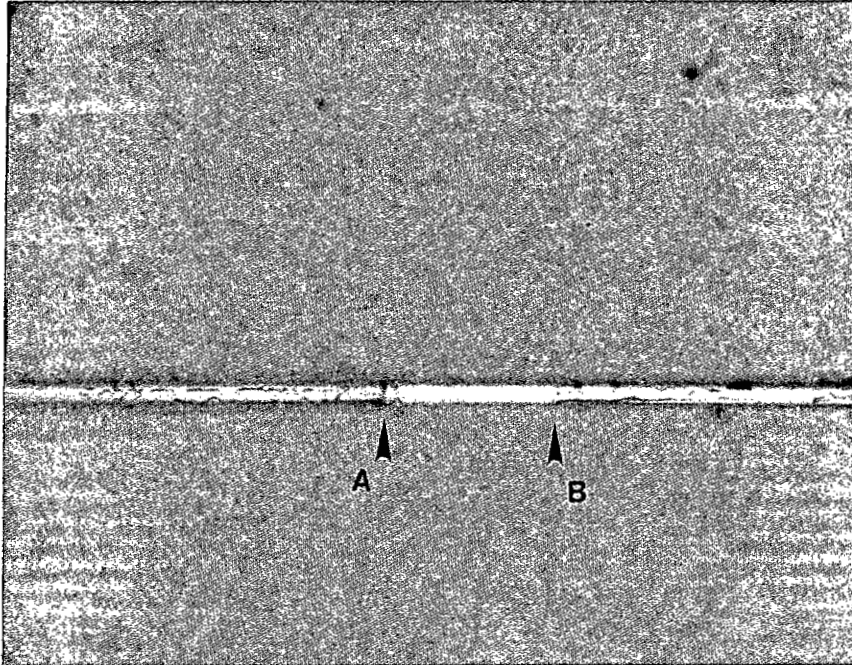
ORIGINAL PAGE IS  
OF POOR QUALITY



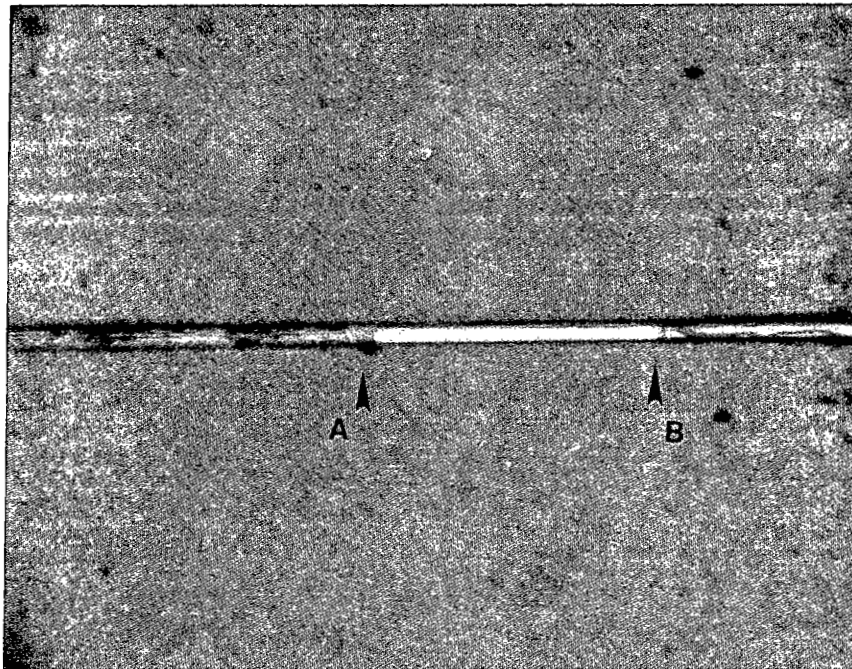
Specimen AERZ02: Unsized AS4/4001 (320X)



Specimen AERZ21: PVA-Sized AS4/4001 (320X)

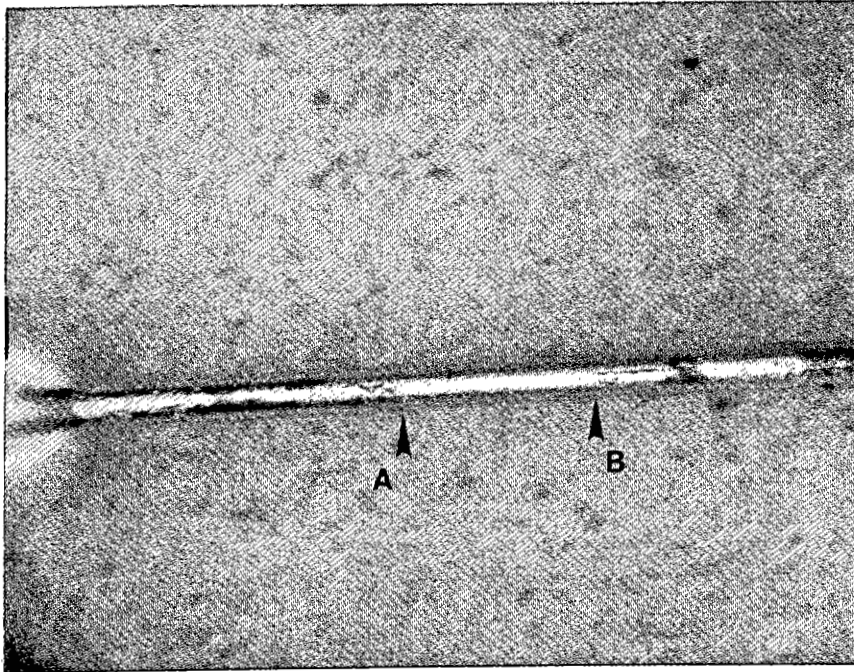


Specimen AERZ22: PVA-Sized AS4/4001 (320X)

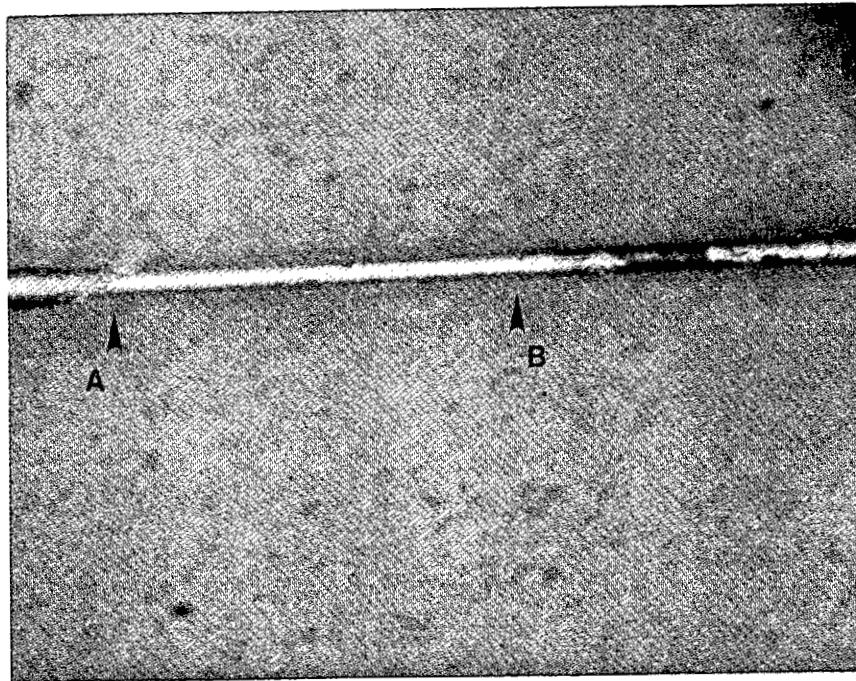


Specimen AERZ34: Polysulfone-Sized AS4/4001 (320X)

ORIGINAL PAGE IS  
OF POOR QUALITY



Specimen AERX32: Polysulfone-Sized AS4/F155 (320X)



Specimen AERX33: Polysulfone-Sized AS4/F155 (320X)



APPENDIX D

CHARACTERIZATION OF GRAPHITE FIBER SURFACE COATINGS

Preceding Page Blank

ANK NOT IN INDEX



CHARACTERIZATION OF GRAPHITE FIBER SURFACE COATINGS

by

Lynn Penn  
Gaylord Atkinson

FINAL REPORT

March 30, 1984

MRI Project No. 8044-G

For

University of Wyoming  
P.O. Box 3295  
University Station  
Laramie, Wyoming 82071

Attn: Mr. Ed Odom  
College of Engineering

Preceding Page Blank

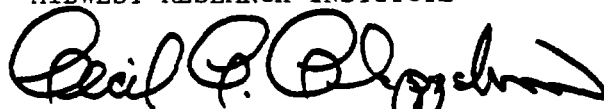
PREFACE

This report describes the characterization of graphite fiber surface coatings by infrared spectroscopy.

The program was conducted under the supervision of Dr. Lynn Penn, Principal Scientist. Mr. Gaylord Atkinson, Principal Scientist, also participated in the investigation.

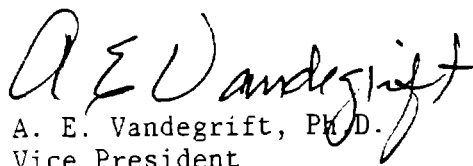
Sincerely,

MIDWEST RESEARCH INSTITUTE



Cecil C. Chappelow, Head  
Materials Science Section

Approved:



A. E. Vandegrift, Ph.D.  
Vice President

March 25, 1984



## CHARACTERIZATION OF GRAPHITE FIBER SURFACE COATINGS

### ABSTRACT

After consideration of available surface analysis methods (ESCA, AES, SIMS, IR, etc.) for characterizing polymeric coatings on graphite fiber yarns, infrared spectroscopy was selected as the most suitable because of its ability to identify functional groups of organic molecules and because of its ability to produce a "fingerprint" of the polymeric coating. Spectra were obtained of the coatings and were compared with handbook spectra of nominally identical polymers. The experimental spectra agreed with the handbook spectra for all of the coatings--epoxy, polysulfone, and polyvinyl alcohol.

## I. INTRODUCTION

This report describes the characterization of the surface coatings of graphite fiber yarns. First is a discussion of the available surface analysis methods. The discussion is followed by a description of our use of infrared spectroscopy, the technique selected for this work. Last, the spectroscopy results are presented and discussed.

## II. AVAILABLE SURFACE ANALYSIS METHODS

The chemical properties, and therefore such things as bonding capabilities and moisture resistance, of surfaces are determined by the presence or absence of various chemical functional groups. The ideal surface analysis method would identify the atoms present, determine how they are arranged or bonded to each other as chemical functional groups in molecules, and also determine whether the functional groups are chemically bonded to the bulk beneath or are simply adsorbed. In reality, however, no single technique can do all of the above. For cases in which there is no prior information on the nature of a surface, it is best to use a combination of techniques.

Surface analysis is simplified if the surface can be removed and studied separately, without any interfering effects from the bulk. If the surface cannot be easily removed, then it must be studied in situ. For cases in which both the surface and bulk of a substance are organic polymers, it is very important that the analysis technique be surface-sensitive; that is, the technique must analyze only the surface and not penetrate deeply into and analyze the bulk. ESCA\* (energy spectroscopy for chemical analysis) is a surface-sensitive technique giving the atomic composition of only the first 100 Å or less.

Although its surface sensitivity makes ESCA attractive, it does have a major limitation. This limitation is ESCA's inability to identify chemical functional groups.<sup>1,2</sup> ESCA yields the identities of atoms in the surface (and their relative amounts), but it does not yield unambiguous information about their bonding to other atoms. It is true that one can obtain some information about the bonding state of some atoms by examination of binding energy shifts in the ESCA spectrum, but these shifts are often difficult to interpret and cannot be definitively assessed. In addition, while ESCA equipment is no longer a rarity, it is not yet commonplace. Many who decide it would be useful must undertake a lengthy search for available equipment and an ESCA expert willing to provide this service.

---

\* ESCA is also called XPS or x-ray photoelectron spectroscopy.

Auger electron spectroscopy (AES) and secondary-ion mass spectrometry (SIMS) are also surface-sensitive techniques.<sup>3,4</sup> Unfortunately, AES is not suitable for polymers because the energetic electron beam required for this technique alters the sample.<sup>2</sup> In addition, AES gives only elemental information and little chemical information. SIMS gives chemical information, but the effects of the ion beam on the sample during measurements are not well characterized.<sup>2,4</sup> Moreover, instrumental facilities for these techniques are even less available than ESCA facilities.

For chemical analysis of organic materials, infrared spectroscopy is excellent. It is especially useful for functional group identification.<sup>5</sup> Briefly described, it is a vibrational spectroscopy in which the sample absorbs light at wavelengths corresponding to the frequencies of vibration of each different functional group. Although it is usually used for bulk analysis, special procedures permit it to be used for surface analysis. In the simplest case, the surface coating or layer can be removed from the bulk and collected for spectroscopic analysis. Where removal is not possible, infrared spectroscopy can be adapted for in situ surface analysis. When so adapted, it is called attenuated total internal reflectance (ATIR) and has an analysis depth of 10,000 Å.<sup>2</sup> With most specimens this large depth includes not only the surface but some of the bulk, which is a drawback when only surface analysis is desired. However, if the material below the surface is not very responsive to infrared spectroscopy, (such as a metal, graphite, or inorganic glass), then the response of the surface layer will dominate. The infrared spectrum, then, serves as a "fingerprint" of the substance being investigated and can be conveniently compared with other spectra. In addition, infrared equipment is very widely used and is therefore readily available.

### III. SELECTION OF AN ANALYTICAL METHOD FOR COATED GRAPHITE FIBER

In making the final selection of an analysis method, the researcher must be sure to understand what information is desired. In the present case of coated graphite fibers, a characterization of the coatings themselves was desired. This characterization will serve as a standard against which future lots of coated fibers can be checked, or against which aged samples of the initial lots can be studied for chemical changes such as polymerization, moisture degradation, or oxidation. A method of analysis which gives a fingerprint of the coating is required.

It should be pointed out that the question of whether actual chemical bonding rather than just physical bonding occurs between the organic coating and the functional groups in the graphite surface remains unresolved. The technical difficulties of assessing the exact chemical details of a small-volume region between an opaque fiber and a polymerized solid are extreme, and cannot be overcome in a short study.

For the coated graphite fibers used in this study, the information we already had about the material made the choice of an appropriate surface analysis method easier. The three coatings were identified as

polysulfone, polyvinyl alcohol, and diglycidylether of bisphenol A (epoxy). Since these are organic polymers that absorb infrared (IR) radiation, they will each give distinct IR spectra. In contrast, ESCA would not provide unambiguous characterization of the many different carbon-, hydrogen-, or nitrogen-containing functional groups. Infrared spectroscopy was therefore chosen as the most suitable characterization method.

The simplest approach would be to remove the polymeric coating from the surface of the graphite fiber. Then spectral analysis could be carried out on the coatings alone.

If removal is not possible then the ATIR adaption described above can be used.

#### IV. USE OF INFRARED SPECTROSCOPY TO CHARACTERIZE THE COATING ON GRAPHITE FIBER SURFACES

The four fiber yarn samples received for analysis were designated as follows:

AS4 unsized  
AS4 828 sizing (epoxy)  
AS4 polysulfone sizing  
AS4 PVA sizing

The expected chemical structures of the three sizing materials are shown in Figure 1. The word sizing here means coating.

First, we tried the simplest approach--dissolving the coating from the fiber surface in order to take a spectrum of the isolated coating. A length of fiber was packed in a disposable pipette, and solvent was dripped down through the fiber. The solvent dripped out the narrow end of the pipette into a vial. This procedure is depicted in Figure 2.

Fortunately, by use of appropriate solvents ample amounts of coating were extracted from the coated fiber surfaces. The extractions were for the purpose of obtaining material for the IR analyses and were therefore thorough but not exhaustive. The data from the extraction procedure are shown in Table 1.

ORIGINAL PAGE IS  
OF POOR QUALITY

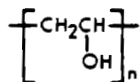
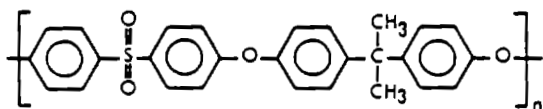
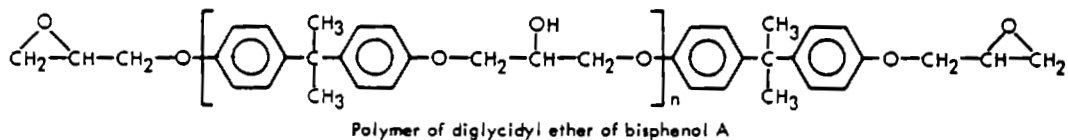


Figure 1 - Chemical structures of polymers identified as the coating materials for graphite fibers.

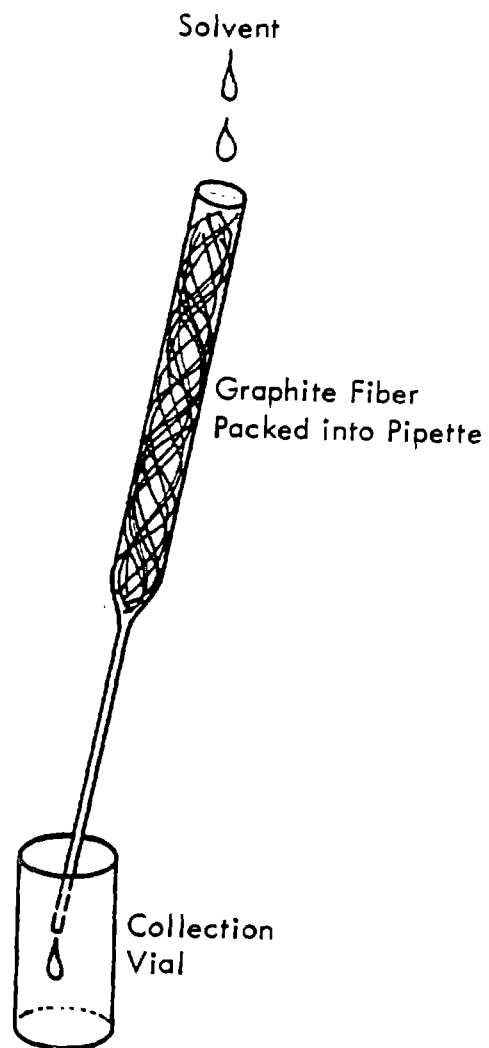


Figure 2 - Extraction of polymeric coating (sizing) from graphite fiber yarns.

TABLE 1

EXTRACTION DATA FOR FOUR FIBER SAMPLES

	<u>Wt Coated Fiber, g</u>	<u>Wt Dried Extracted Material, g</u>	<u>Wt Percent Coating*</u>	<u>Color of Extract</u>
Unsize:				
Methylene chloride	0.5851	0.0002	0.03	orange
Epoxy-sized:				
Methylene chloride	0.9197	0.0127	1.38	colorless
Polysulfone-sized:				
Methylene chloride	0.6477	0.0021	0.32	pale yellow
PVA-sized:				
Methylene chloride	0.5611	0.0009	0.16	colorless
Water	0.5611	0.0035	0.63	colorless
Total	0.5611	0.0044	0.79	

---


$$* \text{ wt percent coating} = \frac{\text{wt dried extract}}{\text{wt coated fiber}} \times 100$$

For the epoxy-sized and polysulfone-sized fibers, methylene chloride was a sufficiently good solvent to remove adequate amounts of coating. For the PVA-sized fiber, methylene chloride removed only about 20% of the coating. Therefore, water was used to remove more of the PVA coating.

Interestingly, the small amount of material extracted from the unsized fiber appeared bright orange, while the greater amounts extracted from the sized fibers showed little or no color. No significance is attributed to this result, however, since extremely small amounts of some impurities can display bright hues while large amounts of many organic compounds can be colorless.

To obtain the spectrum of each coating, the extracted material, dissolved in solvent, was placed on a supporting disc (pressed KBr, transparent to infrared light) and mounted in the sample chamber. The solvent was allowed to evaporate before spectra were obtained. These spectra are displayed in Figures 3, 4, and 5. Also displayed, for comparison, are handbook spectra of the same polymers. Because some spectra are linear in the wave number scale and others are linear in the wavelength scale, caution must be exercised in peak by peak comparison.





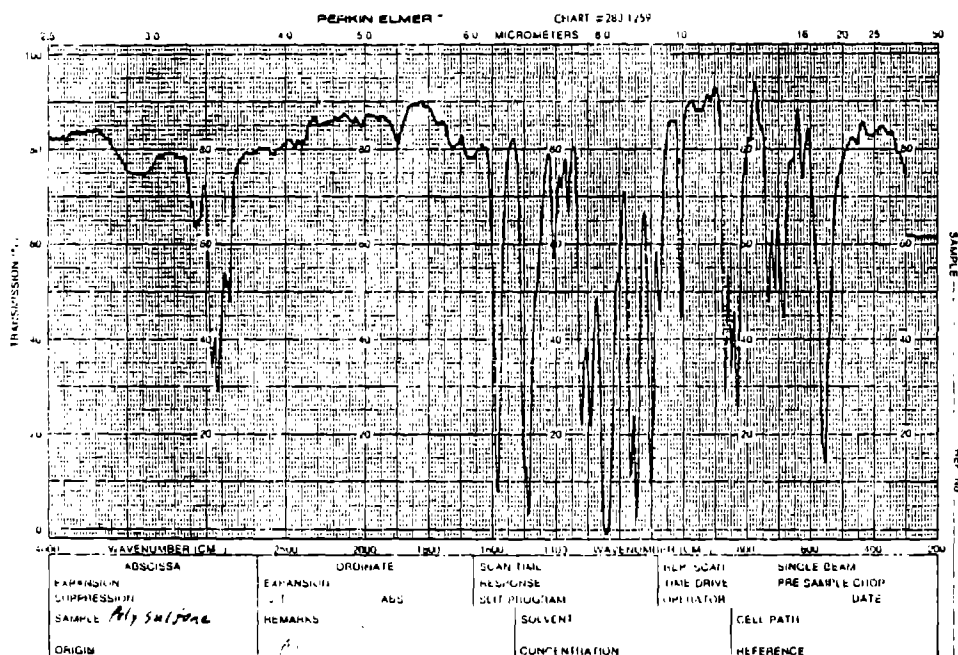
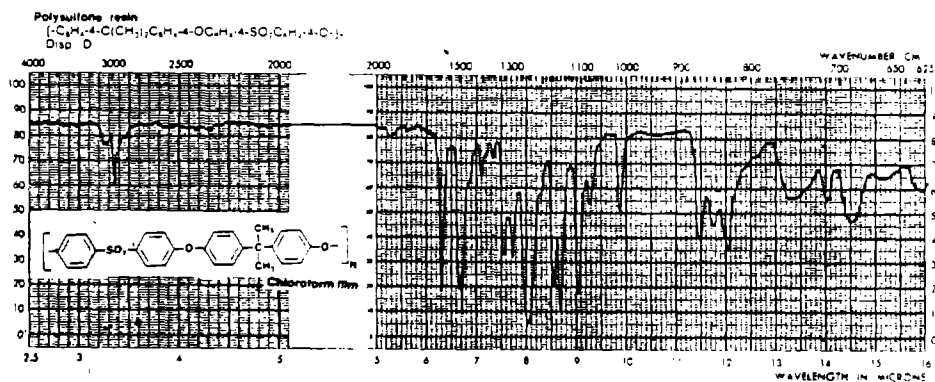


Figure 4 - Comparison of IR handbook spectrum with experimental spectrum, showing identical features.

Top: Handbook spectrum of commercial polysulfone.<sup>7</sup>

Bottom: Spectrum of coating from coated graphite fiber AS4 polysulfone sizing.

ORIGINAL PAGE IS  
OF POOR QUALITY

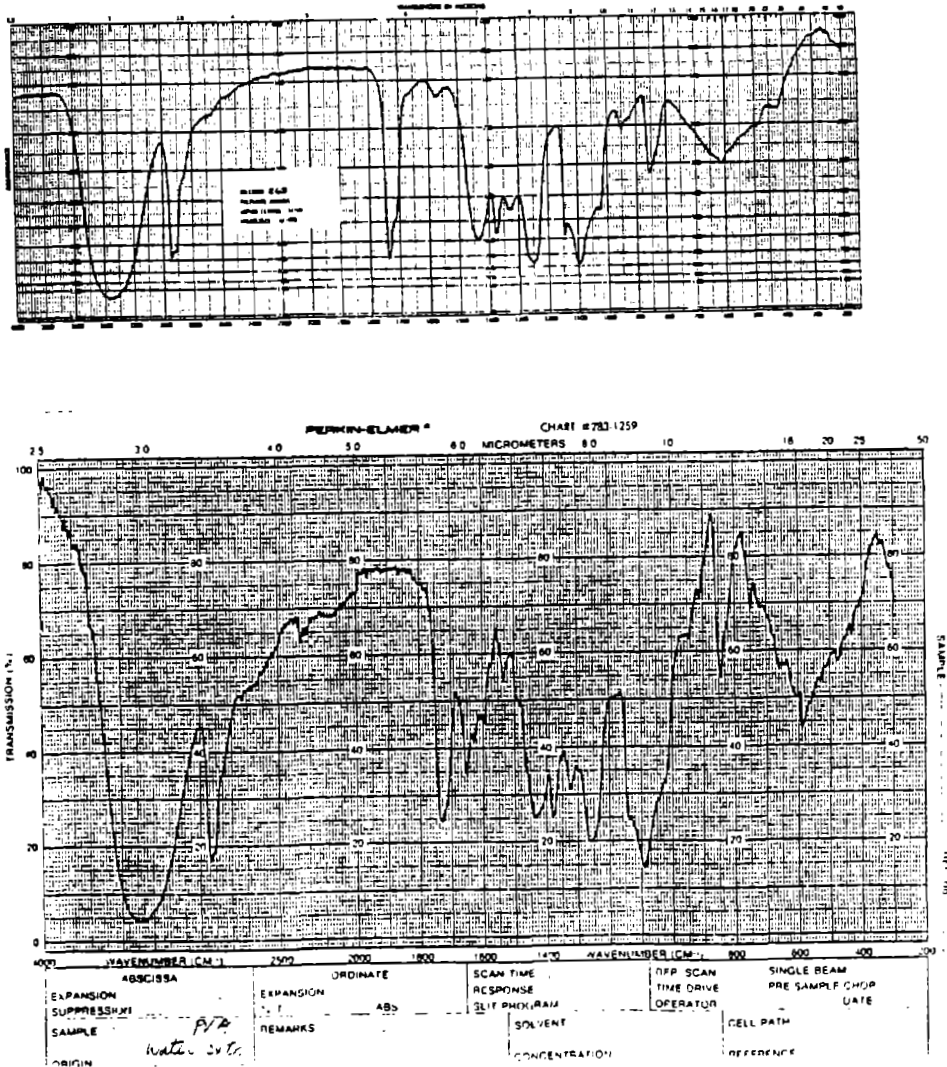


Figure 5 - Comparison of IR handbook spectrum with experimental spectrum, showing identical features.

Top: Handbook spectrum of commercial polyvinyl alcohol.<sup>8</sup>

Bottom: Spectrum of water-extracted coating from coated graphite fiber AS4 PVA sizing.

The spectrum of the coating from epoxy-sized graphite is almost exactly the same as the handbook spectrum for diglycidyl ether of bisphenol A. This is confirmation that the 828 epoxy coating is diglycidyl ether of bisphenol A, as had been expected.

The spectrum of the coating from polysulfone-coated graphite is the same as the handbook spectrum for polysulfone, which verifies that this polymeric coating on the graphite is a fairly standard polysulfone.

The spectrum of the water-extracted coating from PVA-coated graphite is the same as the handbook spectrum of commercial PVA. The coating on the graphite contains pure PVA but also contains a small amount of other substances. This was discovered by examining the spectrum of the methylene chloride-extracted portion of the PVA-sized graphite (Figure 6). Note the strong peak at  $1100\text{ cm}^{-1}$  indicating presence of aliphatic ether groups. In addition, the large amplitude of the peak at  $2950\text{ cm}^{-1}$  indicates presence of more alkane groups than are normally found in the commercial PVA. These too could be from an aliphatic ether.

The handbook spectrum of the commercial PVA (Figure 5) also shows evidence of apparent aliphatic ether. Such additional components are no cause for concern since polymeric aliphatic ethers have no negative indications in the performance or durability of composites.

Figure 7 shows the spectrum of the small amount of extract from the unsized graphite. This spectrum exhibits no strong peaks, which proves that the spectra of the extracted coatings in Figures 3, 4, and 5 can be attributed solely to the coatings.

## V. SUMMARY

Infrared spectra were obtained for the polymer coatings (sizings) on each of three coated graphite yarns. The epoxy coating, the polysulfone coating, and the polyvinyl alcohol coating proved to be the standard widely used types.



ORIGINAL PAGE IS  
OF POOR QUALITY

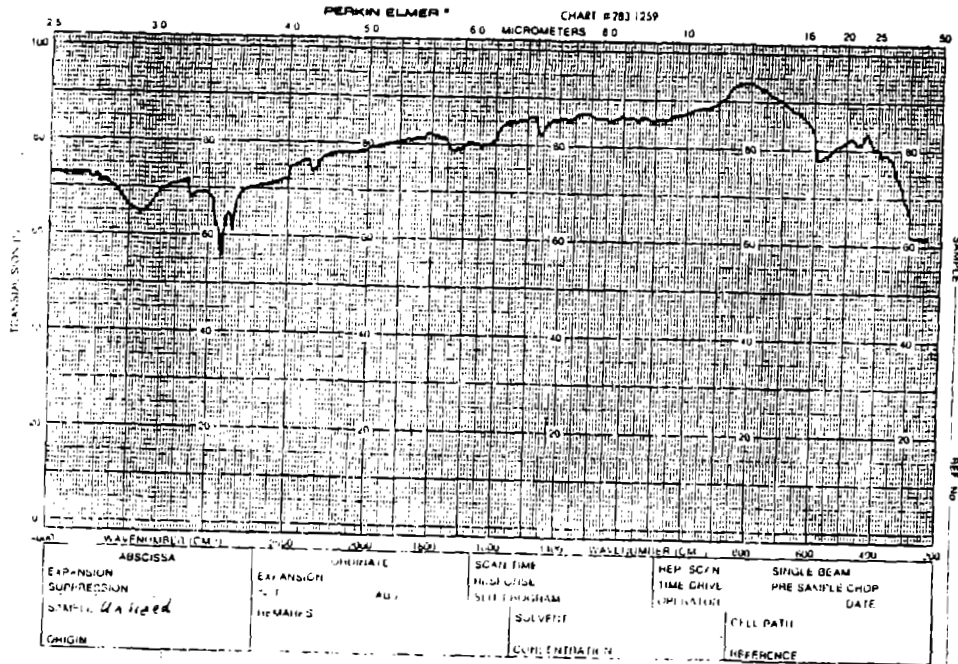


Figure 7 - IR spectrum of the small amount of material extracted from surface of the unsized graphite fiber. The lack of any strong spectral features verify that the spectra in Figures 3, 4, 5, are of the sizing only.

## REFERENCES

1. Leary, H. J., Jr., and D. S. Campbell, "Surface Analysis of Aromatic Polyimide Films Using ESCA," Surf. Interface Anal., 1, 75 (1979).
2. Reilley, C. N., and D. S. Everhart, "ESCA Analysis of Functional Groups on Modified Polymer Surfaces," in Applied Electron Spectroscopy for Chemical Analysis, H. Windawi and F. Ho, Eds., John Wiley and Sons, Inc., New York, 1982, p. 105.
3. Gettings, M., and A. J. Kinloch, "Surface Characterization and Adhesive Bonding of Stainless Steels," Surf. Interface Anal., 1, 189 (1979).
4. Gardella, J. A., Jr., and D. M. Hercules, "Static Secondary Ion Mass Spectrometry of Polymer Systems," Analytical Chemistry, 52, 226 (1980).
5. Colthup, N. B., "Introduction to Infrared and Raman Spectroscopy," Academic Press, New York, 1964.
6. Lee, H., and K. Neville, Handbook of Epoxy Resins, McGraw-Hill, Inc., New York, 1967 (1982 Classic Handbook Reissue), p. 4-39.
7. Pouchert, C. J., The Aldrich Library of Infrared Spectra, 3rd Ed., Aldrich Chemical Co., Milwaukee, 1981, p. 1604.
8. "Infrared Spectroscopy: Its Use in the Coatings Industry," Federation of Societies for Paint Technology, Philadelphia, Pennsylvania, 1969, p. 221.